AD -776-998

SUMMARY OF PROPELLER DESIGN PROCEDURES AND DATA. VOLUME III. HUB, ACTUATOR, AND CONTROL DESIGNS

Edward Sand, et al

Nov 73

U.S. Department of Commerce
National Technical Information Service
NTIS

Task 1G162207AA7203
Contract DAAJ02-72-C-0033
USAAMRDL Technical Report 73-34C
November 1973

SUMMARY OF PROPELLER DESIGN PROCEDURES AND DATA

VOLUME III
HUB, ACTUATOR, AND CONTROL DESIGNS

By

Edward Sand
Douglas A. Elliott, Jr.
Henry V. Borst

Prepared by

HENRY V. BORST & ASSOCIATES
Rosemont, Pennsylvania

REPRODUCED BY
NATIONAL TECHNICAL
INFORMATION SERVICE
US DEPARTMENT OF COMMERCE
SPRINGFIELD, VA. 22161

for

EUSTIS DIRECTORATE
U.S. ARMY AIR MOBILITY RESEARCH AND DEVELOPMENT LABORATORY
FORT EUSTIS, VIRGINIA

Approved for public release;
distribution unlimited.

330

DISCLAIMERS

The findings in this report are not to be construed as an official Department of the Army position unless so designated by other authorized documents.

When Government drawings, specifications, or other data are used for any purpose other than in connection with a definitely related Government procurement operation, the United States Government thereby incurs no responsibility nor any obligation whatsoever; and the fact that the Government may have formulated, furnished, or in any way supplied the said drawings, specifications, or other data is not to be regarded by implication or otherwise as in any manner licensing the holder or any other person or corporation, or conveying any rights or permission, to manufacture, use, or sell any patented invention that may in any way be related thereto.

Trade names cited in this report do not constitute an official endorsement or approval of the use of such commercial hardware or software.

DISPOSITION INSTRUCTIONS

Destroy this report when no longer needed. Do not return it to the originator.

Unclassified
Security Classification

AD 776 998

DOCUMENT CONTROL DATA - R & D

(Security classification of title, body of abstract and indexing annotation must be entered when the overall report is classified)

1. ORIGINATING ACTIVITY (Corporate author) Henry V. Borst & Associates 353 Yorkshire Road Rosemont, Pennsylvania	2a. REPORT SECURITY CLASSIFICATION Unclassified 2b. GROUP

3. REPORT TITLE
SUMMARY OF PROPELLER DESIGN PROCEDURES AND DATA
VOLUME III - HUB, ACTUATOR, AND CONTROL DESIGNS

4. DESCRIPTIVE NOTES (Type of report and inclusive dates)
Final Report

5. AUTHOR(S) (First name, middle initial, last name)
Edward Sand
Douglas A. Elliott, Jr.
Henry V. Borst

6. REPORT DATE November 1973	7a. TOTAL NO. OF PAGES 329	7b. NO. OF REFS 22

8a. CONTRACT OR GRANT NO. DAAJ02-72-C-0033 b. PROJECT NO. c. Task 1G162207AA7203 d.	9a. ORIGINATOR'S REPORT NUMBER(S) USAAMRDL Technical Report 73-34C 9b. OTHER REPORT NO(S) (Any other numbers that may be assigned this report) None

10. DISTRIBUTION STATEMENT
Approved for public release; distribution unlimited.

11. SUPPLEMENTARY NOTES Volume III of a 3-volume report	12. SPONSORING MILITARY ACTIVITY Eustis Directorate U.S. Army Air Mobility R&D Laboratory Fort Eustis, Virginia

13. ABSTRACT

The technology needed for the design and installation of propellers is presented and summarized in three volumes.

Volume III (Hub, Actuator, and Control Design) contains material on the design of the hub and actuator systems. The theories of propeller controls are presented with the details of the types used with conventional and V/STOL airplanes. A brief discussion of past and future propeller installations is given along with recommendations for future work. Design criteria, airfoil data, and a computer program are given.

DD FORM 1 NOV 65 1473 REPLACES DD FORM 1473, 1 JAN 64, WHICH IS OBSOLETE FOR ARMY USE.

Unclassified
Security Classification

14 KEY WORDS	LINK A		LINK B		LINK C	
	ROLE	WT	ROLE	WT	ROLE	WT
Propellers - Design						
Dual-Rotation Propellers						
Controls - Propellers						
Aerodynamics - Propellers						
Propeller Performance						
Blades - Propellers						
Propulsion						
Turboprops						
Aircraft						
V/STOL Aircraft Propellers						
STOL Aircraft Propellers						
Composite Structure Blades						
Propeller Deicing						
Propeller Maintenance						

DEPARTMENT OF THE ARMY
U S ARMY AIR MOBILITY RESEARCH & DEVELOPMENT LABORATORY
EUSTIS DIRECTORATE
FORT EUSTIS, VIRGINIA 23604

This report was prepared by Henry V. Borst & Associates under the terms of Contract DAAJ02-72-C-0033. It describes and summarizes available propeller design and performance methods and data needed for the design and installation of propellers for conventional and V/STOL airplanes.

The technical manager for this contract was Mr. James Gomez, Technology Applications Division.

SUMMARY

This report contains background material for the design of the blade actuator system, the blade retention and the propeller hub. Included is a comparison of the various actuation systems that have been used, including the details of their operation, and the advantages as well as the disadvantages of each type. The design of the blade retention is discussed, including the integral blade bearing type. Also covered is the design consideration used for the layout of the hub.

The background theory for the design of propeller control systems is presented, including a development of block flow diagrams, engine propeller control loops and calculation of transfer function derivatives. The propeller control system's characteristics are considered with the engine and propeller response, block diagrams and control system elements. Proportional control, integral control and the proportional plus integral control system are also discussed. Controls for special functions such as phase synchronizing are covered. Finally, new types of adaptive propeller controls are considered for advanced types of installations.

For background information a number of past propeller installations are covered. In this light, considerations of new applications are discussed with the factors needed to prevent some of the problems encountered in the past. The type of future propellers to be considered is also discussed.

As no technology can remain static and still be used, the recommendations for additional propeller research are also covered.

The appendixes contain the propeller design criteria, airfoil data for performance analysis and an outline for a computer program to calculate propeller performance.

TABLE OF CONTENTS

Page

SUMMARY iii

LIST OF ILLUSTRATIONS ix

LIST OF TABLES xx

LIST OF SYMBOLS xxi

HUB AND BLADE ACTUATOR DESIGN 1

INTRODUCTION 1

BLADE ACTUATOR TYPES 1

- Electric Motor/Speed Reducer Type 1
- Electromechanical Clutch Type 1
- Hydromechanical Type 1

RELATIVE ADVANTAGES OF BLADE ACTUATION SYSTEMS 2

ELECTRIC MOTOR/SPEED REDUCER BLADE ACTUATION SYSTEM 5

- General Description 5
- Motor Assembly 5
- Brake Assembly 7
- Speed Reducer 7
- Blade Angle Limit Switches 8

ELECTROMECHANICAL CLUTCH TYPE BLADE ACTUATION SYSTEM 8

- General 8
- Details of Operation 9
- Clutch Design 11

HYDROMECHANICAL BLADE ACTUATION SYSTEM 12

- Controls 14
- Blade Actuator Torque Design Requirements 15
- Hub Design Considerations 16
- Influence of Blade Retention on Hub Design 18
- Selection of Blade Shank Size 20
- Selection of Retention Bearing 21
- Retention Nut and Hub Barrel Interface 21
- Final Hub Design Consideration 22

Preceding page blank

TABLE OF CONTENTS (Continued)

Page

Integral Blade Bearing Hub 23

PROPELLER CONTROLS 28

INTRODUCTION 28

PROPELLER CONTROL DEVELOPMENT 29

Control Criteria 29
Control and Safety Analyses 29

CONTROL DESIGN 30

Testing 31

PROPELLER CONTROL THEORY 32

Basic Dynamic Equations 32
Operational Notation 35
Solutions of Operational Equations 38
Block Diagram Notation 39
Obtaining Transfer Functions From Block Diagrams 41
Propeller Engine Control Loops 43
Transfer Function Derivatives 49

PROPELLER CONTROL SYSTEM CHARACTERISTICS 60

Engine and Propeller Response 61
Propeller Control System - Block Diagram 63
Control System Elements 63
Proportional Control Function 64
Integral Control Function 68
Proportional-Plus-Integral Control Function 73

CONTROL FUNCTIONS FOR SPECIAL CONDITIONS 80

Fuel and Propeller Coordination 80
Speed Synchronizing 83
Phase Synchronizing 83

ADAPTIVE PROPELLER CONTROLS 90

Compensation for Varying Flight Conditions 90
Correlation of Gain and Time Constants 90

TABLE OF CONTENTS (Continued)

Page

Control Gain Compensation 95

TURBOPROP CONTROL DESIGN 99

Design Philosophy 99
Speed Governor 100
Actuator Relations 102
Synchronized Constant Speed 103
Limit Switches and Stops 103
Ground Operation 103
Feathering Manual 104
Negative Torque Controlled Feathering 106

PROPELLER APPLICATION 109

REVIEW OF PAST APPLICATIONS AND TESTS 109

Republic P-47 109
The Boeing B-29, B-50 Airplanes 111
The Consolidated B-36 112
Boeing B-47D 113
Douglas DC-6 113
Convair CV-240 114
Lockheed L-749, L-1049, L-1649 114
Boeing Model 377, C-97 115
Douglas C-124A and C-124C 115
Lockheed C-130 116
Douglas C-133 117
V/STOL Propeller Installations 118

FUTURE PROPELLER APPLICATIONS 119

Development Testing 122

FUTURE PROPELLER DESIGNS 123

Present Technology 123
Future Propellers 123

RECOMMENDATIONS FOR PROPELLER FUTURE DEVELOPMENTS .. 126

GENERAL 126

Optimum Propeller - Hover 126
Reduced Weight Propellers 127
High-Speed Performance 128

TABLE OF CONTENTS (Continued)

Page

Propeller Design Specification 129

PROPELLERS FOR STOL AIRCRAFT 129

Propeller Cyclic Pitch 130
Propeller Performance 131
Variable Geometry Propellers 131

PROPELLER NOISE 132

CONCLUSIONS 133

LITERATURE CITED 134

APPENDIXES

I. Propeller Design Specification and Criteria 136

II. Two-Dimensional Airfoil Data 159

III. Computer Program Procedure for Propeller Forward Flight Strip Analysis 292

DISTRIBUTION 306

LIST OF ILLUSTRATIONS

Figure		Page
1	Electric Motor/Speed Reducer Blade Actuator System Schematic	6
2	Electromechanical Clutch Type Blade Actuation System	10
3	Schematic - Hydromechanical Blade Actuation System	13
4	Section of Typical Blade Retention	19
5	Integral Race Retention	24
6	Vibrating Spring-Mass System	33
7	Effect of Damping on Rotational Spring-Mass System	37
8	Summation of Forces on a Spring-Mass System	40
9	Block Diagram of Spring-Mass System	41
10	Typical Negative Feedback Loop	42
11	Propeller Engine Response Characteristics	44
12	Typical Turbine Engine Characteristics	49
13	Typical Propeller Torque Relations	51
14	Propeller Efficiency and Blade Angle Map ..	52
15	Generalized Propeller Torque-Speed Derivatives	55
16	Generalized Propeller Torque-Angle Derivatives	56
17	Propeller Proportional Control Schematic	65
18	Control Response to Load Disturbance	69

LIST OF ILLUSTRATIONS (Continued)

Figure		Page
19	Propeller Integral Control Schematic	70
20	Propeller Proportional Plus Integral Control Schematic	74
21	Effect of Servo Lag on Speed Response	79
22	Propeller Control With Speed Set Applied to Integral Term	82
23	Speed Synchronizing Control Relations	84
24	Phase Synchronizing Propeller Control Approaches	86
25	Variation of Engine and Propeller Time Constant With Airspeed, Power and Altitude	92
26	Variation of Engine and Propeller Time Constant With Blade Angle, Power and Altitude	93
27	Variation of Engine and Propeller Gain With Propeller Speed, Power, Altitude and Airspeed	94
28	Variation of Engine and Propeller Time Constant Related to Gain Ratio Compensation	97
29	Propeller Control Gain Compensation Relations	98
30	Mechanical Governor Schematic Diagram	101
31	Speed Response During Blade Angle Reversal	105
32	Windmilling Propeller Drag	107
33	Controlled Feathering	108

LIST OF ILLUSTRATIONS (Continued)

Figure Page

34 Two-Dimensional Lift Data, NACA 16-004 Airfoil 162

35 Two-Dimensional Lift Data, NACA 16-104 Airfoil 163

36 Two-Dimensional Lift Data, NACA 16-204 Airfoil 164

37 Two-Dimensional Lift Data, NACA 16-304 Airfoil 165

38 Two-Dimensional Lift Data, NACA 16-404 Airfoil 166

39 Two-Dimensional Lift Data, NACA 16-504 Airfoil 167

40 Two-Dimensional Lift Data, NACA 16-604 Airfoil 168

41 Two-Dimensional Lift Data, NACA 16-006 Airfoil 169

42 Two-Dimensional Lift Data, NACA 16-106 Airfoil 170

43 Two-Dimensional Lift Data, NACA 16-206 Airfoil 171

44 Two-Dimensional Lift Data, NACA 16-306 Airfoil 172

45 Two-Dimensional Lift Data, NACA 16-406 Airfoil 173

LIST OF ILLUSTRATIONS (Continued)

Figure Page

46 Two-Dimensional Lift Data, NACA 16-506 Airfoil 174

47 Two-Dimensional Lift Data, NACA 16-606 Airfoil 175

48 Two-Dimensional Lift Data, NACA 16-706 Airfoil 176

49 Two-Dimensional Lift Data, NACA 16-009 Airfoil 177

50 Two-Dimensional Lift Data, NACA 16-109 Airfoil 178

51 Two-Dimensional Lift Data, NACA 16-209 Airfoil 179

52 Two-Dimensional Lift Data, NACA 16-309 Airfoil 180

53 Two-Dimensional Lift Data, NACA 16-409 Airfoil 181

54 Two-Dimensional Lift Data, NACA 16-509 Airfoil 182

55 Two-Dimensional Lift Data, NACA 16-609 Airfoil 183

56 Two-Dimensional Lift Data, NACA 16-709 Airfoil 184

57 Two-Dimensional Lift Data, NACA 16-012 Airfoil 185

58 Two-Dimensional Lift Data, NACA 16-112 Airfoil 186

59 Two-Dimensional Lift Data, NACA 16-212 Airfoil 187

60 Two-Dimensional Lift Data, NACA 16-312 Airfoil 188

LIST OF ILLUSTRATIONS (Continued)

Figure		Page
61	Two-Dimensional Lift Data, NACA 16-412 Airfoil	189
62	Two-Dimensional Lift Data, NACA 16-512 Airfoil	190
63	Two-Dimensional Lift Data, NACA 16-612 Airfoil	191
64	Two-Dimensional Lift Data, NACA 16-712 Airfoil	192
65	Two-Dimensional Lift Data, NACA 16-015 Airfoil	193
66	Two-Dimensional Lift Data, NACA 16-115 Airfoil	194
67	Two-Dimensional Lift Data, NACA 16-215 Airfoil	195
68	Two-Dimensional Lift Data, NACA 16-315 Airfoil	196
69	Two-Dimensional Lift Data, NACA 16-415 Airfoil	197
70	Two-Dimensional Lift Data, NACA 16-515 Airfoil	198
71	Two-Dimensional Lift Data, NACA 16-615 Airfoil	199
72	Two-Dimensional Lift Data, NACA 16-018 Airfoil	200
73	Two-Dimensional Lift Data, NACA 16-118 Airfoil	201
74	Two-Dimensional Lift Data, NACA 16-218 Airfoil	202
75	Two-Dimensional Lift Data, NACA 16-318 Airfoil	203

LIST OF ILLUSTRATIONS (Continued)

Figure		Page
76	Two-Dimensional Lift Data, NACA 16-418 Airfoil	204
77	Two-Dimensional Lift Data, NACA 16-518 Airfoil	205
78	Two-Dimensional Lift Data, NACA 16-021 Airfoil	206
79	Two-Dimensional Lift Data, NACA 16-121 Airfoil	207
80	Two-Dimensional Lift Data, NACA 16-221 Airfoil	208
81	Two-Dimensional Lift Data, NACA 16-321 Airfoil	209
82	Two-Dimensional Lift Data, NACA 16-421 Airfoil	210
83	Two-Dimensional Lift Data, NACA 16-521 Airfoil	211
84	Two-Dimensional Drag Data, NACA 16-004 Airfoil	212
85	Two-Dimensional Drag Data, NACA 16-104 Airfoil	213
86	Two-Dimensional Drag Data, NACA 16-204 Airfoil	214
87	Two-Dimensional Drag Data, NACA 16-304 Airfoil	215
88	Two-Dimensional Drag Data, NACA 16-404 Airfoil	216
89	Two-Dimensional Drag Data, NACA 16-504 Airfoil	217
90	Two-Dimensional Drag Data, NACA 16-604 Airfoil	218

LIST OF ILLUSTRATIONS (Continued)

Figure		Page
91	Two-Dimensional Drag Data, NACA 16-006 Airfoil	219
92	Two-Dimensional Drag Data, NACA 16-106 Airfoil	220
93	Two-Dimensional Drag Data, NACA 16-206 Airfoil	221
94	Two-Dimensional Drag Data, NACA 16-306 Airfoil	222
95	Two-Dimensional Drag Data, NACA 16-406 Airfoil	223
96	Two-Dimensional Drag Data, NACA 16-506 Airfoil	224
97	Two-Dimensional Drag Data, NACA 16-606 Airfoil	225
98	Two-Dimensional Drag Data, NACA 16-706 Airfoil	226
99	Two-Dimensional Drag Data, NACA 16-009 Airfoil	227
100	Two-Dimensional Drag Data, NACA 16-109 Airfoil	228
101	Two-Dimensional Drag Data, NACA 16-209 Airfoil	229
102	Two-Dimensional Drag Data, NACA 16-309 Airfoil	230
103	Two-Dimensional Drag Data, NACA 16-409 Airfoil	231
104	Two-Dimensional Drag Data, NACA 16-509 Airfoil	232
105	Two-Dimensional Drag Data, NACA 16-609 Airfoil	233

LIST OF ILLUSTRATIONS (Continued)

Figure Page

106 Two-Dimensional Drag Data, NACA 16-709 Airfoil 234

107 Two-Dimensional Drag Data, NACA 16-012 Airfoil 235

108 Two-Dimensional Drag Data, NACA 16-112 Airfoil 236

109 Two-Dimensional Drag Data, NACA 16-212 Airfoil 237

110 Two-Dimensional Drag Data, NACA 16-312 Airfoil 238

111 Two-Dimensional Drag Data, NACA 16-412 Airfoil 239

112 Two-Dimensional Drag Data, NACA 16-512 Airfoil 240

113 Two-Dimensional Drag Data, NACA 16-612 Airfoil 241

114 Two-Dimensional Drag Data, NACA 16-712 Airfoil 242

115 Two-Dimensional Drag Data, NACA 16-015 Airfoil 243

116 Two-Dimensional Drag Data, NACA 16-115 Airfoil 244

117 Two-Dimensional Drag Data, NACA 16-215 Airfoil 245

118 Two-Dimensional Drag Data, NACA 16-315 Airfoil 246

119 Two-Dimensional Drag Data, NACA 16-415 Airfoil 247

120 Two-Dimensional Drag Data, NACA 16-515 Airfoil 248

121 Two-Dimensional Drag Data, NACA 16-615 Airfoil 249

LIST OF ILLUSTRATIONS (Continued)

Figure		Page
122	Two-Dimensional Drag Data, NACA 16-018 Airfoil	250
123	Two-Dimensional Drag Data, NACA 16-118 Airfoil	251
124	Two-Dimensional Drag Data, NACA 16-218 Airfoil	252
125	Two-Dimensional Drag Data, NACA 16-318 Airfoil	253
126	Two-Dimensional Drag Data, NACA 16-418 Airfoil	254
127	Two-Dimensional Drag Data, NACA 16-518 Airfoil	255
128	Two-Dimensional Drag Data, NACA 16-021 Airfoil	256
129	Two-Dimensional Drag Data, NACA 16-121 Airfoil	257
130	Two-Dimensional Drag Data, NACA 16-221 Airfoil	258
131	Two-Dimensional Drag Data, NACA 16-321 Airfoil	259
132	Two-Dimensional Drag Data, NACA 16-421 Airfoil	260
133	Two-Dimensional Drag Data, NACA 16-521 Airfoil	261
134	Basic Low-Speed Lift Coefficient - C_{LB} Symmetrical Sections - 25% to 90%	263
135	Correction to Basic Lift Coefficient for Camber C_L^C	264
136	Shape Correction to Basic Lift Coefficient C_{LC}/C_{LP}	264

LIST OF ILLUSTRATIONS (Continued)

Figure		Page
137	Correction to Lift Increment for Camber - fc	265
138	Critical Mach Number, Thick Airfoils, $C_L = 0$	266
139	Critical Mach Number Correction for Lift $-\Delta M_{CRL}$	266
140	Lift Coefficient Increment at Mach Numbers Above the Critical	267
141	Minimum Profile Drag for Thick Airfoil Sections	269
142	Drag Coefficient Increment for Angle of Attack $-\Delta C_{D_\alpha}$	270
143	Drag Correction for Elliptic Airfoil Sections	271
144	Drag Correction for Camber Sections	272
145	Drag Coefficient Increment at Mach Numbers Above the Critical	273
146	Incremental Lift Coefficient for 65 Airfoil Sections	274
147	Lift Increment Correction to NACA-16 Sections	275
148	Maximum Lift Coefficient NACA-66 Sections	276
149	Maximum Lift Coefficient NACA-65 Sections	277
150	Change in Maximum Lift Coefficient Due to Mach Number	278
151	Angle of Attack at Stall	279
152	Angle of Attack at Stall	280

LIST OF ILLUSTRATIONS (Continued)

Figure		Page
153	Stall Angle Increment Due to Reynolds Number NACA-16 and NACA-65 Sections	281
154	Variation of Lift Beyond the Stall	282
155	Drag Coefficient at 8° Angle of Attack Thickness Ratio = 4%	283
156	Drag Coefficient at 8° Angle of Attack Thickness Ratio = 6%	284
157	Drag Coefficient at 8° Angle of Attack Thickness Ratio = 9%	285
158	Drag Coefficient at 8° Angle of Attack Thickness Ratio = 12%	286
159	Drag Coefficient at 8° Angle of Attack Thickness Ratio = 15%	287
160	Drag Coefficient at 8° Angle of Attack Thickness Ratio = 18%	288
161	Change in Drag Coefficient at $\alpha = 8^\circ$ With Reynolds Number	289
162	Design C_L Drag Factor	290
163	Increment in Drag Coefficient Beyond $\alpha = 8^\circ$	291

LIST OF TABLES

Table Page

I Summary of Typical Propeller Installations 110

II Calculation Procedure for Operating Lift Coefficient of Thick Airfoils - 25% to 100% 262

III Calculating Procedure for Operating Drag Coefficient of Thick Airfoils - 25% to 100% 268

LIST OF SYMBOLS

AF	activity factor
a	acceleration - ft/sec^2
a	proportional gain
B	number of blades
b	integral gain
CF	centrifugal force
C_P	power coefficient
C_T	diameter thrust coefficient
c	synchronizing control gain
D	damping coefficient
D	disc diameter - ft
e	natural log base
F	force - lb
g	any function of s in forward path
h	any function of s in feedback path
I	moment of inertia
J	advance ratio
K	spring constant, lb/ft
K_T	bearing design factor
M_B	static bending moment
M_V	vibratory bending moment
M	total steady and vibratory moment
m	mass
n	diameter

LIST OF SYMBOLS (Continued)

Q	torque
Q_{BF}	blade twisting moment due to friction, in.-lb
ΔQ	external torque variation
R	bearing radius
s	differential operator, d/dt
t	time
V	velocity
v	linear velocity
w_f	fuel flow
x	displacement
α	angular acceleration
β	blade angle
ζ	damping ratio
η	efficiency
θ	displacement - radius
μ	coefficient of friction
ρ	air density
σ	propeller solidity
τ	disc thickness
τ	characteristic time
ϕ	angular position
ω	natural frequency
ω	angular velocity
ω_n	undamped natural frequency

LIST OF SYMBOLS (Continued)

SUBSCRIPTS

acc	acceleration
e	engine
f	fuel
p	propeller
ref	reference

HUB AND BLADE ACTUATOR DESIGN

INTRODUCTION

The propeller hub with the actuator for changing the blade angle generally comprises approximately 50 percent of the weight of the system. The hub must retain the blade and react the forces to the airplane structure. The blades must be retained in the hub so that the blade actuation system can rotate then about their centerline to obtain the desired blade angle. Generally the blade angle travel must cover the range from reverse to feather, which is approximately 115 degrees. The blade actuator must have the capability to provide the rate of pitch change necessary to satisfy the control system requirements of the propeller.

Since the hub and blade actuator are important elements of the propeller and make up a large portion of the weight, the various types will be discussed. Included in this section will be the design consideration and detailed descriptions, including the advantages and disadvantages of each system.

BLADE ACTUATOR TYPES

The blade actuation system is considered to be synonymous with the pitch changing mechanism, which is defined by MIL-P-5447, Reference 1, as follows: "The pitch-changing mechanism is defined as compromising all the components needed to translate the pitch-changing power into angular blade movement."

There are many types of blade actuation systems possible; however, only the following are discussed in detail.

Electric Motor/Speed Reducer Type - This type of system was used, and is still in use, on aircraft powered by reciprocating engines. Typical aircraft employing this system include the C-54, DC-6, DC-7, CV-240, 1049, P-47, B-29.

Electromechanical Clutch Type - This is the type of system used on aircraft powered by turboprop engines. Typical aircraft employing this system include the C-130 and C-133. The forerunner of this type was the hyromechanical clutch used on the B-36 reciprocating engine installation.

Hydromechanical Type - This is the type of system designed specifically for VTOL type aircraft and was used on the X-19 aircraft.

RELATIVE ADVANTAGES OF BLADE ACTUATION SYSTEMS

Each of the blade actuation systems above was developed to satisfy the requirements imposed by the advances in engine technology/aircraft performance of that particular era:

Blade Actuation System	Engine Technology
Electric motor/speed reducer	Reciprocating
Electromechanical	Turboprop
Hydromechanical	Turboprop/V/STOL A/C

Therefore, any comparison of these systems (in terms of advantages/disadvantages) must consider the demands of advancing engine technology/aircraft performance on the design of blade actuation systems.

The electric motor/speed reducer blade actuation system was developed for propellers on reciprocating engines where the need for high rates of pitch change were relatively low, approximately 1 to 3 degrees per second.

A competitive hydraulic actuating system was also used on propellers for reciprocating type engines. Blade angle change was accomplished by an increase or decrease pressure in the governor oil. The high pressure engine oil from the governor was balanced by oil pressure from the engine and the centrifugal blade twisting moment when holding a constant blade angle, Reference 2 . Although this system was relatively simple in operation, difficulty was experienced at high altitude, as the oil tended to freeze causing poor operation. The design of the hydraulic propeller was also poor from maintenance considerations, as complete dissassembly was required for the removal of a blade.

The advantage of the electric propeller blade actuator system was its high altitude operating characteristics. Further, this system made possible designs where the component parts such as the blades could be easily changed thus leading to good maintenance characteristics. This type of actuator also made it possible to easily develop the blade angle reversing feature to provide negative thrust to reduce the landing distance; earlier, this feature was considered to be an important advantage.

One of the main difficulties with the electric motor actuating system was its limitation in terms of pitch change rate and torque output. This limitation led to the clutch type propeller actuating system for use on the larger propellers and turboprop installations. The other disadvantages were due to brush wear at high altitudes and the usual problems with reliability of a system with a large number of mechanical pieces.

The development of high power turbo-propeller engines led to the requirement for larger propellers with a corresponding increase in power required for pitch change. The rate of pitch change was also higher than with reciprocating engines due to their tighter overspeed and over-temperature limits, especially with the coupled engine. In addition, the throttle and power transients were especially critical during a rejected landing maneuver. These requirements for the coupled turboprop engine led to pitch change rates of 15 to 25 degrees per second.

To meet the pitch change requirements of the turboprop engine, propellers were designed with either all mechanical or hydraulic pitch change actuators. The propeller using the mechanical actuator obtained the power directly from the rotation shaft through the use of clutches. As a result sufficient power for pitch change could easily be obtained, the limit being only a function of the size of the clutches.

Although very high rates of pitch change and torque can be developed with the clutch type of propeller the complication and large number of parts required lead to high costs and poor reliability. The system is also poor from the maintenance standpoint as the clutches and the large number of gears and bearings need frequent attention. From a failure standpoint the clutch propeller was somewhat better than the hydraulic type as the blade remained in fixed pitch. However, because of the many problems in development the clutch type blade actuator was used for only a few installations such as the B-36 and C-133 airplanes.

Generally the hydraulic propellers designed for turboprop engines had a lower pitch change rate than the clutch type. This was considered a major disadvantage, especially for the coupled turboprop engine. However, in spite of the lower pitch change rate and the usual problems with a hydraulic system, this system proved to be superior to all mechanical propellers.

With the development of the integral hydraulic type of blade actuator, the problems of some of the earlier hydraulic types were eliminated. The full range of pitch change from reverse to feather is obtained with the later design, with satisfactory rates of pitch change. The use of various types of mechanical stops has also been developed so that the system is protected in the case of a complete hydraulic system failure.

The propeller blade angle control requirements for V/STOL aircraft lead to actuation systems with a much greater degree of safety and reliability than was needed with previous designs. In the case of V/STOL aircraft the propeller is used for hover height and roll control and thus the blade actuation system becomes a primary flight control. This control function leads to a requirement for a highly reliable system. Also, the height and roll control function must be phased out during the conversion maneuver as the control characteristic at cruise is different than at hover. For this reason additional complication in the control system is encountered compared with conventional propellers.

At the cruise condition the propeller control of V/STOL aircraft is like that of conventional airplanes except the system must be much more sensitive. This is due to the use of oversized propellers to satisfy the hover requirement. A blade angle range of one degree between zero and full power at cruise is not unusual for V/STOL propellers.

Because of the difference in control requirements between conventional and V/STOL airplanes the improved actuator systems were required. At the hover condition the use of a follow-up stop that allowed less than a degree change of blade angle was found to be unsafe, therefore, it became necessary to design propellers with dual actuator systems. The dual actuators were designed to be as completely separate as possible so that a failure of one would not induce a failure of the other. Only hydraulic systems were considered for the dual actuator V/STOL propellers as these appeared to be the simplest.

Since the propeller is used as a primary flight control, the question of the use of the aircraft hydraulic system or a separate integral propeller system must be answered. If aircraft hydraulics are used the system already has the degree of redundancy needed. However, problems are encountered with the aircraft system due to contamination and the transfer of the fluids to the rotating propeller. With the use of a separate propeller hydraulic system, the propeller becomes self contained with its own pumps, etc., and this is considered to be a definite advantage.

ELECTRIC MOTOR/SPEED REDUCER BLADE ACTUATION SYSTEM

General Description

The electric motor/speed reducer blade actuation system (see Figure 1) consists of the following major elements: a power unit, including a reversible electric motor (1), a brake (2), and a speed reducer (3), containing two stages of double planetary reduction gearing; and the power gear assembly (4), which includes the master bevel gear that meshes with the blade gear (5) attached to the shank of each blade.

The electrical energy for operating the blade-angle-change motor comes from the electrical power supply of the airplane to the control system of the propeller through switches located in the cockpit. From this point, the current passes through brushes mounted in a housing fixed to the engine nose to the slip rings attached to the rear of the propeller hub and from there through connector rods to cam-operated cut-out switches located in the power unit, then to the blade-angle-change motor. A speed reducer is used to convert the high rotational speed of the electric motor into a slower but more powerful turning force which is transmitted to the blades through the power gear. The angle of the blades is increased or decreased, as required, depending upon the direction of rotation of the electric motor. The brake attached to the front end of the electric motor stops the rotation of the motor when the blade-angle-changing current is cut off, and locks the propeller blades in a fixed position when no blade angle change is in progress.

Motor Assembly

As compared to conventional motors, the design of the pitch change motor is extremely specialized due to the following contributing factors:

a. Propeller rotation - The centrifugal effects of rotation of the entire motor requires careful design of the motor commutator and brush mechanism to insure proper commutation.

b. Vibration - 125 G's at 240 cps is used as a design specification. This requires extreme care and special design of structure, winding retention, coil connection, bearing, etc.

c. Operating requirements - Idealized operation should be as follows:

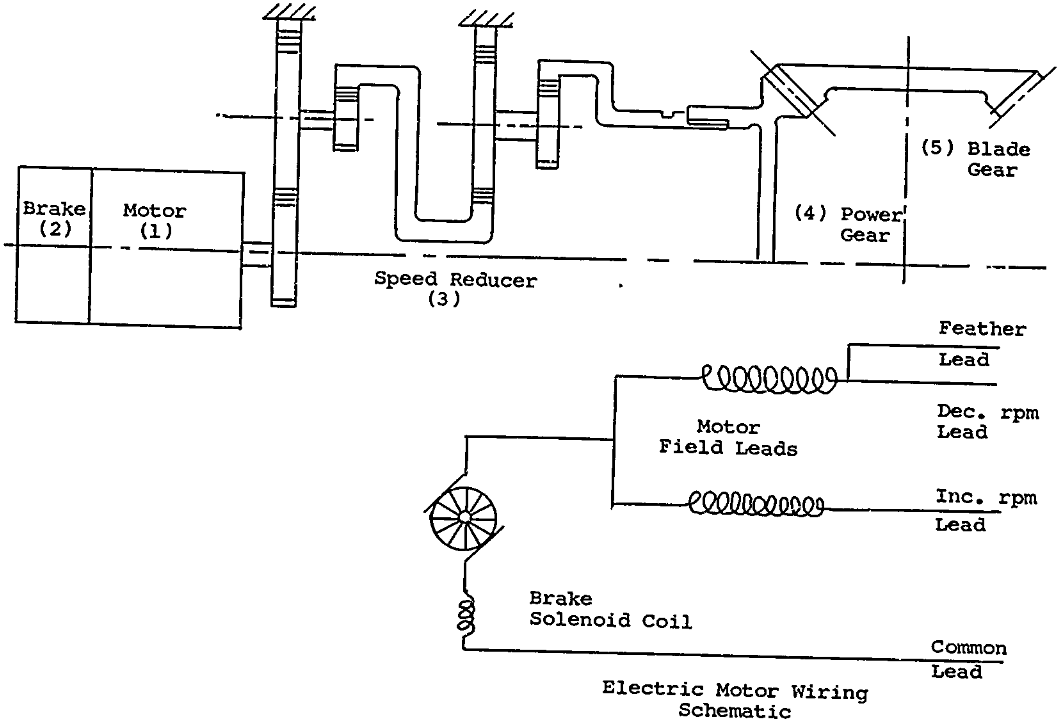
Brake (2)
Motor (1)
Speed Reducer (3)
(4) Power Gear
(5) Blade Gear
Feather Lead
Dec. rpm Lead
Motor Field Leads
Inc. rpm Lead
Brake Solenoid Coil
Common Lead
Electric Motor Wiring Schematic

Figure 1. Electric Motor/Speed Reducer Blade Actuator System Schematic.

1. Increase pitch - constant speed over a wide load range.
2. Decrease pitch - constant speed over a wide range of overhauling load.
3. Feather - 4 to 5 times the speed of increase pitch under the same load conditions.
4. Reverse - rapid acceleration to as high a speed as possible under loads changing from moderate overhauling to opposing.

A reversible series motor has been determined which best meets pitch change requirements.

Brake Assembly

The pitch change motor brake assembly must accomplish two functions. First, it must be capable of holding the blade angle at any position when the pitch change motor is not energized, and second, it must be capable of stopping pitch change upon de-energization of the pitch change motor with a minimum of overrun. The brake is energized (released) by the energization of a flat-faced type lifting magnet which moves the armature away from the brake disc. The disc, which is splined to the pitch change motor shaft, is thus released and pitch change is permitted. Upon de-energization of the motor the magnet armature is released, thus clamping the brake disc between opposing plates and providing braking action. In the design of the brake, the coil and magnetic circuit must be chosen such that the voltage drop across the coil is held to a minimum and such that the brake will operate and release at proper current values in relation to motor operating currents.

Speed Reducer

The speed reducer consists of two stages of double planetary reduction gearing. It is designed for an output torque capacity that will equal or exceed the total twisting moment generated by the propeller blades for the takeoff rpm condition, and with the blades at the blade angle for maximum twisting moment. Speed reducer designs have covered output torque capacities ranging from 65,000 in.lb and reduction ratios varying from approximately 5000:1 to 7500:1. Speed reducer efficiency is in the order of 60 to 70%.

Blade Angle Limit Switches

The pitch change range of the electric type propeller is controlled by cam-operated limit switches. Generally, four such switches are used and are set so that the operation would be within the proper blade angle range. The normal operating range was controlled electrically between the high and low blade angle stops or switches. The low pitch stop was set at the blade angle required for full takeoff power and the high speed stop was set to correspond to the highest blade angle needed at the high speed flight condition.

The low pitch switch was by-passed when it was desired to go to a reverse pitch blade angle required for negative thrust. The reverse pitch limit switch controlled the magnitude of the maximum negative blade angle. Likewise the high pitch stop was overridden when it was necessary to feather the propeller. The feather limit switch controlled the feather angle.

The propeller system was therefore protected from electrical type failures in the governor and airframe since any hard over signal would be overridden by the high and low pitch limit switches. The system, however, was not protected by mechanical failures such as those in the brake. Since the blade will go toward the negative angle due to the high centrifugal twisting moment if the brake fails, a dangerous condition existed with the electrical type propeller. This condition could be eliminated with positive mechanical stops or with counterweights which would prevent the blade angle from going toward low pitch by balancing the centrifugal twisting moment.

ELECTROMECHANICAL CLUTCH TYPE BLADE ACTUATION SYSTEM

General

The electrically actuated mechanical clutch type blade actuation system obtains power to change pitch from the rotation of the propeller shaft, and this power is transmitted through these clutches and suitable gearing to the primary blade angle turning system. This primary system consists of worms mounted in the hub and driving matching worm gears splined to the blade shanks. The pitch change mechanism is contained in a stationary housing between the rotating hub and the engine nose section.

During normal operation, in response to a control signal for a pitch change, electric power simultaneously disengages a multiple disc brake and energizes one or the other of two mechanical clutches to raise or lower blade angle as required. The clutch, through a system of gears, enables power from the propeller shaft to be delivered to the worm and blade gearing in the rotating hub. When the control cycle is terminated, electric power is no longer supplied to the clutches and brake, causing the clutches to disengage and the brake to engage and lock the blades in fixed pitch.

Limit switches are also provided as in the electric motor actuator propeller to limit blade angle travel to the required operating ranges. Such limits are provided at feather, flight idle, flight low pitch, air start, normalizing and reverse. Additional stops can be designed into the system if required.

An electric motor is provided for completion of the feathering cycle, initiation of unfeathering and operation under static conditions.

All blade angle changes above approximately 25% rated propeller rpm are obtained through the action of the clutches, while changes below this speed are accomplished by the electric motor. Shifting between electric motor and clutch operation is accomplished automatically through the use of a centrifugal switch in the propeller.

Self-contained, low-pressure oil lubrication for the gearing, clutches, and for the governor is provided by a small centrifugal pump which is submerged in the oil sump formed by the lower portion of the nonrotating housing.

The operation of the entire system is free of fluid pressure devices and is thus unaffected by ambient temperature or pressure extremes.

Details of Operation

Referring to Figure 2 , two electrically energized clutches are used during normal flight operation, one for increase (1) and one for decrease (2) pitch actuation. When a control signal actuates one of these clutches, it also disengages the fixed pitch brake (3). The gearing from the propeller shaft (4) is then coupled through the actuated clutch and the intergearing movable ring gear (5) to the inter-gearing spider/planetary gearing assembly (8). The inter-gearing assembly enables energy to be transmitted from the stationary pitch changing mechanism to the rotating hub. During fixed pitch, the brake (3) is engaged and the fixed sun gear (6) rotates with the propeller shaft and hub, while the fixed ring gear (9) and movable ring gear (5) remain stationary. The planet gears (8) which are meshed with the fixed ring gear (9) and the movable sun gear (7), rotate with the hub. When power is transmitted by clutch actuation to the movable ring gear (5), it rotates in relation to the fixed ring gear (9). This change of relationship, acting through planet gears (8), causes the movable sun gear (7) to rotate in relation to

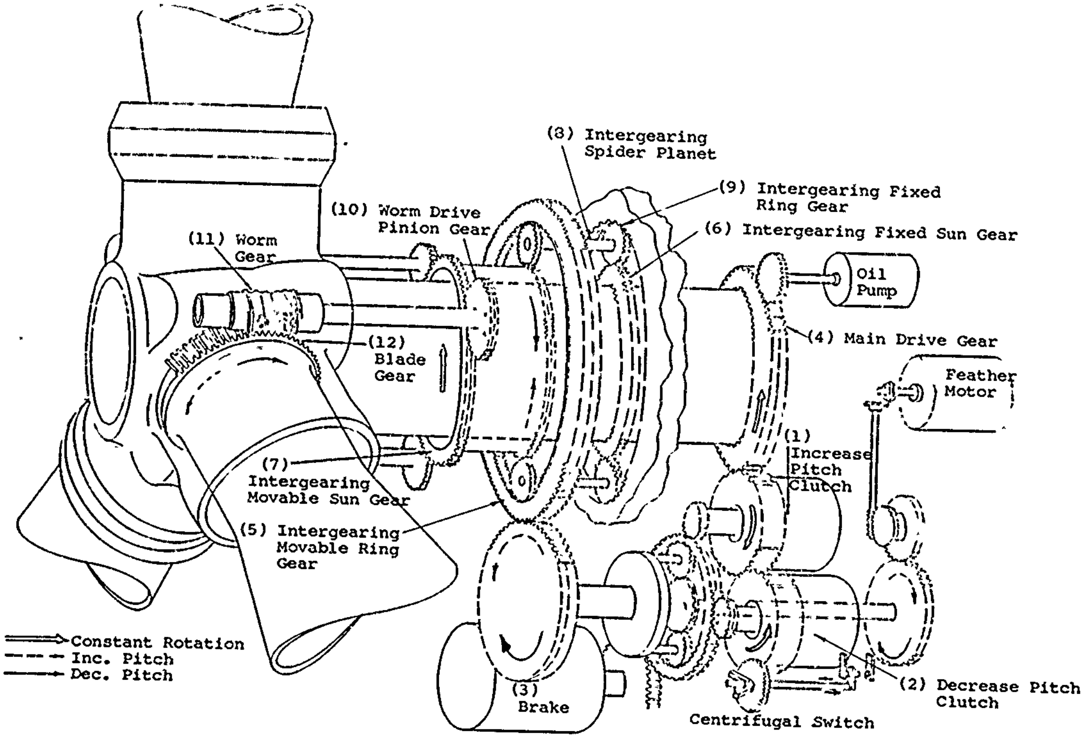
(3) Intergearing Spider Planet
(9) Intergearing Fixed Ring Gear
(10) Worm Drive Pinion Gear
(6) Intergearing Fixed Sun Gear
(11) Worm Gear
Oil Pump
(4) Main Drive Gear
(12) Blade Gear
Feather Motor
(1) Increase Pitch Clutch
(7) Intergearing Movable Sun Gear
(5) Intergearing Movable Ring Gear
Constant Rotation
Inc. Pitch
Dec. Pitch
(3) Brake
(2) Decrease Pitch Clutch
Centrifugal Switch

Figure 2. Electromechanical Clutch Type Blade Actuator System.

to the hub. The movable sun gear (7) is coupled to the blade gear (12) through the worm drive pinion gear (10) and worm gear (11). The blade gear is splined to the blade. Upon completion of the control signal, the clutch disengages and the brake (3) engages to maintain the adjusted blade angle.

When the propeller is stopped or turning slowly, an electric feather motor (13) completes pitch change. When power is supplied to the feather motor, which is normally disengaged from the gearing by the feather motor clutch (14), this clutch couples the motor to the movable ring gear (5). The electric brake (3) is released when power is supplied to either pitch-change clutch (1) or (2) or the electric feather motor (13).

Clutch Design

The heart of the electromechanical clutch type propeller is, of course, the clutches. The design shafting and gearing necessary to transmit the power from the clutches is straightforward, and standard aircraft/engine procedures are used. The clutches, however, must be designed to work over thousands of cycles without problems during the lift cycle of the propeller, and therefore require special attention.

Two types of clutch systems were used on the electrical-mechanical propeller: (1) a high-speed low-torque type, and (2) a low-speed high-torque type. The low-speed type was the more successful of the two and was used on the C-133 airplane.

The main clutches used in the system are of the disc type with the number of plates based on the output torque required. A drag type disc clutch is used to engage the main clutch through a force multiplier which applies the necessary axial pressure for engagement. This drag clutch is energized by a small fixed 24-volt DC electric-magnet.

The design torque requirements of the clutches depend on the blade design as discussed in previous sections and the rate of pitch change required. Pitch change rates in excess of 20 degrees have been used with this system at rated propeller rpm which corresponds to over 30 horsepower.

For the desired action of the clutches the proper friction materials must be selected. The action of the material surfaces used will depend on speed, unit pressure, temperature, lubrication, wear, material heat transfer and the surface finish. A sintered metal surface operating against steel and oil lubricated has been found to be suitable for use in the disc clutches. This combination of materials gives the desired type of engagement as a function of speed and pressure along with the wear characteristics needed for long life.

HYDROMECHANICAL BLADE ACTUATION SYSTEM

The hydromechanical pitch change mechanism considered here is contained within a nacelle gearbox. A simple schematic is shown in Figure 3 . The nacelle gearbox also provides for mounting of the propeller and connection to the engine driven transmission.

The propeller pitch-change system is comprised of an integral hydraulic power unit which contains two independent nacelle-oil pressure systems. No connections to the aircraft hydraulic system are required. The power unit assembly includes two tandem pistons (1 and 2), two hydraulic pump assemblies (3 and 4), two oil reservoirs (5 and 6), a control rod and valve assembly (7), and suitable links (8) for attachment of the blade levers (9) to the front piston (1).

Propeller pitch-change is accomplished by two mechanically-coupled single-acting pistons having independent hydraulic systems. The pistons are single acting in that high pressure oil provides the force to drive the blade angle in the increase pitch direction. Blade centrifugal twisting moment provides the force to drive the blade angle in the decrease pitch direction. Blade angle change results from a transfer of the piston assembly motion, through a link assembly, to a lever which is splined to the blade shank. The pitch-change hydraulic system is basically a position follow-up mechanism in which the pistons follow valve displacement at approximately the same rate while delivering the force required for pitch-change. Valve displacement corresponds to desired blade angle, and piston displacement corresponds to actual blade angle. The pistons move to balance themselves across the valve ports for any given blade angle until both blade loading and piston pressure are in equilibrium.

Both hydraulic systems operate in the same manner, i.e., at a given control signal, oil flows into each piston from independent high-pressure pump assemblies, at a constant rate until the desired blade angle is achieved. Oil is exhausted through the dual control valves to each sump. The valves monitor piston pressures by metering the orifices.

Isolation of the hydraulic systems is obtained in the following manner:

1. The front piston system functions as follows:

   Oil is placed into the hub which acts as the sump for the front piston system. This oil enters the cylinder of the forward hydraulic system through one of the two pump assemblies and is ported through one of the two control valves back into the hub. After being cooled in the hub, the oil

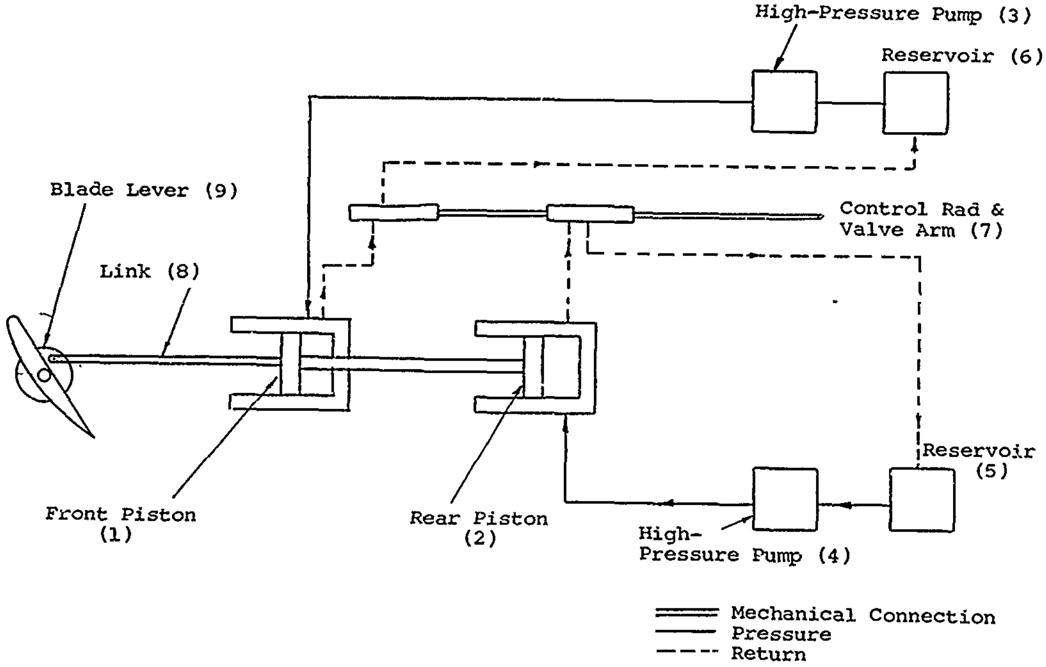
High-Pressure Pump (3)
Reservoir (6)
Blade Lever (9)
Control Rad &
Valve Arm (7)
Link (8)
Reservoir
(5)
Front Piston
(1)
Rear Piston
(2)
High-
Pressure Pump (4)
Mechanical Connection
Pressure
Return

Figure 3. Schematic - Hydromechanical Blade Actuation System.

returns to the rotating sump provided in the pump housing, which feeds the oil back into the pumps.

2. The rear piston hydraulic system functions as follows:

Oil enters this cylinder from the other pump assembly and is exhausted through its control valve into the nacelle housing where it is cooled. A scavenge and lubrication pump mounted in the nacelle housing delivers oil to the rear piston rotating sump assembly which feeds the pitch-change pumps to complete the hydraulic circuit.

Rotation of both sump assemblies acts to eliminate entrapped air in the oil while serving as a centrifugal pump to supply primed oil to the pitch-change pumps. The scavenge pump also supplies lubrication to the propeller mounting bearing, the bevel gear set, and retention bearings.

Each pitch-change pump assembly consists of three pumps of vane type which are mounted in a single housing. This housing is mounted in the hub, so it rotates at propeller speed. A pinion gear, which meshes with an internal fixed ring gear, is attached to each pump shaft. Each of the three pumps in a system is meshed to one of two fixed ring gears. Power to drive the pumps is obtained from propeller rotation since the pumps and pinion gears revolve as a unit within their respective fixed ring gears.

A pivoted torque-reaction bar, for the two fixed ring gears, is installed in the nacelle together with two microswitches. A loss of hydraulic pressure in either system results in an unbalanced reaction-torque on the ring gears, causing movement of one gear relative to the other. This gear movement actuates one of the microswitches and closes an electrical circuit to an indicator light, indicating "loss of hydraulic pressure."

Controls

Pitch-change signals to the propeller are a push/pull, blade angle desired, signal. This signal is transferred through a series of bellcrank linkages and converted into a linear fore-and-aft control rod and valve motion. Each of the two pitch-change control valves is mounted on the end of a differential beam. A mechanically operated relief valve is located aft of each control valve, in the valve assembly. Each relief valve is capable of relieving pressure from one system when actuated by the control valve of the other system. During normal propeller operations, with both pistons and valves operating, there is insufficient movement of either valve to trigger the poppet which actuates the relief valves. In the event of a "stuck" control valve in one system, the greater movement available to the other control valve, due to the differential beam arrangement, allows this valve to actuate the relief valve of the "stuck" system, thus resulting in "dumping" the pressure of the inoperative system. A snap ring type of detent spring on the relief poppet, once actuated, maintains this "dumped" condition until such time as the valve assembly is removed and the relief poppet detent spring is reset.This loss of pressure of a single system due to a "stuck" valve is indicated by a tel-light through the reaction-ring gear bar.

A ball-bearing coupling is installed between the nonrotating control rod and the rotating propeller and valve assembly. Two compression springs are installed between the piston and each control valve to eliminate signal backlash and to provide a unidirectional signal input force.

Blade Actuator Torque Design Requirements

The blade actuator must be designed so that sufficient torque is available to the blade angle under the most adverse conditions. To assure that this design condition is achieved, Reference 3 specifies that it must be possible to initiate feather from the low pitch stop (takeoff blade angle)when operating at 141 percent of the maximum design rotational speed. The feathering cycle must continue as the rpm is reduced linearly from 141 percent to 120 percent at a 45-degree blade angle. From 45 degrees to the feather angle, the propeller must be capable of pitch change at 120 percent of the maximum rpm. The propeller must demonstrate this capability 25 times during the qualification testing. Thus effectively it must be possible to initiate an increase of blade angle at a condition where the centrifugal force is twice that at the maximum design rpm condition. Since the blade centrifugal twisting moment usually is at a peak at the low pitch stop,the demonstrated ability for pitch change required for qualification will assure that feathering can be accomplished under adverse conditions.

The blade actuator must therefore be designed to have sufficient torque to rotate the blade against the maximum centrifugal twisting moment plus the bearing friction when the propeller is operating at a rotational speed corresponding to 141 percent of the maximum design value. Although the aerodynamic twisting moment is generally opposite to the centrifugal blade twisting moment, it is usually neglected in determining the actuator torque requirements.

The centrifugal twisting moment is determined knowing the blade characteristics and geometry as described in the Structural Design section, Volume II. The bearing friction torque is calculated from the equation

$$Q_B = \mu \, E \, \frac{CF}{2} \tag{1}$$

where Q_{BF} = blade twisting moment due to bearing friction

μ = the coefficient of friction $\approx$ .004

E = bearing pitch diameter

CF = blade centrifugal force

In addition to meeting the above requirements, the blade actuator must be designed to provide the rate of pitch change necessary for propeller control. The rate of pitch necessary depending on the engine type and airplane requirements is discussed in the next section on controls. The pitch change actuator torque requirements for this condition are determined knowing the blade inertia about its centerline plus bearing friction and the centrifugal twisting moment discussed above.

Hub Design Considerations

The techniques used for designing conventional aircraft propeller hubs were largely empirical and based on test data and experience. This was due to the highly redundant nature of the hub structure and the difficulty of an analytical analysis as discussed in the structures section, Volume II. With the use of high-speed computers, it is now possible to analyze the hub in greater detail (Reference 4). However, the principles discussed here still apply and would be used during the initial design.

A hub can be considered to be made up of the blade retention components, the structure that transmits torque and reacts the blade forces to the engine and airframe, and the structure for tying these components together and resisting the centrifugal forces and moments. The loadings that the hub must sustain include not only steady centrifugal force, thrust bending moment, and aerodynamically-excited vibratory moments entering from the blades, but also steady torque and vibratory engine orders entering the engine. Some of these are phased symmetrically about the shaft; others are not. Some of the aerodynamic orders are force and/or moment reactionless on the shaft, yet impose heavy duty on the hub.

Most of the older conventional propellers were shaft mounted and were driven and supported on the spline shaft that mated with internal splines. These internal splines are usually part of the tail shaft of the hub. Provision for the blade actuation system must also be considered in the hub design including the gearing or links to transmit the moments to the blade.

The size and configuration of a new hub will depend on the blade size, moment and forces, the mounting system, the actuator system, the rotational speed, and the power input. The success of the final hub configuration will depend on the ability of the designer to come up with a compact and balanced structure that will withstand the steady and vibratory loads and provide the necessary rigidity for the support of the blade. In establishing the design, the proper selection of material, the manufacturing methods used, and the heat treatment must also be considered.

For optimum design of the propeller hub, certain general principles should be borne in mind:

(1) Eliminate stress concentrations wherever possible. Sharp corners, being vulnerable in fatigue, must be avoided. External corners or edges should be broken, and fillet radii made as generous as possible.

(2) The most efficient use of metal, and hence the lightest weight, must be designed in. Removing metal from the finished product to meet predetermined weight limitations has shown that relatively little can be accomplished, percentage-wise, by this method.

(3) To obtain the most effective transfer of blade moments into the tail shaft, the variation in end restraint around the base of the barrel must be minimized. This means that as much stiffness as possible should be built into the forward side of the hub.

(4) Where the design requires any pronounced dissymmetry in the structure, the details should be analyzed carefully, as very large stress concentrations are apt to be introduced. This should start very early in the design process, as it may involve the basic configuration of the hub and compromise the location of the operating mechanism.

(5) Because of thread flexibility characteristics, the inboard hub barrel thread (for the blade nut) carries the greater portion of the total thread loading in standard non-tapered threads. The thread loading produces a thread bending stress and a thread relief stress at the base

of the inboard thread which when combined yields the thread fillet stress.

(6) There is a small relative motion between the bearing and the barrel bore of the hub and the surface of the blade shank under vibratory loads. These conditions are conducive to galling, which results in a substantial reduction of the fatigue strength of the surfaces at these points. Galling fatigue strength is greatly increased by rolling of the shank and shotpeening of the hub barrel bore.

Influence of Blade Retention on Hub Design

One of the key factors in the design of a new hub is the retention. The retention used to react the loads and allow the blade to change angle is determined from a large store of experimental data on the test of various systems. Data was obtained from tests of various shank sizes and number of bearing rows subjected to steady and vibratory loads. The blade angle was usually varied during these tests.

The blade retention system must be designed to have sufficient strength to withstand safely the steady and vibratory loads while allowing the blade to rotate about its centerline for pitch change. The steady loads include the centrifugal force and the bending moment due to thrust. The vibratory load is due to the 1xP and other associated moments.

The basic structural elements of a conventional blade retention system of a propeller that must be considered are shown in Figure 4, and consist of the hub barrel, blade shank, and multiple-row angular contact ball bearings. Bearing thrust loads are transferred from the blade shank to the hub by the integral flange at inboard shank to a blade nut that is threaded to the hub barrel.

The factors which guide the selection or design of the blade retention elements and their corresponding impact on hub design are:

selection of blade shank size

selection of retention bearing

retention nut and hub barrel interface

retention bearing friction

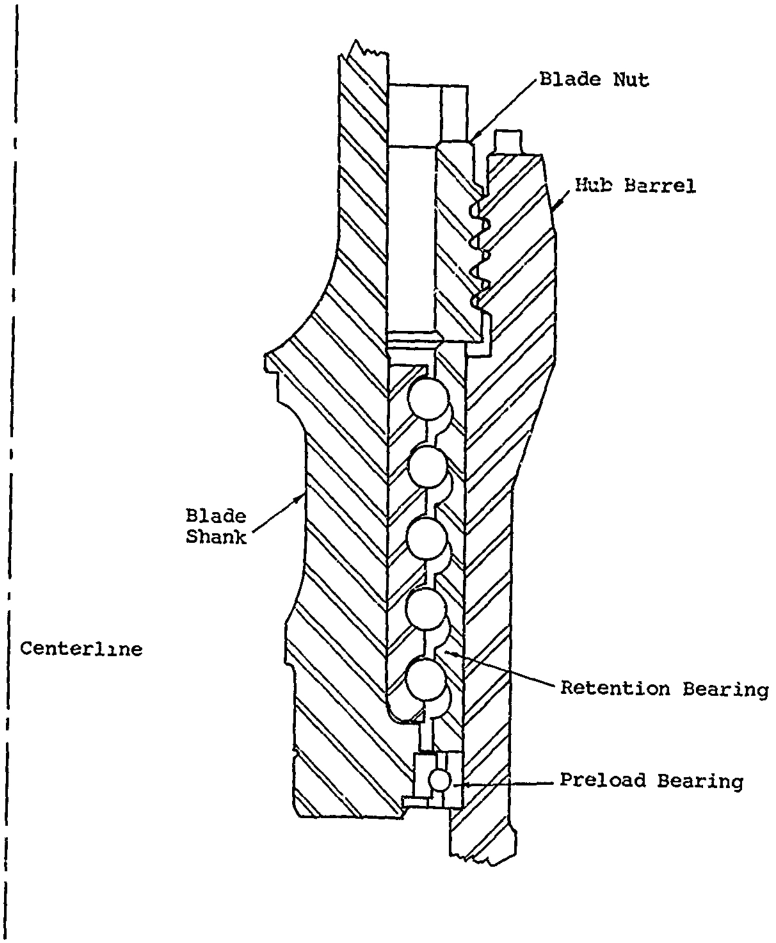
Blade Nut
Hub Barrel
Blade Shank
Centerline
Retention Bearing
Preload Bearing

Figure 4. Section of Typical Blade Retention.

Selection of Blade Shank Size

The blade structural analysis determines the shank size. The selection of the shank size must also include the consideration of the adequacy of the wear and strength of the blade gear for the intended service. This is the starting point in determining the ultimate hub barrel dimensions. Typical shank sizes for steel blades are No. 2, 4, 4¼, 5, 6 and 8. The following table shows blade shank diameter as a function of shank size and lists typical aircraft installations:

Shank Size	Shank Dia. - Inches (Measured at Brg. Seat)	Aircraft
No. 2 Steel	4.5262	DC-6, CV-240
No. 4 Steel	5.5100	B-29, B-50, C-124S, 1049, C-130
No. 4¼ Steel	5.7713	
No. 5 Steel	6.5056	C-133, KC-97J C-124 B,C
No. 6 Steel	6.8880	B-36
No. 8 Steel	8.0724	XF-84

Prior to the selection of the final shank size which will influence the blade bearing radius, a check must be made to determine the overturning moment and determine any unloading. This is an especially important design consideration in the case of propellers for V/STOL aircraft. If the bearing is unloaded, failure will occur due to bearing pounding, and this will occur if

$$\frac{2M}{R} > \frac{CF}{2} \qquad (2)$$

where M = the total steady and vibratory blade moment

R = the bearing radius

CF = the centrifugal force

Preload of the bearing can be used to eliminate the bearing unloading; however, it is usually more desirable to increase the blade shank size, and if possible, reduce the blade moments.

Selection of Retention Bearing

Given the blade shank diameter, the retention bearing O.D. and stack length can next be sized. The bearing design is based on the equivalent centrifugal loading (ECF) and the bearing design factor, K_T. The K_T factor is an indication of the magnitude of the mean compressive Hertzian contact stress between the balls and raceways. It is desirable to use a K_T of 150 to 175 to obtain contact stresses in the range of 350,000 psi for blade bearing design. The equivalent ECF is a combination of blade CF, static bending moment and vibratory bending moment. For this calculation the following formula is used:

$$ECF = CF + \frac{(M_B + M_V)}{E} \tag{3}$$

where CF = blade CF

M_B = static bending moment

M_V = vibratory bending moment

E = pitch diameter of bearing

The bearing size is then configured by the following formula, using a K_T value that does not exceed 175:

$$K_T = \frac{ECF}{\text{No. of Rows} \times \text{No. of Balls/Row} \times (\text{Ball Dia.} \times 8)^2} \tag{4}$$

The hub design considerations then are the hub barrel diameter and length to accommodate the bearing stack and uniform fixity of the barrel to assure uniform loading of the bearing.

Retention Nut and Hub Barrel Interface

The fillet at the base of the inboard hub thread is one of the most important hub design points relative to the retention. Because of thread flexibility characteristics, the inboard thread carries the greater portion of the total thread loading in standard nontapered threads. The thread loading produces a thread bending stress and a thread relief stress at the base of the inboard thread which, when combined yields the thread fillet stress at this critical point in the hub. The details of the analysis of this stress are given in the structures section, page 189.

Hub designs have used a 4-pitch buttress thread of from 2.79 to 4.00 full turns depending on loading, and a barrel wall thickness at the thread relief varying from 0.42 inch to 0.65 inch, depending upon the thread relief stress. Hub barrel walls have varied from 0.27 inch on No. 2 steel bladed hubs to 0.37 inch on No. 5 and No. 6 steel bladed hubs.

Final Hub Design Consideration

After the design of the blade retention components, the remainder of the hub is laid out. This includes the design of the hub tail shaft, the mounting system, provision for the blade actuator system including the necessary gear or links to the blade butt and the necessary structure. The structure between the blade retention barrels, the tail shaft, and the front face of the hub must be designed with the necessary stiffness to provide support for the steady centrifugal, moment and vibratory loads as are discussed in the structures section, Volume II.

The hub tail shaft generally contains the splines that mate with the shaft which transmits the engine torque to the hub. The size of the tail shaft is a function of the size of engine shaft and depends on the engine torque and the blade moments. Over the years, considerable difficulty has been experienced with the engine shaft / propeller tail shaft combination. To eliminate this problem and reduce weight, these two components are combined into the integral shaft configuration. This has been an important propeller development for not only saving weight but improving reliability and safety. The design procedures used for this type of mounting and drive are discussed in Reference 10.

After the hub has been designed and stress analyzed, it must be redesigned to correct for any deficiencies that are found and to reduce weight. The use of experimental stress analysis procedures to confirm the analytical work is also desirable and can be an important tool for preventing difficulties before the first hubs are built. In the past, full-scale hubs were stress coated and tested on a large fixture that could produce the steady loads to determine the critical areas. Although this was an effective method, the results came late in the program, leading to costly redesigns if problems were encountered.

After the first hubs are built, an adequate test program to confirm the design must be carried out. The hub should be tested simulating actual conditions of steady and vibratory loads as nearly as possible. For this testing, strain gages should be installed to check critical areas. The testing could continue for a period of time to confirm that the hub has adequate fatigue strength.

Integral Blade Bearing Hub

To eliminate the number of parts and reduce the hub size, integral blade retention bearings have been designed for a number of new propeller installations. This type of retention uses the walls of the blade and hub barrel for the bearing raceway. The integral blade bearing hub has a number of design considerations in addition to those discussed due to differences in the retention, assembly, and the use of integral races on the hub and blade. These features have a large impact on the hub design and are therefore treated separately.

The integral bearing retention is designed without the conventional threaded (hub nut provisions) and flanged (blade shank) connections . The blade centrifugal force is therefore reacted directly into the hub and blade structure. Because of this, the blade nut is eliminated and special means of assembling the propeller must be provided. One method of assembling the blade into the hub is by the use of loading holes in the side of the barrel. After each blade row is filled with the required number of balls, the blade is pulled into place. When the propeller is rotating, the centrifugal force gives the retention the necessary stiffness. In the design of this system, additional material must be placed around the loading holes to eliminate stress concentrations on the highly loaded hub barrel. To minimize any problems around the loading holes of the barrel, they are placed in an area where the stresses are a minimum. The initial experience with this type of blade retention has been favorable.

A second method of blade hub assembly using the integral bearing concept is with the use of an internal ball loading system. A two-row integral blade bearing retention using this concept developed for the supersonic propeller on the XF-84 is shown on Figure 5. This retention had the following characteristics:

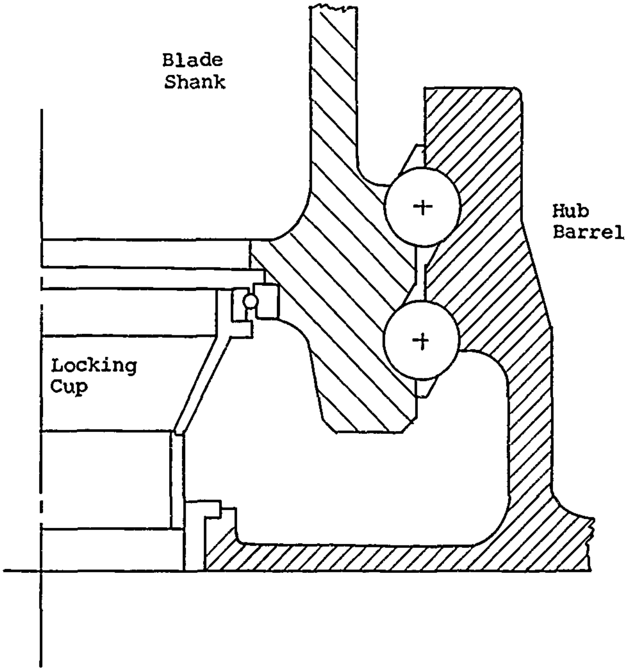
Blade
Shank
Hub
Barrel
Locking
Cup

Figure 5. Integral Race Retention.

Number of bearing rows	2
Number of balls/row	26
Raceway hardness	R_C61-63
Ball diameter	1.1875
Raceway curvature	
Outer raceway (hub)	51.2
Inner raceway (blade)	50.8

A plain nylon retainer is used for the outboard row; a nylon retainer incorporating a "snap ring type" spring (for assembly purposes) is used for the inboard row.

The assembly of the propeller is accomplished with this system by:

a. Inserting inboard retainer with balls in the bottom of hub barrel.

b. Spreading retainer with a "snap ring" type tool and then inserting blade into hub barrel so that blade butt passes through inboard retainer.

c. Remove spreading tool so that inboard retainer can close around the inboard raceway on the blade.

d. Spiral the outboard retainer (with balls) onto the outboard raceway of the blade.

e. Properly position blade with respect to hub using screw jack assembly that is a subassembly of the hub.

Independent of the method of assembly, the integral raceway retention offers important advantages in reduced hub weight and size. However, because the bearing is no longer an expendable part, it becomes necessary to examine the problem of race life very critically. Probably the most important hub design consideration is the hub structural characteristic that permits bearing mounting flexibilities. Nonuniformity of hub barrel fixity can cause nonuniform elastic deflections of barrel and integral races. This, in turn, causes unequal load distribution between rows and overloading balls within each row. The end result is higher Hertz stresses and corresponding reduction in bearing life. Careful attention must be given to the design of the hub web structure so that the inter-barrel openings are reduced so that barrel flexibilities are uniform.

Bearing design generally follows that of the conventional retention bearing design relative to K_T factor and allowable Hertzian stress (e.g., K_T = 150 to 175 and Hertzian stress in the order of 350,000 psi). In the case of the bearing using internal ball loading, a limited bearing race is used since it is impossible to use the "overlap" feature because of assembly limitations. The raceway curvatures are lower in order to reduce Hertz stress. With the use of loading holes this problem is somewhat reduced.

The two major manufacturing processes developed for the integral type retention were raceway grinding and flame hardening.

a. Raceway Grinding

Both raceways are ground simultaneously by one wheel in order to insure optimum control over spacing and concentricity of the raceways. The grinding wheels are diamond dressed as the most desirable means of maintaining the specified size and finish of the raceways. Crush dressing is not considered suitable because of the depth of the grooves and the high raceway shoulders. The tendency is for the crushed wheel to break down at the high shoulders and the crusher rolls wear too rapidly.

b. Flame Hardening

The raceways are hardened by the simultaneous hardening method. With this method the entire internal circumference of a hub barrel (or external circumference of a blade shank) is simultaneously heated with a ring type burner (using propane-oxygen fuel in this case) and then immediately quenched in oil. The hub barrels are hardened and quenched one at a time. Due to the close proximity of the inboard raceways of adjacent hub barrels, cooling protection must be provided to prevent tempering of a portion of the inboard raceway of the previously hardened hub barrel.

Briefly, the flame hardening process is as follows:

1) Hardening: Parts are heated in the flame hardening machine according to specified gas pressures, time cycles, and flame head configuration. At the end of the time cycle, parts are quenched in Houghton K oil which is temperature controlled between 90° and 110° F.

2) Refrigeration: After quenching, the parts are refrigerated and held at -60°F. This treatment provides additional hardness and is beneficial in reducing the danger of grinding checks.

3) Tempering: A double temper at 225° is specified to help minimize residual stresses.

PROPELLER CONTROLS

INTRODUCTION

Controls are required for a variable-pitch propeller where a change in blade angle will give differences in the torque requirements and the thrust output. These controls can be designed to choose the proper blade angle for a given rotational speed at a given power input or directly determine the level of thrust output. The controls must be designed to give the required response to the system without undesirable transient conditions. To achieve this, the controls and blade angle actuators must be considered as a package. The control system must also be designed to protect against failures in the system so that unwanted levels of thrust will not be obtained.

With fixed-pitch propellers, no control is present, and the nominal blade angle is fixed at a value that provides an acceptable compromise between static thrust for initiating takeoff and cruising thrust at higher airspeed. Initial variable-pitch approaches provided two positions: a low blade angle for takeoff and a high blade angle for cruise conditions. This could be shifted at appropriate times in a manner similar to a gear shift. The two-position propeller progressed to a continuously variable blade angle type controlled by a speed governor. When used on reciprocating engines, the propeller regulated the engine speed, while the throttle varied the manifold pressure to adjust power.

In some cases an opposite arrangement of the control functions was provided, with speed governor control of throttle position and manual variation of blade angle. This type of control was particularly useful for blimp applications, where direct variation of blade angle through a range from full reverse to full forward was desirable for maneuvering purposes. This arrangement is also used in some blade angle regimes of turboprop control systems, where it is termed the "Beta Range".

In the case of gas turbine engines, more complex control configurations may be encountered than with reciprocating engines. Many single-spool turboprop controls include a Beta Range at low powers for ground operation and a normal governing range for the higher powers used in flight. In the governing range, the propeller control regulates engine speed, while fuel adjusts compressor discharge pressure to vary power. Because of the high inertia of the system, the control task of the single-spool turboprop engine is much more demanding than with the reciprocating engine. The gas generator, which consists of a compressor and its driving turbine, is controlled separately by a fuel control that regulates its speed.

PROPELLER CONTROL DEVELOPMENT

Control Criteria

The first step in the development of a propeller control system is the definition of the tasks it must perform. The tasks will be dependent on the airplane and engine configurations and their operating requirements and characteristics. As described in Appendix I, the control requirements must be set up for all modes of propeller operation including reverse, feather and ground handling. The type of operation at each condition must be specified. For instance, constant rotational speed control may be desired for the takeoff, climb, and cruise conditions, while "Beta" control is needed for reverse and ground handling. On multi-engine aircraft, blade synchronization may be required to reduce noise. The propeller control stability and response characteristics must also be specified and must be compatible with the engine control and the rest of the aircraft system.

Safety features and criteria must also be defined that will accomplish those requirements determined from safety analyses of failure conditions. These safety features might include low pitch stops, follow-up stops, negative thrust control and backup control functions. The protection of the airplane from unwanted propeller signals as a result of failures is of primary importance in establishing an acceptable control system.

In the development of the control criteria, the special requirements of the airplane must be considered. This is especially true for STOL and V/STOL airplanes due to their specialized takeoff and landing characteristics. In the case of some V/STOL airplanes, the propeller control becomes a primary flight control and thus must be designed with a dual system to provide the required safety. The functions that the control must handle will also be more complex for systems of this type.

The control criteria developed will lead to the blade actuator requirements in terms of rate, response and safety. The type of actuator system required as discussed in the previous section will also be established by the control requirements.

Control and Safety Analyses

Once the concept and criteria for the desired control system have been established, the control configuration to accomplish the required functions may be defined. Computer simulation is particularly helpful in this stage of the development. The most suitable control equation can be determined for compatibility with the engine characteristics, and magnitudes of control constants may be established which give the desired response characteristics over the necessary range of flight conditions. (Use of computer simulation overlaps into both development of the concept and development of the control configuration).

For purposes of control analysis, the dynamic response characteristics of the engine and propeller must be expressed in mathematical form. Similar mathematical expressions for the control terms are combined with those of the engine and propeller to form complete control loops. Using the computer, or various control analysis techniques, the most satisfactory control equation and values of control constants are determined.

Safety analyses must also be conducted to establish features which must be included in the propeller control system to minimize the effect of failures which may occur in the engine or propeller system. In some cases, the use of computer simulation is also helpful in these studies for examining the effects of various failures and the effectiveness of possible corrective control features.

CONTROL DESIGN

When the functions that must be performed by the control system have been established, the essential step of translating the control relations into practical hardware must be accomplished. Control methods such as hydraulic, mechanical, or electrical means must be compared and evaluated on the basis of ability to accomplish the desired functions with acceptable reliability, cost and performance. Adaptation of components available from control manufacturers may be more satisfactory than developing new devices in-house.

Actuation methods that convert the control system output into physical motion of the propeller blade angle must also be developed. Actuators become an integral part of the propeller structure and are deeply involved in the overall propeller design task; they are discussed in the previous section.

The design task is not separate from the tasks of control analysis and safety analysis, but must be constantly considered while developing the control concepts. Compromises in control functions that will permit practical design and manufacturing approaches must be examined during the control analysis phase of the propeller development.

Testing

Proper operation and reliability of the propeller control system obviously must be verified by testing. Initially, laboratory tests of elements of the prototype system are subjected to functional tests to verify the soundness of the principles selected for control and actuation. Life tests must also be conducted on individual components to verify design criteria. Design modifications must be made as indicated by the results of component testing to obtain the desired performance. After satisfactory individual components are developed, they may be combined into more complete systems and subjected to tests of compatibility and proper interaction.

The final system is a complete propeller assembly with fully operating controls. When mounted on a whirl stand, the propeller is driven at normal operating speeds and subjected to typical control commands. An effective method for verifying proper control response characteristics is accomplished by connecting a computer simulation of engine response characteristics directly to the propeller control system so that a complete control loop is established. Provision of a signal of propeller blade angle as a computer input is relatively simple, but the connection from the computer output signal of engine speed response may be more difficult. For propeller control systems that utilize a mechanically driven governor, the solution has been to use a small synchronous motor to drive the governor independently of the main propeller shaft drive. The computer output is used to control the frequency of an oscillator which drives the motor through power amplifiers. With adequate instrumentation and recording of propeller and engine parameters, this type of system testing permits complete analysis of propeller control response characteristics at any flight conditions that may be represented on the computer. The test results may be compared with initial analytical predictions and later with engine test and flight test results as they become available.

After laboratory testing of the propeller assembly alone, combined testing of the engine and propeller combination must be conducted on test stands large enough to contain the complete assembly. These tests are limited to the region of static thrust testing, but serve to prove the operation with actual engine characteristics. Comparison of records of control performance under these conditions with previous testing and analytical predictions provides the justification for proceeding to flight testing.

When the engine and propeller are mounted on an aircraft, tests may be conducted over a full range of flight conditions. Variations in airspeed, altitude, temperature, and density may be examined and evaluated.

At each step in the testing program, various design changes may be required. By providing adequate control analysis and computer simulation during the initial stages of the design, the need for extensive redesign at later stages can be minimized.

PROPELLER CONTROL THEORY

The subject of control analysis involves a few useful and effective analytical techniques by which the response and stability of a control system such as a propeller may be examined. Since control systems are dynamic, they must be described and examined in terms of time responses. This requires that system equations must be written in terms of the time derivatives of the system, such as velocities and accelerations. These become differential equations which may be easily handled by expressing the relations in block diagram form and using operational notation to represent time differentiation. Such techniques reduce the differential equations to simple algebra so that they may be manipulated easily. The methods that have been used in the development of propeller control system relations are defined in the following discussion (Reference 5).

Basic Dynamic Equations

In organizing a physical system for dynamic analysis, a balance between the motions and forces in the system is defined mathematically by the familiar relations of acceleration to force or torque:

$$\Sigma F = m\,a \qquad (5)$$

$$\Sigma Q = I\alpha$$

where F = force, lb

a = acceleration, ft/sec^2

m = mass, slugs (lb-sec^2/ft)

Q = torque, ft-lb

α = angular acceleration, rad/sec^2

I = moment of inertia, slug-ft^2 (also ft-lb-sec^2/rad)

t = time, sec

In these relations, ΣF and ΣQ include not only the externally applied force or torque but also those resulting from velocity or position of the mass. A physical system which is commonly encountered is the typical spring-mass system which provides a good example of this method of analysis, and is illustrated in Figure 6.

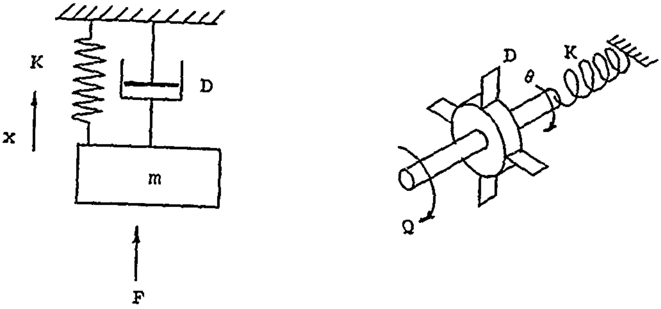

TRANSLATION

ROTATION

Figure 6. Vibrating Spring-Mass System.

where

F = externally applied force, lb

Q = externally applied torque, ft-lb

K = spring constant, lb/ft (ft-lb/rad for rotation)

D = damping coefficient, lb/(ft/sec), ft-lb/(rad/sec) for rotation)

m = mass, slugs or $\text{lb}/(\text{ft}/\text{sec}^2)$

I = moment of inertia, slug-ft^2 or ft-lb/(rad/sec^2)

x = displacement, ft

θ = angular displacement, rad

v = linear velocity, ft/sec

ω = angular velocity, rad/sec

a = linear acceleration, ft/sec^2

Damping is always present in systems of this type (although not always easy to evaluate). Damping is represented by a dashpot or paddles in Figure 6, and is defined as the force (or torque) reacting to velocity. Damping is usually assumed to be viscous or directly proportional to velocity. In this way, coefficients are provided for the forces reacting to the motion and each of its derivatives: K for position, D for velocity and m for acceleration. Although the assumption of direct proportion is often not strictly accurate for damping, it is usually quite reasonable for mathematical representation of most systems.

The equation of motion of each of these systems may be written as follows by observing that the external force or torque is opposed by the reactions:

Translation | Rotation

$$\Sigma F = ma = F - Dv - Kx \qquad \Sigma Q = I\alpha = Q - D\omega - K\theta$$

$$\text{or} \quad F = ma + Dv + Kx \qquad Q = I\alpha + D\omega + K\theta \tag{6}$$

These expressions may be written as differential equations in terms of the time derivatives or in the common "dot" notation by defining a single dot as a first derivative and a double dot as a second derivative:

$$\left.\begin{array}{ll} F = m\dfrac{d^2x}{dt^2} + D\dfrac{dx}{dt} + Kx & Q = I\dfrac{d^2\theta}{dt^2} + D\dfrac{d\theta}{dt} + K\theta \\ F = m\ddot{x} + D\dot{x} + Kx & Q = I\ddot{\theta} + D\dot{\theta} + K\theta \end{array}\right\} \quad (7)$$

Operational Notation

Although the above forms of presenting the equations are commonly used, the form that is most useful for control analysis is that of operational calculus, in which "operator" is substituted for the time derivative. The most commonly used form of operational calculus is that of Laplace which has a rigorous and complex mathematical derivation. However, in practice, a few simple rules are sufficient for its use in control analysis applications. Basically, the letter s is used as an operator to denote time differentiation. In general use, this principle is expressed as follows:

$$s = \frac{d}{dt} \qquad \text{(example:} \quad sx = \frac{dx}{dt} = \dot{x}) \qquad (8)$$

From this, the second derivative is

$$s^2 = \frac{d^2}{dt^2} \qquad \text{(example:} \quad s^2x = \frac{d^2x}{dt^2} = \ddot{x}) \qquad (9)$$

And time integrals are expressed as the reciprocal of differentiation:

$$\frac{1}{s} = \int_0^t (\ )\, dt \qquad \text{(example:} \quad \frac{x}{s} = \int_0^t x\, dt) \qquad (10)$$

Use of operators in this manner converts differential equations into algebraic equations in which the operators may be multiplied, factored, canceled and in general treated in accordance with the normal rules of algebra.

These rules may be illustrated by applying them to the spring mass system. With application of operators, the equations of motion above appear as follows:

$$F = ms^2x + Dsx + Kx \qquad Q = Is^2\theta + Ds\theta + K\theta$$

The variable may be factored out to yield

$$F = (ms^2 + Ds + K)\,\dot{x} \qquad Q = (Is^2 + Ds + K)\,\theta \qquad (11)$$

The response of the variable to externally applied force or torque then becomes

$$\frac{x}{F} = \frac{1}{ms^2 + Ds + K} \qquad \frac{\theta}{Q} = \frac{1}{Is^2 + Ds + K} \qquad (12)$$

This type of equation is of a quadratic form that is frequently encountered in control analysis. Such relations are normally expressed in terms of the natural frequency and damping ratio since these two terms define the nature of the response in a general form. In this form, the equations appear as follows:

$$\frac{\text{output}}{\text{input}} = \frac{C_1}{s^2 + (2\zeta\omega_n)s + \omega_n{}^2} \qquad (13)$$

or

$$\frac{\text{output}}{\text{input}} = \frac{C_2}{\frac{s^2}{\omega_n{}^2} + \frac{2\zeta}{\omega_n} s + 1} \qquad (14)$$

where ω_n = undamped natural frequency of the vibrating system, rad/sec

ζ = damping ratio, dimensionless

C_1, C_2 = gain coefficients resulting from system constants

Either the translational or rotational system may be converted to this form. The means of conversion is illustrated for the rotational system as follows:

$$\frac{\theta}{Q} = \frac{1/I}{s^2 + \frac{D}{I} s + \frac{K}{I}} \qquad (15)$$

From this relation, ω_n and ζ may be obtained as follows:

$$\omega_n = \sqrt{\frac{K}{I}} \qquad (16)$$

$$\zeta = \frac{D}{2\sqrt{K\,I}}$$

Depending upon which general form is chosen, the gain coefficients are as follows. (The form using C_2 provides the steady-state gain.)

$$C_1 = \frac{1}{I} \tag{17}$$

$$C_2 = \frac{1}{K} \tag{18}$$

Depending upon the values of ζ, the quadratic equation may be underdamped ($\zeta<1$), critically damped ($\zeta = 1$), or overdamped ($\zeta>1$). In either the critically damped or overdamped cases the equation can be factored into two real roots. These are equal in the critically damped case. For the underdamped case the roots are complex conjugates. Typical time plots showing the response of a spring-mass system for the three damping cases are shown in Figure 7.

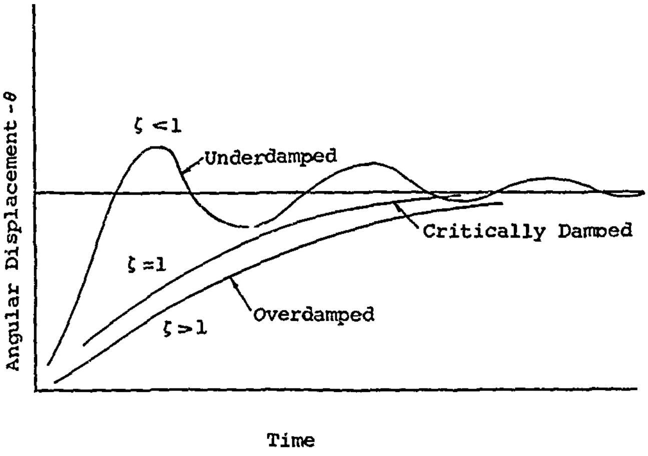

Figure 7. Effect of Damping on Rotational Spring-Mass System.

Solutions of Operational Equations

In general, control systems can be reduced to operational forms similar to those shown for the spring mass system. The resulting algebraic equations relating output to input are called "transfer functions". The output response is then the input multiplied by the transfer function.

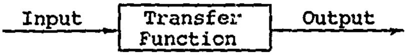

Tables of operational transforms are used to relate time expressions to their equivalent operational forms. In order to use these tables, the output response must be expressed as a single operational equation resulting from the product of the transfer function and the operational form of the input.

Initially, the input transform is obtained from the table and then combined with the transfer function. The table is then used to find the time solution, or "inverse transform", equivalent to this combined operational expression.

The most commonly used input is a step function, although ramp functions are also frequently used as inputs. The output responses resulting from these inputs are termed "transient responses" since the output variations occur briefly in time while proceeding from one steady-state condition to another.

Typical input functions in time and operational forms are included in the following short table, which also shows some common response functions in Laplace transform notation:

Typical Laplace Transforms

	Operational Form	Time Form
Step of magnitude a	$\frac{a}{s}$	a
Ramp with rate a/sec	$\frac{a}{s^2}$	at
Exponential Decay	$\frac{1}{s+a}$	e^{-at}

Exponential Time Lag Response to Step	$\frac{1}{s(\tau s+1)}$	$1-e^{-t/\tau}$
Exponential Time Lag Response to Ramp	$\frac{1}{s^2(\tau s+1)}$	$t-\tau(1-e^{-t/\tau})$
Underdamped quadratic response to Step	$\frac{1}{s\left(\frac{s^2}{\omega_n^2}+\frac{2\zeta}{\omega_n}s+1\right)}$	$1+\frac{1}{\sqrt{1-\zeta^2}}e^{-\zeta\omega_n t}\sin(\omega_o t-\psi)$ where: $\omega_o=\omega_n\sqrt{1-\zeta^2}$ $\psi=\tan^{-1}\frac{\sqrt{1-\zeta^2}}{-\zeta}$
Critically damped quadratic response to step	$\frac{1}{s(\tau s+1)^2}$	$1-\left(1+\frac{t}{\tau}\right)e^{-t/\tau}$
Overdamped quadratic response to step	$\frac{1}{s(\tau_1 s+1)(\tau_2 s+1)}$	$1+\frac{1}{\tau_2-\tau_1}(\tau_1 e^{-t/\tau_1}-\tau_2 e^{-t/\tau_2})$

where τ = characteristic time (or time constant)

e = 2.718, the natural logarithmic base

More complete tables can be found in References 6 and 7.

Block Diagram Notation

By the use of block diagrams, problems are organized into a form which defines all of the operations which occur and the manner in which they are related. Once the diagram has been established, the operation of the system is easier to visualize and the equations to define the system can be written by inspection using closed-loop transfer function techniques.

Common practice in drawing block diagrams follows a few logical rules:

1. Boxes are used to represent gain coefficients or dynamic operations that relate the variables in the system.

2. Lines which interconnect the boxes represent the variables in the system, with arrows drawn on the lines to indicate flow toward a box as an input and away from the box as an output.

3. Circles are used for algebraic summation of variables that occur in the system. An arrow leaving the circle is the algebraic sum of all the arrows entering the circle. The proper algebraic sign must be indicated for each entering arrow. Sometimes an X or Σ is included in the circle. The meaning remains the same. The following example shows a typical representation of summation such as might be used in a propeller analysis:

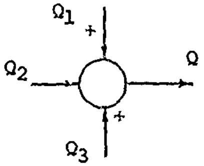

To illustrate the construction of a block diagram, consider again the rotational spring-inertia system shown in Figure 6. The summation of torques acting on the inertia is equal to the product of inertia and acceleration. If an external torque, Q, is applied to the inertia, its motion is resisted by "internal" torques, namely, a damping torque, proportional to velocity, and a spring torque, proportional to displacement. This summation is shown in Figure 8.

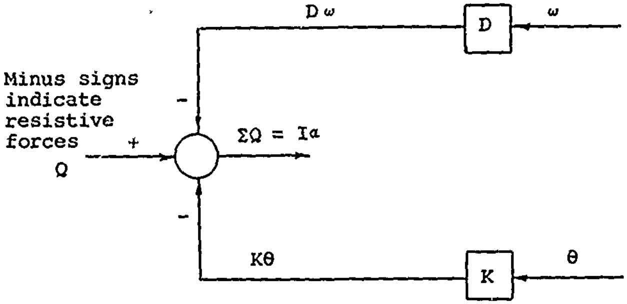

Figure 8. Summation of Forces on a Spring-Mass System.

By successive time integration of acceleration, the velocity and displacement can be developed to complete the block diagram as shown in Figure 9.

Since all variables entering the summing point must have the same dimensions, in this case torque, the gain coefficients, D and K, must have dimensions to relate velocity and position respectively to torque, thus:

$$D = \text{ft-lb-sec/rad}$$

$$K = \text{ft-lb/rad}$$

In a similar manner, 1/I relates torque to acceleration and s has dimensions of 1/time.

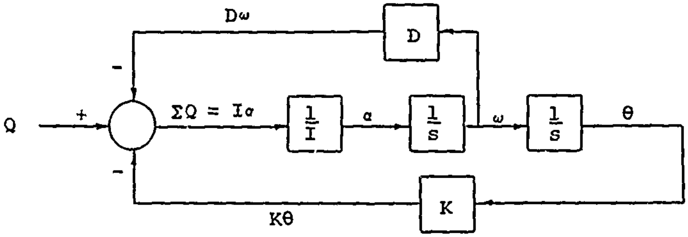

Figure 9. Block Diagram of Spring-Mass System

Obtaining Transfer Functions From Block Diagrams

Having obtained the block diagram for a system, the closed-loop transfer function relating the response of any variable to an input disturbance can be calculated by simple methods. As shown before, these transfer functions lead to time solutions by inverse Laplace transform techniques.

Consider a general negative feedback system shown in block diagram form by Figure 10.

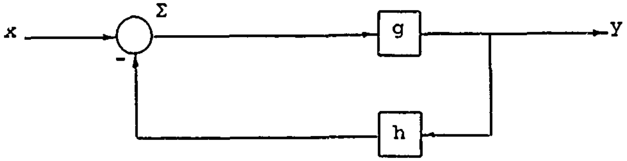

Figure 10. Typical Negative Feedback Loop.

where g is any function of s in the forward path (between input and output)

h is any function of s in the feedback path (between output and input)

It is desired to know the relationship between output (y) and input (x).

From the diagram above,

$$y = g\Sigma$$

but $$\Sigma = x - hy$$

therefore, $$y = g(x - hy)$$

combining $$y(1 + gh) - gx$$

The transfer function is the ratio of output to input. Thus

$$\frac{y}{x} = \frac{g}{1 + gh} \qquad (19)$$

This relation can be applied to sub loops to simplify complex systems in the spring mass system. The damping sub loop can be simplified as follows:

$$g = \frac{1}{Is} \quad \text{and} \quad h = D$$

and $$\frac{g}{1+gh} = \frac{\frac{1}{Is}}{1 + \frac{D}{Is}} = \frac{1}{Is+D} \qquad (20)$$

The block diagram now takes the form

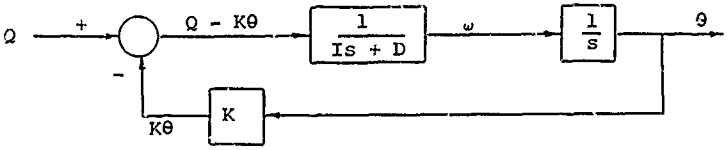

The complete transfer function relating θ to Q is obtained in a similar manner. In this case

$$g = \frac{1}{s(Is + D)}$$

$$h = K$$

$$\frac{g}{1 + gh} = \frac{\theta}{Q} = \frac{1}{Is^2 + Ds + K} \qquad (21)$$

This is recognized as being the same equation developed in the section covering operational notation.

In the case of the spring-mass system, either the block diagram method or the direct mathematical approach yields the final transfer function with equal ease. However, in more complex cases, block diagrams provide the easier method for determining complete transfer functions.

Propeller Engine Control Loops

Using the mathematical procedures developed in the previous paragraphs, the propeller engine transfer function can be examined.

The dynamic response characteristics of the combined engine and propeller may be expressed as a typical first-order exponential time lag transfer function. The block diagram of Figure 11 illustrates the mathematical relations that represent engine and propeller response characteristics.

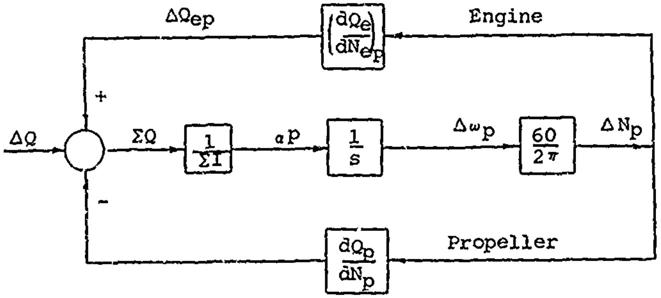

Figure 11. Propeller Engine Response Characteristics.

The nomenclature used in this diagram is as follows:

ΔQ = external torque variation, ft-lb (resulting from fuel flow or blade angle change)

$\Delta Q_p, \Delta Q_{ep}$ = propeller and engine torque variation resulting from speed variation, ft-lb

ΣQ = summation of nonequilibrium torque variations, ft-lb

$\Sigma I = I_p + I_{ep}$, summation of propeller and engine moments of inertia, ft-lb-sec^2/rad. (Engine inertia is referred to propeller shaft by the relation $I_{ep} = I_e(Ne/Np)^2$)

$\left(\frac{dQ}{dN}\right)_P$ = Torque vs. speed derivative of propeller, ft-lb/rpm

$\left(\frac{dQ_e}{dN_e}\right)_P$ = Torque vs. speed derivative of engine referred to propeller shaft, ft-lb/rpm

$$\left(\frac{dQ_e}{dN_e}\right)_P = \frac{dQ_e}{dN_e}\,(Ne/Np)^2 \qquad (22)$$

where

s = differential operator d/dt, 1/sec

α_p = angular acceleration of propeller shaft, rad/sec^2

$\Delta\omega_p$ = propeller speed variation from equilibrium point, rad/sec

ΔN_p = propeller speed variation from equilibrium point, rpm

The moments of inertia of the engine and propeller (referred to a common shaft) are additive, since the shafts are geared together. In the case of reciprocating engines or single-spool gas turbines, the full engine inertia is used. For free-turbine engines, only the power turbine inertia is added. The inertia of reduction gearing may also be considered, but is usually insignificant. All inertia values must be referred to a common shaft before the terms are added. Since the control system is regulating propeller speed, the propeller shaft is a logical reference point. Each inertia value must be multiplied by the square of the gear ratio which links it to the propeller shaft. Shafts that are rotating faster than propeller speed will have greater inertia when referred to the propeller shaft.

In a similar manner, the torque versus speed derivative of the engine must be referred to the propeller shaft. This engine derivative must be multiplied by the square of the gear ratio between propeller and engine, just as in the case of inertia. Since the engine speed is greater than propeller speed, the engine derivative is increased when referred to the propeller shaft. The ratio of torque speed derivative to inertia is unchanged by reference to the propeller shaft.

In combining the torque versus speed derivatives of propeller and engine, the signs are such that the two effects are additive. Visualized in a physical sense, an increase in speed causes the propeller load torque to increase and the engine driving torque to decrease. Both influences combine to oppose the speed change.

The additive influence of the engine and propeller torque versus speed derivatives may also be shown mathematically. When referred to a common shaft, any difference between engine torque and propeller torque causes angular acceleration of the combined moment of inertia. This accelerating torque may be expressed as

$$Q_{acc} = \alpha_p \Sigma I = Q_{ep} - Q_p \qquad (23)$$

where α_p is the angular acceleration of the propeller shaft in rad/sec^2

ΣI is the combined inertia of engine and propeller referred to the propeller shaft

Q_p is propeller load torque

Q_{EP} is engine torque referred to the propeller shaft by the engine to propeller speed ratio: $Q_{eP} = \frac{N_e}{NP} Q_e$

Q_e is engine torque at the engine shaft

Expressed as variations from a steady-state operating point so that linearized derivatives may be used, the engine and propeller variables become

$$Q_e = Q_{eo} + \Delta Q_e \qquad (24)$$

$$Q_p = Q_{po} + \Delta Q_p \qquad (25)$$

$$N = N_o + \Delta N \qquad (26)$$

$$w_f = w_{fo} + \Delta w_f \qquad (27)$$

$$\beta = \beta_o + \Delta \beta \qquad (28)$$

The terms with subscript 0 represent values at the equilibrium operating point, and the Δ terms are variations from the equilibrium value. The symbols w_f for engine fuel flow and β for propeller blade angle have also been included.

Since steady-state torque values are in equilibrium, the accelerating torque relation may be expressed in terms of the torque variations alone:

$$\Sigma I(\alpha_p) = \Delta Q_{ep} - \Delta Q_p \qquad (29)$$

The variation of engine torque is a function of speed and fuel flow, and may be expressed in terms of linearized partial derivatives at the engine as

$$\Delta Q_e = \left(\frac{\delta Q_e}{\delta N_e}\right) \Delta N_e + \left(\frac{\delta Q_e}{\delta W_f}\right) \Delta w_f \qquad (30)$$

When referred to the propeller, this expression becomes

$$\Delta Q_{ep} = \left(\frac{\partial Q_e}{\partial N_e}\right)_p \Delta N_p + \left(\frac{\partial Q_e}{\partial w_f}\right)_p \Delta w_f \qquad (31)$$

where $\Delta Q_{ep} = (N_e/N_p)\,\Delta Q_e$

$$(\partial Q_e/\partial N_e)_p = (N_e/N_p)^2(\partial Q_e/\partial N_e)$$

$$(\partial Q_e/\partial w_f)_p = (N_e/N_p)(\partial Q_e/\partial w_f)$$

The variation of propeller torque is a function of propeller speed and blade angle. Expressed in terms of linearized partial derivatives, the propeller torque variation is

$$\Delta Q_p = \left(\frac{\partial Q_f}{\partial N_p}\right)\Delta N_p + \left(\frac{\partial Q_p}{\partial \beta}\right)\Delta\beta \qquad (32)$$

The resulting expression for accelerating torque in terms of the partial derivatives becomes

$$\Sigma I(\alpha_p) = \left[\left(\frac{\partial Q_e}{\partial N_e}\right)_p - \left(\frac{\partial Q_p}{\partial N_p}\right)\right]\Delta N_p + \left(\frac{\partial Q_e}{\partial w_f}\right)_p \Delta w_f - \left(\frac{\partial Q_p}{\partial \beta}\right)\Delta\beta \qquad (33)$$

In the normal operating range, the derivative $\partial Q_e/\partial N_e$ is negative and $\partial Q_p/\partial N_p$ is positive. These terms combine as a summation of negative influences that oppose variations of speed.

Expressed in these terms, the block diagram of engine and propeller relations becomes

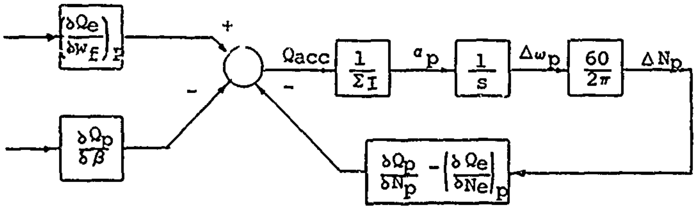
$\left(\frac{\partial Q_e}{\partial w_f}\right)_p$
+
Q_{acc}
$\frac{1}{\Sigma I}$
α_p
$\frac{1}{s}$
$\Delta\omega_p$
$\frac{60}{2\pi}$
ΔN_p
–
–
$\frac{\partial Q_p}{\partial \beta}$
$\frac{\partial Q_p}{\partial N_p} - \left|\frac{\partial Q_e}{\partial N_e}\right|_p$

This diagram may be reduced to a simpler form by combining the feedback term with the other system constants so that unity feedback is obtained while preserving the mathematical relationships between input and output variables. Expressed in terms of combined coefficients, the diagram reduces to the following form:

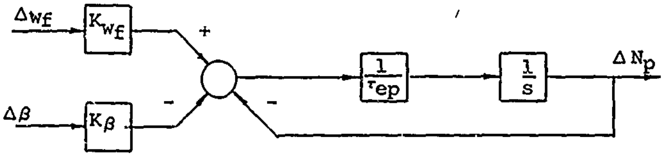

Δwf
K_{w_f}
+
Δβ
K_β
-
-
$\frac{1}{\tau_{ep}}$
$\frac{1}{s}$
ΔN_p

Solving for the closed-loop expression, the diagram becomes

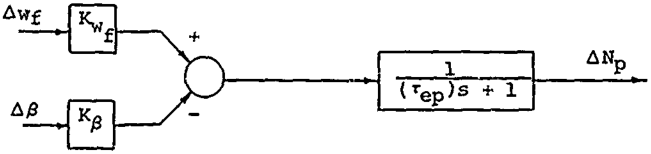

Δwf
K_{w_f}
+
Δβ
K_β
-
$\frac{1}{(\tau_{ep})s + 1}$
ΔN_p

The combined coefficients have the following relations to the original system derivatives:

$$K_{wf} = \frac{(\partial Q_e/\partial wf)p}{(\partial Q_p/\partial N_p) - (\partial Q_e/\partial N_e)_p} \qquad (34)$$

$$K_\beta = \frac{(\partial Q_p/\partial \beta)}{(\partial Q_p/\partial N_p) - (\partial Q_e/\partial N_e)_p} \qquad (35)$$

$$\tau_{ep} = \frac{2\,\pi(Ip + 1ep)}{60\left|(\partial Q_p/\partial N_p) - (\partial Q_e/\partial N_e)_p\right|} \qquad (36)$$

These three coefficients describe the major response characteristics of the engine and propeller combination. As defined here, the term K_{wf} is the fuel gain coefficient which represents the steady-state response of propeller speed to fuel flow changes, and the term K_β is the blade angle gain coefficient which defines the steady-state response of propeller speed to blade angle changes. The term τ_{ep} is the engine and propeller time constant, which defines the dynamic response of propeller speed variations to fuel or blade angle changes. Although other influences such as aircraft velocity and air density also influence propeller speed, they vary at slow rates and are normally not significant in propeller control analysis.

Transfer Function Derivatives

The expression of engine and propeller response characteristics in terms of a transfer function represents a linearization of their relationships for small perturbations about any selected operating point. The derivatives which make up the coefficients in the transfer function are partial derivatives defined by the slope of the engine or propeller characteristic curve at the specified operating point. Each derivative expresses the linearized variation of torque in response to variations of one variable (such as speed, fuel flow, or blade angle) when all other variables are held fixed.

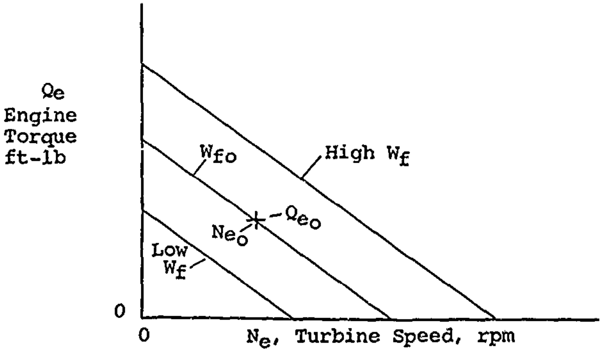

Figure 12 . Typical Turbine Engine Characteristics.

In the case of a turbine engine, the characteristic plot of engine torque vs. speed and fuel flow will appear somewhat as illustrated in Figure 12.

In normal practice, performance curves for the engine which is to be used with a particular propeller would be available for the evaluation of derivatives. However, for preliminary design purposes when no engine curves are available, rough approximations of engine derivatives may be made from the following general relations:

Engine Torque versus Speed

Normal engine operating points will occur in the most efficient region, where horsepower output is maximum at a specified fuel flow. Typical torque vs. speed lines are reasonably linear, and the peak horsepower will occur at approximately half of the stall torque and half of the no-load speed. If the horsepower, speed and fuel flow are known for a specified condition, the torque may be calculated. The stall torque may then be expressed as twice this computed torque, and the no-load speed as twice the specified speed:

$$\begin{aligned} Q_{stall} &= 2\ Q_{eo} \\ N_{no\ load} &= 2\ N_{eo} \end{aligned} \qquad (31)$$

The negative slope of a straight line between these two points is a fair approximation of the engine torque vs. speed derivative at constant fuel flow:

$$\frac{\partial Q_e}{\partial N_e} = - \frac{2\ Q_{eo}}{2\ N_{eo}} = - \frac{Q_{eo}}{N_{eo}} = - \frac{5250\ hp}{(N_{eo})^2} \qquad (32)$$

Engine Torque versus Fuel Flow

The influence of fuel flow on engine torque is an external disturbance which is not involved in the propeller control loop. Therefore, for analysis of propeller control response and stability, it is not necessary to know the engine torque vs. fuel flow derivative accurately. If the actual derivative is not known, a suitable approximation can be obtained by assuming that torque varies in direct proportion to fuel flow, so that the derivative is defined by the ratio of torque to fuel flow at the specified operating condition. The approximate derivative of torque vs. fuel flow at constant speed is then

$$\frac{\partial Q_e}{\partial W_f} = \frac{Q_{eo}}{W_{fo}} \tag{33}$$

Propeller Derivatives

At a particular airspeed and altitude, the relation of propeller torque to propeller speed and blade angle may be plotted in the form of Figure 13.

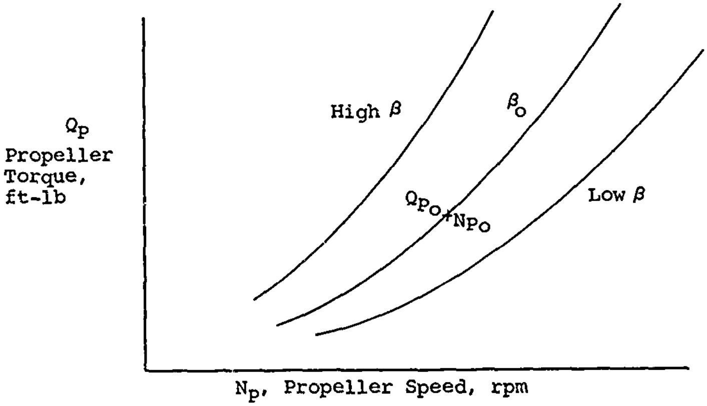

Figure 13. Typical Propeller Torque Relations.

Partial derivatives for the propeller may be obtained from this plot or its crossplot by measuring slopes at any desired operating point. These partial derivatives are $\partial Q_p/\partial N_p$, which defines the variation of propeller torque in response to variations of propeller speed at constant blade angle, and $\partial Q_p/\partial \beta$, the variation of propeller torque in response to blade angle at constant propeller speed. In practice, plots of propeller torque vs. speed and blade angle are seldom made in that form, since the full range of airspeeds and altitudes over which the propeller must operate would require a large number of plots. Instead, a generalized plot is normally used, which presents the relation of propeller power coefficient, C_p to advance ratio, J, and blade angle, β. A plot of this type is illustrated in Figure 14.

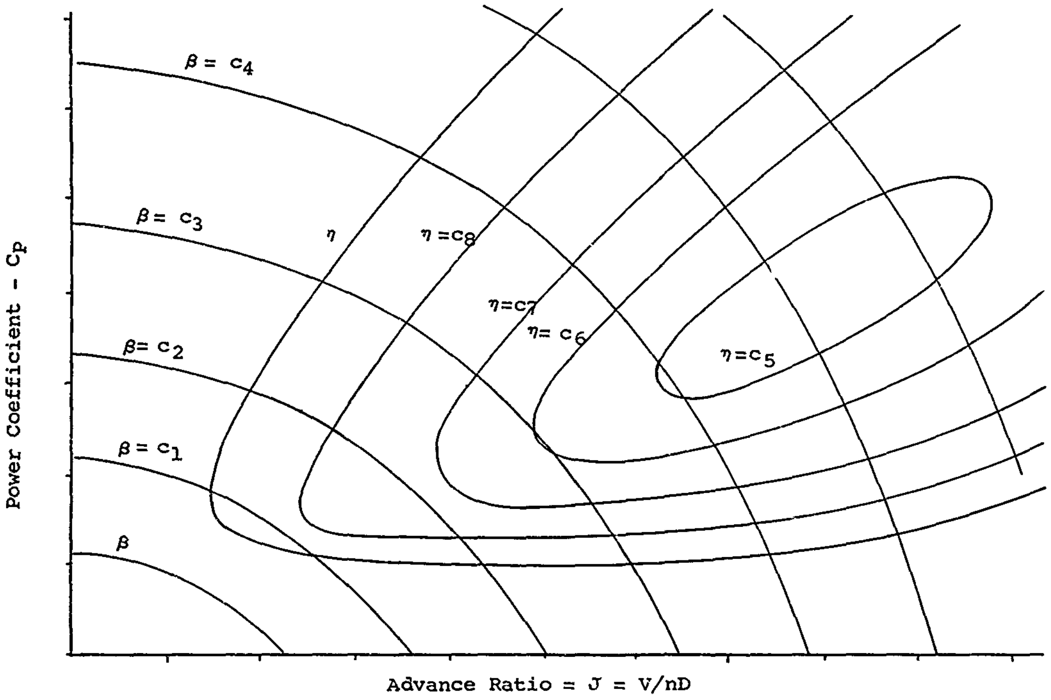

Figure 14. Propeller Efficiency and Blade Angle Map.

In this plot, the significant parameters are

β = Blade angle, deg

$C_P = \frac{P}{\rho n^3 D^5}$, power coefficient (33)

$J = V/nD$, advance ratio (34)

where $P = 2\pi Qn$, power absorbed, ft-lb/sec

Q = torque, ft-lb

n = propeller speed, rev/sec

ρ = air density, slugs/ft^3

D = propeller diameter, ft

V = airspeed, ft/sec

In a similar manner, thrust relations are frequently plotted in terms of a thrust coefficient, C_T, related to advance ratio and blade angle. The thrust coefficient is defined as

$$C_T = \frac{T}{\rho n^2 D^4} \tag{35}$$

where T = thrust, lb

ρ, n, D are as defined above

The propeller efficiency, η , is related to the thrust and power coefficients by the following expression which includes the advance ratio:

$$\eta = J\frac{C_T}{C_P} \tag{36}$$

where $J = 60V/ND$ = advance ratio

V = airspeed, ft/sec

D = propeller diameter, ft

N = propeller speed, rpm

Determination of propeller derivatives from C_P and C_T plots: To obtain dimensional values for propeller derivatives from the nondimensional coefficient plots, the following sets of partial derivative expressions are used. The subscripts used with the derivatives represent the variables which are held fixed while the specified derivative varies. For example, $\delta Q/\delta N|_{\beta,V}$ represents the variation of torque with variation of propeller rpm while blade angle and airspeed are held constant. Similarly, $\delta C_P/\delta J|_{\beta}$ represents the variation of C_P with J at constant β.

Torque derivatives:

$$\frac{\delta Q}{\delta N}\bigg|_{\beta,V} = \frac{Q}{N}\left[2 - \frac{J}{C_P}\left(\frac{\delta C_P}{\delta\beta}\bigg|_{\beta}\right)\right]^{*} \tag{37}$$

$$\frac{Q}{\delta\beta}\bigg|_{N,V} = \frac{Q}{C_P}\left(\frac{\delta C_P}{\delta\beta}\bigg|_{J}\right) \tag{38}$$

$$\frac{\delta Q}{\delta V}\bigg|_{\beta,N} = \frac{QJ}{V\ C_P}\left(\frac{\delta C_P}{\delta J}\bigg|_{\beta}\right) \tag{39}$$

Thrust derivatives:

$$\frac{\delta T}{\delta N}\bigg|_{\beta,V} = \frac{T}{N}\left[(2 - \frac{J}{C_T}\left(\frac{\delta C_T}{\delta J}\bigg|_{\beta}\right)\right]^{*} \tag{40}$$

$$\frac{\delta T}{\delta\beta}\bigg|_{N,V} = \frac{T}{C_T}\left(\frac{\delta C_T}{\delta\beta}\bigg|_{J}\right) \tag{41}$$

$$\frac{\delta T}{\delta V}\bigg|_{\beta,N} = \frac{TJ}{VC_T}\left(\frac{\delta C_T}{\delta J}\bigg|_{\beta}\right) \tag{42}$$

* In the static case, the second term becomes zero.

When only the C_P plot is available, thrust derivatives may still be obtained from the following expressions:

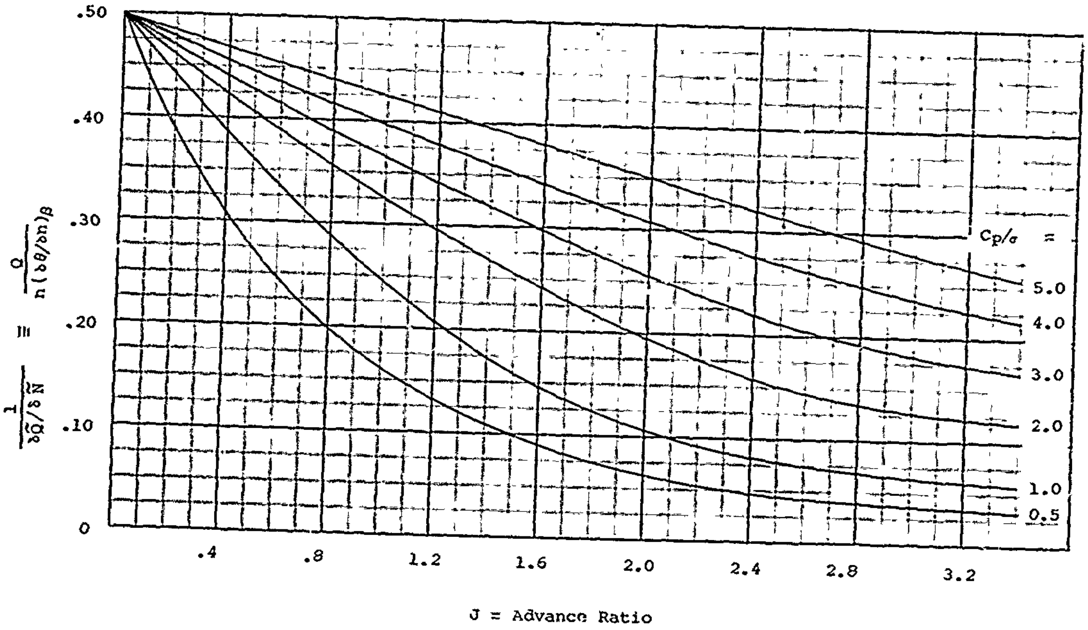

Figure 15. Generalized Propeller Torque-Speed Derivatives.

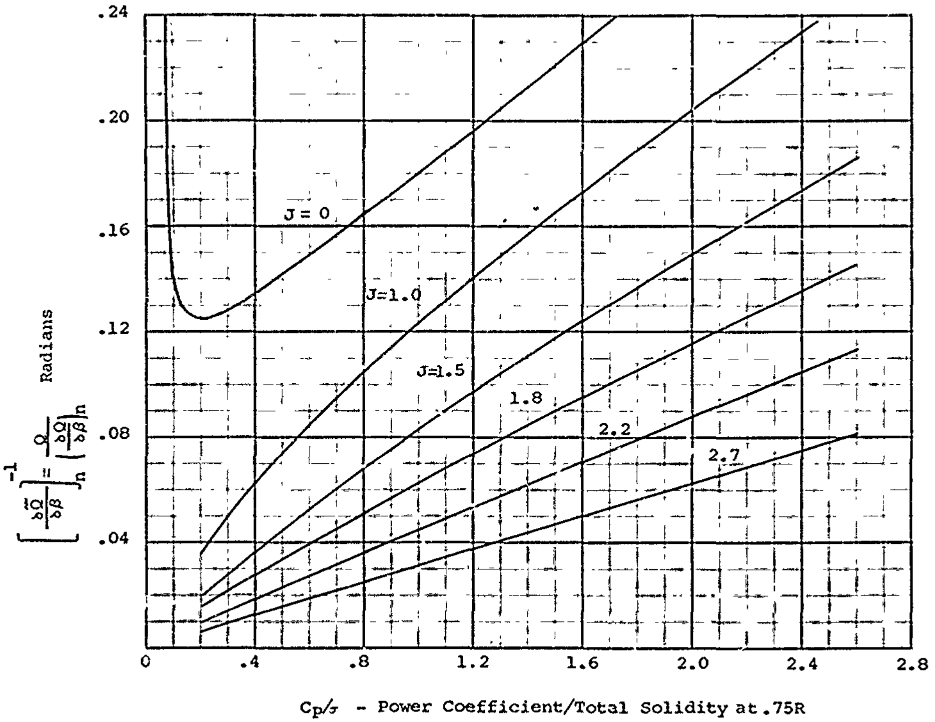

Figure 16. Generalized Propeller Torque-Angle Derivatives.

$$C_T = \frac{\eta C_P}{J} \tag{43}$$

$$\left.\frac{\partial C_T}{\partial J}\right|_\beta = -\frac{C_T}{J} + \frac{C_T}{C_P}\left(\left.\frac{\partial C_P}{\partial J}\right|_\beta\right) + \frac{C_T}{\eta}\left(\left.\frac{\partial \eta}{\partial J}\right|_\beta\right) \tag{44}$$

$$\left.\frac{\partial C_T}{\partial \beta}\right|_J = \frac{C_T}{C_P}\left(\left.\frac{\partial C_P}{\partial \beta}\right|_J\right) + \frac{C_T}{\eta}\left(\left.\frac{\partial \eta}{\partial \beta}\right|_J\right) \tag{45}$$

For the static case, when a plot of C_t vs. C_P is available, these derivatives are

$$\left.\frac{\partial C_T}{\partial J}\right|_\beta = \left(\frac{\partial C_T}{\partial C_P}\right)\left.\frac{\partial C_P}{\partial J}\right|_\beta \tag{46}$$

$$\left.\frac{\partial C_T}{\partial \beta}\right|_J = \left(\frac{\partial C_T}{\partial C_P}\right)\left.\frac{\partial C_P}{\partial \beta}\right|_J \tag{47}$$

For rapid approximation of propeller gain and time constant values when propeller performance curves are not available, the two propeller torque derivatives $\partial Q_P / \partial N_P$ and $\partial Q_P / \partial \beta$ may be found from the generalized derivative plots of Figures 15 and 16 . These plots are reasonably accurate for most propellers.

To use these plots, values must be determined for C_P and J at desired power conditions, and the solidity, σ , must be computed for the propeller under consideration. Solidity at the .75 radius point is determined from the expression

$$\sigma = \frac{bB}{.75\,\pi D} \tag{48}$$

where b = blade chord at .75 radius

B = number of blades

The results obtained from the plots are expressed in generalized form, using the relationships

$$\partial \tilde{Q} = \frac{\partial Q}{Q} \qquad (49)$$

$$\partial \tilde{N} = \frac{\partial N}{N} \qquad (50)$$

The dimensional derivatives then have the relations

$$\frac{\partial Q_P}{\partial N_P} = \frac{Q_P}{N_P}\left(\frac{\partial \tilde{Q}}{\partial \tilde{N}}\right) \qquad (51)$$

$$\frac{\partial Q_P}{\partial \beta} = Q_P\left(\frac{\partial \tilde{Q}}{\partial \beta}\right) \qquad (52)$$

Inertia Computation:

Calculation of the propeller and engine time constant also requires a value for the combined polar moment of inertia of the propeller and engine. During the preliminary design phase, when final inertia values are not available, estimated values for propeller inertia are used.

The inertia for a hollow steel blade may be estimated from the equation

$$I_B = 7.16 \times 10^{-6}(AF)D^4, \text{ Slug-Ft}^2 \qquad (53)$$

where D = Propeller diameter, ft

I_B = Inertia of one blade, slug-ft^2

AF = Activity Factor per blade

$AF = 1562\ b/D$ for rectangular planform blades

b = Blade chord, ft

Using the approximation for the activity factor of rectangular blades, the following approximate expression for the moment of inertia for a hollow steel blade based on b at .75R is obtained:

$$I_B = .0112 \ b \ d^3, \ \text{slug-ft}^2 \qquad (54)$$

An approximate value for the inertia of a solid propeller blade may be found by using the activity factor in the following expression:

$$I_B = K\left(\frac{AF}{100}\right)\left(\frac{D}{10}\right)^5, \ \text{slug-ft}^2 \qquad (55)$$

where K = 5.29 for steel

3.02 for titanium

1.90 for aluminum

Based on the approximate relation for AF, the expression for the inertia of a solid blade becomes

$$I_B = 1.5625 \ K \ b\left(\frac{D}{10}\right)^4 , \ \text{slug-ft}^2 \qquad (56)$$

The total moment of inertia of the propeller about its drive shaft is obtained by summing the inertia of all blades and the propeller hub:

$$I_P = B \ I_B + 1 \ , \ \text{slug-ft}^2 \qquad (57)$$

where B = number of blades

1 = typical hub inertia

The nominal value of 1 slug-ft^2 has been found to be typical of the hub inertia for turboprop propellers, and sufficiently accurate for preliminary calculations.

Values of engine inertia are normally obtained from data supplied by the engine manufacturer. In some cases, where dimensions of rotating turbine elements are known, but no value of inertia has been supplied, a reasonable estimate can be obtained from a standard equation for polar moment of inertia of a disc:

$$I = 6.02 \times 10^{-6}\ T\ D^4,\ \text{slug-ft}^2 \qquad (58)$$

where T = disc thickness, in.

D = disc diameter, in.

Weight density of steel = .284 lb/in.^{3}

A rough approximation of engine inertia may also be obtained for preliminary control analysis purposes from the following typical ratios, which are based on a number of comparisons of engine inertia with the inertia of steel propellers. The values given by these ratios represent the apparent engine inertia when referred to the propeller shaft by the square of the gear ratio

COUPLED TURBINE ENGINE (Spool, including turbine and compressor, geared to propeller):

$$(I_e)_p = 1.25\ I_p \qquad (59)$$

FREE TURBINE (Power turbine separate from compressor spool):

$$(I_e)_p = 0.2\ I_p \qquad (60)$$

RECIPROCATING ENGINES:

$$(I_e)_p = 0.1\ I_p \qquad (61)$$

where $(I_e)_p$ = engine inertia referred to propeller shaft

I_p = inertia of steel propeller designed to absorb power of engine

As shown by these ratios, the combined inertia of a propeller and coupled-turbine engine is more than double that of the propeller alone, but the free turbine or reciprocating engine does not cause a significant inertia increment.

PROPELLER CONTROL SYSTEM CHARACTERISTICS

The principal purpose of a normal propeller control system is to maintain the speed of the engine and propeller at a desired magnitude in flight. When controlling speed, the propeller control system compares actual engine speed with the desired speed setting. If a difference exists, blade angle is varied as a function of the error. This modifies the propeller torque load, and causes engine speed to change in a direction to reduce the error. Although other control functions may be present, such as reversing, feathering, and direct blade angle scheduling at low powers, the analysis of control system dynamic performance will apply only to the closed-loop speed control operation.

The objective of control system analysis is the selection of propeller control system equations and gain values that will provide good response and stability over the full range of flight conditions. This selection involves a certain amount of compromise. High control gains will achieve rapid response in opposing disturbances or following changes of speed setting, but will reduce system stability. Low control gains have the opposite effect of good stability but sluggish response. Control gains that are good at one flight condition may provide poor stability or poor response at other conditions.

The best control functions and gain values for a particular engine and propeller may be determined by combining control system equations with the engine and propeller transfer function that has been derived previously. Using values of engine and propeller derivatives for all significant flight conditions, the following approach provides a method for selecting the control characteristics that will achieve the best combination of performance and stability.

Engine and Propeller Response

In a previous section, the response of engine and propeller speed to variations of blade angle or fuel flow has been defined in terms of a mathematical transfer function which may be expressed in the following block diagram form:

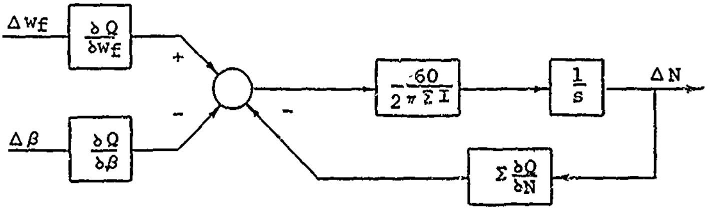

ΔW_f
$\frac{\delta Q}{\delta W_f}$
+
$\Delta\beta$
$\frac{\delta Q}{\delta\beta}$
-
-
$\frac{60}{2\pi\Sigma I}$
$\frac{1}{s}$
ΔN
$\Sigma\frac{\delta Q}{\delta N}$

where ΔN = speed variation

Δw_f = fuel flow variation

$\Delta \beta$ = blade angle variation

ΣI = moment of inertia summation

$\Sigma \partial Q/\partial N$ = torque vs. speed summation

$\partial Q/\partial w_f$ = torque vs. fuel flow derivative

$\partial Q/\partial \beta$ = torque vs. blade angle derivative

$\frac{1}{s}$ = time integration

In simplified form, this block diagram becomes

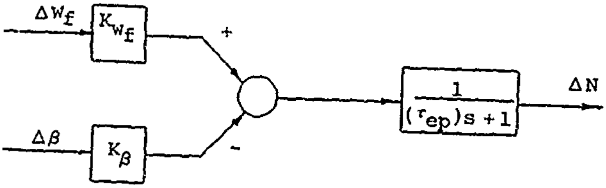

where K_{wf} = steady-state gain of ΔN vs. Δw_f, rpm/(lb/sec)

K_β = steady-state gain of ΔN vs. $\Delta \beta$, rpm/deg

τ_{ep} = engine and propeller characteristic time, sec

The derivation of each of these coefficients has been detailed in a previous section of this report. The response of speed to fuel flow is typical of the response to any external disturbance, and may be expressed as the following transfer function:

$$\frac{\Delta N}{\Delta w_f} = \frac{K_{wf}}{(\tau_{ep})s + 1} \qquad (62)$$

Some external variables, such as airspeed and air density, influence the speed response much more slowly than fuel flow. In this discussion, the effect of fuel flow changes will be used to represent the response to any external disturbance.

Propeller Control System - Block Diagram

The typical propeller control system, which varies blade angle to control speed, includes three elements: an error sensor, which senses actual speed and compares it with a reference level of desired speed to develop a measure of speed error; a control function, which computes the necessary response of blade angle to oppose the speed error; and a servo, or power amplifier, to manipulate the blade angle as required by the control function. The addition of a control system to the basic engine and propeller relation is shown in block diagram form as follows:

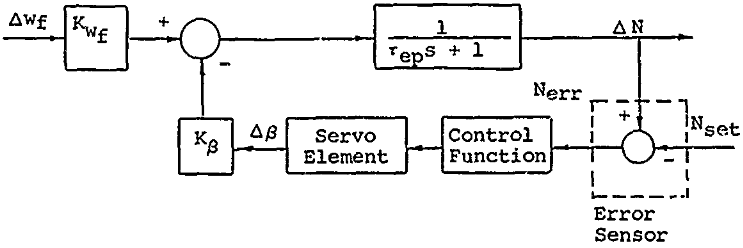

Control System Elements

A typical error sensor consists of a flyweight governor balanced against a spring. The governor is mechanically driven by the engine, and develops a force proportional to speed. The spring force which opposes the flyweight force is manually adjusted to represent a desired speed magnitude. At the proper propeller speed, the flyweight and spring forces will be in equilibrium. For speeds above or below the equilibrium level, the governor will have a mechanical motion proportional to speed error. This motion may be utilized to stroke a hydraulic valve, operate electrical contacts, or actuate a mechanical linkage.

Other error-sensing approaches compare the speed of an engine to the speed of a master reference such as an electric motor or an oscillator frequency, to develop a shaft rotation or an electrical signal proportional to speed error.

Typical control functions consist of simple computing operations that respond to the error sensor output to develop a signal of the required blade angle change. These operations may be proportional to the speed error, or the time integral or time derivatives of the error, individually or combined in various proportions. Hydraulic, mechanical, or electrical methods for developing the control functions may be used, depending upon the particular control design approach.

The servo element is a power amplifier which includes an actuator to drive the blade angle to the position determined by the computer element. The actuator may consist of a hydraulic cylinder, an electric motor, or mechanical clutches. Feedback elements may also be present for matching the servo output to the desired angle from the computer.

In some simple control systems, the separation into individual control elements is not very definite, as in the case of a hydraulic cylinder servo actuated directly by a governor valve. However, as the control becomes more complex, the roles of each element become more definite, and the proper mathematical control functions must be established to provide the best performance and stability.

Proportional Control Function

The most obvious mathematical control relation is one in which the blade angle varies in proportion to speed error. This is termed proportional control, since speed also varies in direct proportion to blade angle, and the net loop gain is a proportional coefficient without any time functions such as integration or differentiation. With proportional control, a servo actuator is generally necessary to move the blade angle through an increment proportional to the speed error measured by the governor. A sketch of a proportional control system is shown in Figure 17.

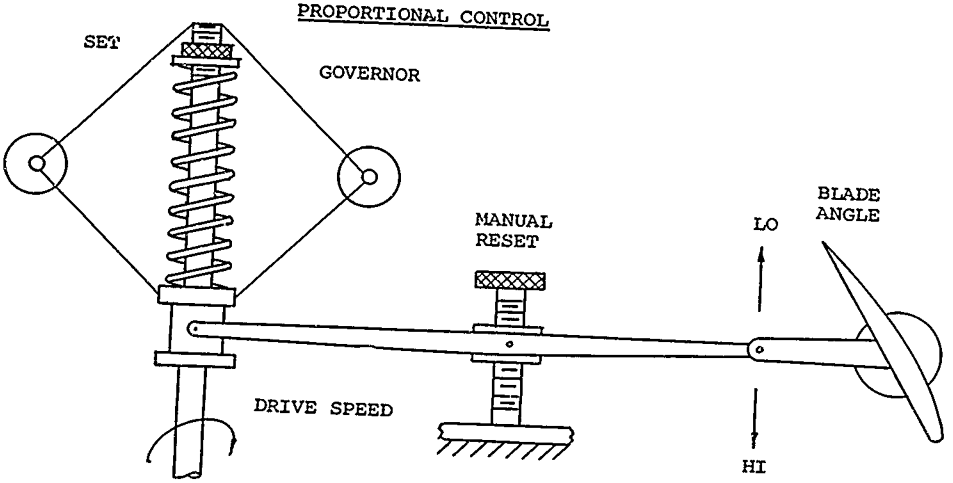
PROPORTIONAL CONTROL
SET
GOVERNOR
MANUAL
RESET
LO
BLADE
ANGLE
DRIVE SPEED
HI

Figure 17. Propeller Proportional Control Schematic.

The mathematical relation for proportional control, when servo dynamics are ignored, may be expressed as the simple control function

$$\frac{\Delta\beta}{N_{err}} = a$$

where a = proportional gain, deg/rpm

In block diagram form, the proportional control function is

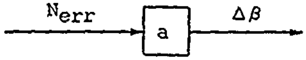
N_{err}
a
$\Delta\beta$

When combined with the block diagram of engine and propeller relations, the proportional control system provides the following loop diagram:

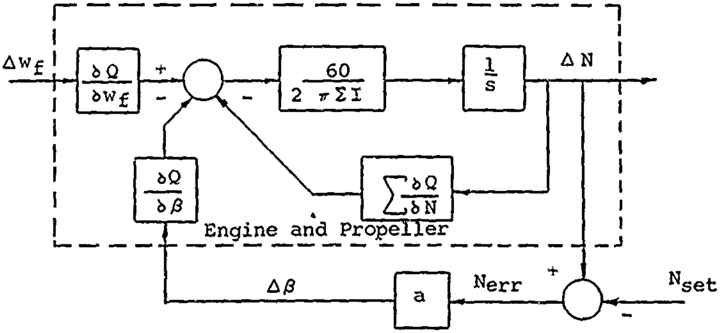
Δw_f
$\frac{\delta Q}{\delta w_f}$
+
-
-
$\frac{60}{2\pi\Sigma I}$
$\frac{1}{s}$
ΔN
$\frac{\delta Q}{\delta\beta}$
$\sum\frac{\delta Q}{\delta N}$
Engine and Propeller
$\Delta\beta$
a
N_{err}
+
N_{set}
-

PROPORTIONAL CONTROL

This diagram shows that the proportional control adds to the natural damping of the engine and propeller expressed by the term $\Sigma \delta Q / \delta N$. This results in increased stiffness of speed response in resisting torque changes caused by external disturbances such as fuel flow.

In a simplified form, the proportional control block diagram becomes

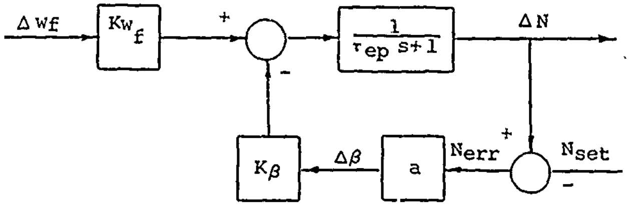

SIMPLIFIED PROPORTIONAL CONTROL LOOP

The resulting mathematical transfer functions which relate speed response to changes of an external disturbance or of speed setting are

$$\frac{\Delta N}{\Delta w_f} = \frac{\left(\frac{K w_f}{1 + aK_\beta}\right)}{\left[\left(\frac{\tau_{ep}}{1 + aK_\beta}\right) s + 1\right]} \qquad (63)$$

$$\frac{\Delta N}{\Delta N_{set}} = \frac{\left(\frac{aK_\beta}{1 + aK_\beta}\right)}{\left[\left(\frac{\tau_{ep}}{1 + aK_\beta}\right) s + 1\right]} \qquad (64)$$

The form of the transfer function has remained the same as for the engine and propeller without control, but the steady-state gain and the characteristic time have both been reduced by the factor $1 + aK_\beta$, where aK_β is the loop gain of the system. The response obtained with proportional control is compared to the uncontrolled system in Figure 18 . Since a proportional control permits an offspeed error when a disturbance is present, it is often called a "droop" control. The effect of the control has been to improve the regulation of the system by reducing the natural response of the engine and propeller to disturbances, but the error will not be entirely eliminated. A very high control gain may appear desirable to reduce the error to a very small value. However, in practical cases, additional dynamics such as servo and governor lags become significant and will cause instability at very high gains.

Integral Control Function

Another simple control function is one in which the rate of blade angle change varies in proportion to speed error. Therefore, the blade angle position is the time integral of speed error. Since speed varies in proportion to blade angle position in the steady state, the loop gain includes one time integration. With this type of control, the system will always seek zero speed error in the steady state.

As shown on Figure 19, a typical example of an integral control system consists of a governor which moves a hydraulic valve to vary flow to and from a hydraulic cylinder. The rate of flow through the valve, and therefore the rate of piston travel in the cylinder, is proportional to speed error. The piston output is linked to blade angle, so that blade angle then varies as the time integral of speed error.

The mathematical relation for integral control may be expressed as the following control function:

$$\frac{\Delta\beta}{N_{err}} = \frac{b}{s} \qquad (65)$$

where b = integral gain, $\left(\frac{\text{deg/sec}}{\text{rpm}}\right)$

$\frac{1}{s}$ represents time integration, sec

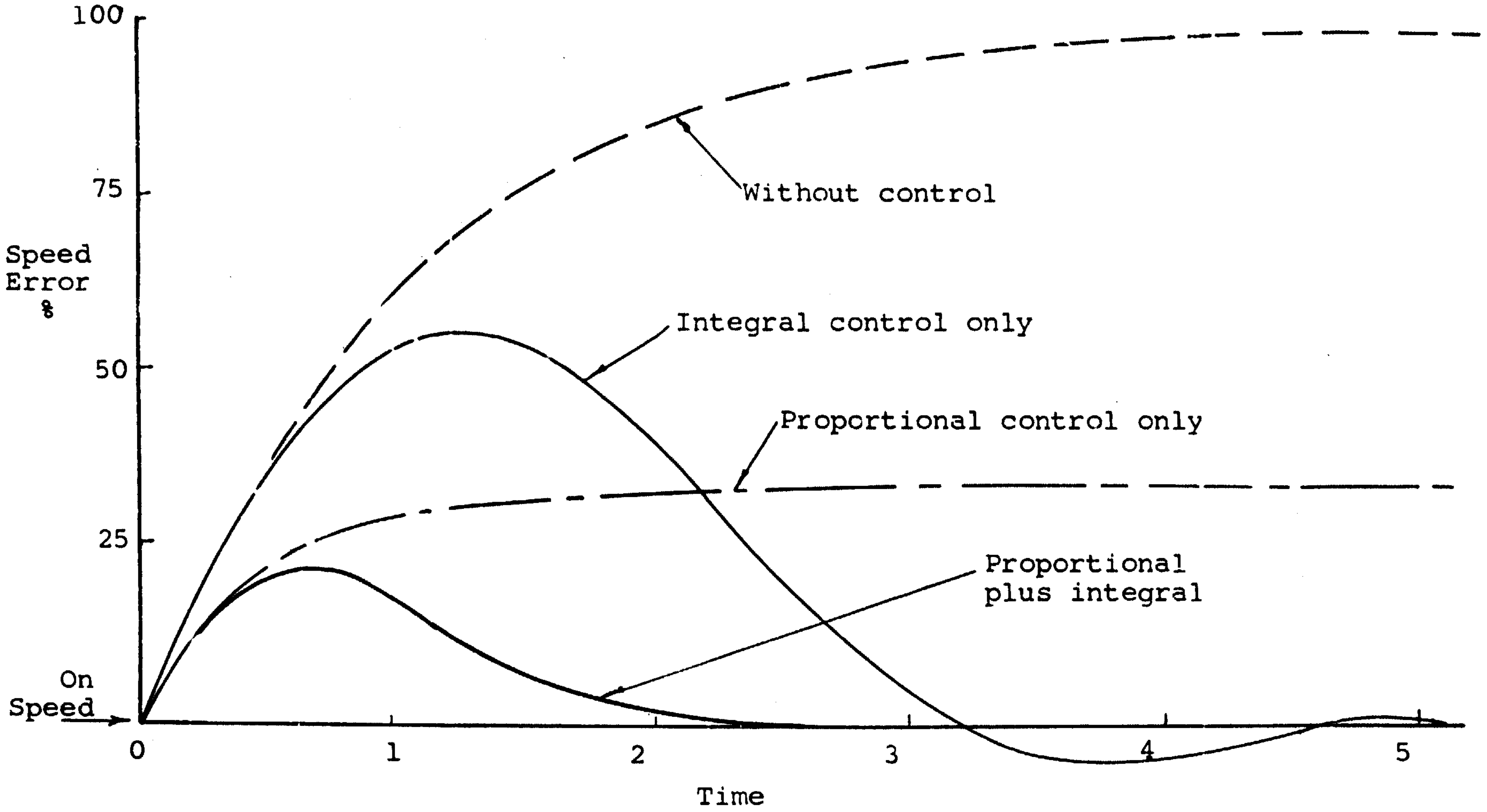

Figure 18. Control Response to Load Disturbance.

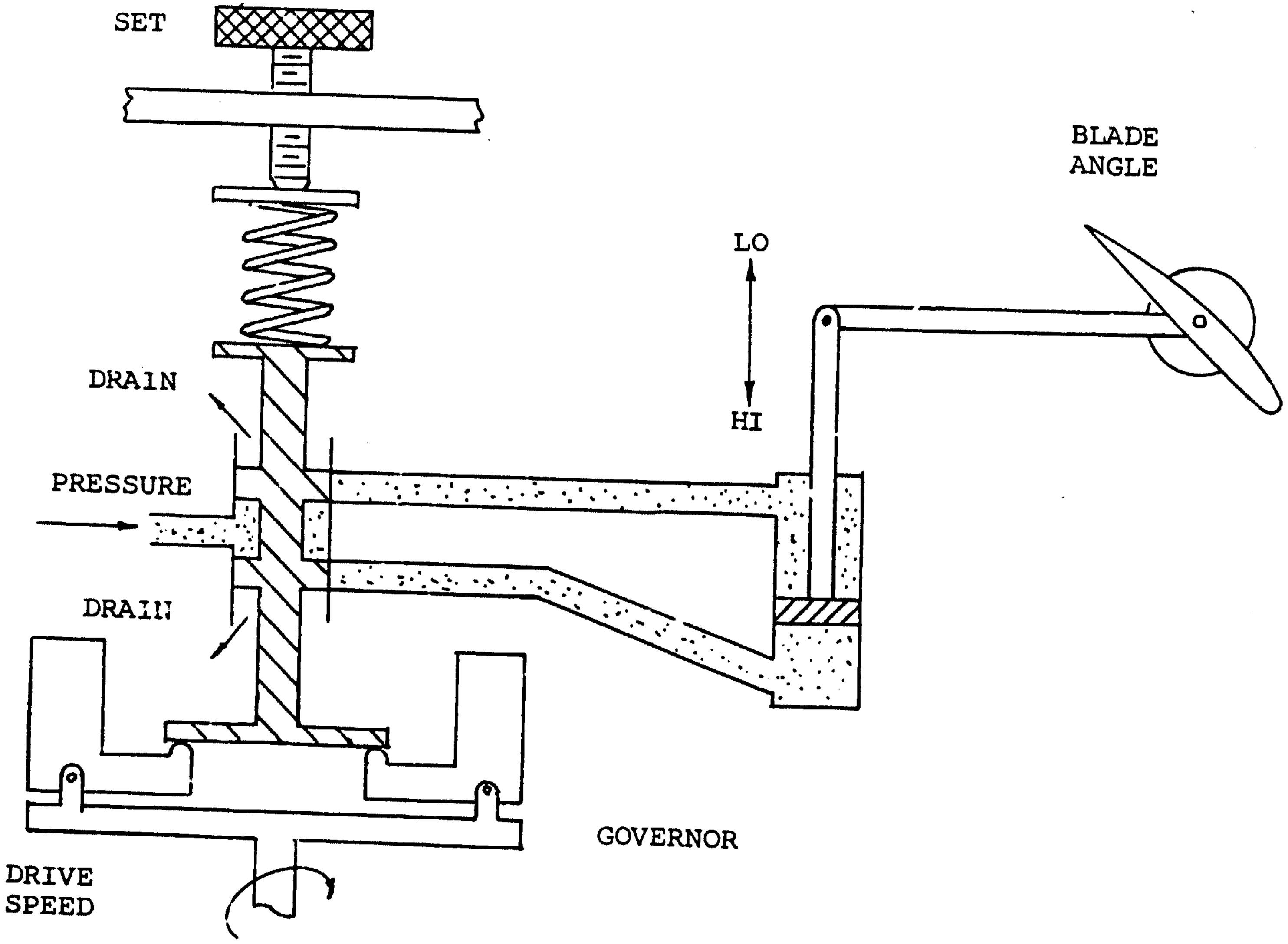
SET
BLADE
ANGLE
LO
HI
DRAIN
PRESSURE
DRAIN
GOVERNOR
DRIVE
SPEED

Figure 19. Propeller Integral Control Schematic.

In block diagram form, the integral control function is

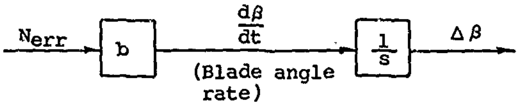
N_{err}
b
$\frac{d\beta}{dt}$
(Blade angle rate)
$\frac{1}{s}$
$\Delta\beta$

When combined with the block diagram of engine and propeller relations, the integral control system provides the following loop diagram:

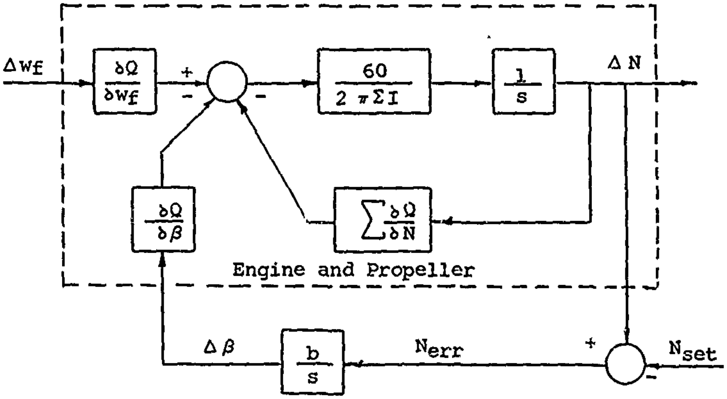
ΔW_f
$\frac{\delta\Omega}{\delta W_f}$
+
−
−
$\frac{60}{2\pi\Sigma I}$
$\frac{1}{s}$
ΔN
$\frac{\delta\Omega}{\delta\beta}$
$\sum\frac{\delta\Omega}{\delta N}$
Engine and Propeller
$\Delta\beta$
$\frac{b}{s}$
N_{err}
+
−
N_{set}

INTEGRAL CONTROL

The diagram shows that two integrations are present in the loop: one for engine-propeller dynamics and one for the control. This is equivalent to a typical second-order system, such as a spring-mass oscillating system. The inertia term is equivalent to mass, the integral control has the effect of a spring, and damping is provided by the $\Sigma \partial Q/\partial N$ term. Increasing the integral gain increases the frequency of oscillation and reduces the relative damping.

Expressing the block diagram in simplified form, the system with integral control becomes

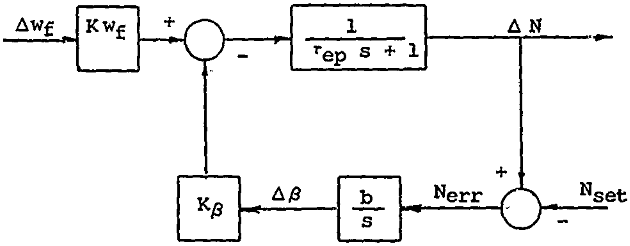

The resulting integral control transfer functions which relate speed response to changes of an external disturbance or speed setting are

$$\frac{\Delta N}{\Delta w_f} = \frac{\left(\frac{K w_f}{b K_\beta}\right) s}{\left(\frac{\tau_{ep}}{b K_\beta}\right) s^2 + \left(\frac{1}{b K_\beta}\right) s + 1} \tag{66}$$

$$\frac{\Delta N}{\Delta N_{set}} = \frac{1}{\left(\frac{\tau_{ep}}{b K_\beta}\right) s^2 + \left(\frac{1}{b K_\beta}\right) s + 1} \tag{67}$$

In the steady state, when time is large, S approaches zero and the response to a fuel flow disturbance becomes zero. In the case of a speed set change, the speed response equals the set change in the steady state.

The denominator of these transfer functions is a quadratic term which may be expressed in the form typical of second-order vibrating systems:

$$\frac{s^2}{\omega_n^2} + \frac{2\zeta s}{\omega_n} + 1 \qquad (68)$$

where $\omega_n = \sqrt{\frac{bK_\beta}{\tau_{ep}}}$, $\frac{rad}{sec}$, the undamped natural frequency

$\zeta = \frac{1}{2\sqrt{bK_\beta \tau_{ep}}}$, the dimensionless damping ratio

The time response of this type of transfer function is of a sinusoidal nature which becomes more oscillatory as the integral gain is increased. If additional dynamic terms are present such as servo and governor lags, the system may easily be made unstable by raising the gain too high. The curve labeled "integral control only" on Figure 18 illustrates the nature of the response that may be expected from this type of control. Although a reduction of gain sufficiently to provide a reasonably damped system will result in a large initial offspeed peak and a relatively long time to reach the onspeed condition, the integral control may still be quite satisfactory for some applications such as the control of reciprocating engines. Calculation of the proper value for the integral gain, b, can be made by using the damping ratio equation to solve for a damping of approximately $\zeta = .707$ using values of K_β and τ_{ep} obtained from engine and propeller derivations.

Proportional-Plus-Integral Control Function

The advantages of both proportional and integral controls can be obtained by combining both actions in one control function as illustrated in Figure 20 . The proportional term reduces the amount of offspeed and adds stabilization by increasing the system damping. The integral term continues to trim the blade angle until zero speed error is obtained. This action is equivalent to automatically resetting the governor to eliminate the droop that results from a load change when proportional control is used alone. For this reason, integral control was called "reset" in early control terminology. A proportional-plus-integral control device, Figure 20, is thus a governor having both "droop" and "reset" action. This type of control is also termed an "isochronous governor" since it maintains a

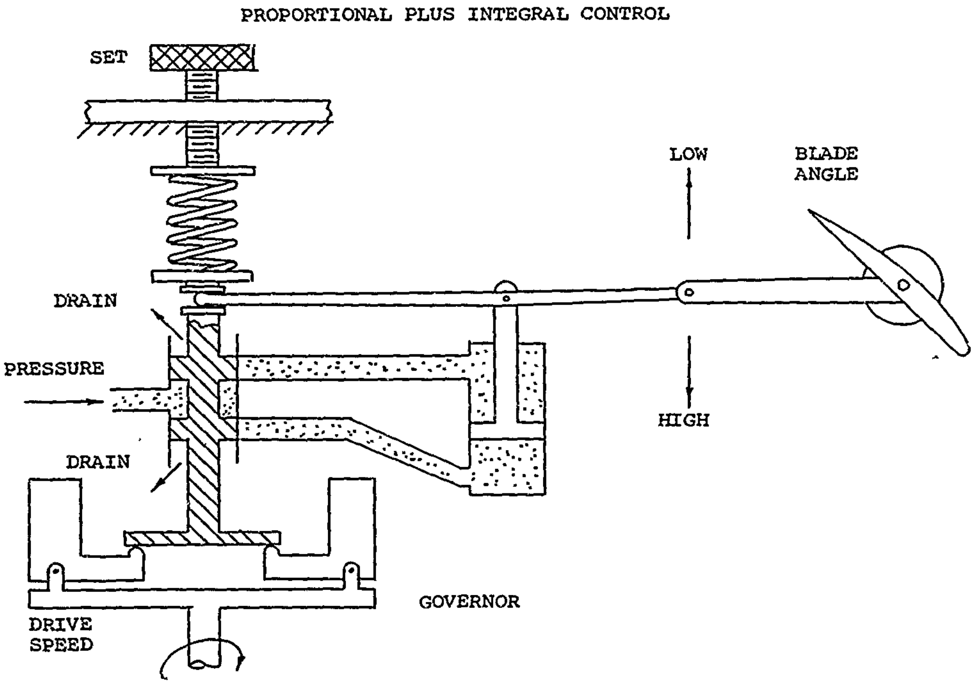
PROPORTIONAL PLUS INTEGRAL CONTROL
SET
DRAIN
PRESSURE
DRAIN
DRIVE
SPEED
GOVERNOR
LOW
HIGH
BLADE
ANGLE

Figure 20. Propeller Proportional Plus Integral Control Schematic.

constant speed. The curve labeled proportional-plus-integral control on Figure 18 compares the response of this control function with other approaches.

The mathematical relation for proportional-plus-integral control, including the dynamics of a blade angle servo actuator, may be expressed as the following control function:

$$\frac{\Delta\beta}{N_{err}} = \frac{a + b/s}{(\tau_c s + 1)} \qquad (69)$$

where a = proportional gain, deg/rpm

b = integral gain, $\frac{(\text{deg/sec})}{\text{rpm}}$

τ_c = servo time constant, sec

s = time differentiation, 1/sec

$1/s$ = time integration, sec

In block diagram form, the proportional-plus-integral control function is

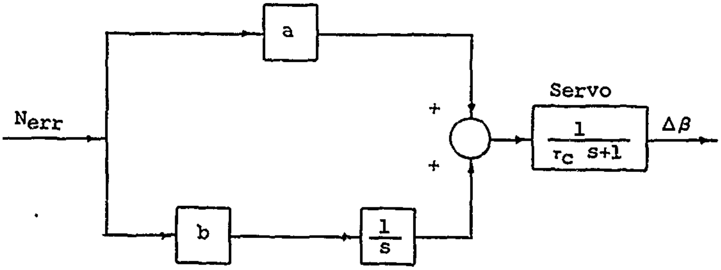

When combined with the block diagram of engine and propeller relations, the proportional-plus-integral control provides the following loop diagram:

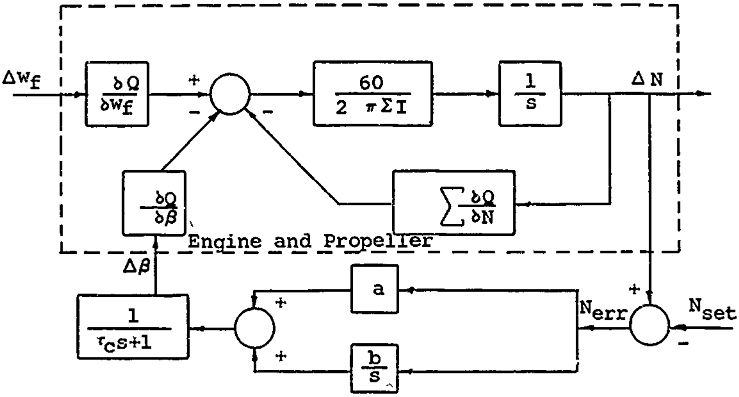

Δw_f
$\frac{\partial Q}{\partial w_f}$
+
−
−
$\frac{60}{2\pi\Sigma I}$
$\frac{1}{s}$
ΔN
$-\frac{\partial Q}{\partial \beta}$
$\sum\frac{\partial Q}{\partial N}$
Engine and Propeller
$\Delta\beta$
a
+
+
N_{err}
−
N_{set}
$\frac{1}{\tau_c s+1}$
$\frac{b}{s}$
+

PROPORTIONAL-PLUS-INTEGRAL CONTROL

This diagram has a form similar to that of integral control alone, except that the proportional "a" term adds increased damping to that provided by the $\Sigma\partial Q/\partial N$ term. This not only reduces the speed offset resulting from disturbances, but stabilizes the system so that higher values of the integral gain "b" may be used to produce a more rapid return to zero speed error.

The proportional-plus-integral control function may be simplified to the following form:

$$\frac{\Delta\beta}{N_{err}} = \frac{b(\tau_a\ s + 1)}{s(\tau_c\ s + 1)} \qquad (70)$$

where $\tau_a = a/b$

Combining this simplified control relation with the simplified engine and propeller expression results in the following block diagram:

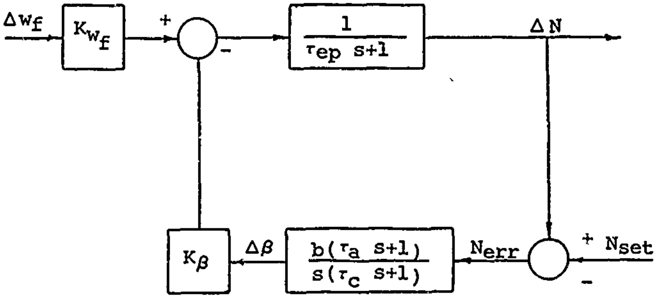

SIMPLIFIED PROPORTIONAL-PLUS-INTEGRAL CONTROL

The ratio of control gains (a) and (b) may be selected to give a value of the leading time constant, τ_a, which is equal to the lagging time constant, τ_{ep}, of the engine and propeller. This is an optimum value for the a/b ratio and permits simplification of the closed-loop transfer functions by cancelling the leading and lagging terms. The resulting transfer functions for proportional-plus-integral control, when $a/b = \tau_{ep}$, are

$$\frac{\Delta N}{\Delta w_f} = \frac{\left[\dfrac{(K_{wf})s(\tau_c s + 1)}{bK_\beta(\tau_{ep} s + 1)}\right]}{\left(\dfrac{\tau_c}{bK_\beta}\right)s^2 + \left(\dfrac{1}{bK_\beta}\right)s + 1} \qquad (71)$$

$$\frac{\Delta N}{\Delta N_{set}} = \frac{1}{\left(\frac{\tau_c}{bK_\beta}\right) s^2 + \left(\frac{1}{bK_\beta}\right) s + 1} \tag{72}$$

These expressions are similar to those for integral control alone, except for two significant differences: the servo time constant, τ_c, has replaced the engine and propeller time constants in the left denominator term, which indicates a higher response frequency; and the ratio of the τ_c lead to the τ_{ep} lag appears in the numerator of the fuel flow response, which indicates that the peak offspeed has been reduced below the magnitude that would have occurred with integral control alone. Figure 21 shows the influence of the ratio τ_c/τ_{ep} on the offspeed peak.

The natural frequency and damping terms for the proportional-plus-integral control are

$$\omega_n = \sqrt{\frac{bK_\beta}{\tau_c}} \quad \text{rad/sec} \tag{73}$$

$$\zeta = \frac{1}{2\sqrt{bK_\beta \, \tau_c}} \quad \begin{array}{l}\text{dimensionless}\\ \text{damping ratio}\end{array} \tag{74}$$

These terms are similar to those for integral control alone, except that τ_c has been substituted for τ_{ep}.

For good control performance, it is apparent that the blade angle servo must be designed so that τ_c is small in comparison with the engine and propeller characteristic time τ_{ep}. This will permit a large value of "b" for a given damping ratio, a high natural frequency, and a low offspeed response to an external disturbance.

Selection of the best gain values for a given flight condition can be made once the servo time constant, τ_c, has been established, using values of K_β and τ_{ep} determined by the flight condition. The integral gain, b, may be found from the damping ratio expression:

$$bK_\beta \, \tau_c = \frac{1}{(2\zeta)^2} \tag{75}$$

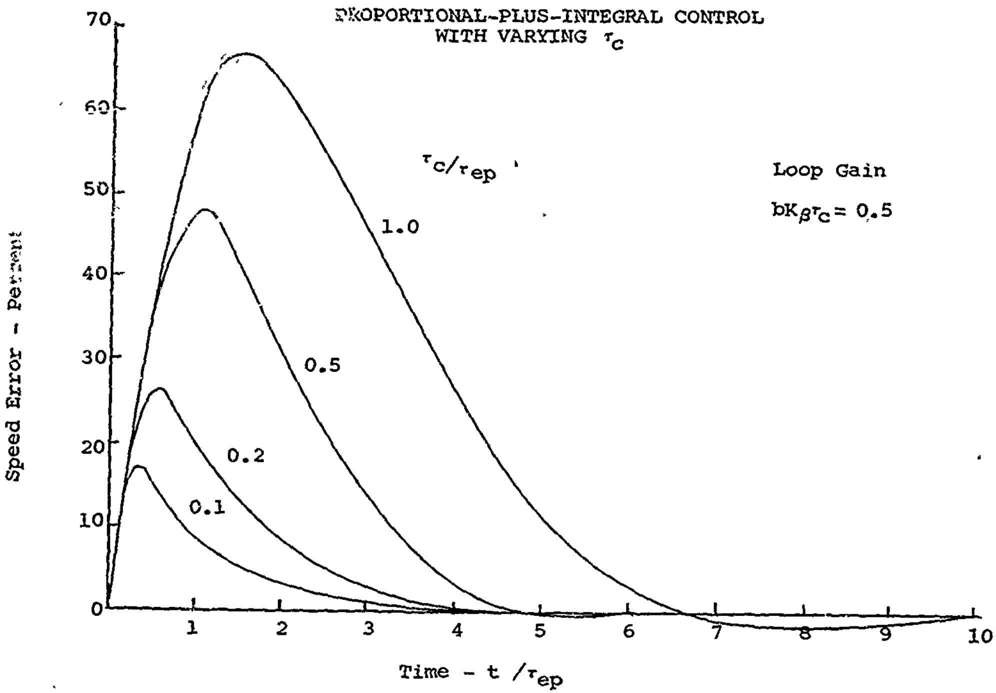

Figure 21. Effect of Servo Lag on Speed Response.

Defining a desirable response as that which results from a damping ratio of $\zeta = .707$ provides the following relationship for the integral gain:

$$b = \frac{.5}{K_\beta \ \tau_c} \qquad \frac{(\text{deg/sec})}{\text{rpm}} \tag{76}$$

The proportional gain is found from the integral gain value by utilizing the optimum control condition, in which the control lead cancels the engine and propeller lag:

$$\frac{a}{b} = \tau_a = \tau_{ep} \tag{77}$$

From this, the proportional gain is

$$a = b\,\tau_{ep} \qquad \text{deg/rpm} \tag{78}$$

The criteria that have been used here will determine optimum values for the proportional and integral control gains, a and b, at one particular flight condition. However, as K_β and τ_{ep} vary over a range of flight conditions, the optimum values of a and b will also vary. Some studies have been made of adaptive control methods for propellers, which are discussed later in this report. But normal propeller control systems have fixed gain values, which must be selected to give satisfactory performance over the full range of flight conditions. Reasonably acceptable gain values can be obtained by using the average between the maximum and minimum values of each gain, computed at the flight condition extremes. However, by using analog computer simulation of the engine and propeller control loop, a more thorough evaluation may be made to determine the gain values that are the best compromise for all conditions.

CONTROL FUNCTIONS FOR SPECIAL CONDITIONS

Fuel and Propeller Coordination

A desirable control arrangement for a turboprop engine is one in which a single lever in the cockpit varies power by simultaneously manipulating the engine fuel control and the speed setting of the propeller governor. Such a single lever control is desirable for use as a height control on VTOL airplanes. However, this approach leads to some problems. Advancing the lever to increase power applies a command for increased speed to the propeller governor as well as increased fuel flow to the engine. As a result of the lag of engine response, speed is not influenced initially by the fuel change. The propeller governor therefore reduces blade angle in order to initiate a speed increase. The first reaction to advancing the power lever is then a reduction in thrust, which is just the opposite of the response desired. As the delayed influence of fuel flow becomes effective, the engine accelerates in response to both increased fuel flow and decreased blade angle. This results in a large overspeed transient before coming to equilibrium at the new power setting. At this new equilibrium point, the blade angle returns to approximately the same position as before the power change, since increased power would naturally cause a speed increase if blade angle remained fixed. This implies that the power transient would be smoother if blade angle were prevented from varying until the fuel response was finished.

As a result of large power changes a compressor surge condition is approached in some cases. This approach to surge is from either an increase of fuel flow or a decrease of blade angle. If both occur together, the worst approach to surge is obtained.

In order to prevent a reduction in thrust, a speed overshoot, and the approach to surge, it is desirable to have a control system in which acceleration is caused by fuel flow change alone, and blade angle is prevented from varying until the fuel transient is completed.

In some turboprop controls, fuel and speed coordination has been achieved by introducing a mechanical lag in the linkage to the speed set input of the governor. By approximately matching this lag to the engine response, satisfactory response of speed and fuel flow to a single lever is obtained.

A better approach uses the system shown schematically in Figure 22 . In this case, the speed-set signal is applied only to the integral term, and the proportional term responds to angular acceleration of the propeller. The sum of these two terms is a signal of blade angle rate, which is converted to blade angle position by an integrating servo. With this control system, a combined speed and fuel flow command results in very little blade angle change. The decreasing blade angle rate resulting from a higher speed set command to the integral term is opposed by an increasing blade angle rate caused by the speed response to fuel flow change sensed by the proportional term. With proper limits and gain values, these two responses effectively cancel so that the response is approximately that caused by fuel flow alone. The control provides a final trimming action of blade angle to achieve the proper equilibrium speed.

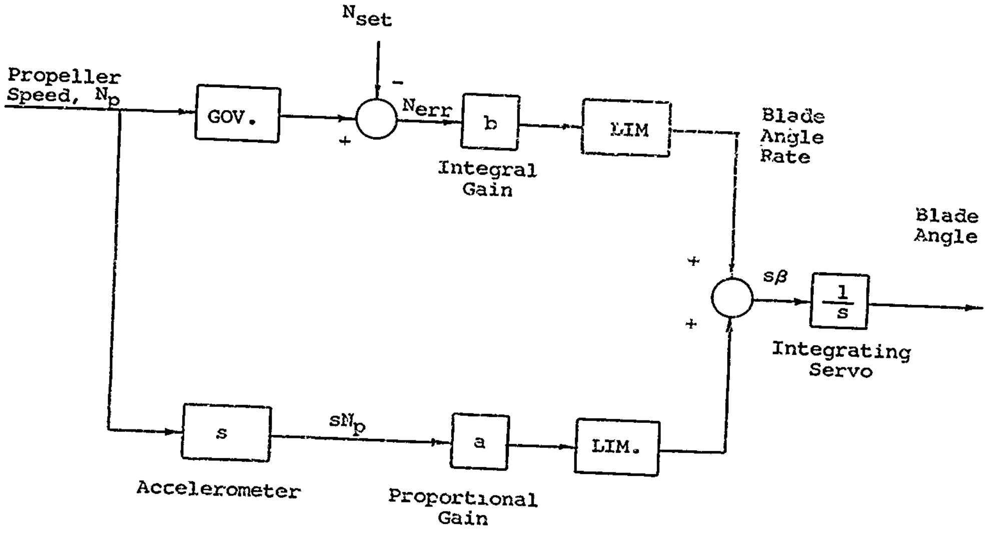
N_{set}
Propeller Speed, N_p
GOV.
+
-
N_{err}
b
Integral Gain
LIM
Blade Angle Rate
Blade Angle
+
+
$s\beta$
$\frac{1}{s}$
Integrating Servo
s
Accelerometer
sN_p
a
Proportional Gain
LIM.

Figure 22. Propeller Control With Speed Set Applied to Integral Term.

An added advantage of this control approach is the response to the startup condition, in which a system accelerates toward the onspeed condition after being initially underspeed. Some control configurations require a crossing of the onspeed point before control action occurs to limit the speed increase. This results in an overspeed peak. The revised system anticipates the approach to onspeed by commencing control action at a lower threshold level where the speed error through the integral term is cancelled by the acceleration response through the proportional term. Speed overshoot is then reduced or eliminated entirely.

Speed Synchronizing

Automatic synchronization of the speeds of multiple engines can be achieved by applying a common speed reference signal to the propeller control systems of all engines. This is typically done by electrical means, such as a synchronous motor in each propeller control for speed reference. An alternator driven by one engine, or a master electric motor in the fuselage, is used to drive all reference motors at a common speed. Comparison of each individual propeller speed with that of each reference motor provides a speed error signal to the propeller control, which varies blade angle until the speeds agree. The diagram of Figure 23 illustrates schematically the speed synchronizing relations.

Using the proportional-plus-integral control function which has been described previously, the blade angle of each propeller will vary until the propeller speed matches the common speed reference. The use of speed synchronizing does not change the response or stability of the control system, and the analytical treatment of each propeller control loop is the same as the analysis that has been previously presented for control of a single propeller.

Phase Synchronizing

When the speeds of multiple propellers are unsynchronized, beats of sound are produced which are uncomfortable to crew and passengers. As the speeds approach synchronism, the beat frequency decreases and the peaks and nodes of sound vary more slowly until they stop at the point of synchronization. The point at which they stop may be a peak or a node, and may slowly alternate between them at random. In addition to speed synchronization, it is therefore desirable to control the relative angular blade positions between propellers so that the sound remains at a node when synchronized. This will provide minimum noise to improve the comfort of crew and passengers, and also reduce vibration levels in the aircraft

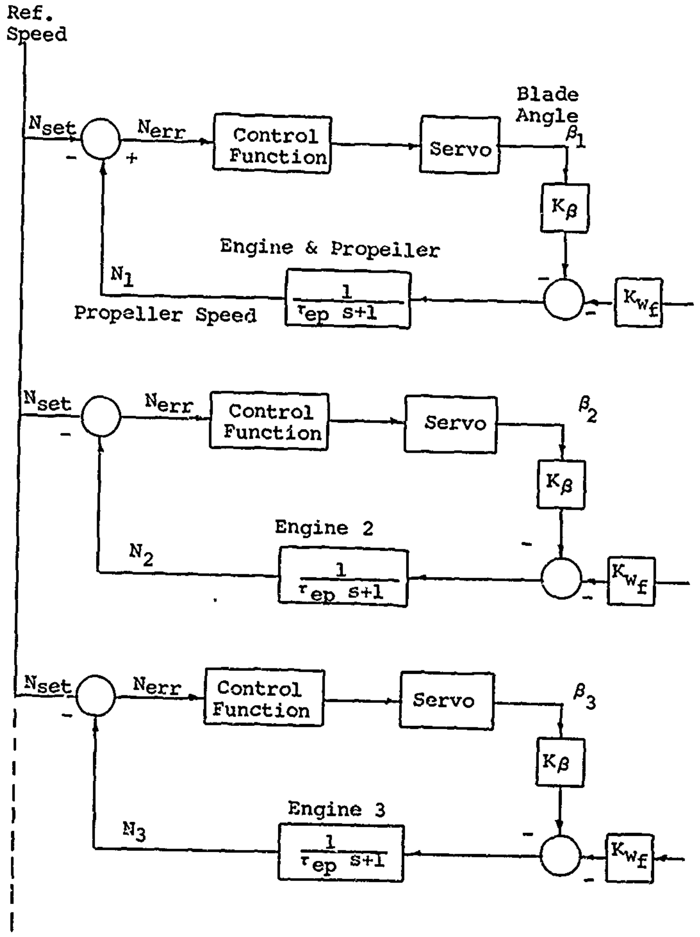
Ref. Speed
N_{set}
N_{err}
-
+
Control Function
Servo
Blade Angle
β_1
K_β
Engine & Propeller
N_1
$\frac{1}{\tau_{ep}\, s+1}$
Propeller Speed
K_{w_f}
-
-
N_{set}
N_{err}
-
Control Function
Servo
β_2
K_β
Engine 2
N_2
$\frac{1}{\tau_{ep}\, s+1}$
K_{w_f}
-
-
N_{set}
N_{err}
-
Control Function
Servo
β_3
K_β
Engine 3
N_3
$\frac{1}{\tau_{ep}\, s+1}$
K_{w_f}
-
-

Figure 23. Speed Synchronizing Control Relations.

structure. In general, this minimum sound level is achieved when adjacent propellers are out of phase so that the blade passage of one propeller is between two blade passages of the next. The exact phase relation for minimum noise can be adjusted experimentally in flight when a phase synchronizing control term is present.

Control approaches for achieving blade phase synchronization are shown schematically in Figure 24. In all of the arrangements, a basic requirement is the phase sensing device which compares the angular position of each propeller with a common phase reference source. One phase sensing approach utilizes engine-mounted alternators that produce an a-c signal as an indication of propeller position. A phase discriminator then compares the signal from each engine alternator with that of a common reference alternator and emits an electrical signal of the phase error.

Arrangement A shown on Figure 24 illustrates the addition of a phase synchronizing term to a typical proportional-plus-integral propeller speed control system. The phase error provided by the phase discriminator is applied to a phase control gain term which develops a rate of blade angle change proportional to phase error. This represents a blade angle increment varying as the time integral of phase error, which is added to the basic blade angle signal from the speed control terms. A limited magnitude of blade angle variation is permitted for the phase control term so that the speed control has full authority until speed is synchronized, after which the phase term adjusts blade angle until propeller phase is synchronized.

Arrangement B shown on Figure 24 illustrates a method for adding phase synchronization to a speed control that is basically mechanical. A mechanical signal of speed error is developed by comparison of a shaft driven by propeller speed with the speed reference provided by a synchronous motor driven by a master alternator. The proportional and integral control terms are provided mechanically in the propeller governor to drive a mechanical pitch change servo. The electrical phase error term from the phase discriminator is applied to the propeller control by adding an electrical speed change, or frequency shift, to the alternator frequency which drives the synchronous motor. The speed change is typically a sinusoidal function of phase error, with inherent limited authority. In this case, the phase term is fed through both the proportional and integral terms of the propeller speed control so that gain relationships among the three terms are somewhat interdependent.

Arrangement C shows the addition of a phase synchronizing term to a propeller control in which the speed error signal is applied only to the integral term. This may be desirable for

Arrangement A. Phase Control Correction Added to Blade Angle Output of Control.

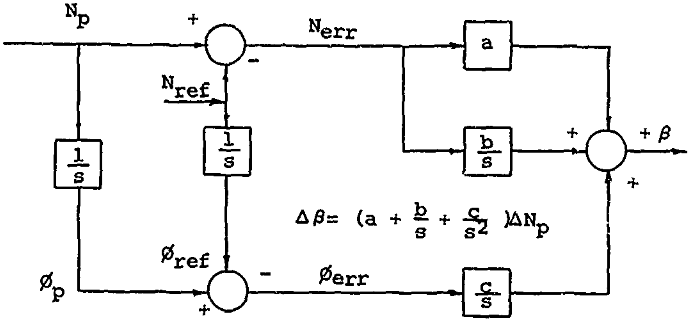

N_p
+
N_{err}
-
N_{ref}
a
$\frac{b}{s}$
+
$+\beta$
+
$\frac{1}{s}$
$\frac{1}{s}$
$\Delta\beta = (a + \frac{b}{s} + \frac{c}{s^2})\Delta N_p$
ϕ_{ref}
ϕ_p
-
ϕ_{err}
$\frac{c}{s}$
+

Arrangement B. Phase Control Correction Added to Speed Reference Input of Control.

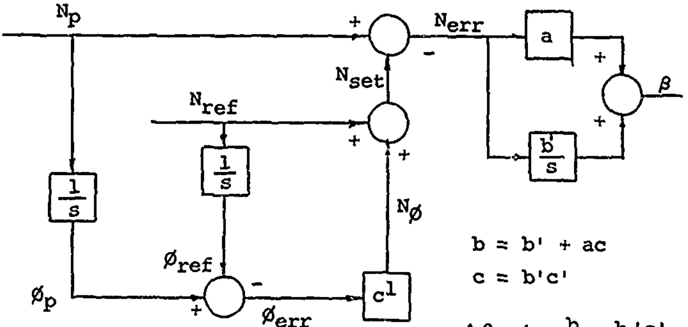

N_p
+
N_{err}
a
-
+
N_{set}
β
N_{ref}
+
+
+
$\frac{b'}{s}$
$\frac{1}{s}$
$\frac{1}{s}$
N_ϕ
$b = b' + ac$
$c = b'c'$
ϕ_{ref}
-
ϕ_p
+
c^1
ϕ_{err}

$$\Delta\beta = (a + \frac{b}{s} + \frac{b'c'}{s})\Delta N_p$$

N_p = Propeller speed
N_{ref} = Reference speed
N_{err} = Speed error
ϕ_p = Angular position of propeller
ϕ_{ref} = Reference angular position
ϕ_{err} = Angular (phase) error
a = Proportional gain
b = Integral gain
c = Phase sync. gain
s = Differential operator

Figure 24. Phase Synchronizing Propeller Control Approaches.

Arrangement C. Phase Control With Speed Set Applied to Integral Term.

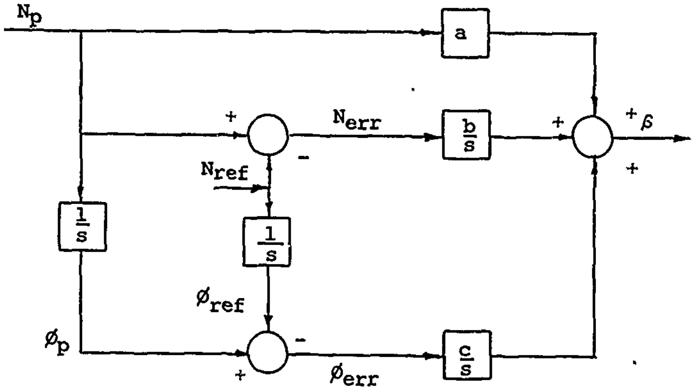
N_p
a
+
N_{err}
$\frac{b}{s}$
+
+ β
-
+
N_{ref}
$\frac{1}{s}$
$\frac{1}{s}$
ϕ_{ref}
ϕ_p
-
$\frac{c}{s}$
+
ϕ_{err}

Arrangement D. Phase Control With Acceleration Sensing Speed Control

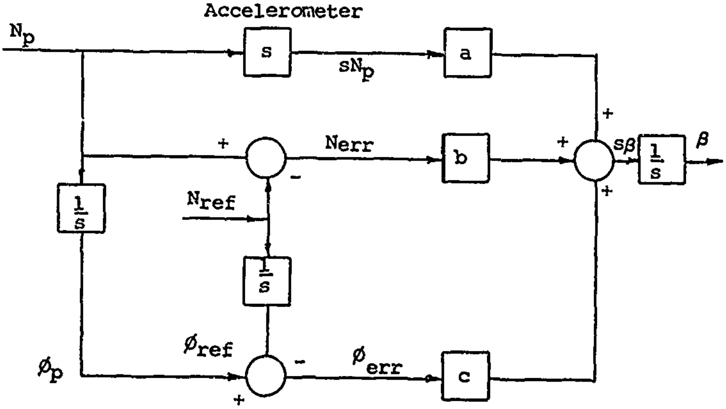
Accelerometer
N_p
s
sN_p
a
+
+
N_{err}
b
+
$s\beta$
$\frac{1}{s}$
β
-
+
N_{ref}
$\frac{1}{s}$
$\frac{1}{s}$
ϕ_{ref}
ϕ_p
-
ϕ_{err}
c
+

Figure 24. Continued.

purposes of fuel and propeller coordination using a single power lever, as discussed previously. In this arrangement, the proportional term must be provided by a speed sensing method which can cover the full range of control speed variation. A mechanical flyweight governor is not practical for this purpose, since it can only sense speed errors for a limited range about a nominal reference point.

Arrangement D illustrates a more practical approach for a mechanical phase synchronizing control in which the speed error signal is applied only to the integral term. The arrangement shown here is similar to that presented in the previous paragraphs on Fuel and Propeller Coordination, in which the proportional control term responds to angular acceleration of the propeller. The proportional, integral and phase synchronizing terms all provide signals of blade angle rate, which are summed and then integrated by the servo actuator to provide an output proportional to angle position. Appropriate limits of authority in which proportional and integral terms are approximately equal, and the phase term is much smaller, will permit smooth speed control followed by phase synchronizing after speed equilibrium is reached.

In all of the phase synchronizing arrangements which have been shown, the basic response of blade angle to propeller speed variation is the same. Ignoring the dynamics of the servo actuator, the control response equation is

$$\frac{\Delta\beta}{\Delta N_p} = a + \frac{b}{s} + \frac{c}{s^2} \qquad (79)$$

When this control transfer function is combined with the servo actuator dynamics and the transfer function for engine and propeller response, the open-loop transfer function becomes

$$\text{Open-loop function} = \frac{K_\beta\,(as^2 + bs + c)}{s^2(\tau_{ep}s + 1)(\tau_c s + 1)} \qquad (80)$$

A good value for the phase synchronizing gain coefficient, c, can be determined by using a damping ratio of approximately .7 to .8 in the numerator quadratic term. This has been found to give the best performance by servo analysis methods and by analog computer simulation. Having obtained values for proportional and integral control gains, (a) and (b), by use of the relationships which have been discussed previously under speed control descriptions, a value may be obtained for the coefficient (c) by the following steps:

Express the numerator in the form

$$\text{Numerator} = cK_\beta(\frac{a}{c}\, s^2 + \frac{b}{c}\, s + 1)$$

The natural frequency and damping may be expressed as

$$\omega = \sqrt{\frac{c}{a}}$$

$$\frac{2\zeta}{\omega} = \frac{b}{c}$$

From these, the expression for (c) is

$$c = \frac{b^2}{4\, a\, \zeta^2}$$

For example, typical values for the proportional and integral terms of a turboprop speed control are

$$a = .1\ \frac{\text{deg}}{\text{rpm}}$$

$$b = .2\ \frac{\text{deg/sec}}{\text{rpm}}$$

Using a numerator damping ratio of $\zeta = .8$, the three gain terms of a phase synchronizing control become

$$a = .1\ \frac{\text{deg}}{\text{rpm}}$$

$$b = .2\ \frac{\text{deg/sec}}{\text{rpm}}$$

$$c = .156\ \frac{\text{deg/sec}^2}{\text{rpm}}$$

ADAPTIVE PROPELLER CONTROLS

With the requirement for improved controls for use with turboprop engines the concept of adaptive propeller controls was examined. Although the adaptive controls were never used for production propellers, it became apparent that with advanced installation where a large range of flight conditions is encountered, such controls are needed to provide satisfactory operation over the entire flight range. The concept of adaptive propeller controls is therefore presented, as it may also be desirable for use on V/STOL aircraft.

Compensation for Varying Flight Conditions

Typical turboprop governors were made to provide good propeller control performance over the normal range of operating conditions by the selection of suitable fixed values of proportional and integral control gains. With the addition of phase synchronizing and further aircraft developments which extended the ranges of airspeed, altitude, and power variations, the fixed integral control gains did not give satisfactory control characteristics over the entire range. Thus the need developed for some form of adaptive propeller control system to compensate for the increased variations of engine and propeller response characteristics.

The objectives of the adaptive control approach are the use of simple control gain manipulations in response to easily obtainable measurements within the engine and propeller system that will compensate for variations of response characteristics that are encountered. An effective approach is established by determining the correlation of the engine and propeller gains and time constants with variations of airspeed, altitude, and power conditions. Correlation is also obtained of propeller speed and blade angle with power conditions and airspeed. From these correlations, a relatively simple approach is developed for varying control gains in accordance with propeller rpm and blade angle to accomplish a major portion of the adaptation necessary to compensate for gain and time constant variations.

Correlation of Gain and Time Constants

Using the methods that have been presented previously, engine and propeller derivatives are computed for a broad range of airspeeds, altitudes and power conditions. These derivatives can be combined into the form of engine and propeller gain and time constant which define the propeller control characteristics. When these gain and time constant values are plotted against the corresponding values of airspeed, altitude, blade angle, and propeller speed, the conditions for correlation are apparent.

An example of the type of correlation that is found is shown in Figure 25, which illustrates the relation of engine and propeller time constant to variations in airspeed, power and altitude. The time constant decreases as airspeed increases, but higher altitudes cause the time constant to become greater. The influence of engine power variation on the time constant is present but is not very strong. A similar plot showing the relation of time constant to blade angle instead of airspeed is shown in Figure 26. This plot is almost identical to the airspeed relation, showing that there is a strong correlation between blade angle and airspeed. The trend with altitude is also similar in these two plots, but the weak response to power variation is reversed.

Plots of the relation between time constant and variations of turbine speed and engine power showed no correlation. This indicated that turbine speed is not a useful parameter for the indication of time constant variation.

The plot of engine and propeller gain, K_β, shown in Figure 27, illustrates the variation of the gain coefficient with engine speed, power and altitude. In this case there is a strong correlation between the gain K_β and engine speed. Correlation of the gain with power and altitude is not sufficient.

Plots of the relation of gain to airspeed, power and altitude showed that no correlation existed between gain and airspeed. As might be expected from the close relationship between airspeed and blade angle, there was also no correlation between gain and blade angle.

The results of these correlation studies showed that the two significant engine and propeller performance parameters of gain and time constant can be related to three measurable conditions. These conditions are blade angle, propeller speed and altitude. This implies that control system gains could be manipulated by functions of these three parameters in such a manner as to completely compensate for variations of engine time constant and gain variations. Measurements of altitude might be difficult to introduce into a control system, but measurements of propeller speed and blade angle exist in some form in any propeller control. Ignoring altitude variations and adjusting control system gains in relation to the other two parameters, propeller speed and blade angle will still provide a major portion of the necessary compensation for variations of flight conditions. Even without altitude compensation, the resulting variable-gain control system will provide

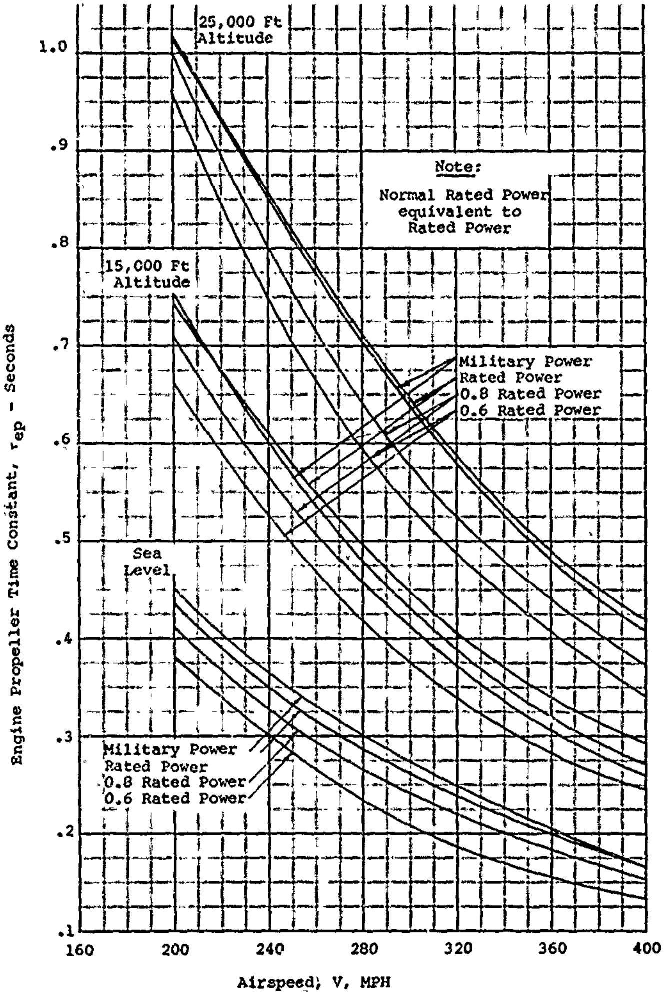

Figure 25. Variation of Engine and Propeller Time Constant With Airspeed, Power and Altitude.

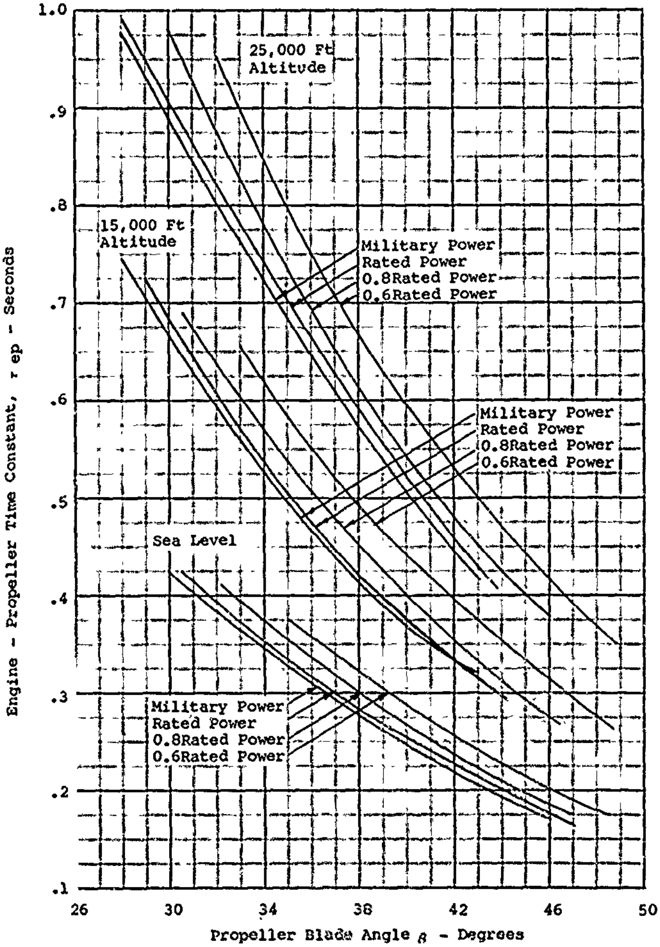

Figure 26. Variation of Engine and Propeller Time Constant With Blade Angle, Power and Altitude.

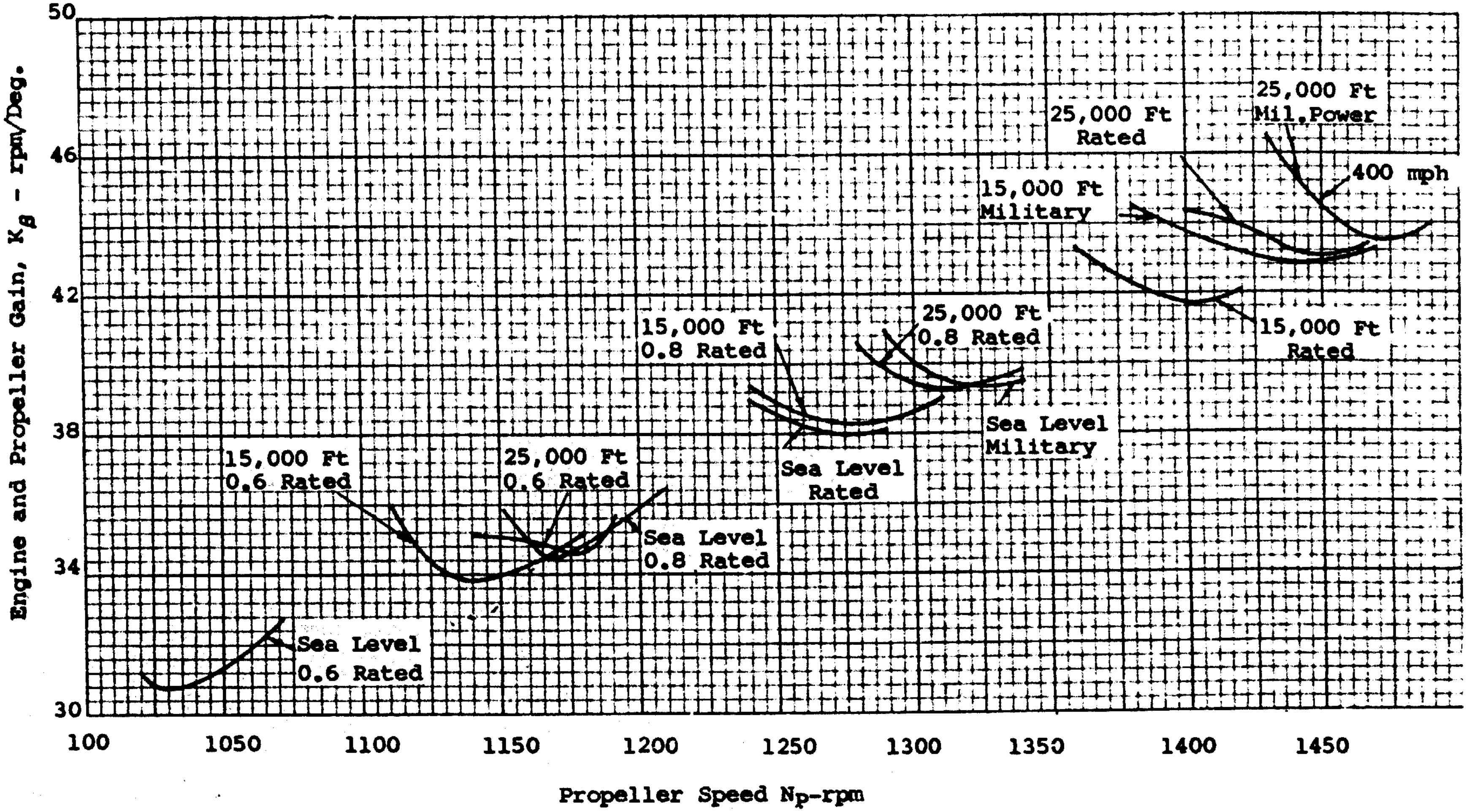

Figure 27. Variation of Engine and Propeller Gain With Propeller Speed, Power, Altitude and Airspeed.

a major improvement over the normal fixed-gain system.

Control Gain Compensation

Having determined the influence of flight conditions on engine and propeller response characteristics, the final step is to establish the corresponding variations that must be made in control gains to preserve uniform system response at all conditions. As shown previously, the complete open-loop transfer function for a phase synchronizing control system combined with engine and propeller characteristics is

$$\frac{K_\beta \, (as^2 + bs + c)}{s^2(\tau_{ep} \, s + 1)(\tau_c \, s + 1)} \tag{81}$$

In this expression, the τ_c control lag may actually be two or more lags in series. However, for purposes of establishing control gain relations, the essential principle is illustrated by expressing the control lags by a single unvarying time constant. This represents the relatively constant control system dynamic terms which are unaffected by variation of flight conditions.

The initial step in determining control gain requirements is to examine the system with (a) and (b) terms alone. The phase synchronizing term, (c), does not become effective until speed has become stabilized. The initial open-loop expression for speed control is the proportional-plus-integral function that has been previously defined as

$$\frac{bK_\beta \, (\frac{a}{b} \, s + 1)}{s(\tau_{ep} \, s + 1)(\tau_c \, s + 1)} \tag{82}$$

The criteria that have been previously defined for good control performance are

$$\frac{a}{b} = \tau_{ep} \tag{83}$$

$$bK_\beta \tau_c = \text{constant} \tag{84}$$

Using these relations and the correlations with flight conditions that show a relation of τ_{ep} to blade angle and K_β to propeller rpm, the necessary relations of the control gains to speed and rpm can be determined. Since τ_c is a constant, the integral gain, the value of (b), must vary in inverse proportion to the engine-propeller gain K_β in order to preserve the product $bK_\beta\tau_c$ as a constant. As K_β varies in proportion to propeller speed, (b) must therefore vary in inverse proportion to propeller speed.

Figure 28 repeats the plot of time constant variation in relation to blade angle and altitude conditions. Superimposed on this plot are a line representing an average value of τ_{ep} and a negative proportional line for the ratio a/b which provides a good compromise for control purposes. By using this a/b relationship to blade angle, and the inverse relationship of (b) to propeller speed, a well compensated speed control is obtained.

Compensation for the phase synchronizing control gain, (c), can be determined from the damping relationship that has been presented previously:

$$\frac{c}{b} = \frac{1}{(4\,\zeta)^2}\left(\frac{b}{a}\right) \qquad (85)$$

This shows that ratio c/b should vary in inverse proportion to the ratio a/b which has been related to the time constant τ_{ep}. Since τ_{ep} has been shown to vary inversely in relation to blade angle, this indicates that the ratio c/b should vary in direct proportion to blade angle. The plot of Figure 29 shows the resulting relationship between the a/b ratio, the c/b ratio, blade angle and τ_{ep}.

The resulting gain-compensated control system, which has been defined by this analytical approach and verified by computer simulation, has been included in the design of an advanced propeller development program. In summary, the control compensation relations that have been used are:

1. To compensate for variations of engine and propeller gain, K_β, all three gain terms, (a), (b), and (c), should vary simultaneously in inverse proportion to K_β. This may be accomplished by varying an overall gain term in an inverse or negative proportional relation to propeller speed.

2. The ratio of the proportional gain, (a), to the integral gain, (b), should vary in proportion to the time constant, τ_{ep}. A satisfactory compensation

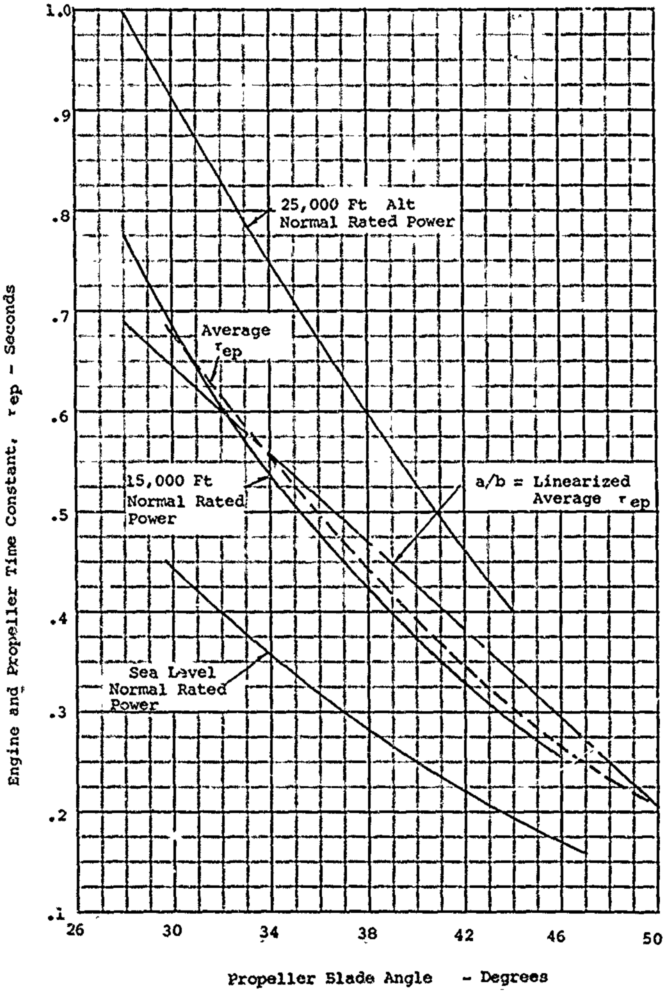

Figure 28. Variation of Engine and Propeller Time Constant Related to Gain Ratio Compensation.

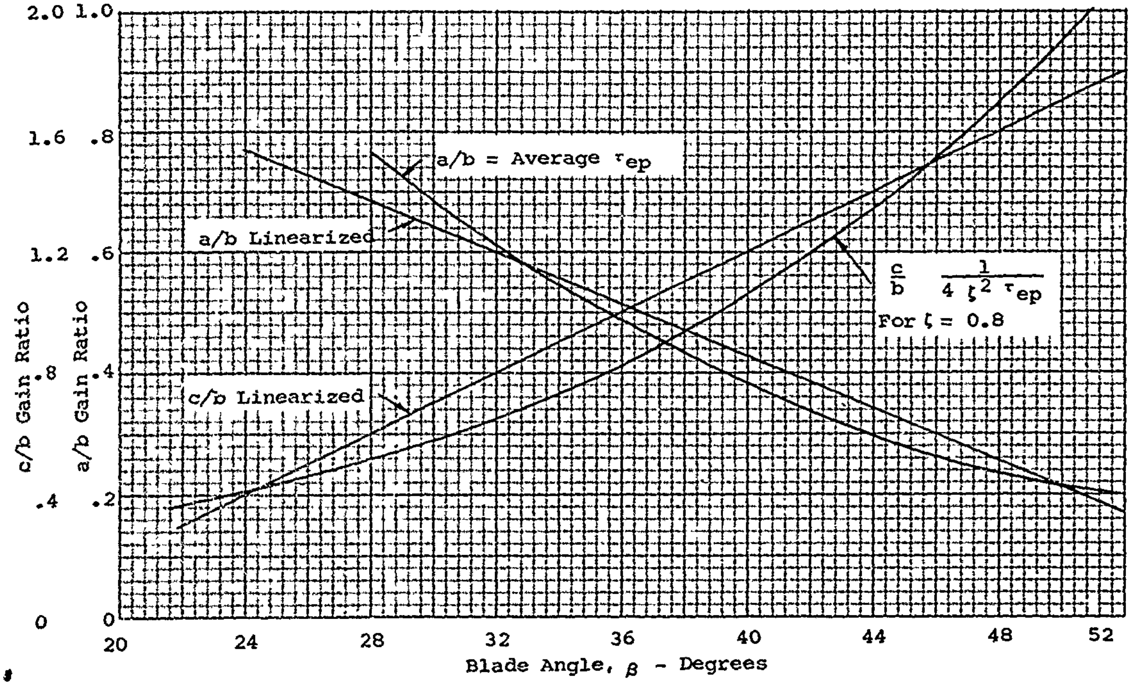

Figure 29. Propeller Control Gain Compensation Relations.

for this a/b ratio can be obtained by varying this term in negative proportion to blade angle alone, since the relation of τ_{ep} to blade angle is negative.

3. The ratio of the phase synchronizing gain, (c), to the integral gain, (b), should vary in negative proportion to τ_{ep}. Satisfactory compensation can be obtained by causing the ratio c/b to vary in direct proportion to blade angle.

Further work is needed on the application of the concept of adaptive propeller controls to work out the hardware requirements and to prove the system by test over the entire range of operation.

TURBOPROP CONTROL DESIGN

Design Philosophy

The basic concept of propeller controls for turboprop engines follows the original approach used for reciprocating engines. In that system, the blade angle actuator consisted of an electric motor, with a suitable gear reduction, acting to increase or decrease blade angle in response to governor offspeed signals. When the onspeed condition was reached, the motor was de-energized and a brake was engaged to hold the blade angle fixed. The maximum rate of pitch change during speed governing was of the order of 3 degrees per second. By means of oscillating contacts at the governor, the motor was energized in a series of pulses, with the "on" time varying in proportion to the speed error. This resulted in a varying average rate of pitch change proportional to speed error, which is an integral control function, as discussed in the previous section concerning control relations.

A maximum rate of 3 degrees per second was adequate for speed governing purposes, but an increased rate of approximately twice the basic rate was provided for feathering or reversing the propeller on reciprocating engines by applying a booster generator to increase the motor voltage for short periods of time.

For turboprop engines, the blade angle rate requirements are much higher than for reciprocating engines. This is particularly true in the case of reversing, where rates of the order of 20 degrees per second are required to prevent engine overspeeds. An electric motor of sufficient power to achieve such blade angle rates would be prohibitive in size. To provide the necessary rates with reasonable size and weight, one approach was to use the power of the engine itself to vary blade angle. This was accomplished by mechanical clutches which are electrically engaged to couple the rotation of the engine shaft through suitable gearing to the propeller blades. Two clutches are utilized, one geared to produce increasing blade angle, and one to produce decreasing blade angle. When neither clutch is energized, a brake is engaged to hold the blade angle fixed.

Electrical signals to engage the appropriate clutch and disengage the brake are obtained from a set of contacts driven by the speed governor. For the higher response requirements and the greater range of flight conditions encountered with turboprop engines, a simple integral control system is not adequate. Therefore, a proportional-plus-integral governor is used as the speed control system.

The output of the speed control is a shaft position proportional to the desired blade angle. Comparison of the governor output shaft with a shaft driven by actual blade angle provides a mechanical error position which actuates the electrical contacts to engage the clutches. This makes the clutch system a closed-loop servo actuator which drives the propeller blade angle to match the desired angle from the speed control governor. The actuator arrangement used in this system is described in the section Hub and Blade Actuator Design.

Speed Governor

A schematic diagram of the mechanical governor and actuator arrangement is shown in Figure 30. As shown in this diagram, one shaft rotates at a "reference speed" which represents the desired propeller speed. The reference speed is developed either by the electrical reference motor for speed synchronizing, or by a mechanical flyweight governor which strokes a variable ratio drive. The relation between governor stroke and the variable drive ratio is matched so that the reference speed is maintained at approximately the correct level during offspeed conditions. An electrically operated solenoid clutch selects between the synchronous motor reference and the mechanical reference.

The difference between propeller speed and reference speed is obtained with gear differential D1. The output shaft of this differential rotates at a rate proportional to speed error, and the shaft position is therefore the time integral of speed error.

Variable ratio drive V2 and gear differential D2 are combined in a feedback loop that acts to match the output speed of V2 to the reference speed. The output shaft of differential D2 rotates to the angular position necessary to stroke the ratio

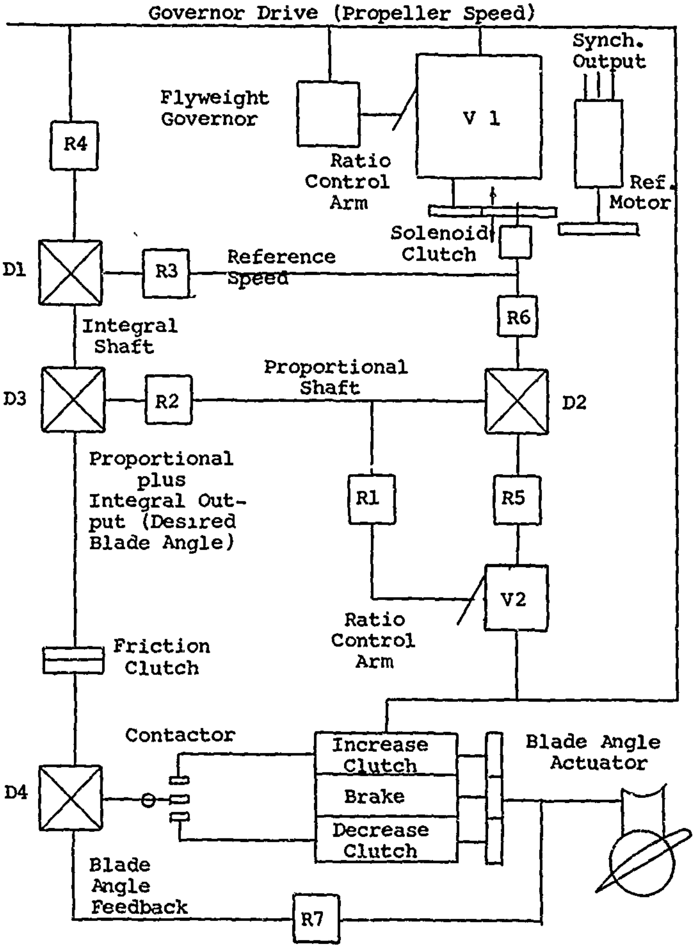
Governor Drive (Propeller Speed)
Synch. Output
Flyweight Governor
V 1
R4
Ratio Control Arm
Ref. Motor
Solenoid Clutch
D1
R3
Reference Speed
R6
Integral Shaft
Proportional Shaft
D3
R2
D2
Proportional plus Integral Output (Desired Blade Angle)
R1
R5
V2
Ratio Control Arm
Friction Clutch
Contactor
Increase Clutch
Brake
Decrease Clutch
Blade Angle Actuator
D4
Blade Angle Feedback
R7

R = Gear Ratio
D = Gear Differential
V = Variable Ratio Drive (Speed Changer)

Figure 30. Mechanical Governor Schematic Diagram.

control arm of V2 to the proper speed ratio. When the output speeds are matched, the ratio control arms of V1 and V2 have equal positions, which are proportional to speed error. This loop is essentially a mechanical power amplifier that repeats the governor speed error position that appears at the ratio control arm of V1. Since the force capability of the governor is low, this amplification has been used to provide a shaft position at the output of D2 which is proportional to speed error and has adequate torque and stroke. By suitably high gear ratios around the loop, a short time constant is maintained for this mechanical amplifier stage.

The integral control signal from the output of differential D1 and the proportional control signal from the output of differential D2 are added in differential D3. The output of D3 is then a shaft position which is a proportional-plus-integral function of speed error. This shaft position is the governor output signal of desired blade angle.

By appropriate selection of gear ratios, the desired values of proportional and integral gain are obtained. For typical turboprop engines and propellers with which this governor system has been used, a proportional gain of $a = .1$ deg/rpm, and an integral gain of $b = .2$ (deg/sec)/rpm have given good performance over the full range of flight conditions.

Actuator Relations

The schematic diagram of the governor system, Figure 30 , also illustrates the manner in which the actuator is connected to the governor. The governor output shaft representing desired blade angle is connected through a friction clutch to gear differential D4. The friction clutch has the purpose of permitting the output of the governor to rotate and avoid damage when the actuator is not able to respond. This can occur during the Beta regime or under power conditions where low blade angle limits have been reached.

During normal governing operation, the actual blade angle is compared with the desired blade angle in gear differential D4. Any disagreement between the two appears as a blade angle error at the output shaft of D4. Rotation of this output shaft moves the arm of a contactor to energize the appropriate actuator clutch and disengage the brake. The actuator clutches are designed for full engagement without slipping. When engaged, the blade angle rate is much higher than the governor output rate, so that a small pulse of blade angle change occurs and returns the contactor arm to the neutral position through the feedback path. This releases the clutch and engages the brake. Sufficient dead-zone is present in the contactor to permit the brake to bring the blade angle drive to a stop before the opposite contact is energized.

Synchronized Constant Speed

The synchronizer control consists of two basic elements: the synchronizer master unit, which is mounted in the fuselage, and a synchronous reference motor mounted on each propeller governor. The synchronizer master unit is an accurately controlled motor-generator set, operating from the 28-volt DC power source, which supplies an AC output of the desired frequency. This output frequency represents the desired propeller speed, and is adjusted by the power lever. The output operates the synchronous reference motors in each propeller governor to provide a stable speed reference which is identical for all propellers.

The synchronous reference motor in each governor is supplemented by the standby mechanical speed reference, to make the governor completely self contained. The speed of the mechanical reference is varied by a linkage from the engine power coordinator, which sets the governor reference at approximately the same speed as the synchronizer master unit.

In the event of failure of the synchronizing system, the mechanical speed reference is automatically engaged by a governor speed error switch which releases the solenoid clutch and disengages the synchronous motor.

Individual nonsynchronized control of engine speed may also be selected manually by operation of the synchronizer reset switch. When this switch is opened, the governor clutch is de-energized, and the mechanical speed reference is engaged.

Limit Switches and Stops

Electrical limit switches are provided to confine blade angle travel to the required operating ranges. Mechanical limit stops are provided at feather, air start and low pitch blade angles, as well as at high reverse pitch. Intermediate stops at air start or low pitch limits are retracted under conditions where they are not needed, such as during reverse operation.

Ground Operation

Blade angle follow-up operation for reversing and ground handling is provided by motion of the power lever into the Beta range. The Beta control signals are transmitted mechanically from the power lever to one side of the Beta differential. Actual blade angle is transmitted to the other side of the differential. The output of the Beta differential moves the arm of a contactor which is similar to that at the governor output. During Beta operation, electrical power is removed from the governor contactor and applied to the Beta contactor, which then energizes the appropriate actuator clutch until the desired blade angle is obtained.

Reverse thrust operation for ground braking after landing is achieved by moving the power lever into the reversing region of the Beta range. This retracts low pitch stops and applies a signal of negative blade angle to the blade angle actuator, which causes the decrease pitch blade angle clutch to be engaged until the desired reverse pitch angle is reached.

Motion of the power lever in the reversing range also varies engine power, which can be a high percentage of rated power at the maximum reverse position. Rapid motion of the power lever to the full reverse position immediately after landing will apply a command for high engine power to the fuel control while propeller blade angle is varying from forward to reverse pitch. A high blade angle rate is necessary to prevent overspeeding of the engine and propeller as blade angle varies through low angles before reaching a sufficiently high reverse pitch position to absorb the engine power.

This reversing condition defines the required maximum blade angle rate for propeller actuator design. The plot of Figure 31 presents the results of computations used in selecting the required blade angle rate for a typical turboprop installation. This plot illustrates the time response of engine and propeller speed as blade angle varies to the reverse position while a constant fuel flow equivalent to 1250 horsepower is applied. The response shows that a blade angle rate of 20 deg/sec is satisfactory for avoiding an overspeed limit of 1440 rpm using either of two propeller inertia values.

Feathering Manual

Feathering is accomplished by energizing the increase-pitch clutch and releasing the brake by one or both of two parallel systems. Normally the energization is electrical, either from a cockpit control or as an automatic feathering signal from the engine. A parallel mechanical feathering system may also be provided, which can be actuated by a cable or shaft system from the cockpit control. The mechanical system releases the brake and engages the increase pitch clutch by cam action.

Mechanical and electrical feathering may be accomplished simultaneously from independently actuated cockpit controls without compromising the operation of either system. This is particularly important for turboprop installations which require

Initial Conditions: 60 mph, 1200 N_p, 1250 hp,
Sea Level, Standard Day

Propeller: 14 feet Diameter, Three Blades

Engine: T-55 - Fixed Fuel Flow

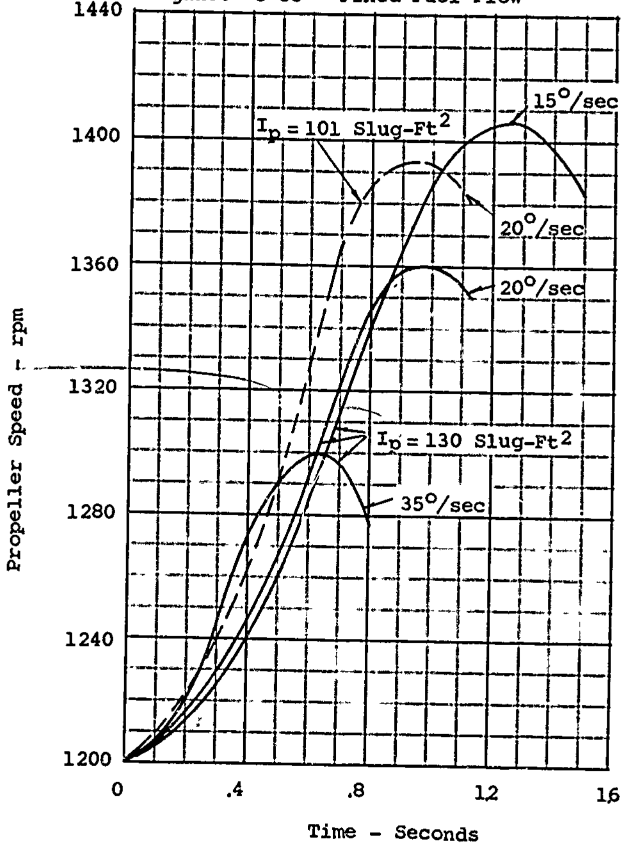

Figure 31. Speed Response During Blade Angle Reversal.

reliable feathering in the event of turbine failure.

Negative Torque Controlled Feathering

Controlled feathering is utilized to avoid high drag forces in the event of engine failure. This type of feathering is initiated automatically by a torque switch in the engine reduction gearing which is actuated whenever negative torque occurs.

Without controlled feathering, the governor would attempt to maintain propeller speed by reducing blade angle if an engine power failure should occur. When the propeller drives a turboprop engine, the resulting drag can be very high, and may endanger control of the aircraft if allowed to continue. This high drag results from the large amount of energy that can be absorbed by the compressor, which is derived from the windmilling propeller in forward flight. As shown by Figure 32 this drag can be of the order of 40% of takeoff thrust in the case of a burner-off power failure. Even greater drag will result if the turbine wheel fails and can no longer recover a portion of the compressor energy. In this case, the drag can exceed 100% of takeoff thrust.

Controlled feathering converts the characteristics of the turboprop engine into an advantage by utilizing the kinetic energy stored in the rotating parts of the dead engine on a controlled basis to provide positive thrust until almost all of the energy has been converted to help propel the airplane. Controlled feathering also prevents excessive torque on the engine shaft and gearing which would result if the propeller went immediately to feather at high engine rpm.

This system operates on a cyclic basis as follows: When the no-torque or negative torque signal is obtained, the torque switch closes, disconnecting the governor circuit and starting the propeller blades toward feather at a high rate of pitch change. As this occurs, the blades absorb positive torque from the decelerating engine and thus produce positive thrust. The positive torque reopens the torque switch and returns the propeller to governor control. This causes the propeller to decrease pitch until zero or a slight negative torque is again obtained, at which point the torque switch will close and the cycle repeats itself.

Figure 33 illustrates the effect of controlled feathering under typical flight conditions. Excessive propeller drag is prevented, and much of the kinetic energy remaining in the propeller and turbine is converted to useful positive thrust.

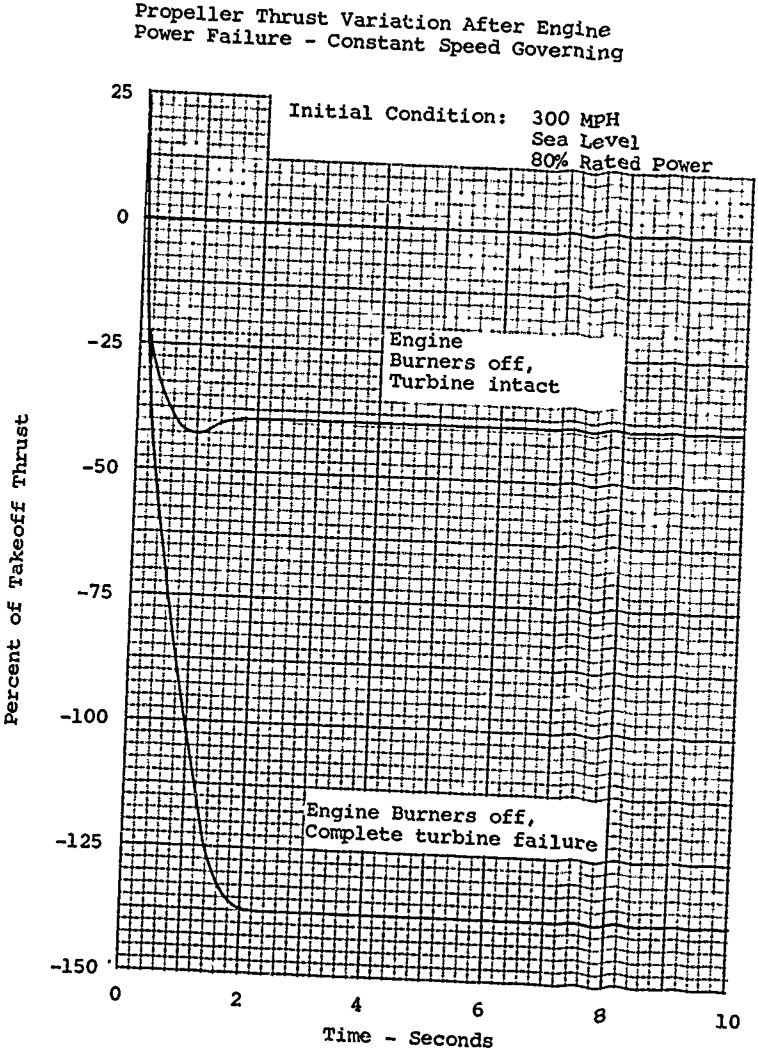
Propeller Thrust Variation After Engine Power Failure - Constant Speed Governing

Figure 32. Windmilling Propeller Drag.

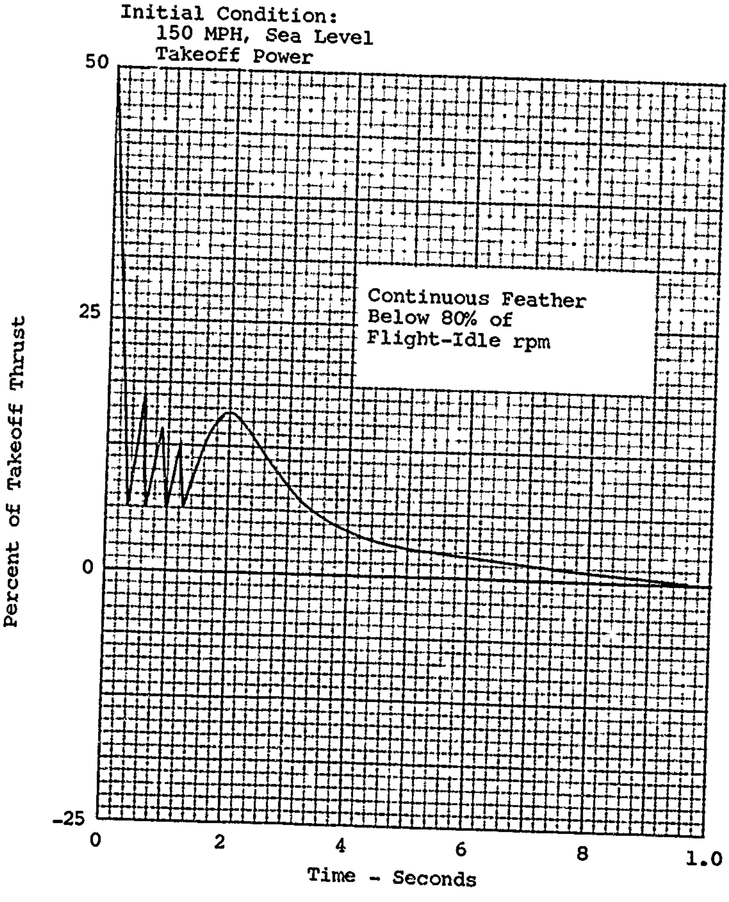

Propeller Thrust Variation
After Engine Power Failure
Controlled Feathering

Figure 33. Controlled Feathering.

PROPELLER APPLICATION

REVIEW OF PAST APPLICATIONS AND TESTS

Some typical propeller installations will be reviewed and discussed to provide an insight for possible future applications and designs. Covered will be the problems encountered in the areas of performance, control, weight, noise, vibrations and structural failures. Also discussed will be the propeller selected for typical CTOL, STOL and V/STOL aircraft and some propeller test results of importance. From this discussion it is hoped to provide a background that will enable the designer to eliminate the many problems that have been encountered, and will provide the basis for the design and selection of propellers for optimizing the total system.

The propeller installations considered cover a range of single and multi-engine configurations for conventional aircraft with reciprocating engines such as the P-47, C-124, B-50, DC-6 and L-1049. Turboprop engine installations such as the C-130, C-133 and B-47 are also covered. Table I gives the important parameters of the typical propeller installations. The power and rotational speed given are the maximum operating values, generally takeoff.

Republic P-47

The Republic P-47 airplane was equipped with a four-blade propeller, and is of interest because it was a very successful WW II fighter aircraft. The airplane first used propellers with narrow blades of approximately 70 activity factor, but as the power rating was increased, the so-called paddle blades were installed which had an activity factor in the range of 100. These blades improved the climb and altitude performance of the airplane as the blade sections operated at lower lift coefficients and thus higher lift drag ratios at these flight conditions.

The P-47 was one of the fastest propeller-driven airplanes of the time, attaining speeds in the range of 475+ mph at altitude. A great deal of effort was made to improve the high-speed performance of the propellers for the P-47 airplane. These efforts were generally unsuccessful as the blades were operating near peak efficiency for the given blade number and propeller diameter; also the techniques for optimizing the blade design were not available, so the last increment of efficiency could not be realized.

Because of its high-speed characteristics, the P-47 airplane was used as a propeller test bed. One of the tests of interest

TABLE I. SUMMARY OF TYPICAL PROPELLER INSTALLATIONS

Airplane	Propeller Model	Blade No.	Dia. Ft	No. of Blades	Blade		Max. rpm	hp_{max}	Engine Type
					A.F.	IC_{Li}			
P-47	C5432S-B	836-3C2-18	13'2"	4	98	.506	1400	2800	Recip.
B-29	C644S-A38	1052-7C4-30	16'8"	4	113	.500		2800	"
B-36	C736SP-A	1129-17C6-30	19'2"	3	135	.370	1000	3800	"
B=50	C644S-A44	1052-20C4	16'8"	4	113	.379		3200	"
B-47	CT8465-A	920-3C6-12	15'0"	4	200	.195		7000	T.P.
DC-6	C632S-B	744-6C2-0	13'6"	3	120	.489	1260	2500	Recip.
CV-240	C632S-B	740-6C2-0	13'0"	3	146	.461	1260	2500	"
L-749	C634S-C500	830-20C4-0	15'0"	3	120	.488	1270	2900	"
L-1049	C634S-C500	858-5C4	15'0"	3	124	.496	.270	3500	"
L-1049C	C634D-A	109652	15'0"	3	115	.500	1270	3500	"
L-1649	C634S-C	958-1C4	16'10"	3	121	.336	1030	3500	"
B-377	C644S-B300	1052	16'8"	4					
C-124A	C634S-C300	1056-7C5	16'6"	3			1150	3500	"
C-124C	C735S-A	1060-6C5	17'0"	3	136	.444	1050	3800	"
C-130	CT6345S-E	862-4C4-0	15'0"	3	150	.338	1020	4400	T.P.
C-133	CT735S-B-102	1060-21C5-12	18'0"	3	128	.355	1000	7000	"
XFV	C(6L8)65S	1060/1061	16'1"	6	146			5000+	"
XFV	"	"	"	"	"				
X-19	-	13166	13'0"	3	166		1200		"
XC-142	5008C	2FE16A3-4	15'6"	4	86	.475	1232	3400	"
CL-84	CHG44PA1	1490A2P3	14'0"	4	90	.498	1228	1500	"

was an investigation of the use of reverse thrust propellers in flight to limit dive speeds. Rather than using dive breaks on the wing for limiting the speed, it was reasoned that the propeller operating at negative blade angles could be used and at a much lower installed weight.

Flight tests of the propeller as a dive brake on the P-47 airplane indicated that high values of negative thrust could be obtained in a dive. Indeed, the tests showed that negative values of thrust in excess of 13,000 pounds could be obtained with the propeller windmilling. Higher values of negative thrust were known to be possible with the addition of small amounts of power. These values of negative thrust can be calculated using the data of Reference 8, and the method given in Volume I. Although high values of negative thrust could be obtained with the reverse pitch propeller which was more than adequate for the intended application, many problems were encountered. One such problem occurred when the blade angle was changed from a positive to a negative value in flight. In this case a region is encountered where large values of negative torque are obtained; as this torque is much higher than that of the engine, severe over-speeding is obtained unless the propeller has a very high rate of pitch change. The pitch change rate required is in the range of 25 to 30 degrees per second. Also, when the propeller is operating at high values of negative thrust, the wake is extremely unsteady with a large amount of energy. This unsteady wake caused very high loads on the tail surfaces of the airplane with shaking, and in one case the loss of a horizontal tail surface. If negative thrust propeller is considered again, these factors must be accounted for in the design.

The P-47 airplane was equipped with a thrust and a torque meter so that the performance of propellers in flight could be measured. Tests were conducted up to forward Mach numbers of 0.8. To obtain this Mach number the airplane was operated in shallow dives. Included in the testing were tests of swept-back blades and blades with very low thickness ratios. These tests indicated that thin blades are equivalent to swept-back blades when designed for equal blade stress. That is, the gain in critical Mach number due to a reduction in thickness ratio is equivalent to that obtained due to sweep. A more complete discussion of these tests is given in Reference 9.

The Boeing B-29, B-50 Airplanes

The B-29 airplane was equipped with four-blade propellers in 16'8" diameter. While the bulk of the fleet used hydraulic propellers, a few special airplanes used electric controlled propellers. The electric propeller was chosen at that time because of ability to provide reverse thrust for an aborted takeoff and breaking during landing. The electric propeller was also chosen as the hydraulic propeller tended to freeze at altitude, thus preventing pitch change.

The B-50 airplane was an increased power version of the B-29. It was equipped with four-blade propellers using an electric motor for pitch change. Although this was a reasonably trouble free installation, there was one serious accident caused by a propeller malfunction. In this case the brake on the electric pitch change motor failed, allowing the blade angle to go to low pitch. This resulted in a large value of negative thrust on one propeller that was uncontrollable and caused the loss of the airplane. This accident was typical of several accidents caused by malfunctioning propellers. The propellers using hydraulic power for changing blade angle also had the tendency to go toward reverse, and several accidents were caused by this type of failure.

The Consolidated B-36

The B-36 airplane used six 3-blade pusher propellers with a diameter of 19 feet. This propeller was the largest production propeller in the world and was one of the few pusher propeller installations. The pusher propeller was chosen for the B-36 as it was considered from an airplane drag point of view desirable to maintain clean free-stream air over the wing. Thus the propeller slipstream could not be tolerated over the wing, and the pusher propeller was selected.

Although the drag penalty caused by the interference of the propellers slipstream was unfavorable, the effects of the wing slipstream produced high alternating blade stresses. These blade stresses were especially high when the wing flaps were lowered. In this case the wake of the flaps caused a severe velocity gradient in the plane of the propeller disc. As a result, each time a blade passed through the wing wake it was unloaded and then loaded, causing a large increase in the vibratory blade stress. The magnitude of this vibratory stress was very high and led to many problems in structural blade fatigue.

Performance and weight were important considerations in the design of the propeller for the B-36, and every effort was made to achieve peak efficiency, especially at the cruise condition. Because of the blade size and pitch change rate requirements, the clutch system shown on page 10 was used for this propeller. Another unusual feature was used on the B-36 propeller was hot air deicing. This system is further discussed on page 293, Volume II.

Boeing B-47D

Although the Boeing B-47 airplane was originally designed using six jet engines, studies indicated that important improvements in terms of extended range could be obtained by replacement of the four jet inboard engines with two turboprop engines. An experimental program was therefore undertaken to evaluate this concept.

To obtain good cruise performance and delay compressibility losses to as high a Mach number as possible, a transonic type propeller was selected. This four-blade propeller used very wide 200 activity factor blades. The blades were designed with low values of thickness ratio and design lift coefficient to delay the compressibility losses and thus give good high-speed performance.

The propeller installation on the B-47D airplane was also unusual, as an "E" cowl was used to maintain high levels of ram recovery. This is the only known installation that used a full-scale "E" type cowl. As predicted, the ram recovery obtained was excellent. Unfortunately the cost, weight and maintenance time requirements are serious problems with the "E" type cowl.

The B-47D program was not a success because of the many problems encountered with the engine and the dangers associated with malfunctioning propellers. Because of asymmetrical thrust, the loss of an engine on takeoff was particularly dangerous. For this and many other reasons the program was dropped. The B-47D program emphasized the need for propellers with additional safety features and more complete initial design criteria.

Douglas DC-6

The DC-6 airplane used both dural and steel blade propellers. Because of the advantages of the steel blades in terms of foreign object damage and improved maintenance, these blades were originally used on a large segment of the DC-6 fleet. At that time the problems associated with 1xP stresses due to flow angularity into the propeller were not too well understood and the original steel blades used may have been under-designed. As a result, on at least two occasions, blades were lost in flight with the loss of the engine in both cases. Fortunately the airplanes were landed safely. As a result of the problems with the DC-6 program, the theory for calculating the 1xP blade stresses was developed. The application of this new theory led to more realistic blade designs.

Since the advantages in weight of the hollow steel blade is small compared to the dural blade when the diameter is 13 feet, the steel blades were replaced with dural blades on almost all the DC-6 fleet. This was done because of the adverse experience with the steel blades.

During the early development of the DC-6, concern was had regarding a loss of cabin pressure at altitude. One solution proposed was the reversal of all four propellers with the airplane in nearly level flight. This would result in very rapid rates of descent, as a considerable amount of wing lift is lost aft of the reversed propeller, which allows the airplane to descend rapidly. Tests with a C-54 airplane confirmed this idea, as descents at 10,000 feet per minute were made under complete control. The concept was never used, however, because of safety problems.

Convair CV-240

The steel blade experience with the Convair CV-240 airplane was better than with the DC-6. These blades were similar, but in the case of the CV-240, longer trailing-edge extensions were used. The performance of these blades was excellent and better than the dural blades also used on the airplane. The excellent performance of these blades led to the investigation of blade section types and indicated that the trailing-edge sections were similar in performance to NACA 65 sections. The 65 series sections also proved to be excellent blade sections and were applied to many future designs.

Lockheed L-749, L-1049, L-1649

The Lockheed Constellation series of airplanes used larger diameter propellers than the DC-6 and DC-7, and as a result the weight advantage of the hollow steel blade was more pronounced. The airplane was equipped with both steel and dural blades, depending on the choice of each airline. The overall operation of the airplane with the steel blades was generally excellent, and blade lives in excess of 30,000 hours were recorded.

Early in the Constellation program, it was found necessary to balance the propellers aerodynamically. The methods described in the aerodynamics section of this report were developed at this time and were found to be satisfactory for the purpose. The aerodynamic balancing, in addition to normal static balancing of propellers, gave the desired results.

The flight performances of the Constellation airplane was below the desired level and the competition. As a result, an attempt was made to make a large improvement with the use of a new wing and propeller. The propeller diameter was increased from 15 feet to 16'8", and the wing aspect ratio became 12, to convert the 1049 series to the 1649 airplane series. Associated with this change in diameter was a change in gear ratio. The results of these changes were disappointing to Lockheed, and it was later found that the propulsion efficiencies of the 15'0" and 16'8" propellers were nearly the same when operating at the cruise condition.

The Lockheed 1649 was the only known airplane to use hollow dural blades. These blades were in service only a short time, as cracks in the area of the tips developed within a very short period of time. The hollow dural blades were replaced with solid dural blades, and this resulted in a large weight penalty compared with the competitive steel blade propellers.

Boeing Model 377, C-97

The Boeing Stratocruiser Model 377 and its military version C-97 used two different types of steel blades, and finally a solid dural blade. One of the steel blades used was the welded type described in Volume II, and the other steel blade was the spar type with the steel cover brazed to the spar. In general, the welded type blade gave excellent service with no known failures. The spar type blade developed cracks in the outer skin which would be transmitted to the spar, causing a failure. On the C-97 airplane this situation became so bad that the entire fleet was refitted with dural blades. Since the diameter of the propeller was 16'8", this change to solid dural blades was done at the expense of a large increase of weight for the airplane.

Douglas C-124A and C-124C

The C-124A and C-124C airplanes were the last of the cargo airplanes designed with reciprocating engines. These airplanes used three-blade propellers approximately 17 feet in diameter with both welded and extruded steel type blades. This installation is of interest as it was necessary to increase the engine shaft size because of problems with cracking found with earlier models. The shaft cracking was believed to be caused by high loads generated by the 1xP propeller forces and moments. The original welded steel blades used on this airplane were replaced with extruded steel blades because of their improved overall characteristics. After these changes, the propeller history of the C-124 fleet has been good.

Lockheed C-130

The Lockheed C-130 is one of the most successful turbo-propeller airplanes built to date. Well over 1000 airplanes have been built, and it has been used for a number of different missions.

The C-130 airplane, since the first flight of the "Y" model in 1954, has used four different propellers designed by all three of the major manufacturers. The first propeller was 15 feet in diameter and used 150 activity factor steel blades. This propeller was designed to meet very high rates of blade angle change that were thought to be necessary for the control of the coupled T-56 turboprop engine used on the C-130 airplane.

High rates of blade angle change were considered to be necessary on the C-130 airplane, as a failed fixed turbine turboprop engine is capable of absorbing large amounts of power from the windmilling propeller. This in turn means the drag of the windmilling propeller will be very high. To eliminate this possibility, large rates of pitch change were specified. These rates of pitch change were also considered desirable to reduce the time required for the propeller to go from the flight idle stop to reverse. A minimum time to change blade angle was considered desirable to maximize the effectiveness of braking action of the propellers and reduce landing roll.

To achieve high rates of pitch change, the propeller was designed with a mechanical pitch change mechanism using high-speed clutches. Thus the relative motion between the propeller and the engine casing was converted to blade angle change by the clutches and a suitable gear train. Although the desired characteristics were obtained, the original clutch type propeller was replaced early in the program due to an extensive series of mechanical difficulties.

The mechanical propeller was replaced by a three-blade hydraulic propeller also in 15'0" diameter. This propeller gave satisfactory operation except it was reported that the noise level produced was 7 db above the original propeller. This change in noise is of interest, as both propellers operated at the same power and rotational speed. The change in noise level is considered to be due to the change in load distribution between the two propellers.

Because of the high internal noise characteristics of the C-130A airplane equipped with the 15-foot-diameter propellers, the next model of the airplane was equipped with four-blade 13'6" diameter propellers. These 13'6" diameter propellers will have lower takeoff and climb performance compared with the 15'0" diameter three-blade propellers, and about the same cruise performance. This compromise to reduce the noise was considered to be necessary.

It is believed that had the criteria been realistically established for the propeller, the difficulties and many propeller changes could have been avoided on the C-130 airplane.

Douglas C-133

The C-133 airplane was a large cargo airplane using 3-bladed, 18-foot-diameter propellers. The T-34 turboprop engine was used. This engine is also of the fixed turbine type. Pitch change on the C-133 propeller was accomplished with the use of low-speed clutches, as the power requirements were high due to the high rate of pitch change required and the size.

The propeller was originally designed for the engine operating at approximately 5500 shaft horsepower. When the power rating of the airplane was increased to 7000 shaft horsepower, blade stall flutter was encountered. While the flutter disappeared at a speed in the range of 30 to 50 knots and restrictions to eliminate the flutter did not affect the takeoff distance, such a flutter condition was considered to be unsatisfactory.

The stall flutter encountered was also very bad because the original blade had a fundamental torsional frequency very near the operating rpm. Thus when flutter was encountered, high blade stresses were encountered as well as high blade gear loads. These high stresses caused problems with the blade gears, including several failures. In one case the blade pitch change gear failed in flight, causing one blade to go to the low pitch setting in flight. Although this caused a very large unbalance, the pilot was able to maintain control and land safely.

To eliminate the flutter and blade gear problems, a new blade was designed. This blade was designed with an increased thickness ratio in the critical area to increase the torsional stiffness. To compensate for the increase in thickness, the design lift coefficient of the blade was reduced so that the cruise performance would be maintained. Calculations indicated that this change would not increase the takeoff distance, and this was confirmed by tests. With the blade modifications as described, the flutter and torsional problems encountered with the first blade design were eliminated.

One of the major problems of the C-133 airplane was the high noise. Since the engine was a fixed turbine turboprop, the rotational speed was nearly constant. For this reason, to obtain high performance with a reasonable size propeller, it was necessary to operate at fairly high tip speeds. Unfortunately these high tip speeds were also encountered in cruise, with the result that the noise level in the airplane was extremely high. In fact, the noise level was so high in the airplane that it was restricted for use as a troop carrier and therefore could only be used for cargo.

V/STOL Propeller Installations

With the advent of lightweight turboprop engines, high values of thrust to weight became possible so that vertical takeoff with propeller-driven airplanes became possible. Using the principle of tilting the propeller and/or the wing, it appeared that much higher speeds than are possible with helicopters would be possible.

One of the first major attempts to develop propeller-driven VTOL airplanes was with the Convair XFV and the Lockheed XFY tail sitter airplanes. These airplanes used six-blade dual-rotation propellers in 16'0" diameter to eliminate the torque reaction. Control of the airplane was obtained at low speeds using control surfaces operating in the propeller slipstream. With these configurations the whole airplane was rotated from the takeoff and landing position to the cruise condition.

Although the Convair airplane did make several successful flights, the project was abandoned because of the difficulty of backing in for a landing and the recognition that many safety features in the engine and propeller system were lacking. Further studies showed that in spite of the use of dual-rotation propellers, the blades tended to unload at the high-speed condition, which along with compressibility losses would result in low values of efficiency.

There were several other propeller-driven V/STOL airplanes using tilting propellers and for tilt wings, thus making it possible to maintain a level fuselage at all flight conditions. These included the XC-142, CL-84 and X-19 airplanes. So far, none of these airplanes have been produced in any quantities and have not been too successful.

During the development of the propellers for V/STOL airplanes, it was recognized that the reliability features, safety and weight of the propellers must be better than the propellers of the past. Important improvements were made in the weight with the use of composite materials and integral gearboxes. Safety was improved through the use of dual blade actuators and improved control systems. Reliability was improved with better analysis and testing. As a result, the overall characteristics of propellers for these airplanes were better than past designs.

In spite of the improvements, unexpected difficulties were encountered with the propellers on the V/STOL airplanes. One of the most serious problems was the inability to design and predict the performance of propellers operating at the hover condition. In almost all cases the thrust predicted was much higher than measured. This problem is still not completely resolved.

In the case of the composite monocoque blades using a foam filler, separation of the foam from the plates was encountered. Various types of foam materials were tried; however, this problem was never completely resolved. It appears that the spar blade might be better in this respect, as less dependence on the filler is needed. Rain erosion with composite blades can be a problem unless proper materials are used to protect the leading edges of the blades.

In some cases difficulties have been encountered with much higher vibratory blade stresses than expected with propellers on V/STOL airplanes. Some of these difficulties can be traced to the structure of the airframe, which is extremely flexible due to need to attain a minimum weight. In other cases the propeller was at fault due to a misplaced blade resonance frequency. These problems, in addition to difficulties in obtaining a true propeller balance, have caused the airplane to be rough and give the V/STOL propeller airplane a bad image.

FUTURE PROPELLER APPLICATIONS

From the previous discussion it was noted that many of the problems associated with propeller-driven airplanes did not show up until the program was well advanced. In several cases the problems were encountered well after the airplane had been placed in service and had been operating over a period of time. Such problems with the propellers were caused by structural fatigue, control problems, blade resonance, engine growth, and the initial failure to design, test and qualify the propeller to meet the installation requirements with adequate margins. As a result, satisfactory propeller installations were often not obtained until the propeller had been completely redesigned at least once. In some cases it took two or more redesigns to obtain a satisfactory installation. No wonder the propeller got a bad name in this country and other forms of propulsion became favored.

When developing a new propeller installation, it is desirable to consider some of the factors that led to the difficulties discussed above. One of the major problems is believed to be inadequate lead time. In the case of engines, five years is considered to be required to develop a satisfactory design.

Although a propeller is not as complicated as an engine, consideration should be given to starting the development of new propellers for the engine shortly after the engine program is under way, rather than allow a development time of only 18 months to 2 years as had been done in the past.

Another factor to consider with the development of a new propeller installation is the establishment of a complete criterion and specification for the design. Such a criterion should include all the items of Appendix I, with due consideration for the design criteria discussed in the section Propeller Blades.

After the design criterion is developed, the aerodynamic characteristics of the propeller must be established for the new installation. The procedures used have been discussed previously and are usually determined based on estimated blade characteristics that will satisfy the structural requirements. In establishing the aerodynamic design of the blades, it is important to consider the structural and weight requirements. This is desirable to have a practical design without compromises in the basic structure which could lead to dynamic, fatigue and weight problems. By carefully adjusting the structural and aerodynamic parameters, the desired performance can be obtained with little or no losses from the peak.

With a new installation, the establishment of the flow field in the plane of the propeller at all flight conditions is of great importance, as this will determine the magnitude of the vibratory loading on the blades. The flow field can be established by test or by calculations. There are several computer programs that are very powerful for calculating flow fields so that an accurate estimate can be made. Thus, from an analysis of the propeller operating in proper flow field, a stress analysis can be conducted to establish adequate design margins in the final design.

Of great importance in the successful design of a new propeller airplane is the complete dynamic analysis of the entire system. Such an analysis can prevent the occurrence of a dangerous dynamic condition and indicate the suitable modifications required. The dynamic analysis is of particular importance in the design of large, lightly loaded, flexible blades for VTOL airplanes. The system must be designed so that whirl, stall and wake flutter are not encountered at any operating condition. Also, the blade must be designed so that the first three coupled flap/chord, torsion natural frequencies are well out of the operating range; see page 146, Appendix I. In considering the design to meet the above objectives, the propeller supporting system must also be completely evaluated to assure that even with a structural failure of a component, adequate stiffness and strength remain to prevent whirl flutter.

With the use of high-speed computers and improved theoretical approaches, it is possible to conduct studies so that configurations can be established that meet the above requirements. These analyses can be much more complete than those used in the past, and when coupled with proper test programs can provide the necessary data to assure safe designs.

In considering a new installation, the placement of the propeller on the airplane must be carefully considered. For instance, if the blade tip clearance with respect to the fuselage is too small, damage of the airframe structure can be encountered as a result of the pressures of the tip vortex. This also influences the cabin noise level. A poor propeller placement on the airplane can result in blade damage due to foreign objects. When this occurs, additional allowances must be made in the blade structure to withstand such damage with corresponding weight penalties. Proper placement can also reduce the stress due to flow angularity with a corresponding weight saving.

When any new propeller is developed, it is necessary to examine the flight envelope to determine the time spent at the various conditions. From this study, realistic duty cycles can be established and the design adjusted accordingly.

Although it is difficult to build a propeller with a completely redundant structure, many steps can be taken to achieve the desired level of safety. These include the choice of conservative operating stress, multiple load paths, a primary structure that can be easily inspected, and a mature design that eliminates all possible areas for stress risers.

The proper design of the propeller control is also essential for a successful installation. The control system is essentially the thrust control of the airplane and must provide satisfactory response, maintain the thrust established, and protect the airplane against malfunctions. The control system should also have a high degree of reliability.

In the design of the basic control system, the need for backup systems or a dual actuation system must be completely determined. For some types of missions, a follow-up blade angle stop is all that is required to achieve the desired safety. On V/STOL airplanes, however, a dual system is probably needed, as when the airplane is operating at the hover condition, the propeller control is the primary flight control of the airplane.

The rate of pitch change required for the control system of the airplane depends on the engine configuration and the thrust response needed. A complete analysis including simulation programs should be done to establish this pitch change rate for a new installation and engine.

Development Testing

Even if all the design steps discussed above were followed, problems will be encountered in the final propeller unless proper development testing is done. The testing required is needed to confirm the original design and point to those "unknown unknowns" that will lead to trouble unless identified. As a minimum, testing should be done on the components to prove their functional capability. The complete schedule of development testing will depend on the installation requirements and available time and will therefore be different for each case.

FUTURE PROPELLER DESIGNS

Present Technology

The present propeller technology as presented in this report and as given in References 10 to 12 has advanced considerably from that used up to the middle 1950's for the design of conventional type propellers. The advances in the technology have been made possible as a result of the work done on propellers for new types of V/STOL airplanes where the requirements are more exacting in all technology areas than are necessary for conventional airplanes.

The improved propeller technology has also been made possible as a result of the use of new materials and the design background achieved in the development of helicopters. The improved dynamic analysis of propellers has benefited by the work done on helicopter rotors, especially rotor-propellers designed for low-disc-loading V/STOL airplanes.

As a result of these developments, the design risk has been greatly reduced for producing propellers suitable for conventional and V/STOL airplanes. Today high-performance, lightweight and reliable propellers can be designed and built for airplanes operating from zero speeds or hover to a Mach number of approximately 0.7. The initial estimates of the performance, weight and operating characteristics will be reliable, and it should be possible to design and build these propellers with little risk to the program. This will be true as long as the proper analytical and test programs are followed, such as are described in this report and References 10 to 12.

Future Propellers

Future propellers will be installed on STOL and V/STOL aircraft where low-speed performance is of utmost importance and cruise speeds in the range of 300 to 400 knots are the maximum required. Propeller-driven aircraft will also provide important advantages where high loiter times are required and fuel costs and supply are important factors. In these cases the high-performance potential of propellers can be used to advantage, especially now that important weight savings can be made with respect to the propellers of the past.

The propellers projected for the STOL aircraft installations will operate at disc loadings in the range of 30 to 60 pounds per square foot disc loading based on the static thrust performance. Since noise as well as performance will be an important design consideration, the tip speed selected will be especially low, requiring the blades to operate at high values of operating C_L times the chord. For this reason the total blade solidity of the propeller will be high unless steps are taken to improve the magnitude of operating C_L at high lift/drag ratios. Thus, if the blade can operate at higher lift coefficients with the same lift/drag ratio than is possible now, the blade solidity can be reduced. This will lead to important weight advantages.

To obtain the maximum weight savings possible, the propeller integral gearbox, Reference 10, and the advanced composite blades will be used. In addition, the concepts of reliability, safety and maintenance discussed in this report will be applied to the new propeller designs.

On STOL airplanes it will be desirable to take advantage of the installed power needed for takeoff and operate at as high cruise speeds as possible. This means that the high-speed performance of the propeller is not to be compromised if good range and costs are to be achieved.

When large-diameter, low-disc-loading propellers are used on STOL aircraft, high forces and moments are generated when operating in gusty air. These forces and moments lead to a poor aircraft ride. For this reason aerodynamic dampers will be developed to reduce the effects of these forces to make possible a good ride. Also, the propellers will be designed so that precise balance can be achieved at all conditions.

The propellers designed for V/STOL airplanes will operate at disc loadings in the range of 15 to 40 pounds per square foot based on the performance at hover. The disc loading chosen will depend on the aircraft configuration and will probably be as low as possible for peak performance (Reference 13). If the slipstream velocity over the wing is of primary importance, the disc loading will be high (35 to 40 psf). Whereas in the case of the tilt-rotor aircraft, low values of approximately 15 to 20 psf will usually be chosen.

The low disc loading is desirable for high values of thrust to horsepower at hover and possible autorotation capability in the case of engine failure. Unlike propellers for STOL airplanes the total solidity will be much less, and long narrow blades will be obtained. The operating C_L spread between hover and cruise required from these blades is much higher than for conventional propeller blades. For this reason, important advantages could be obtained if the presently available C_L range for high lift/drag ratios could be improved.

In addition to improving the operating range of C_L for high lift/drag ratios, airfoils with higher thickness ratios with the same performance as present sections would be an important improvement. The use of such airfoils would make possible lighter propellers.

The V/STOL propellers will probably be designed with the additional function of providing mono or complete cyclic control depending on the airplane configuration. This additional control function is necessary to eliminate the need for special propellers for control only (Reference 10). Considerable testing has been done with propellers using cyclic control. However, the application of the control is extremely limited to date, and further analysis work is indicated.

With some of the first propeller-driven V/STOL airplanes, considerable difficulty was experienced in designing configurations that would give the peak efficiency at the hover condition. This was due to problems in defining the wake at the static condition which is necessary for calculating the induced efficiency and angle of attack at each blade station. Since this time, new methods have been developed for calculating the static performance. These methods depend on the results of test measurements of the wake and are known as the "Prescribed Wake" method (Reference 14).

In using the prescribed wake to calculate the performance, peak levels of hover performance are not necessarily determined, as the wake data used depends on the characteristics of actual propellers. These test propellers have no real optimum value of Figure of Merit, so that propellers or rotors designed on the basis of the results of tests can only approach the test values. Further work is needed to define the optimum Figure of Merit and determine the blade configuration required to obtain this level of performance.

RECOMMENDATIONS FOR PROPELLER FUTURE DEVELOPMENTS

GENERAL

To achieve the maximum potential with future propellers, it is recommended that the following programs be undertaken. These programs are necessary, as the technology in the areas of aerodynamics, materials, and dynamics has not been static in other fields and these developments must be applied to obtain optimum systems and thus remain competitive. Also, the review has shown that the propeller technology is deficient in certain areas and thus requires corrections. To accomplish these objectives, the following programs are therefore recommended:

Optimum Propeller - Hover

To design a propeller for use on V/STOL aircraft with the optimum combination of hover and cruise efficiency, a true definition of the optimum blade configuration for hover must be established. The distribution of blade angle, thickness ratio, design C_L and chord is required which will give the peak Figure of Merit for the given power.

As indicated in the aerodynamics section, the optimum Figure of Merit must include the proper contraction ratio which is a function of the power loading. Further, the optimum configuration will generate a rigid wake that moves downstream in the final wake at a fixed velocity which is a function of the thrust loading. The rigid wake influences the induced velocity at each blade station which results in the optimum loading. For these reasons the optimum load distribution at hover cannot be found using test data for nonoptimum propeller configurations and loading such as used in the prescribed wake concept (Reference 14). This is true since the wake used of nonoptimum propellers is neither rigid nor does it move with a uniform velocity.

The theory for calculating the optimum propeller has been developed (Reference 14) but it has not been applied. To determine if the theory is correct, the available propeller test data should be checked against the optimum Figure of Merit. If this check shows the test data is always below the optimum value, the necessary proof of the theory will be established so that it can be applied for establishing the optimum blade for any hover condition. The checks to date confirm the propeller test data is always below the theoretical peak.

It is therefore recommended that the theory and data of References 15 and 16 be applied to define the optimum blade and propeller for use as the static condition. The performance of this propeller should then be determined when operating at typical cruise conditions to find the change from the optimum cruise propeller. Based on the conclusions of this study, an analysis such as Reference 12 should be made to determine the most desirable disc loading for propeller/rotor V/STOL aircraft.

Reduced Weight Propellers

The results of propeller design analysis studies have been very promising for reducing the installed weight. Composite blades, integral propeller gearboxes and titanium hubs have reduced the propeller weight drastically compared to conventional types. It is believed that the major gains have been achieved in reducing weight as a result of these design programs.

There is one major area, however, where important weight reductions can still be achieved. This is in the area of improving the structural and aerodynamics characteristics of the blade. With the use of new types of airfoil sections which have been developed, it should make possible important reductions in blade size and weight while maintaining the same overall performance.

The maximum design C_L used on propeller blades at the present time is approximately 0.7. It is also the practice to design the blades with as low thickness ratios as possible to avoid compressibility losses. If either the thickness ratio or the design lift coefficient could be increased without affecting the performance, the size and weight of the blade could be reduced. For instance, an increase in design C_L would make possible a decrease in blade chord. This is possible because the blade chord required is almost inversely proportional to the design C_L; thus, if the design C_L could be increased from 0.7 to 1.0, the blade chord could be reduced by 30 percent, an important weight reduction. Another important advantage of a chord reduction would be a reduction of the 1xP force generated by the blade. This could be an advantage with some installations using large propellers.

Propeller blades designed with increased thickness ratios without a decrease of efficiency will also have weight reductions compared with previous blades. This weight reduction would occur because of the increased stiffness of the blade which would allow a reduction in plate thickness.

The last comprehensive examination of airfoils for propellers was one in the early 1950's, approached from the performance point of view only. Many advances have been made in the development of new airfoils such as the work of Whitcomb. For this reason it is recommended that a study be made to determine the reduction in weight possible through the use of new airfoils. It is believed that potential weight savings on the order of 50 percent are possible as a result of such a study.

High-Speed Performance

The design objectives of V/STOL aircraft are good hover performance along with a high potential cruise speed. With propeller-driven aircraft, high performance can be achieved at the hover condition with a corresponding high-speed efficiency at Mach numbers below the values where compressibility losses are encountered. Because the blades operate at low values of C_L lift coefficient at the higher speed condition, the onset of compressibility losses will cause a rapid deterioration of efficiency. The magnitude and forward Mach number at which the compressibility losses are encountered are important for predicting the high-speed performance of propeller-driven V/STOL airplanes. The speed for the occurrence of compressibility losses is also important in designing the blade to obtain the desired split in performance between takeoff and cruise.

As was noted in the section Accuracy of Analysis, Volume I, the efficiency can be predicted accurately by strip analysis procedures when operating in the subsonic range. When drag losses are encountered due to compressibility losses, the accuracy deteriorates, especially at the light loadings encountered with V/STOL aircraft. This decrease in accuracy is believed to be due to inaccuracies in the airfoil data, as the induced losses are low at these conditions.

Since the time of the development of the airfoil data used for strip analysis, there have been a number of improvements developed in the high Mach number testing of airfoils, and a considerable store of data has been obtained. These data can be used to correct the airfoil data of Appendix II currently available for propeller strip analysis calculations and so improve the accuracy of the performance predictions at the high-speed conditions.

A program is therefore recommended for correcting the available airfoil data so that the accuracy of the performance prediction is improved at the high-speed conditions where compressibility losses become important. From such a program, the gaps in the airfoil data that require testing could be identified. Also, it will then be possible to design and predict more accurately the performance of blades for the high-speed conditions.

Propeller Design Specification

The military specification entitled "Propeller Systems, Aircraft, General Specification for", MIL-P-26366A, was set up for conventional propeller type aircraft and was last revised in 1962. The specification is considered outmoded due to advances made in the analysis and understanding of the design of propellers. Further, with the use of propellers on STOL and V/STOL airplanes, the design requirements must be more rigorous than defined in the above specification.

It is therefore recommended that MIL-P-26366A be revised based on the requirements of STOL and V/STOL propeller installations. Also, the specification should reflect the advances in technology as described in References 10 to 12 as well as the design criteria as outlined in Appendix I.

PROPELLERS FOR STOL AIRCRAFT

Present efforts to design STOL aircraft have been based on the use of turbofan engines with various combinations of high lift devices on the wing to obtain the desired performance. These turbofan aircraft are only STOL in comparison with the usual turbofan conventional aircraft that require 8000- to 10,000-foot runways. Further, the noise level of such aircraft is only low in comparison with the same conventional aircraft types.

Several studies have been made of turboprop STOL aircraft in competition with the turbofan types. These studies showed that the turboprop STOL airplane had one-half to one-third the runway requirement and was potentially less noisy than the turbofan type. Further, the turboprop airplane can be designed to operate at lower sound levels than the turbofan type, and the technology is in hand for designing propellers to meet the STOL transport noise level requirements.

The turboprop STOL airplane has many important features that give it excellent STOL characteristics with little or no additional complication compared with a conventional type such as a C-130. For instance, with proper placement, the propeller slipstream will wash the wing with an increase in overall lift. Also the propeller is an excellent device for stopping the airplane by simply reversing the blade angle to obtain negative thrust.

Although the turboprop airplane can be designed to have real STOL capability with low ambient noise level, the large propellers lead to disadvantages that require additional work. One of the difficulties is the placement of the propellers, which have a considerable spacing between the thrust lines and the center line of the airplane. This large spacing leads to problems only in case of engine or propeller failures. Cross shafting has been used on some STOL airplanes to eliminate the asymmetrical thrust problem, but of course this leads to problems of maintenance, cost and reliability. The shafting problem has been effectively solved for tandem helicopters and could also be solved for the turboprop STOL airplane.

Another problem with the use of relatively large propellers on STOL airplanes is the undesirable ride characteristics obtained in gusty air. This is due to the normal forces and moments generated by the propeller operating at a shaft angle of attack. Lateral as well as vertical forces can be generated which lead to very unpleasant ride characteristics.

With the use of narrow blades, the normal force is reduced with a corresponding improvement of the ride. A program for developing narrow blades is described earlier in this section. In addition to reducing the blade chord, other systems must be developed for eliminating gust sensitivity with large propellers. Systems like yaw dampers could be developed to eliminate this problem. A program is therefore recommended to study and find solutions to the ride problem associated with large propellers.

Propeller Cyclic Pitch

The early V/STOL aircraft were controlled at the hover condition by only propeller collective pitch. This led to the use of one or more additional propellers to obtain the required pitch control with a corresponding increase in weight and complication. With the success of cyclic pitch for control of helicopters, this system has been considered for use on propeller-driven V/STOL aircraft. As part of the advanced V/STOL technology program, considerable experimental work has been done to evaluate the use of cyclic pitch for control (References 17 and 18). This work was done with both model and full-scale propellers.

A review of the data of References 17 to 18 indicates that further work is necessary before the technology is in hand for the application of cyclic pitch propellers for the control of V/STOL aircraft. This is especially true when the propeller is operating at high shaft angles. At these conditions the methods of analysis underestimate the thrust change due to cyclic pitch change with a corresponding error in the other forces and moments produced by the propeller. A program should be undertaken to improve the accuracy of the calculation forces and moments produced by a cyclic pitch propeller.

The effects of the application of cyclic pitch propellers on the characteristics of V/STOL airplanes have been determined (Reference 19). However, little analysis work was done to determine the impact of the use of cyclic pitch on the propeller design. The effects of the airplane characteristics on the design of the cyclic pitch propeller also appear to be lacking. A program to improve the design technology of cyclic pitch props is therefore indicated.

Propeller Performance

At any one operating condition, propellers can be designed to operate at very high levels of efficiency. On some airplanes, however, the important operating conditions will give widely different requirements with the result that the blade will be operating at a low C_L at one condition and a very high C_L at another condition. This condition is encountered especially with V/STOL airplanes.

With fixed-geometry propellers, the only solution to this problem is with the use of airfoils designed to have improved performance over the range of required operating C_L. A program is recommended to investigate this possibility. Although the performance of the airfoils chosen may be below the optimum at any one condition, it should be possible to find configurations that give a net improvement over the range of conditions.

Variable-Geometry Propellers

Another way of improving the performance of propellers that must operate over a wide range of conditions is through the use of variable geometry. On aircraft wings, variable geometry is obtained through the use of flaps, slats, etc., to improve the range of operating C_L between takeoff and cruise conditions. Flaps, slats and blowing have been considered for propellers to improve performance; however, no serious work has been done to apply such devices to a propeller blade.

The only important investigation of variable-geometry propellers was through the use of two closely spaced blades to effect a change in camber (Reference 20). This system gives a high camber at low blade angles for the takeoff condition and a low camber at high blade angles for cruise condition. The variable camber system has been extensively tested in both model and full-scale configurations, but so far no production airplane has used this propeller.

Although the variable-camber propeller does approach the desired characteristics, the degree of improvement obtained does not warrant the additional complication, especially with the use of the free turbine engine.

The use of composite structure blades would appear to improve the possibilities for the development of variable-geometry blades. Variable pitch and camber blades are considered to be good possibilities. Propellers with variable diameter, such as discussed in Reference 21, are also feasible. For this reason a review of the possible approaches should be done, especially in conjunction with the application of new airfoils as discussed above.

PROPELLER NOISE

The noise generated by propellers has always been a problem as with any device for producing thrust. Large slow-turning propellers can be designed to reduce the noise level to avoid aural detection (Reference 22). Likewise, the noise level can be reduced to almost any level desired with the proper selection of tip speed and propeller size. No decrement in the aerodynamic performance is encountered with low-noise propellers, but the weight increases can be high depending on the noise level desired.

There is evidence that the favorable effects of tip speed in terms of noise reduction are underestimated by the standard methods of calculation when operating at forward flight conditions. It appears that when the rotation tip speed is in the range of 500 to 600 feet per second, the noise level is 7 to 10 decibels below that calculated. Since a reduction of this magnitude is important from both the weight and noise level considerations, it is recommended that additional research be conducted in this area.

An experimental program should be undertaken to measure the noise as a function of tip speed when operating in flight. These data should be correlated with the theoretical results so that the noise level can be accurately predicted on new installations. If possible, the testing should include the effects of blade loading as well as spanwise variations. Some tests run at the static condition indicated that tip end plates gave a reduction in noise level of approximately three decibels along with an improvement of the stall flutter characteristics of the blade. The propeller noise research should therefore include the testing of such devices.

CONCLUSIONS

From the material on propeller controls, hubs, actuators, installation considerations, and future research requirements, the following conclusions are made:

1. Important propeller weight advantages can be achieved with the proper integration of the propeller hub and gearbox.

2. Advanced propellers with hydraulic blade angle actuators can be designed with the required level of safety, reliability and ease of maintenance for any aircraft type.

3. For aircraft with a large operating flight envelope, new types of propeller blade angle controls are needed.

4. Further research and development is indicated for propellers to maintain the technology in a competitive position.

5. With the use of advanced airfoils, propellers can be designed with further reductions of weight and blade excitation.

LITERATURE CITED

1. MIL-P-5447, PROPELLERS; CONTROLLABLE PITCH, GENERAL SPECIFICATION FOR

2. ANC-9, AIRCRAFT PROPELLER HANDBOOK, Issued jointly by Departments of the Air Force, Navy and Commerce, Sept. 1956.

3. Military Specifications MIL-P-26366A, PROPELLER SYSTEMS, AIRCRAFT, GENERAL SPECIFICATION FOR, 15 November 1962.

4. Currie, D. P., DETAILED DESIGN OF A 2000-SHP ADVANCED TECHNOLOGY V/STOL PROPELLER SYSTEM, Hamilton Standard Div., United Aircraft Corp., USAAVLABS Technical Report 69-59, U.S. Army Aviation Materiel Laboratories, Fort Eustis, Virginia, Sept. 1969, AD 864446.

5. Harrison, Howard L., and Bollinger, John G., INTRODUCTION TO AUTOMATIC CONTROLS, International Textbook Co., Scranton, Pa. 1963.

6. Gardner and Barns, TRANSIENTS IN LINEAR SYSTEMS, Wiley.

7. Nixon, Floyd E., PRINCIPLES OF AUTOMATIC CONTROLS, Prentice-Hall.

8. Holford, F. R., and Kasley, J. H., FLIGHT TEST COMPARISON OF PROPELLERS WITH 836-14C2-18R1, 109390, 109394 AND 109498 BLADES IN LEVEL FLIGHT CONDITIONS, Curtiss Wright Corp., Propeller Division, C-1799, 6 March 1947 AT1-163-675.

9. Gray, W. H., and Gilman, Jean, Jr., CHARACTERISTICS OF SEVERAL SINGLE AND DUAL ROTATION PROPELLERS IN NEGATIVE THRUST, NACA MR L5C07, March 1945. WR L-634.

10. Adamson, W. M., FEASIBILITY STUDY OF ADVANCED V/STOL PROPELLER TECHNOLOGY, Hamilton Standard Div., United Aircraft Corp., U.S. Army Aviation Materiel Laboratories, USAAVLABS Technical Report 68-33, June 1968, AD 671029.

11. Adams, G. N., ADVANCED V/STOL PROPELLER TECHNOLOGY - CONTROL SYSTEMS STUDY, Technical Report AFFDL-TR-71-88, Volume VIII, December 1971.

12. Deabler, H. E., and Young, F. A., ADVANCED V/STOL PROPELLER DESIGN, Technical Report AFFDL-TR-71-88, Volume X, December 1971.

13. Borst, H. V., PROPELLER AND ROTOR VTOL CONCEPTS AND THEIR RELATIVE PLACES IN THE MISSION SPECTRUM, U.S. Air Force V/STOL Technology and Planning Conference, Las Vegas, Nevada, 23-25 September 1969.

14. Ladden, R. M., and Gilmore, D. C., ADVANCED V/STOL PROPELLER TECHNOLOGY - STATIC THRUST PREDICTION METHOD DEVELOPMENT, Technical Report AFFDL-TR-71-88, Volume II, September 1971.

15. Theodorsen, T. T., THEORY OF STATIC PROPELLERS AND HELICOPTER ROTORS, 25th Annual Forum, American Helicopter Society, No. 326, May 1969.

16. Holford, F. R., and Kasley, J. H., FLIGHT TEST COMPARISON OF PROPELLERS WITH 836-14C2-18R1, 109390, 109394 AND 109498 BLADES IN LEVEL FLIGHT CONDITIONS, Curtiss Wright Corp., Propeller Division, C-1799, 6 March 1947, AT1-163-675.

17. Wainauski, H. S., ADVANCED V/STOL PROPELLER TECHNOLOGY - LARGE SCALE CYCLIC PITCH INVESTIGATION Technical Report AFFDL-TR-71-88, Volume VII, June 1972.

18. Watts, A., and Pon, L., ADVANCED V/STOL PROPELLER TECHNOLOGY - SMALL SCALE CYCLIC PITCH INVESTIGATION, Technical Report AFFDL-TR-71-88, Volume XI, June 1972.

19. Kolesar, C. E., CYCLIC PITCH CONTROL ON A V/STOL TILT WING AIRCRAFT, Technical Report AFFDL-TR-71-91, October 1971.

20. Rosen, G., and Adamson, W. M., NEXT GENERATION V/STOL PROPELLERS, Society of Automotive Engineers Paper 680281, April 29 - May 2, 1968.

21. Gray, W. H., and Gilman, Jean, Jr., CHARACTERISTICS OF SEVERAL SINGLE AND DUAL ROTATION PROPELLERS IN NEGATIVE THRUST, NACA MR L5C07, March 1945. WR L-634.

22. Berry, F. W., NOISE DETECTABILITY PREDICTION METHOD FOR LOW TIP SPEED PROPELLERS, Technical Report AFAPL-TR-71-37, June 1971.

APPENDIX I

PROPELLER DESIGN SPECIFICATION AND CRITERIA

1. INTRODUCTION

A propeller design criterion and specification are required early in the development program to firmly establish the design requirements and objectives. This specification should outline the operating requirements, conditions, power plant and airplane configuration that will affect the propeller design and installation. Also specified are the structural, dynamic, control, material and design requirements that are considered necessary to assure the satisfactory propeller. Because reliability, maintenance, safety and survivability are important considerations in the final product, these requirements must also be completely defined. The testing program is also specified in detail along with the inspection requirements and procedures for establishing proof, and therefore quality assurance of the end product.

Much of the material necessary for the design specifications is covered in MIL-P-26366-A, which is the propeller specification mandatory for use by the Department of the Army, the Navy, and the Air Force. Therefore, the propeller must be designed to meet the conditions given in this specification and must pass the qualification tests outlined. In addition, the propellers should be designed to comply with those specifications and requirements listed in the heading "Applicable Documents".

Extensive problems are encountered as well as a large loss of time in redesigning and requalifying a propeller that does not satisfactorily complete the testing outlined in MIL-P-26366-A. For this reason additional requirements have been developed for use in the initial design and analysis stage. Compliance with these requirements should result in a satisfactory design that will complete the necessary testing without extensive redesign. These additional requirements are to be followed as well as those given in MIL-P-26366-A and the referenced specifications. In some cases the design specification of this appendix will contain the same information of the MIL spec. This is done for continuity and clarity.

From the material presented, a detailed specification and criteria can be prepared for the development and qualification of new propellers. This material is recommended for use in the next revision of MIL-P-26366-A. For convenience in comparing the material of this appendix with MIL-P-26366-A, the same major paragraph numbering system has been used.

2. APPLICABLE DOCUMENTS

The following documents will form a part of the propeller design specification. In reviewing these specifications it may be desired to use equivalent comparing specifications that are equal to or better than those given. These specifications as given below will apply only if there is no conflict with the material given in the remainder of the specifications and MIL-P-26366-A.

2.1 Specifications

2.1.1 Military

MIL-D-1000	Drawings, Engineering and Associated List
MIL-F-3541B	Fittings, Lubrication
MIL-S-5002B	Surface Treatments and Metallic Coatings for Metal Surfaces of Weapons Systems
MIL-C5015	Connector, AN Type
MIL-B-5087B	Bonding, Electrical and Lightning Protection, for Aerospace Systems
MIL-W-5088D	Wiring, Aircraft, Selection and Installation of
MIL-E-5272	Environmental Testing Aeronautical and Associated Equipment, General Specification for
MIL-E-5400C	Electronic Equipment, Aircraft General Specification for
MIL-P-5514F	Gland Design; Packings, Hydraulic, General Requirements for
MIL-H-5606B	Hydraulic Fluid, Petroleum Base Aircraft Missile and Ordnance
MIL-C-6021G	Castings, Classification and Inspection of
MIL-E-6051C	Electromagnetic Compatibility Requirements
MIL-P-6074A	Preservation, Packaging and Packing of Propellers, Propeller Spares and Propeller Accessories
MIL-H-6083C	Hydraulic Fluid, Petroleum Base for Preservation and Testing
MIL-S-6721	Steel Corrosion and Heat Resistant (Chemically Stabilized) Plate, Sheet and Strip

MIL-W-6858D	Welding, Resistance: Aluminum, Magnesium, Non-Hardening Steels or Alloys, Nickel Alloys, Heat Resisting Alloys and Titanium Alloys; Spot and Seam
MIL-I-6866B	Inspection, Penetrant Method of
MIL-I-6868C	Inspection Process, Magnetic Particle
MIL-F-7179D	Finishes and Coatings: General Specification for Protection of Aerospace Weapons Systems, Structures and Parts
MIL-F-7190A	Forgings, Steel for Aircraft and Special Ordnance Applications
MIL-S-7742B	Screw Threads, Standard, Optimum Selected Series, General Specification for
MIL-L-7808G	Lubricating Oil, Aircraft Turbine Engine, Synthetic Base
MIL-P-7936	Parts and Equipment Aeronautical Preparation for Delivery
MIL-A-8421B	Air Transportability Requirements, General Specification for
MIL-S-8879A	Screw Threads, Controlled Radius Root with Increased Minor Diameter; General Specification for
MIL-T-9047D	Titanium and Titanium Alloy Bars, Forgings, and Forging Stock
MIL-Q-9858A	Quality Program Requirements
MIL-C-11796B	Corrosion Preventive Compound Hot Application
MIL-C-16173D	Corrosion Preventive Compound, Solvent Cutback, Cold-Application
MIL-W-16878D	Wire Electrical, Insulated, High Temperature
MIL-W-22759B(WP)	Wire, Electric, Fluorocarbon Insulated, Copper and Copper Alloy
MIL-A-22771C	Aluminum Alloy Forgings, Heat Treated

MIL-L-23699B	Lubricating Oil, Aircraft Turbine Engine, Synthetic Base
MIL-E-25499A	Electrical Systems, Aircraft Design and Installation of General Specification for
MIL-P-26366A	Propeller Systems, Aircraft, General Specification for
MIL-P-26367A	Propeller Systems, Aircraft, Model Specification for (Outline and Instructions for Preparation)
MIL-C-26500	Connector General Purpose
MIL-S-38130	System Safety Engineering of Systems and Associated Subsystems and Equipment; General Requirements for
MIL-V-38352	Value Engineering - Program Requirements
MIL-W-45223A	Welding, Spot, Hardenable Steels

2.2 STANDARDS

2.2.1 Military

MIL-STD-100	Drawing Practices
MIL-STD-129E	Marking for Shipment and Storage
MIL-STD-130C	Identification Marking of U.S. Military Property
MIL-STD-143B	Standards and Specifications, Order of Precedence for the Selection of
MIL-STD-210A	Climatic Extremes for Military Equipment
MIL-STD-321B	Definition of Effectiveness Terms for Maintainability and Reliability
MIL-STD-461	Electromagnetic Interference Test Requirements and Test Methods
MIL-STD-470	Maintainability Program Requirements (For Systems and Equipment)
MIL-STD-704	Electric Power, Aircraft Characteristics and Utilization of

MIL-STD-721B	Definition of Terms for Reliability Engineering
MIL-STD-785	Reliability Program for Systems and Equipment
MIL-STD-794B	Parts and Equipment, Procedures for Packaging and Packing of
MIL-STD-810	Environmental Test Methods for Aerospace and Ground Equipment
MIL-STD-826	Electromagnetic Interference Test Requirements and Test Methods
MIL-STD-882	System Safety Program for Systems and Associated Subsystems and Equipment, Requirement for
MIL-STD-889	Metals, Definition of Dissimilar
MIL-STD-1472	Human Engineering Design Criteria for Military Systems, Equipment and Facilities
MS 9241B	Packing, Preformed-Rubber AMS 7272 "O" Ring
MS 24123A	Plate, Identification
MS 28774B	Retainer, Packing Backup, Single Turn, Tetrafluoroethylene
MS 33540F	Safety Wiring and Cotterpinning, General Practices for
MS 33586	Metals, Definition of Dissimilar

2.3 OTHER PUBLICATIONS

2.3.1 Manuals

AFR80-18	Department of Defense Engineering for Transportability Program
AFR127-4	Investigating and Reporting USAF Accidents/ Incidents
AFSCM80-3	Handbook of Instructions for Aerospace Personnel Subsystem Design
AFSCM80-1	Handbook of Instructions for Aircraft Design
MIL-HDBK-5	Metallic Materials and Elements for Aerospace Vehicle Structures

ANC9	Aircraft Propeller Handbook
ASD-TR-66-57	Air Force Structural Integrity Program Requirements
TACM 66-31	Equipment Maintenance/Maintenance Management/ Aircraft and AGE Equipment
MIL-HDBK-17	Plastics for Flight Vehicles
ANA Bulletin No. 343	Specifications and Standards Applicable to Aircraft Engines and Propellers, Use of
	Engine Specification

3. DESIGN REQUIREMENTS

3.1 INSTALLATION CHARACTERISTICS

In developing the detailed design requirements, consideration must be given to the factors as outlined below that influence the propeller configuration, weight, control, safety, reliability, maintainability and performance.

3.1.1 Airplane - Characteristics

Give the airplane configuration for the installation including all dimensions affecting the design. Include the overall performance characteristics. If a separate drive system is to be used, detail its characteristics and how it will interface with the propeller.

3.1.2 Engine - Characteristics

The engine that will be used must be defined, including any additional information affecting the propeller design not normally given in the engine specification as called out in Section 2.0.

3.1.3 Propeller - Characteristics

The propeller overall characteristics required must be described. These shall include:

1. Direction of rotation.
2. Diameter.
3. Blade number.
4. Blade characteristics including chord, design C_L and blade angle distribution.

The propeller characteristics described should be confirmed by analysis using the basic data given in the specification and modified to obtain the optimum configuration.

3.1.3.1 Propeller Functional Characteristics

Describe required operational features, including:

1. Control system.
2. Feather, including feather brake if necessary to prevent rotation.
3. Reverse with or without automatic rpm control.
4. Pitch lock system or pitch stops.
5. Overspeed control.
6. Propeller unfeather requirements.

3.1.3.2 Propeller - Major Components

The major components for the propeller will be described and will consist of the blades, hub, pitch change assembly, propeller control unit and spinner.

3.2 AERODYNAMIC PERFORMANCE REQUIREMENTS

The propeller must be designed to meet the thrust requirements of the airplane at the critical operating conditions using the specified power. The configuration must also be optimized in terms of size, weight and performance based on the performance of the entire airplane system. The relative importance of the parameters affecting the performance must be specified.

3.2.1 Design Conditions

For the major and critical design operating conditions, supply for propeller analysis and aerodynamic design selection the following:

1. Operating velocity.
2. Radial velocity distribution in the propeller plane.
3. Power at propeller shaft.
4. Engine rpm and gear ratio.
5. Altitude - air density & temperature.
6. Diameter limit.
7. Thrust required.

State relative importance of the design conditions and possible trades in required performance between conditions.

3.3 STRUCTURAL REQUIREMENTS

The propellers will be designed to meet the structural requirements of ASD-TR-66-57, "Air Force Structural Integrity

Program Requirements", May 1970 , and the Applicable Documents and Specifications.

3.3.1 Operating Envelope

The following data are to be provided for the structural design of the propeller.

3.3.1.1 Velocity-Load Factor Envelope

The velocity-load factor diagram (V-N) for the aircraft at design gross weight, including gusts.

3.3.1.2 Velocity-Altitude Diagram

The velocity-altitude diagram for the aircraft.

3.3.1.3 Load Conditions Occurrence Table

Give the occurrences of flight conditions to be used for propeller fatigue design at the basic mission flight design weight. Shown are to be IP cycles, vertical load factor N_Z, velocity, propeller speed and flight condition.

3.3.1.4 Propeller Flow Field

The definition of the inflow field for two steady and two accelerated flight conditions is to be given.

3.3.1.5 Gust Loads

The propeller system will not exceed its limit strength when exposed to the gust conditions to be shown, 3.3.1.1, with the gust impinging on the propeller at an angle which generates the highest loads.

3.3.1.6 Fatigue Loads

Dynamic loads and their frequency of occurrence will be calculated for the flight conditions to be specified, using methods which account as a minimum for dynamic amplifications, effect of the wing and fuselage on the flow field, first and higher order harmonics, IP dynamic blade twist, inertia and gyroscopic loads, wing-prop shaft inclination and gusts.

3.3.1.7 Overspeed

The propeller shall be structurally capable of withstanding the loads associated with an overspeed condition (141%) for a period of one hour.

3.3.1.8 Maximum Power

The propeller shall be structurally capable of absorbing an increase in power available. A 1.5 limit load factor shall be applied.

3.3.1.9 Propeller loads

Propeller loads will be based on operation at sea level standard altitude and design gross weight.

3.3.2 Fatigue Design Requirements

The propeller system will be designed so that there will be no calculated fatigue damage between the maximum and minimum loading at the basic mission design weight for all velocities and conditions on any component, and a minimum of 6,000 hours operating life considering all flight and ground conditions. Loads and frequencies of occurrences will be calculated as specified. Lives will be calculated for all components which experience loads above their endurance limit or fatigue strength for 5×10^7 cycles for materials which have no endurance limit.

3.3.3 Material Properties

Material design properties utilized for static strength analysis (limit and ultimate) will be as specified in applicable military specifications and documents. The fatigue strength-life relationship (i.e., S-N curve) for all fatigue critical components will be based on tests of representative components.

3.3.3.1 Design Fatigue Strength

Design S-N curves will be generated from component data in a manner which establishes a design fatigue strength which is no greater than the lesser of: mean -3 standard deviations, assuming a log normal distribution, 80% of the mean value or bottom of scatter. If runouts (non-failures) are used in the analysis, they will be treated as failures. In the event a particular specimen has been run at several load levels, it can only be used as a single data point.

3.3.3.2 Mean Steady Stress

The steady-stress levels shall be selected during design development to insure the specified fatigue life and insure by fracture mechanics analysis that all components have adequate crack retarding characteristics to meet the fail-safe requirements of this specification.

Steel structure in the blade shall be an appropriate low alloy VAR steel heat treated to 180 KSI max. The hub shall be an appropriate low alloy VAR steel heat treated to a maximum of 200 KSI.

3.3.4 Torsional Stresses

The effects of steady and alternating torsion will be accounted for in the fatigue, limit and ultimate strength evaluation.

3.3.5 Crack Propagation

An analysis showing the crack propagation characteristics of the main structural elements of the propeller subsystem under representative loading conditions is to be made.

3.3.6 Final Computed Life of Components

The life of the components shall be recomputed using the fatigue test data points generated as a part of this specification. Appropriate small sample corrections shall be made in establishing the fatigue performance of the components.

3.4 DYNAMIC CHARACTERISTICS

3.4.1 Propeller Frequency

The dynamic response characteristics of the blade shall be considered acceptable when the first three coupled flap/chord/torsion natural frequencies, when mounted on the hub and installed on the aircraft, are displaced at least +0.15/rev from an integer harmonic at the operating rpm +5.5%. No natural frequency can occur within the frequency band of 3.8/rev and 4.3/rev. The fundamental torsion mode frequency including control flexibility shall be sufficiently high to preclude blade stall flutter throughout the operating regime up to 1.5 times takeoff power and up to 125% max. rpm. In addition, the proximity of the fundamental torsion frequency to flap/chord modes shall be such that the frequencies will not exist between the same two integers of rpm for any of the first three predominate flapwise/chordwise frequencies in the cruise or takeoff rpm bands.

Analytical methods will be used which account for significant propeller parameters, including the total propeller system stiffness hub impedances, coupling between flapwise and in-plane response, effect of pitch angle and dynamic twist, and effect of loads on propeller system stiffness. Hub impedances are to be calculated and used in the analyses.

3.4.2 Aeroelastic Instabilities

The propeller blade shall be free of aeroelastic instabilities (such as, but not limited to, classical flutter, stall flutter, divergence, pitch lag, and pitch flap instabilities) at all propeller speeds up to 1.25 times the design speed (including the zero rpm feathering propeller condition), at all thrust conditions from the maximum designed negative thrust to the maximum positive thrust (including the effect of control requirements), for all environmental conditions encompassed by the design flight envelope, for all design conditions of gusts and maneuvers, and for all aircraft speeds up to 1.15 the maximum design dive speed (1.15 V_L).

3.4.3 Balance

Balance of the hub blade and spinner shall be in accordance to that specified in MIL-P-26366A.

3.4.5 Aerodynamic Balance

For the critical thrust and rpm conditions, the blades shall be aerodynamically balanced within blade angle ±0.1 degree.

3.4.6 Acoustics

The overall sound pressure level generated by the propeller measured in the plane of the prop at a given distance shall be specified.

3.5 WEIGHTS

The maximum weights for a single propeller subsystem shall be specified as follows:

a) Dry Weight
b) Operating Fluid
c) Ice Control Components

3.6 CONTROL REQUIREMENTS

The propeller control shall be designed to be compatible with the engine control over the full range of operation.

3.6.1 Basic Operating Modes

The basic mode of control will be established for all operating conditions, including ground handling, and shall meet all the requirements of MIL-P-26366-A and the additional conditions given in this section.

3.6.2 Control System Stability and Response Characteristics

The control system response characteristics shall be adequate to attain the required steady state and transient propeller performance. Further, the system as installed shall be free of instabilities, dither and hunting for all thrust conditions with control application at the required rate.

3.6.2.1 Steady-State Performance

Steady-state performance shall be within ±0.5 percent of the speed set under stabilized flight conditions.

3.6.2.2 Propeller Transients

The propeller system shall respond to scheduled control inputs to maintain freedom from speed instabilities in excess of ±0.5 percent.

3.6.3 Range and Rates of Pitch Change

The pitch change mechanism shall control the blades throughout all regimes of flight and ground operations within the blade angle limits specified.

3.6.7.2 Rate

The estimated rate of pitch change in the governing range shall be established.

3.6.4 Safety

3.6.4.1 Reverse Thrust

No single failure or malfunction in either the control unit or pitch change mechanism during normal or emergency operation shall result in unwanted travel of the propeller blades to a position 4 degrees below the normal flight low pitch limit. Propeller system components which have a failure mode rate less than 1×10^{-7} per hour shall be excepted from these requirements.

3.6.4.2 Overspeed/Underspeed Protection

Protection against propeller overspeed and underspeed from the speed governor setting shall be provided to maintain propeller speed at controllable limits in the event of failure of the normal speed governor system. Overspeed/underspeed protection shall be provided only for the control assembly which is selected to control the propeller when the control is in the governing mode.

3.6.4.3 Feathering

The pitch change mechanism must be capable of feathering the propeller operating at 120 percent of takeoff rpm.

3.6.4.4 Unfeathering

The pitch change mechanism must be capable of unfeathering the propeller operating at zero propeller rpm.

3.7 OPERATIONAL UTILITY REQUIREMENTS

For the requirements of this section, a ratio of operating hour/flight hour shall be established.

3.7.1 Reliability Numerical Requirements

3.7.1.1 Overhaul Frequency

The propeller shall be designed for on-condition maintenance exclusively during its service life; scheduled overhaul (i.e., TBO) will not be practiced.

3.7.1.2 Unscheduled Maintenance Frequency

The propeller subsystem shall have a Mean Time Between Unscheduled Maintenance. Will be specified.

3.7.1.3 Mission Reliability

The propeller subsystem probability of loss of thrust control or other requirement for propeller shutdown shall be established for the design mission.

3.7.2 Maintainability Requirements

The propeller is to be designed to meet the following requirements.

3.7.2.1 Mean Elapsed Maintenance Time

The Mean Elapsed Maintenance Time required to perform organizational level remove and replace tasks and intermediate level repair tasks shall be established. The 90 percentile maximum elapsed task time required to perform corrective and preventive maintenance (M_{max}) on the actuator, control, and propeller blade shall be specified.

3.7.3 Operating Life

The propeller subsystem shall have an operating life established where operating life is defined as the period of time during which it is economically feasible to repair the equipment.

3.7.4 Environmental

The subsystem shall operate with minimum degradation of performance, as specified during and after exposure to the following environmental conditions and possible combinations thereof as encountered during worldwide ground and airborne operations.

3.7.4.1 Temperature

The propeller shall withstand continuous operation of all temperature variations ranging from minus 65°F through plus 160°F at sea level and from minus 65°F through plus 30°F at 20,000 feet above sea level and short-term exposure to temperatures within the range of minus 80°F in the inoperative condition.

3.7.4.2 Temperature Shock

The unit shall be capable of withstanding sudden changes in temperature, from minus 40°F through 130°F of the surrounding atmosphere due to rapid altitude changes.

3.7.4.3 Humidity

The system shall withstand relative humidities up to 100%, including condensation due to temperature change and those conditions under which condensation occurs in the form of frost as well as water.

3.7.4.4 Salt Spray

The system shall withstand salt sea atmosphere as encountered along coastal regions.

3.7.4.5 Sand and Dust

The system shall withstand conditions of fine blowing sand and dust particles as encountered in desert areas. The protection system shall demonstrate flightworthiness of the entire blade for the acquisition prop only surface after operating at the equivalent of 1½ hours at takeoff speed in a sand environment containing 200 milligrams per cubic foot of 80% SiO_2 having 80% of particles between 40 and 400 microns.

3.7.4.6 Rain Damage

The system shall withstand conditions of rain impingement on exposed surfaces.

3.7.4.7 Stone Damage

Limits will be established based on propeller installation and expected operating condition.

3.7.4.8 Bird Strike

The propeller must withstand the impact of a 4-lb bird entering the plane of rotation at any angle, in any operational mode, without loss of propeller control or the requirement of blade spar maintenance.

3.7.4.9 Fungus

No materials which are nutrients for fungus shall be used.

3.7.4.10 Lightning

The system shall be capable of operating in lightning conditions per MIL-B-5087B (ASG). Acquisition phase blades shall demonstrate flightworthiness for at least 3 hours after a 200,000-ampere strike and shall sustain no significant damage from 50,000-ampere strikes.

3.7.4.11 Icing

The ice control features shall allow the propeller subsystem to operate satisfactorily under the meteorological conditions specified in MIL-P-26366A.

3.7.4.12 Vibration

The system shall be capable of withstanding the vibration levels prescribed in MIL-STD-810B, Method 514.1, Category (b) curves (G) and (L) as applicable.

3.7.4.13 Acceleration

The propeller shall be capable of withstanding the shock levels prescribed in MIL-STD-810B, Method 516.1, Procedure I, Figure 516.1-1 as applicable for acquisition system only.

3.7.5 Survivability

The survivability requirements for the propeller shall be established based on the design mission.

3.7.7 Human Engineering Performance

Design standards, human capabilities and limitations set forth in MIL-STD-1471 and Air Force System Command Manual AFSCM 80-3 shall be used as guidelines for design details and human performance requirements.

3.7.8 Safety Requirements

3.7.8.1 Fail-Safe Design Definition

A fail-safe design is one which is capable of safe operation in a partially failed state, and which failure detection is provided and correct action can be taken prior to reaching an unsafe condition.

3.7.8.2 Safety-Critical Propeller Functions

The following propeller assembly functions are considered essential to safety of flight and shall be considered from the prototype prop and shall be provided for the acquisition prop:

Blade retention
Continuity of hub to drive shaft
Inplace pitch lock which limits pitch change to one degree in event of failure of pitch change system
Pitch continuity to blades
Blade pitch feathering except when pitch lock condition exists
Balance

Loss of any of the above functions is classified as non-tolerable to flight safety.

3.8 DESIGN AND CONSTRUCTION

3.8.1 General Design Features

The propeller subsystem design and construction shall comply with or exceed the requirements of MIL-P-26356A. In addition, the design should comply with the features given in the following paragraphs and referenced specifications.

3.8.1.1 Mounting Interface

The proposed mounting interfaces and installation to and within the engine nacelle shall exhibit the necessary maintainability characteristics to permit propeller component replacement in specified time. The removal and reinstallation of the component/assembly shall be accomplished by performing only those operations of manually loosening and fastening mounting hardware and assembly items. Hoisting provisions shall be incorporated for handling large and/or heavy components. Propeller components shall be designed to utilize standard and general removal and installation tools.

3.8.1.2 Special Design Features

3.8.1.2.1 Rigging

The design shall be that actuator or control units of the subsystem can be replaced and rigged on the aircraft within .75 hour. It shall be possible to replace the propeller major components without changing the aircraft control rigging.

3.8.1.2.2 Test Points

The subassembly shall include provisions for test points. The selection of these test points and parameters shall be evolved from an approved maintenance analysis.

3.8.1.3 Maintainability Design

3.8.1.3.1 Locking and Threaded Parts

All threaded parts shall incorporate a positive locking feature except for those fasteners for which this provision is proven unnecessary. Safety wiring (lock wire) shall be the least desirable method, and shall be utilized only where it is proven that self-locking devices, lock nuts, castellated nuts and cotter pins cannot be employed.

3.8.1.3.2 Wire, Cable and Tube Routing

Wire, cable and tubes shall be routed to avoid all areas of extreme temperatures and abrasive hazards.

3.8.1.3.3 Removal and Installation

The removal and installation of components and assembly shall be accomplished exclusively by loosening and fastening or normal mounting hardware and connectors, preferably without the need for special tools.

3.8.2 Selection of Specifications and Standards

Specifications and standards for necessary commodities and services not specified herein shall be selected in accordance with the order or precedence set forth in MIL-STD-143.

3.8.3 Materials, Parts and Processes

3.8.3.1 Materials

Unless otherwise specified herein, all materials used in the design of the subsystem shall conform to the following:

3.8.3.1.1 Electrical Wire

Electrical wire for internal use shall conform to the requirements of MIL-W-22759.

3.8.31.2 Fluorescent Materials

No materials shall be used that will be fluorescent when subjected to ultraviolet light.

3.8.3.1.3 Electrical Cable

Electrical cable for internal use shall conform to the requirements of MIL-W-5088.

3.8.3.1.4 Magnetic Materials

Highly stressed magnetic materials shall be inspected in accordance with MIL-I-6868.

3.8.3.1.5 Mechanical Rubber Components

Mechanical rubber components shall be primarily of elastomeric materials which possess resistance to ozone, weathering, and temperature effects, and shall be compatible with MIL-H-5606B, MIL-L-23699 and MIL-L-7808 fluids.

3.8.3.1.6 Lubrication

Lubrication will be permanent and self-applying wherever possible. In no case shall lubrication requirements be more frequent than 150 flight hours. All servicing functions will be accomplished through quick-access provisions.

3.8.3.1.7 Lubricating Oils

Lubricating oils, used for both lubrication and hydraulic control and power functions, shall conform to the requirements of MIL-L-23699 or MIL-L-7808.

3.8.3.1.8 Preservative Oils

Preservative oils shall conform to the requirements of MIL-L-23699 or MIL-L-7808 for internal protection, and MIL-C-11796 or MIL-C-16173 for external protection.

3.8.3.2 Parts

3.8.3.2.1 Hardened Steel Parts

Steel parts may be hardened in order to achieve required wear characteristics.

3.8.3.2.2 Bosses

All internally threaded bosses shall conform to MS 33649. Bosses shall be made deep enough or shall incorporate stops to prevent damage to internal mechanism or blockage of internal passages when fittings are screwed into the bosses.

3.8.3.2.3 Forgings, Ferrous

Ferrous forgings shall be controlled and inspected in accordance with MIL-F-7190 and MIL-I-6868.

3.8.3.2.4 Forgings, Nonferrous

Nonferrous forgings shall be controlled and inspected in accordance with MIL-T-9047 and MIL-A-22771, as applicable, and MIL-I-6866.

3.8.3.2.5 Castings

Classification and inspection of all castings shall be in accordance with MIL-C-6021.

3.8.3.2.6 Threads

All conventional straight screw threads shall be class 3 in accordance with MIL-S-7742, except that rolled threads shall conform to MIL-S-8879.

3.8.3.2.7 Seals

Seals shall be primarily of elastomeric material which conforms to MS 9241 or MS 29561. Backup rings of Teflon or equivalent material shall conform to MS 28774.

3.8.3.2.8 Packing Glands

Packing glands shall conform to MIL-P-5514, except where improvements are required and approved.

3.8.3.2.9 Lubrication Fittings

The design of lubrication fittings shall be in accordance with MIL-F-3541.

4. PRODUCT ASSURANCE

4.1 Inspection Responsibility

The supplier is responsible for the performance of all inspection requirements as specified herein. Except as otherwise specified, the supplier may utilize his own or any other acceptable inspection facilities. Inspection records of the examination and tests shall be kept complete and be available.

4.2 ENGINEERING DEVELOPMENT TESTS

The inspection and testing of the propeller subsystem for the prototype aircraft propellers shall be classified as follows:

- Component tests
- Preliminary flight release tests

4.3 TEST CONDITIONS

The applicable test conditions given in MIL-P-26366A shall be used.

4.4 COMPONENT TESTS

The supplier shall perform component testing as part of the prototype preflight qualification program. This testing shall include but not be limited to the following:

4.4.1 Experimental Stress Analysis

Experimental stress analysis of the blade root end and hub barrel to define stress distribution.

4.4.2 Fatigue Test Blade

Fatigue tests (resonance type, zero mean stress) on two blades at two stress levels each, for 10^7 cycles. The lower of the two stress levels shall correspond to the maximum design load for zero fatigue damage.

4.4.3 Fatigue Tests Retention

Fatigue tests of the blade root retention system (four specimens) at two stress levels each, for 10^7 cycles. The lower of the two stress levels shall correspond to the maximum design load for zero fatigue damage. This test shall include axial loading to simulate centrifugal force and alternating bending.

4.4.4 Fatigue Tests Pitch Change System

Fatigue tests on one propeller set of pitch change mechanism. This test may consist of the application of design loads alternating between the two sides of the pitch change actuator with blades locked for 20,000 cycles.

4.4.5 Functional Tests

Functional testing of the control and propeller assemblies and of pumps, motors, valves and other components including measurement of performance characteristics (response rates, gains, lags, transfer functions, etc.)

4.4.6 Spinner Tests

Vibration tests of the spinner to check resonances.

4.4.7 Barrel Tests

Fatigue tests of the barrel tail shaft will be performed during gearbox qualification testing.

4.5 PRELIMINARY FLIGHT RELEASE TESTS (PFRT)

The propeller shall complete the preproduction PFRT test in accordance with Section 4.5 of MIL-P-26366A. This test may be performed in conjunction with Engine PFRT Testing per MIL-E-8597.

4.5.1 After the 50-hour PFRT test, propeller test stands shall be kept in operational readiness for solving control and associated problems during the aircraft flight test range.

4.6 ACCREDITATION TESTS

The complete preproduction test shall be completed in accordance with MIL-P-26366A

5. PREPARATION FOR DELIVERY

5.1 PRESERVATION, PACKAGING, AND PACKING

The propeller and components shall be prepared for shipment and storage in accordance with Specification MIL-P-6074. The contractor shall furnish a packing list with each propeller. All parts, components and tools which are not installed on the propeller, but which are shipped with the propeller, shall be included on the packing list.

5.2 MARKING FOR SHIPMENT

In addition to those marking requirements specified in Specification MIL-P-6074, interior packages and exterior shipping containers shall be marked in accordance with Standard MIL-STD-129.

5.3 COVER PLATES

Cover plates, coverings or plugging for all openings on components shall be provided to preclude damage and contamination. Plugs and covers used must be of such a design that it is impossible to install a component without first removing the plug or cover.

6. NOTES

6.1 PREVIOUSLY QUALIFIED COMPONENTS AND ACCESSORIES

Similarity of propeller components and accessories with past propeller components and accessories may form the basis for the deletion of specific tests or portions thereof.

6.2 SYMBOLS AND DEFINITIONS

Definitions in this specification are defined below:

6.2.1 Standard Conditions

Standard conditions are the values of air temperature and pressure given in (MIL-STD-210A). The standard humidity, for the purpose of this specification, is zero vapor pressure at all altitudes.

6.2.2 Propeller

A propeller consists of those components necessary for primary propeller operation, including only the items listed as propeller components in Paragraph 3.1.4.3 of this model specification.

6.2.3 Deleted

6.2.4 Propeller components

Propeller components are items of equipment, rotating or non-rotating, furnished as parts of the propeller system required for propeller operation.

6.2.5 Pitch-Changing Systems

The pitch-changing systems are those systems comprised of all the components required to translate the pitch-changing power into angular movement.

6.2.6 Design Aq

Aq is one times propeller speed (1 x P) excitation factor, where A is the angularity of airflow into the propeller disc in degrees and q is the airplane dynamic pressure in pounds per square foot.

7. DATA REQUIREMENTS

7.1 MODEL SPECIFICATION

An aircraft propeller system model specification conforming to Specification MIL-P-26367 shall be submitted. Where necessary, additional subparagraphs shall be included in the model specification to show compliance with those requirements of this Procurement Specification which are additional to the requirements of Specification MIL-P-26366.

7.2 WORK STATEMENT

The work statement provided shall be developed and approved.

7.3 TECHNICAL DATA

The technical data, curves, estimates, predictions, drawings, reports, manuals and analysis shall be provided to substantiate that propeller performance and design characteristics meet the requirements of this specification.

APPENDIX II
TWO-DIMENSIONAL AIRFOIL DATA

BASIC DATA

The basic two-dimensional airfoil data to be used in strip analysis calculation is for NACA-16 series sections. The data covers a range of thickness ratios of 4 to 21% and design lift coefficients of 0 to .7. The lift data is presented on Figures 34 to 83 in the form of curves of C_L as a function of free-stream Mach number and angle of attack. The corresponding drag data also is presented on Figures 84 to 133 as a function of free-stream Mach number and operating lift coefficient. The data source and procedures used to obtain this set of data are given in the body of the report in the Aerodynamics Section.

To determine the lift and drag coefficients for any airfoil within the range of the data presented, linear interpolation is used to account for the changes of thickness ratio and design lift coefficient. The basic data given on Figures 84 to 133 applies at Reynolds numbers up to 2×10^6.

THICK AIRFOILS

Since the basic data covers only thickness ratios up to 21 percent, additional data are required to find the lift and drag coefficient of sections up to a thickness ratio of 1.0. These data are needed as the inboard sections of propellers often exceed the thickness ratio of 21%. The data for finding the lift and drag coefficients of sections with thickness ratios in excess of 21% are given on Figures 134 to 163 in this appendix. The procedures used to calculate the lift and drag coefficient at a given condition are given on Tables II and III.

To account for changes between NACA 16, NACA 65 and NACA 66 series sections, changes in Reynolds number and to find the variation of the lift and drag coefficients when operating at high values of angle of attack, corrections to the basic data have been developed. The data used to make these corrections is given in Figures 146 to 163. The procedures to be used to apply these data are as follows:

Lift Coefficient

1. Data for NACA 16 series sections Figures 34 to 83 is read at M = .30 (for the desired values of design C_L and h/b) to obtain the low Mach number variation of C_L with α up to 8°.

2. To obtain C_L data for NACA 65 series airfoils, add the lift increment, ΔC_{L65}, to values of C_L at all angles of attack of Item 1. See Figure 146.

3. The value of maximum lift coefficient is determined from Figures 147 to 149 at the section Reynolds number based on the local section velocity. Read the $C_{L\,max}$ for the given section, Figure 147 (16 series), Figure 148 (66 series), or Figure 149 (65 series). To this value of $C_{L\,max}$ ($C_{Li} = 0$) add the C_L at $\alpha = 0^\circ$ for $M = .30$ as evaluated in step 1. From Figure 150 determine the increment in lift coefficient due to Mach number. For 65 series airfoils, add the ΔC_{L65} increment evaluated in step 2. Thus,

$$C_{Lmax} = \underbrace{\left[C_{Lmax} \text{ @ } C_{Li} = 0\right]}_{\text{Figures 147-149}} + \underbrace{\left[C_{L\alpha} = 0\right]}_{\text{Step 1}} + \underbrace{\left[\Delta C_{LM}\right]}_{\text{Fig. 150}} + \underbrace{\left[\Delta C_{L65}\right]}_{\text{Fig. 146}}$$

4. The stall angle of attack is determined from Figure 151 (16 series) or Figure 152 (65 series). These data are for a Reynolds number of 6×10^6. To correct for the existing Reynolds number at any section, obtain the $\Delta\alpha_R$ from Figure 153.

5. The variation of C_L with $\Delta\alpha$ beyond C_{Lmax} is obtained from Figure 154.

Drag Coefficient

1. For NACA 16 series sections, the drag coefficient data is read from Figures 84 to 133 at the given section Mach number for values of C_L up to .80.

2. To obtain the drag coefficient at $\alpha = 8^\circ$, Figures 155 to 160 are used. For a given h/b and C_{Li} and section Mach number, values of $C_{D\alpha} = 8^\circ$ are read at a Reynolds number of 1×10^6 from Figures 155 to 160 . Figures 161 and 162 correct this value to the given Reynolds number. The change in the drag coefficient at 8°, $\Delta C_{DR\alpha} = 8^\circ$, is obtained from Figure 161 for a given RN and h/b. This is multiplied by K obtained from Figure 162 to account for the actual design C_L.

Thus,

$$(C_{D_\alpha} = 8^\circ) = \underbrace{(C_{D\alpha} = 8^\circ)}_{\text{Fig. 155 to 160}} + \underbrace{(\Delta C_{DR\alpha} = 8^\circ)(K)}_{\text{Fig. 161 to 162}}$$

3. Beyond $\alpha = 8^\circ$ obtain the variation of C_D with α from Figure 163 . Thus,

$$C_D = \underset{\text{Step 2}}{(C_{D\alpha} = 8^\circ)} + \underset{\text{Figure 163}}{\Delta C_D}$$

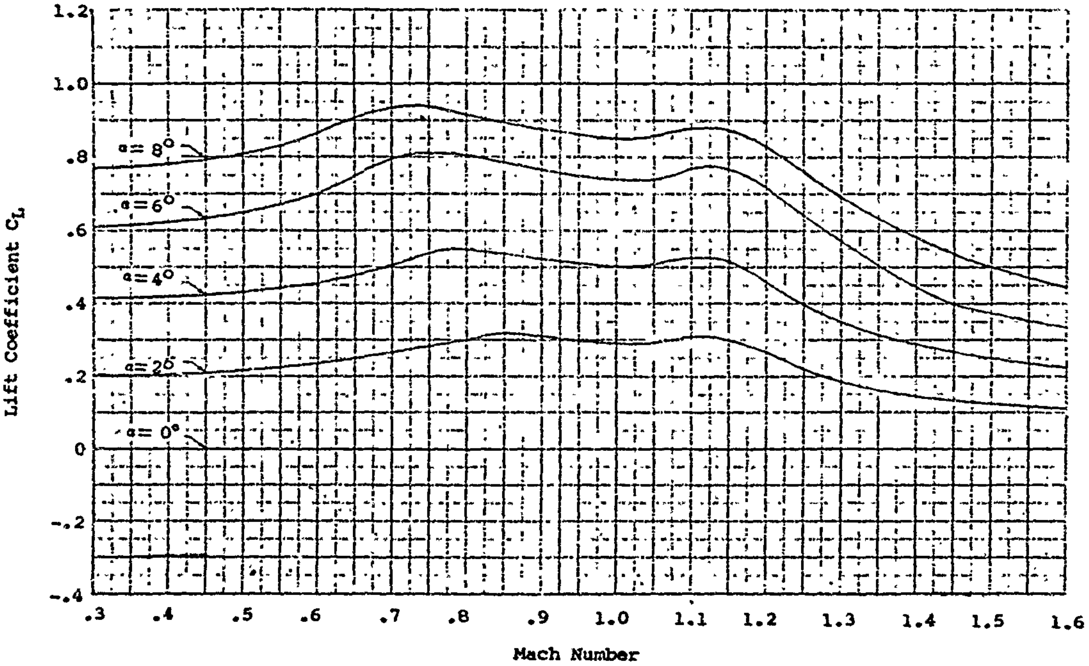

Figure 34. Two-Dimensional Lift Data, NACA 16-004 Airfoil.

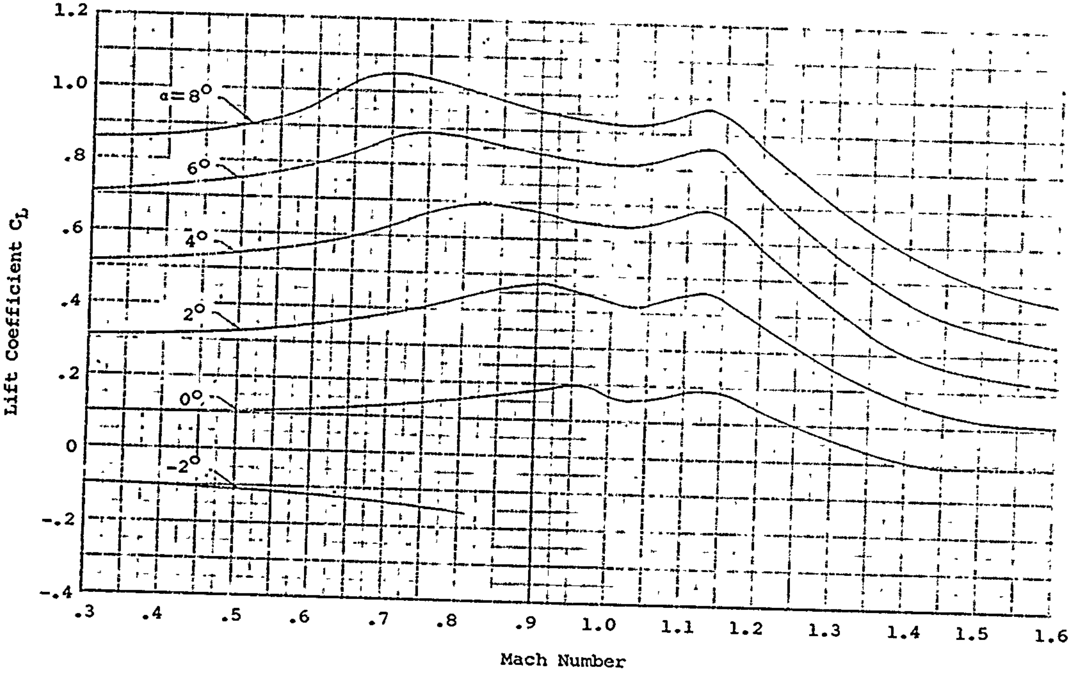

Figure 35. Two-Dimensional Lift Data, NACA 16-104 Airfoil.

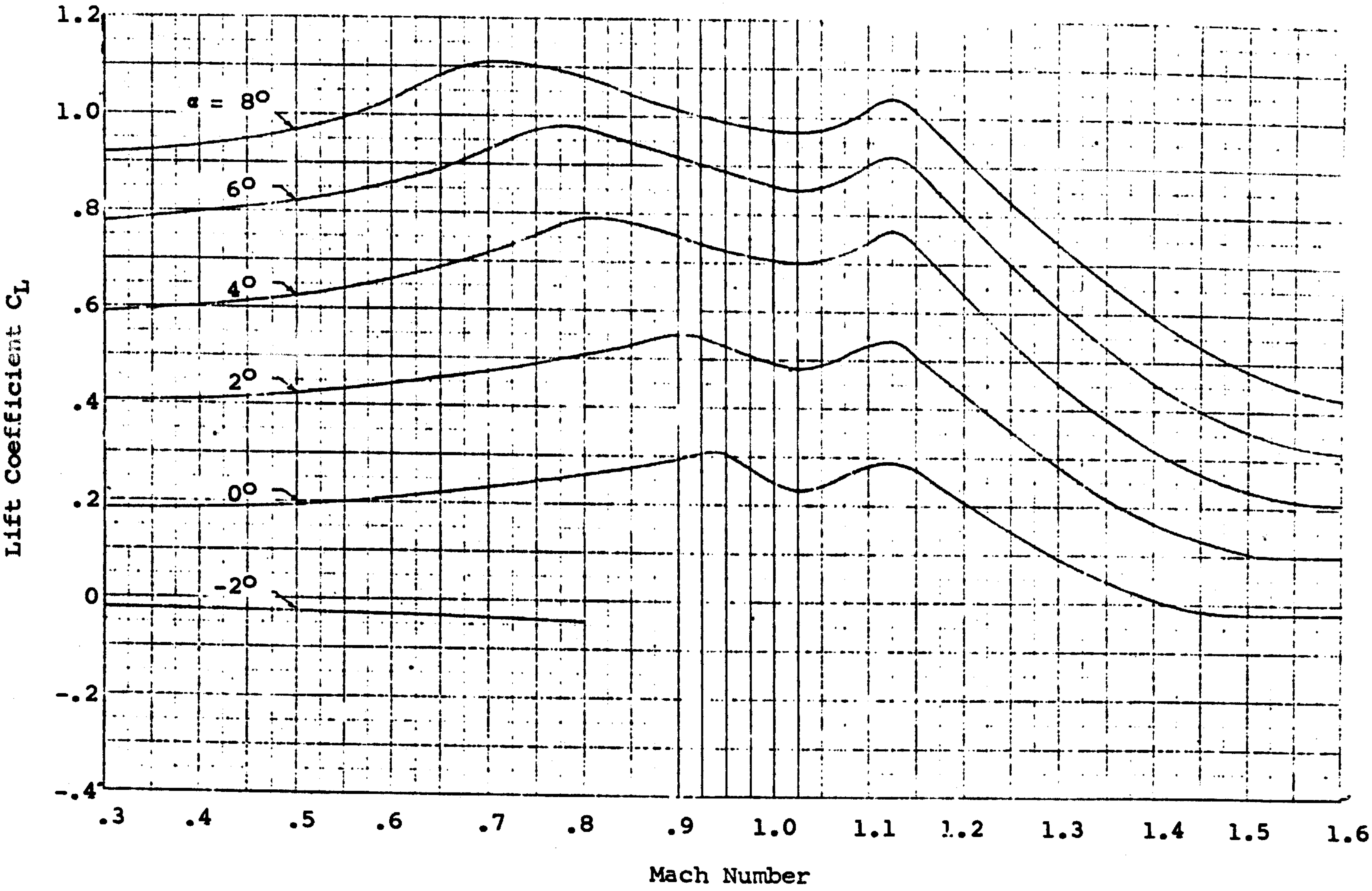

Figure 36. Two-Dimensional Lift Data, NACA 16-204 Airfoil.

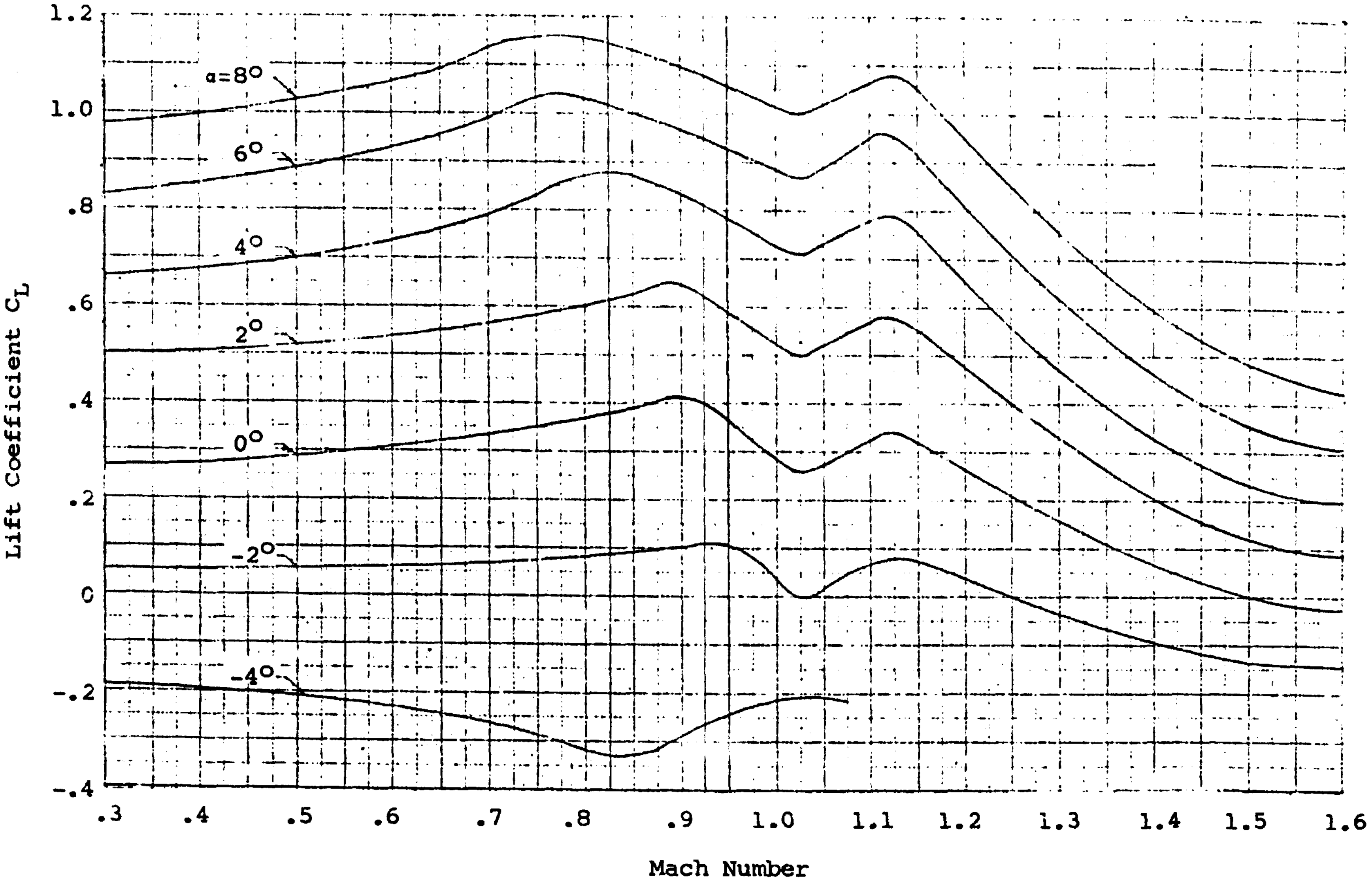

Figure 37. Two-Dimensional Lift Data, NACA 16-304 Airfoil.

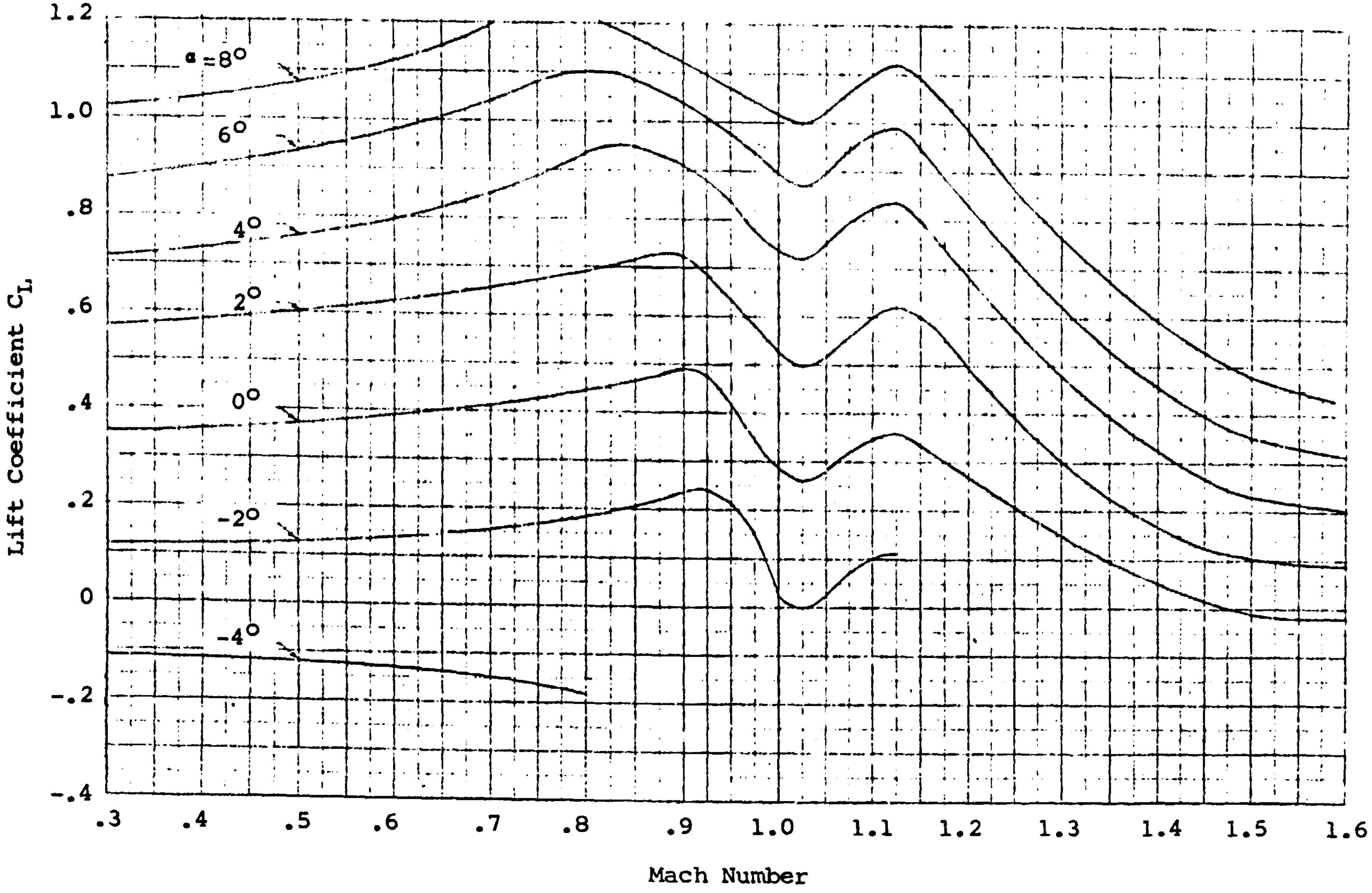

Figure 38. Two-Dimensional Lift Data, NACA 16-404 Airfoil.

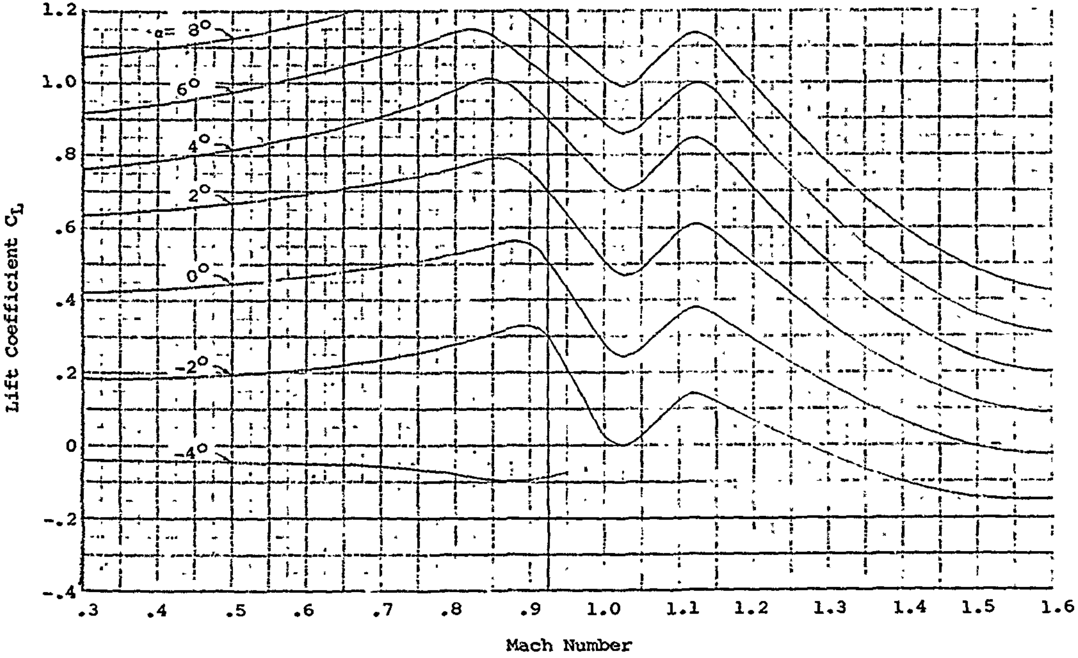

Figure 39. Two-Dimensional Lift Data, NACA 16-504 Airfoil.

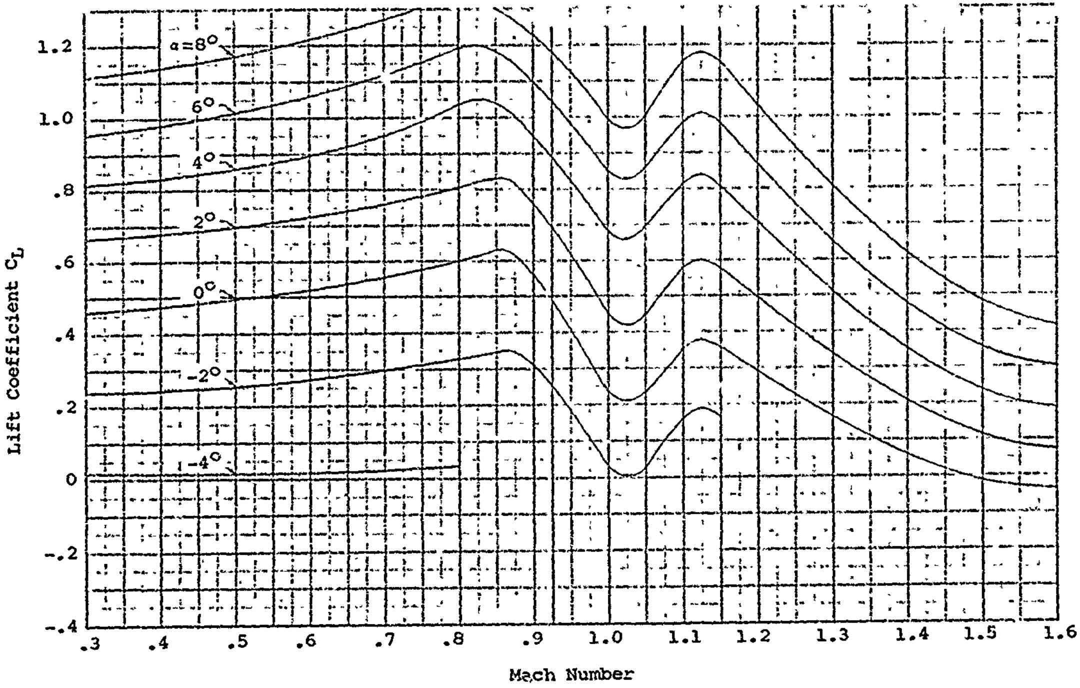

Figure 40. Two-Dimensional Lift Data, NACA 16-604 Airfoil.

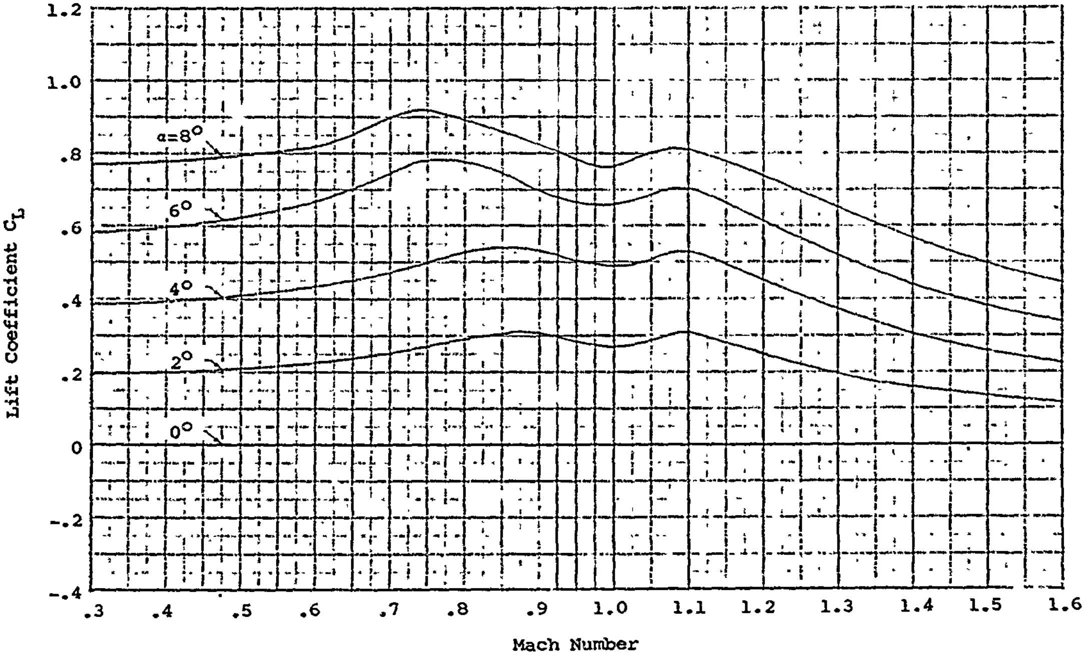

Figure 41. Two-Dimensional Lift Data, NACA 16-006 Airfoil.

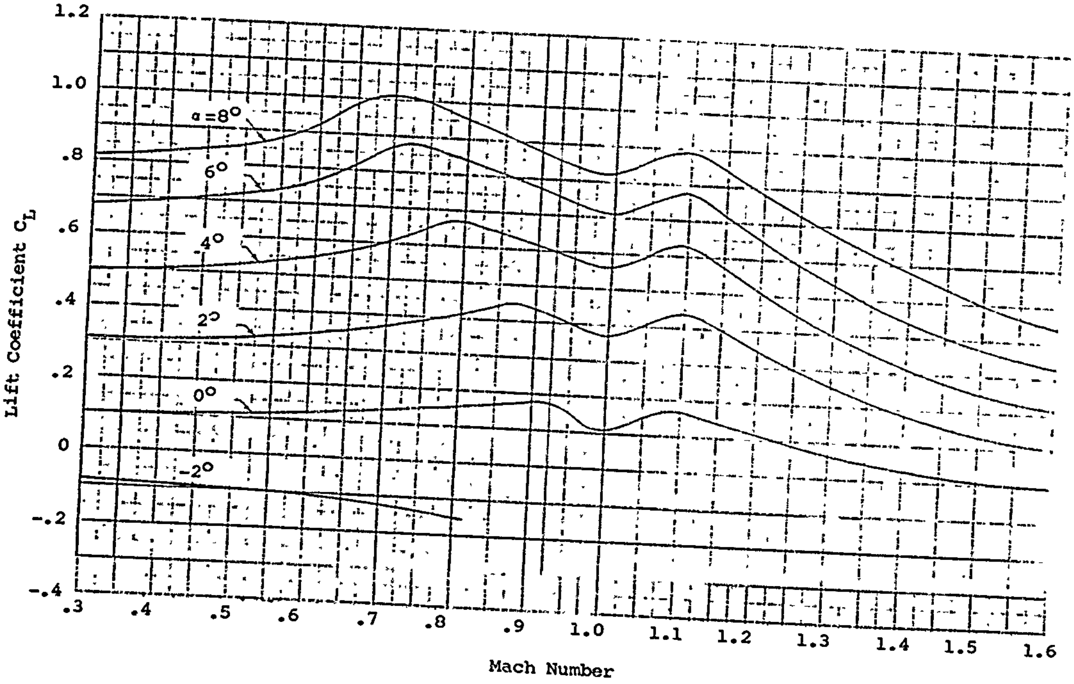

Figure 42. Two-Dimensional Lift Data, NACA 16-106 Airfoil.

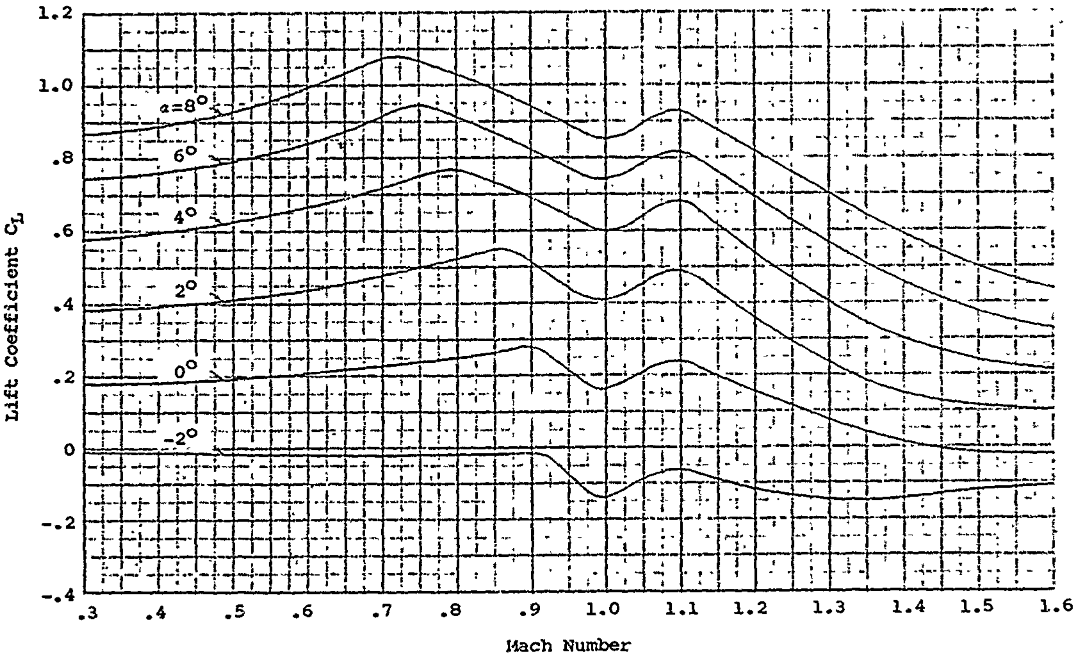

Figure 43. Two-Dimensional Lift Data, NACA 16-206 Airfoil.

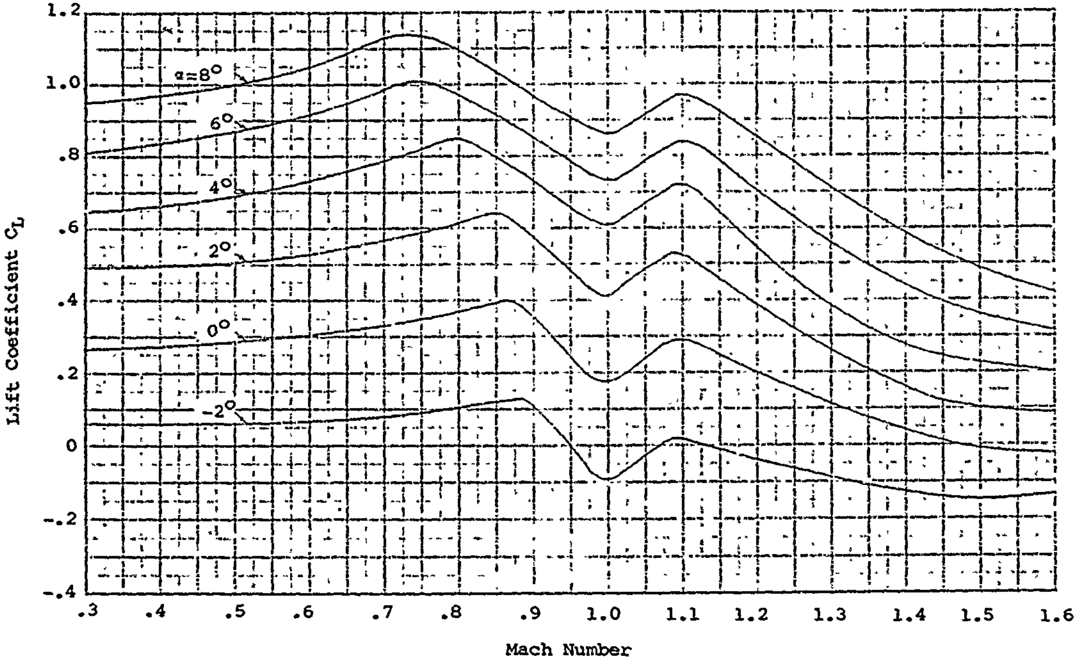

Figure 44. Two-Dimensional Lift Data, NACA 16-306 Airfoil.

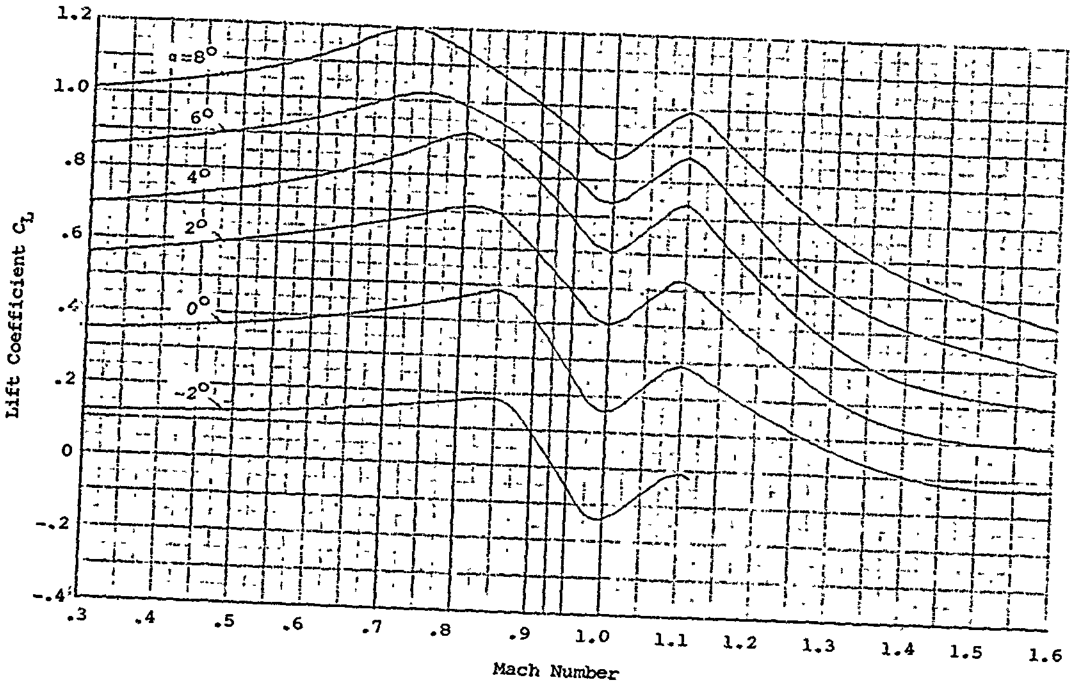

Figure 45. Two-Dimensional Lift Data, NACA 16-406 Airfoil.

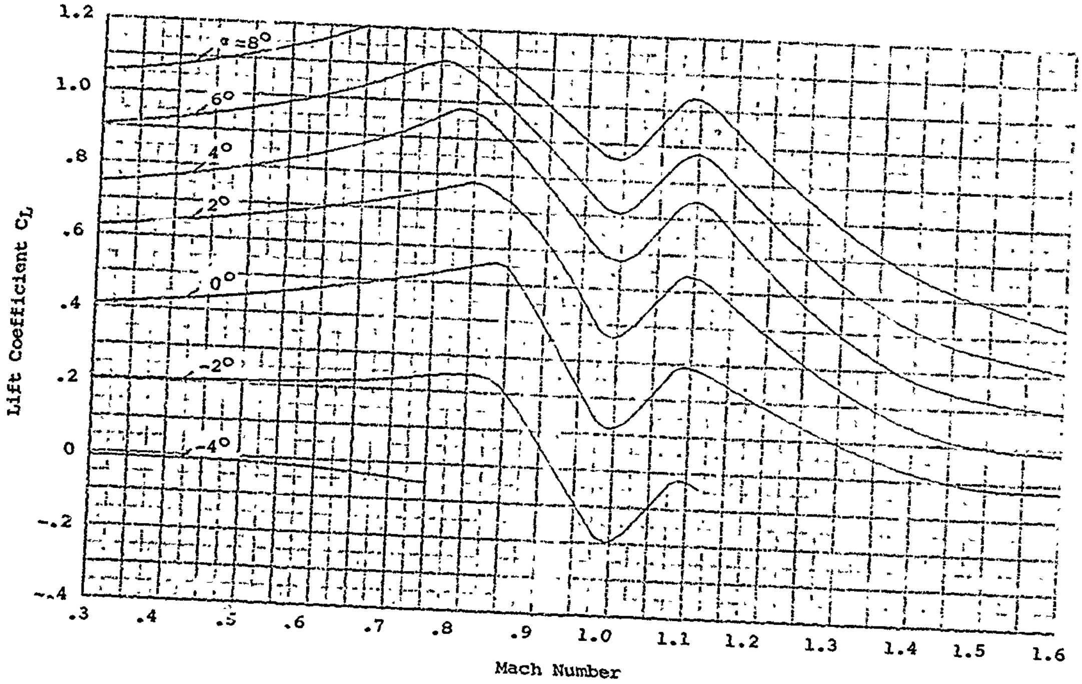

Figure 46. Two-Dimensional Lift Data, NACA 16-506 Airfoil.

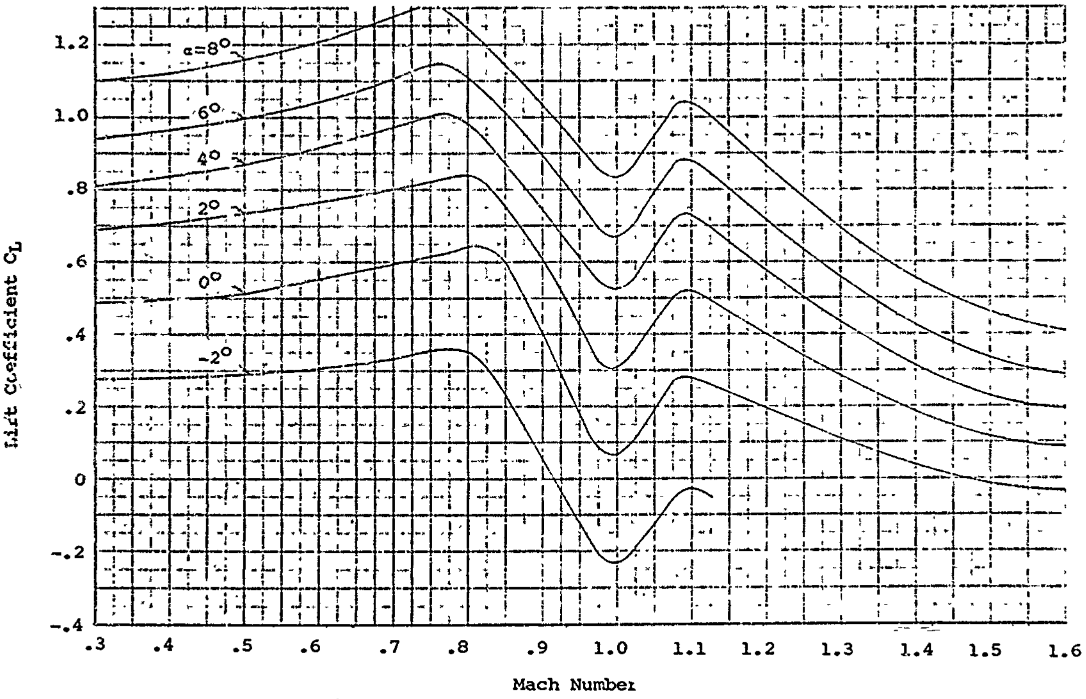

Figure 47. Two-Dimensional Lift Data, NACA 16-606 Airfoil.

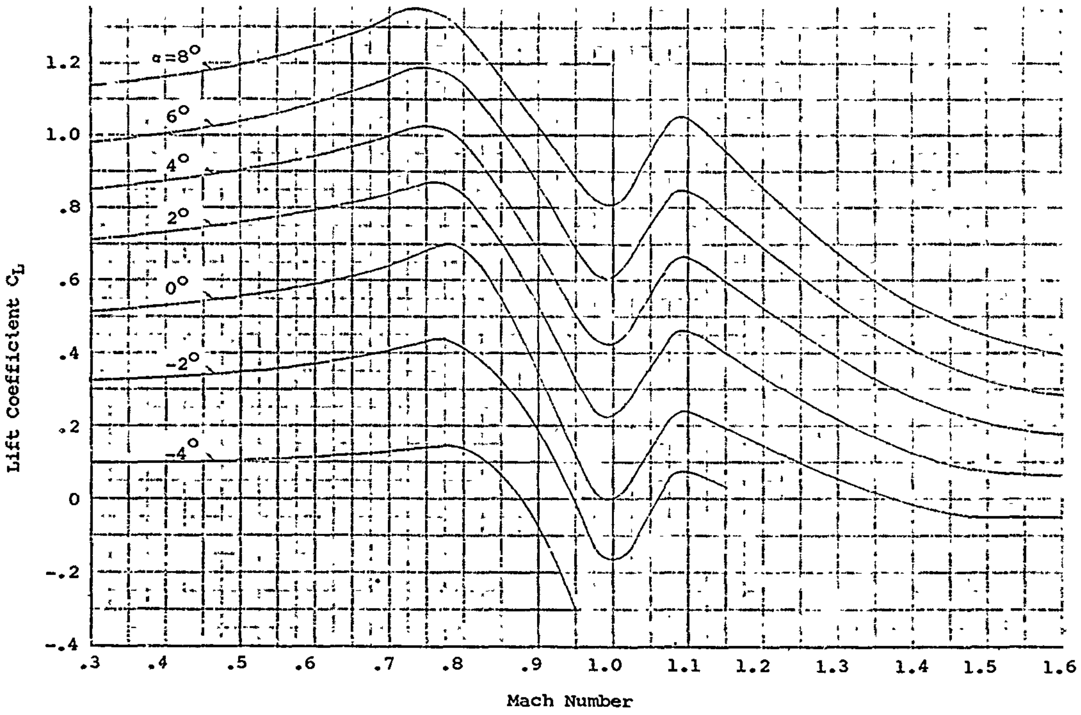

Figure 48. Two-Dimensional Lift Data, NACA 16-706 Airfoil.

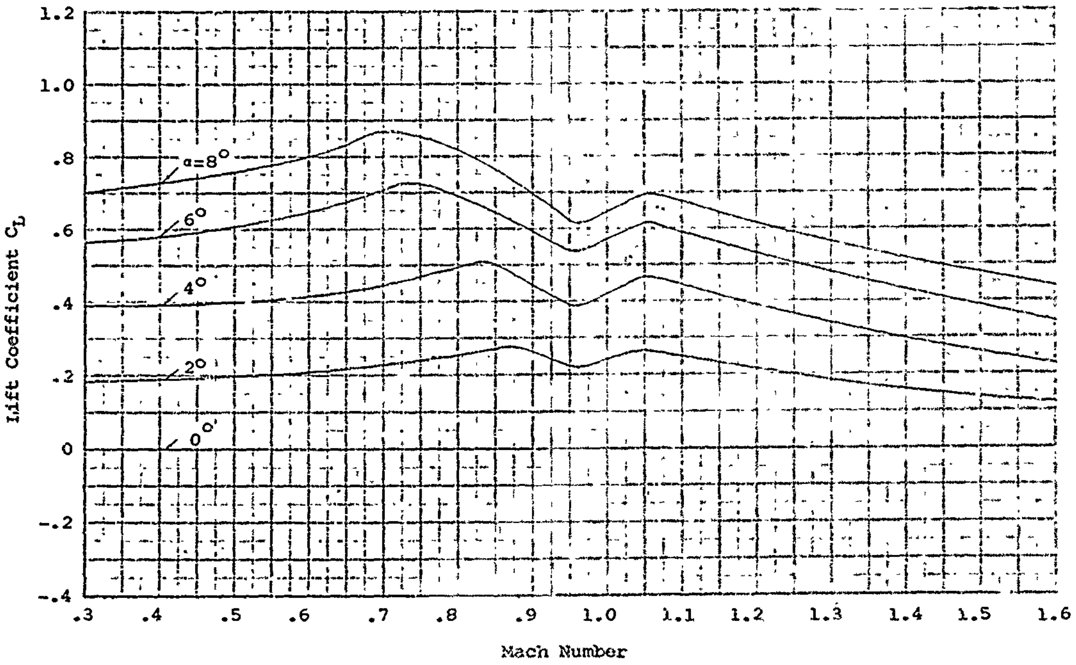

Figure 49. Two-Dimensional Lift Data, NACA 16-009 Airfoil.

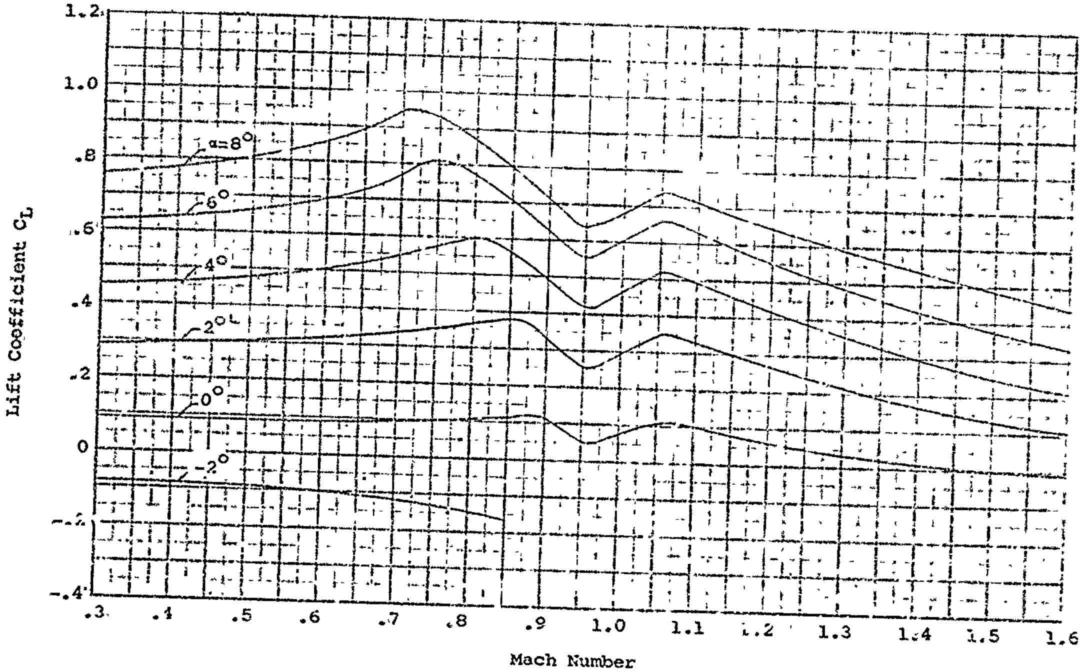

Figure 50. Two-Dimensional Lift Data, NACA 16-109 Airfoil.

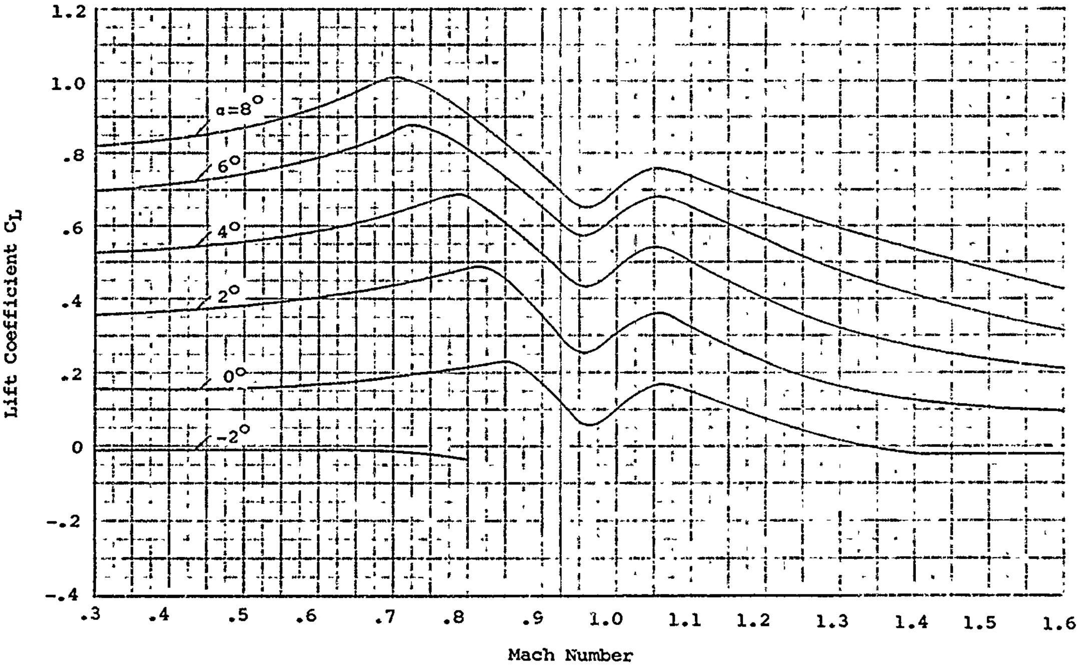

Figure 51. Two-Dimensional Lift Data, NACA 16-209 Airfoil.

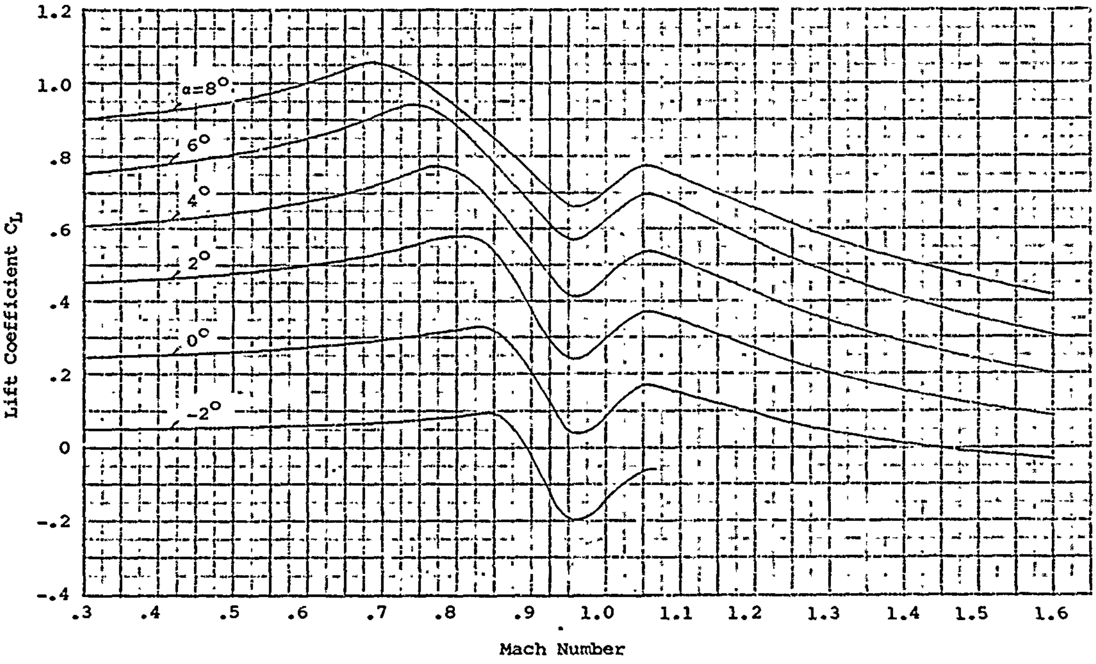

Figure 52. Two-Dimensional Lift Data, NACA 16-309 Airfoil.

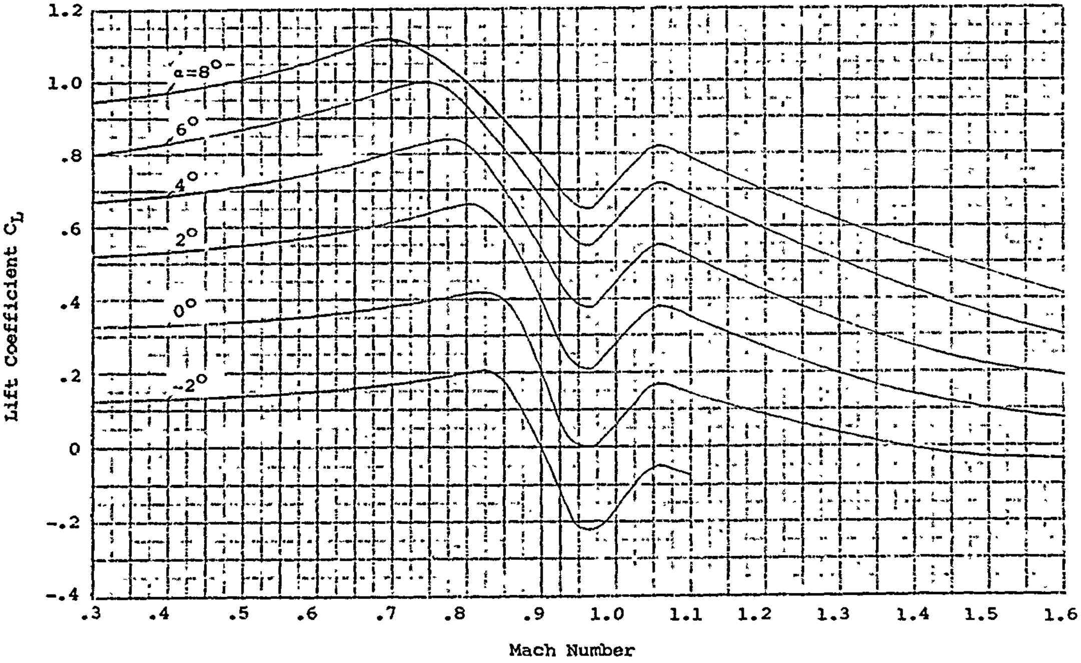

Figure 53. Two-Dimensional Lift Data, NACA 16-409 Airfoil.

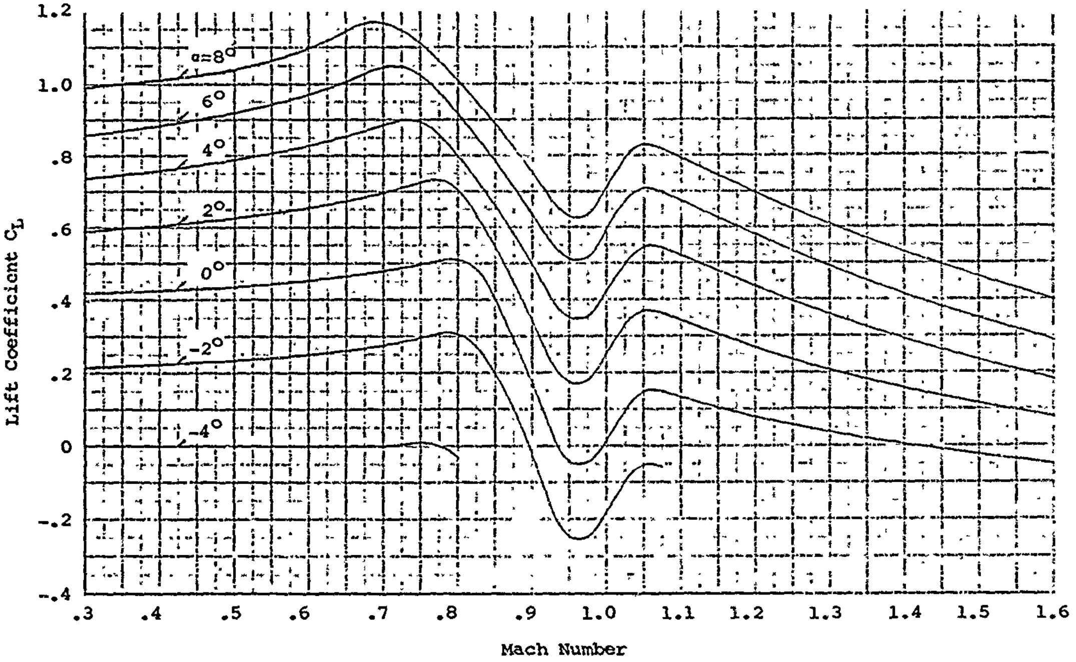

Figure 54. Two-Dimensional Lift Data, NACA 16-509 Airfoil.

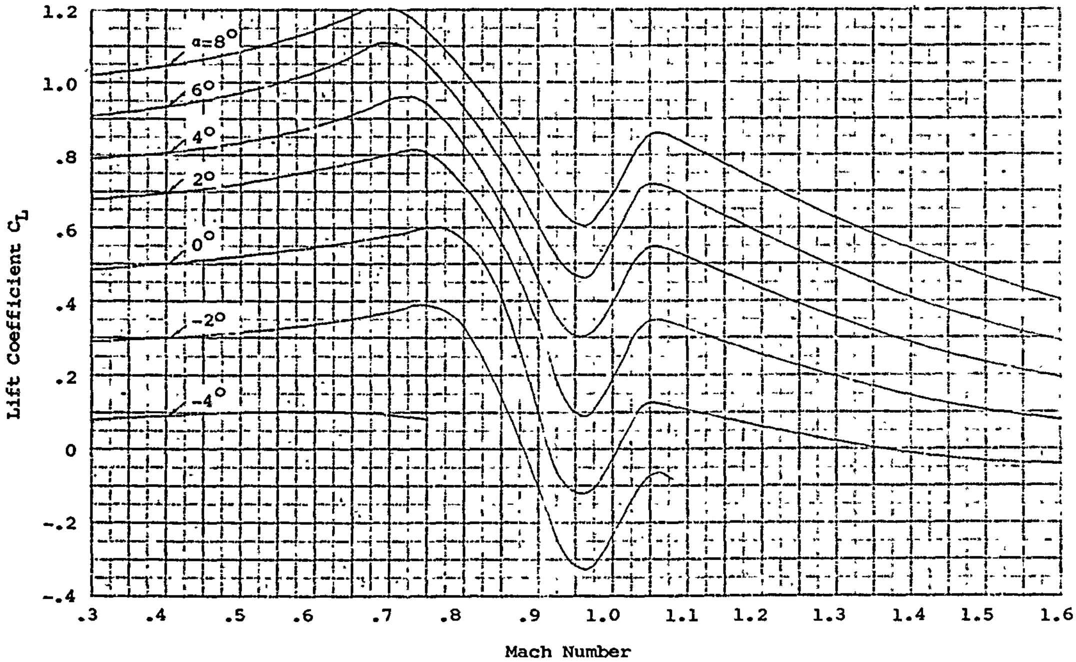

Figure 55. Two-Dimensional Lift Data, NACA 16-609 Airfoil.

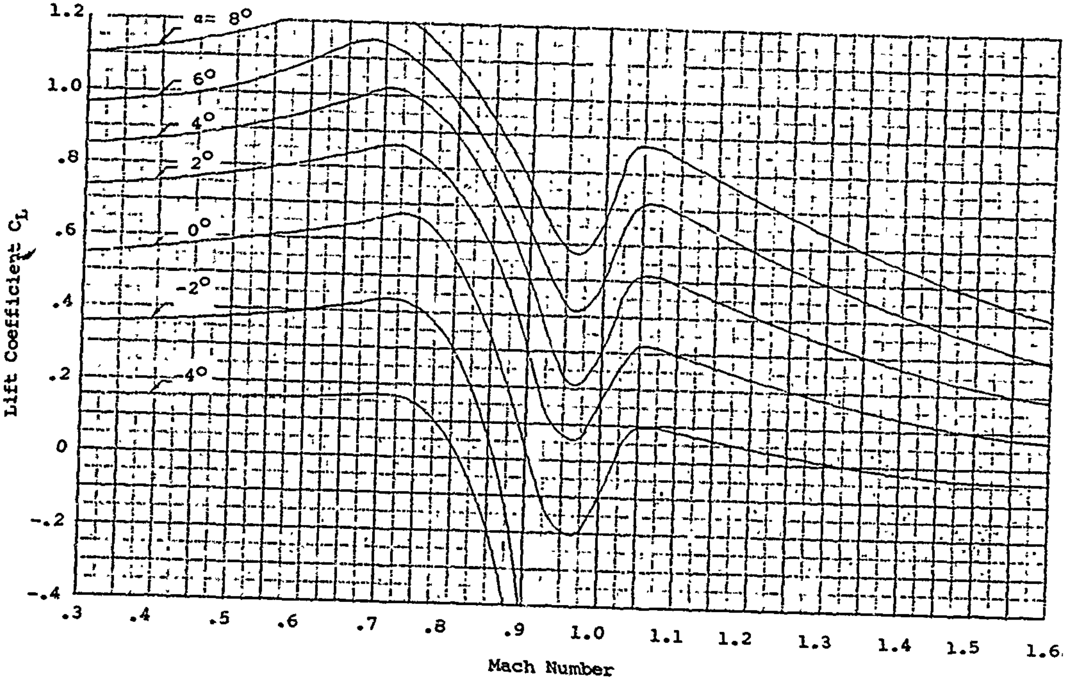

Figure 56. Two-Dimensional Lift Data, NACA 16-709 Airfoil.

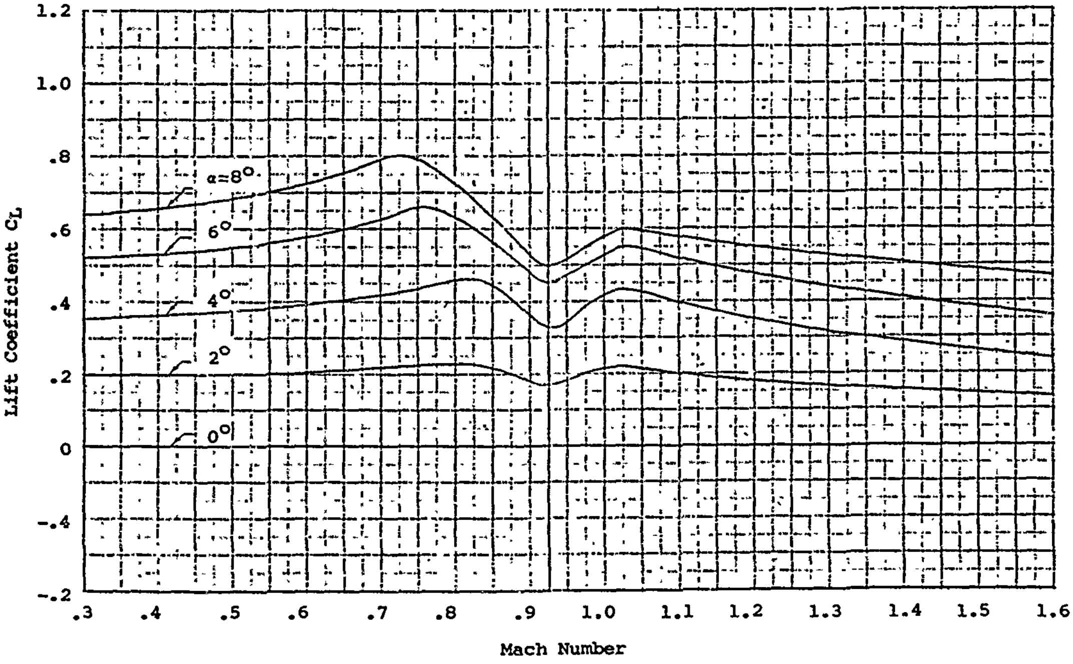

Figure 57. Two-Dimensional Lift Data, NACA 16-012 Airfoil.

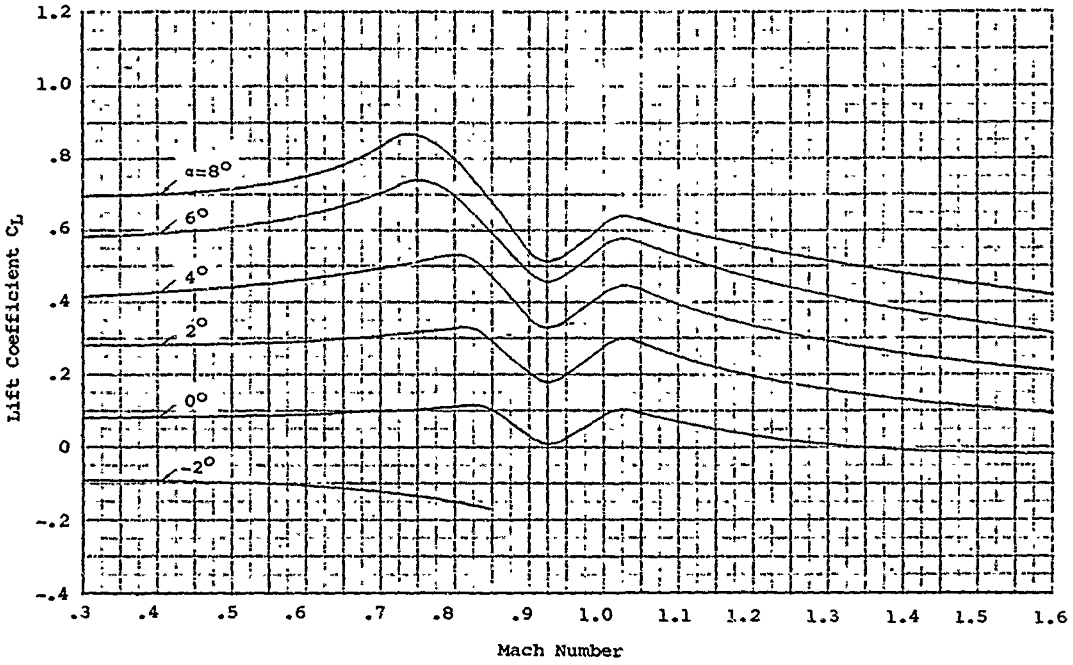

Figure 58. Two-Dimensional Lift Data, NACA 16-112 Airfoil.

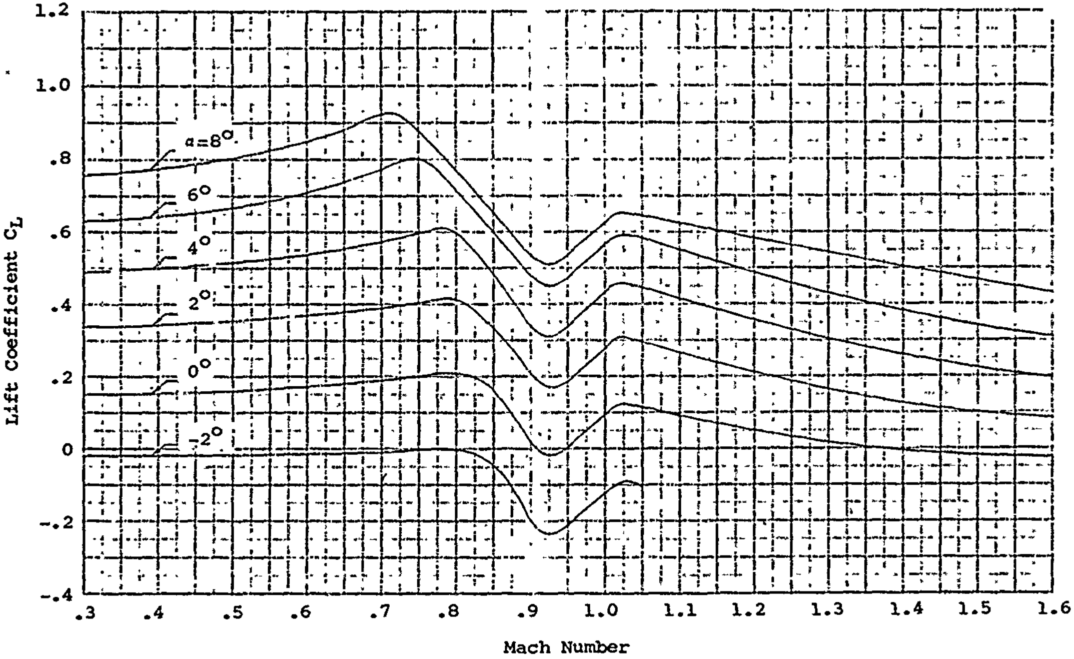

Figure 59. Two-Dimensional Lift Data, NACA 16-212 Airfoil.

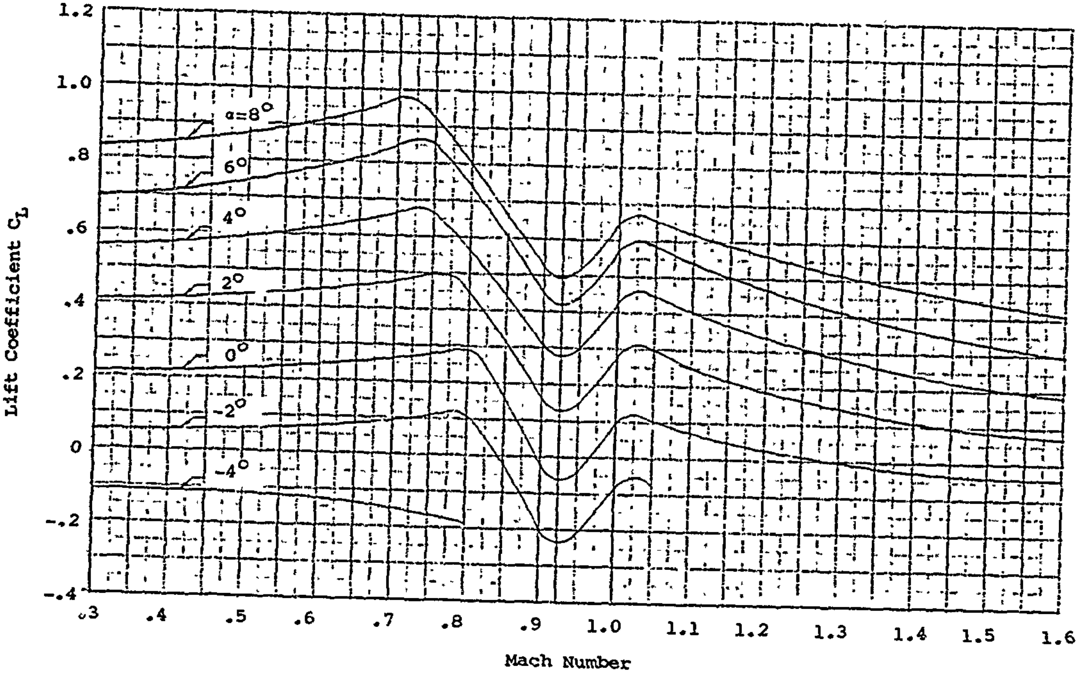

Figure 60. Two-Dimensional Lift Data, NACA 16-312 Airfoil.

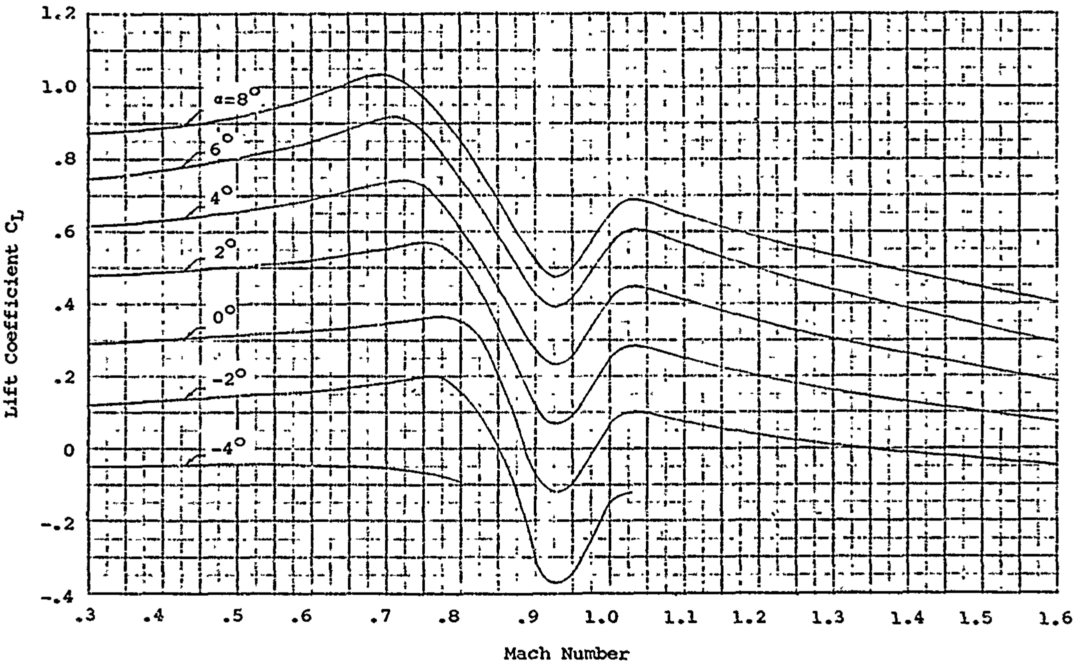

Figure 61. Two-Dimensional Lift Data, NACA 16-412 Airfoil.

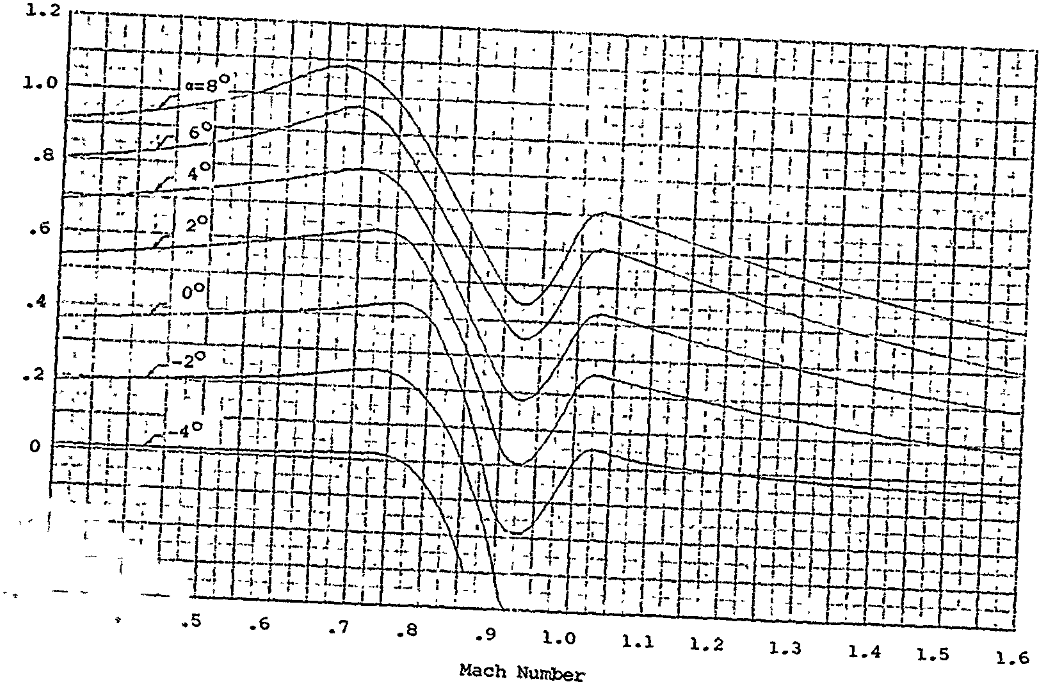

Figure 62. Two-Dimensional Lift Data, NACA 16-512 Airfoil.

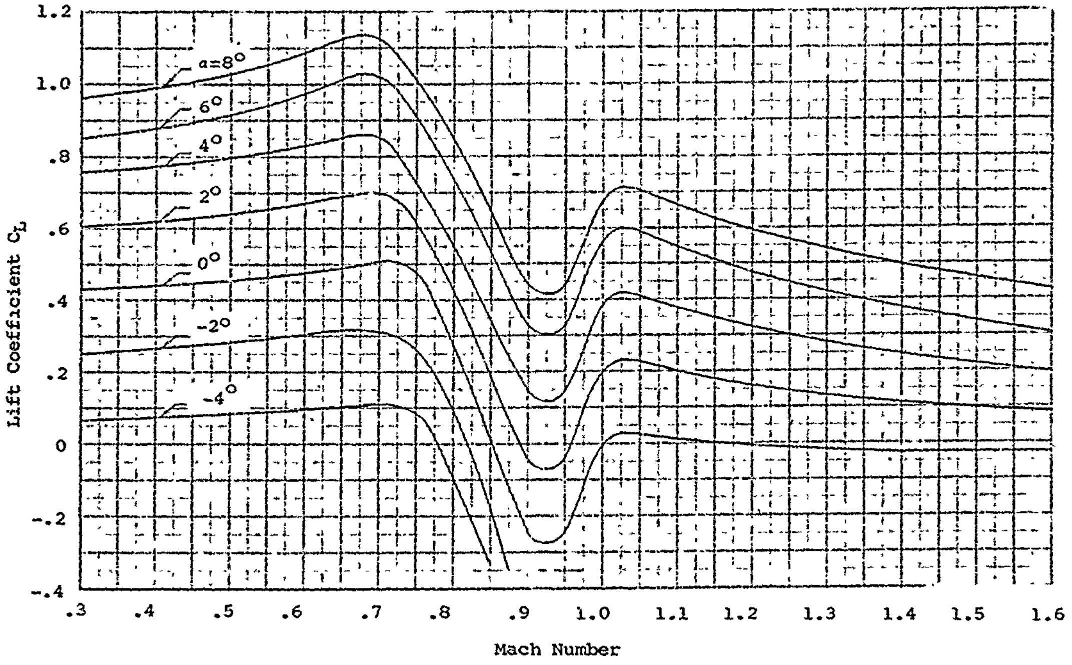

Figure 63 Two-Dimensional Lift Data, NACA 16-612 Airfoil.

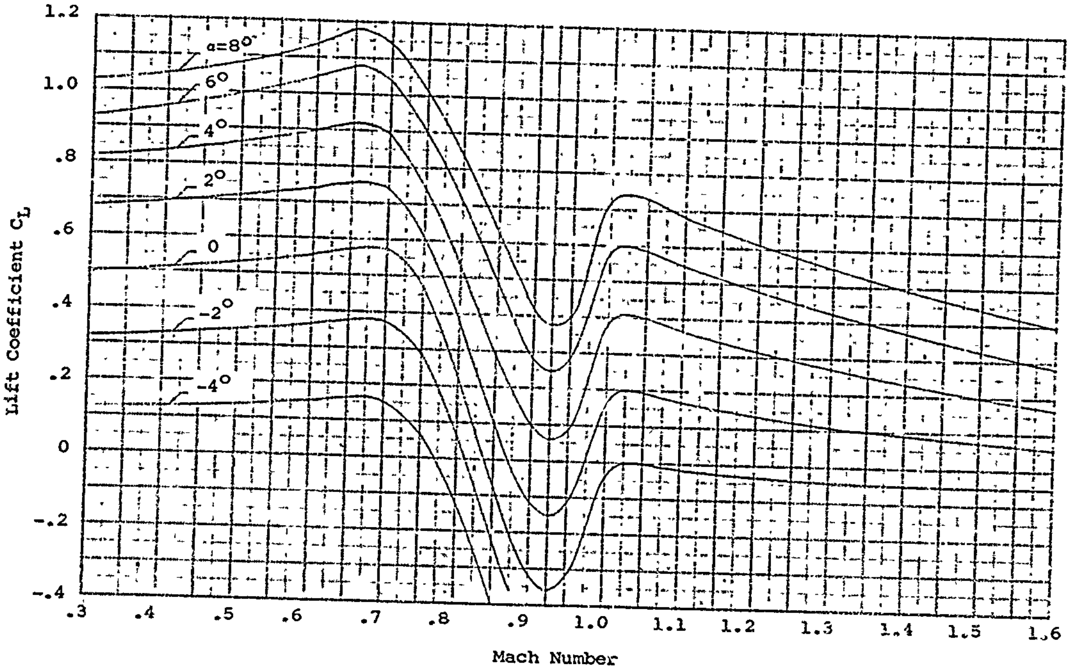

Figure 64. Two-Dimensional Lift Data, NACA 16-712 Airfoil.

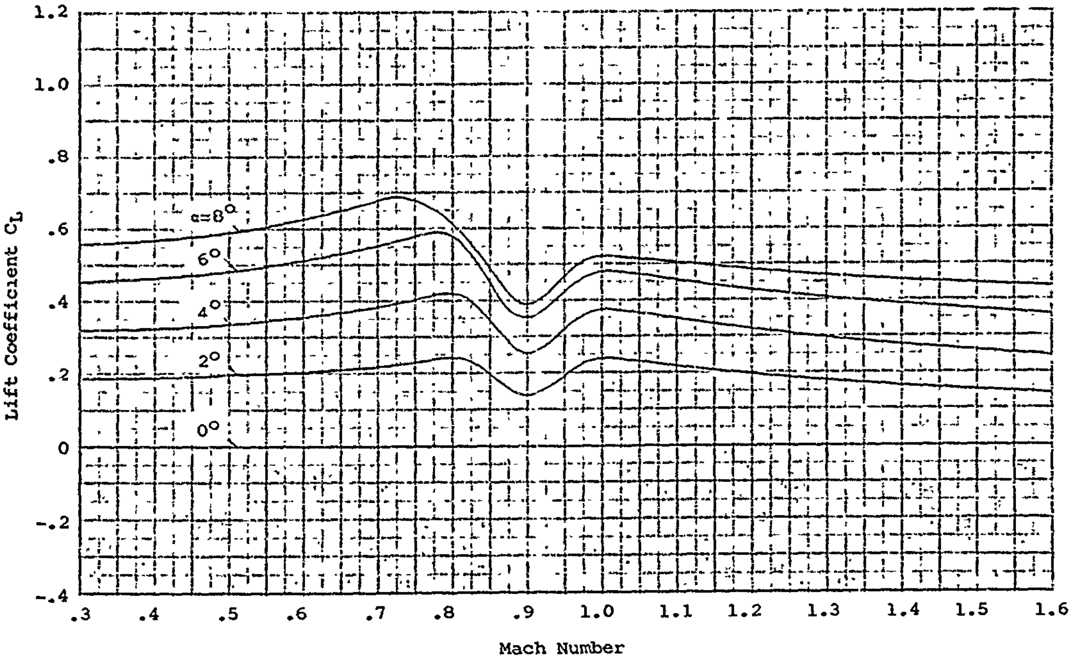

Figure 65. Two-Dimensional Lift Data, NACA 16-015 Airfoil.

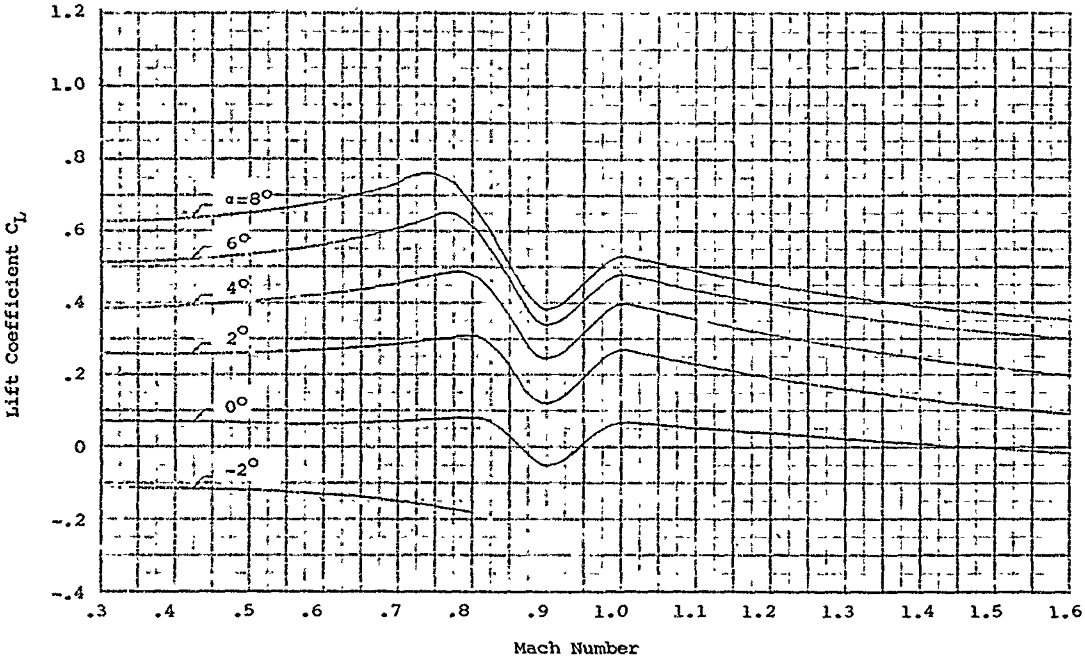

Figure 66. Two-Dimensional Lift Data, NACA 16-115 Airfoil.

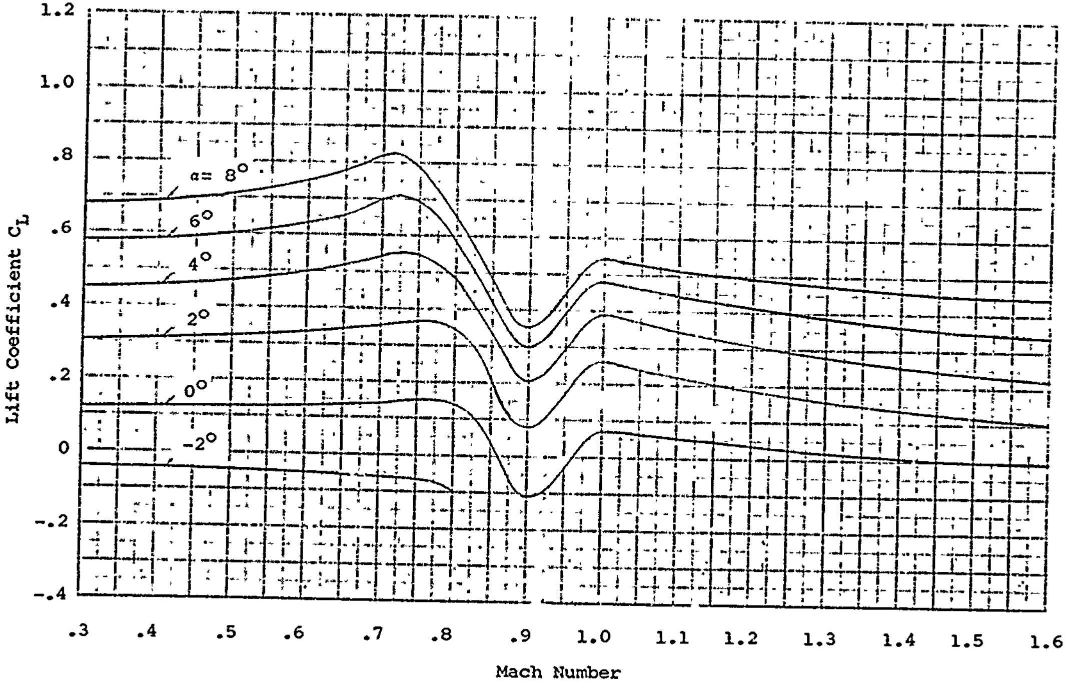

Figure 67. Two-Dimensional Lift Data, NACA 16-215 Airfoil.

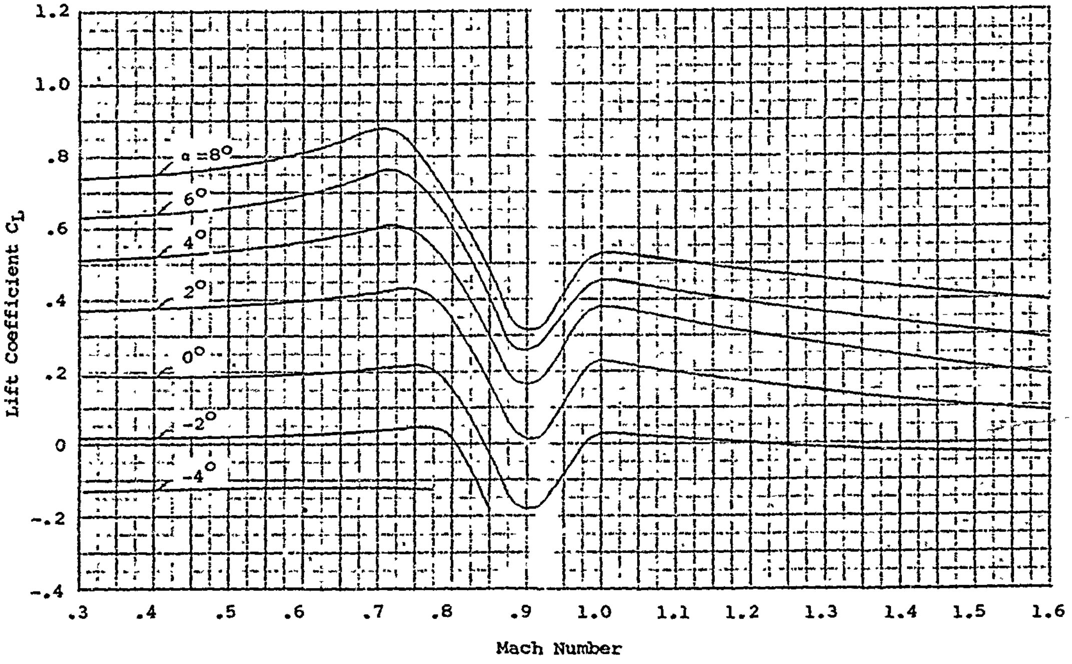

Figure 68. Two-Dimensional Lift Data, NACA 16-315 Airfoil.

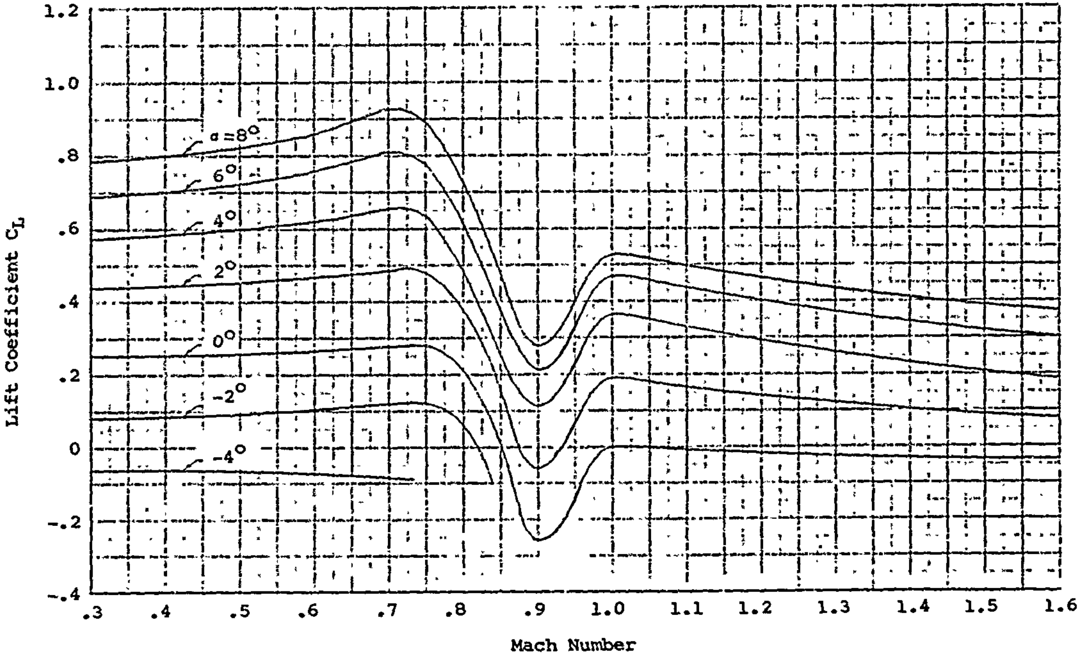

Figure 69. Two-Dimensional Lift Data, NACA 16-415 Airfoil.

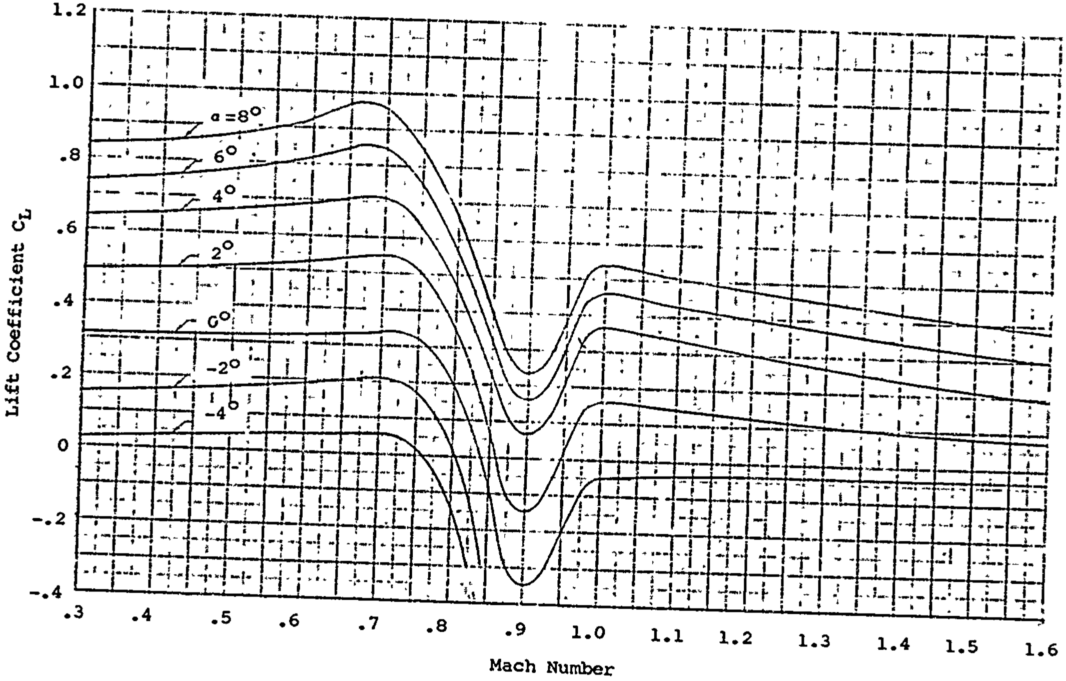

Figure 70. Two-Dimensional Lift Data, NACA 16-515 Airfoil.

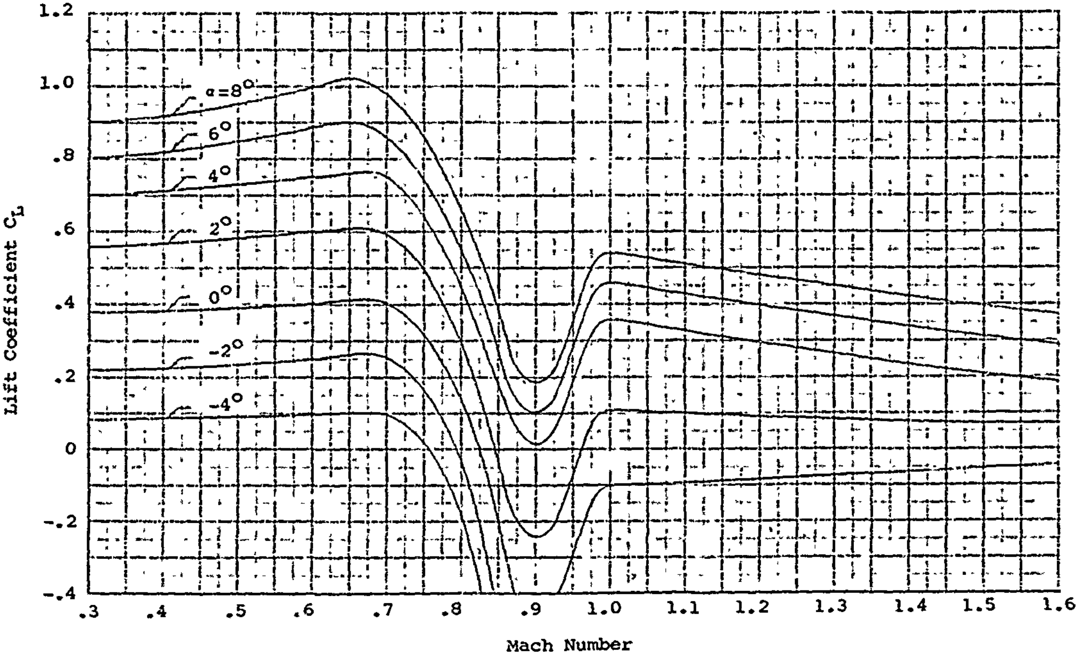

Figure 71. Two-Dimensional Lift Data, NACA 16-615 Airfoil.

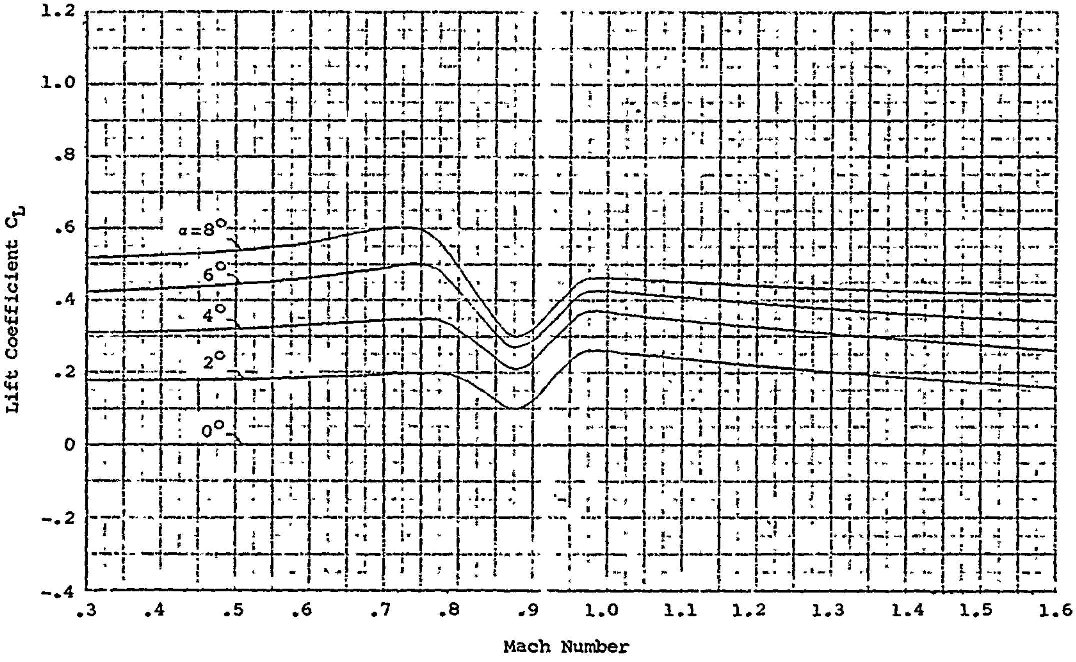

Figure 72. Two-Dimensional Lift Data, NACA 16-018 Airfoil.

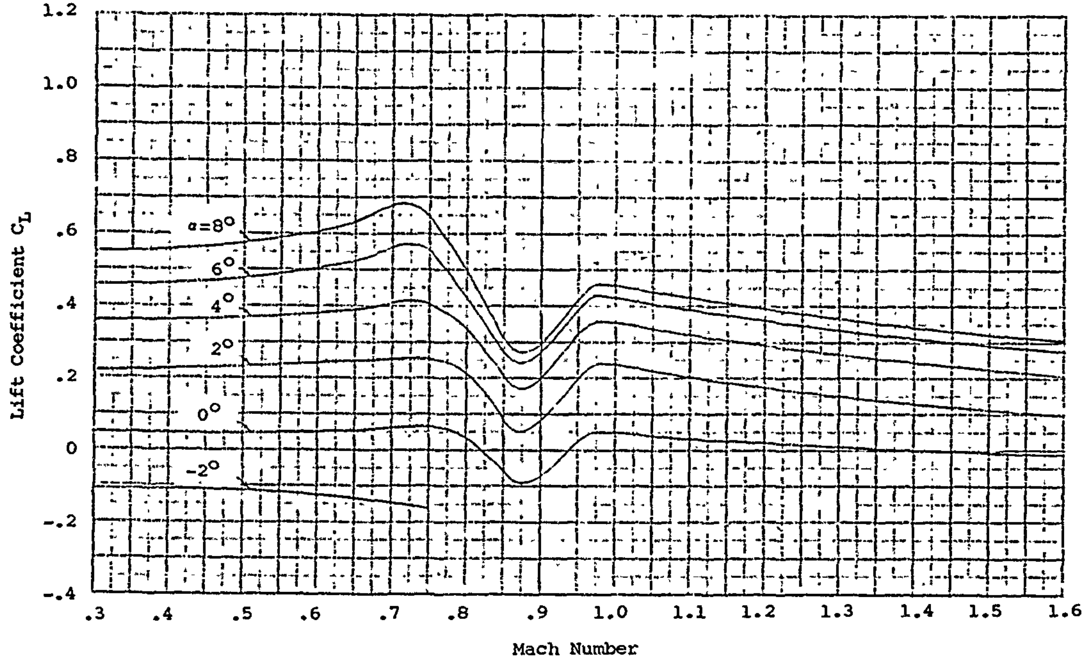

Figure 73. Two-Dimensional Lift Data, NACA 16-118 Airfoil.

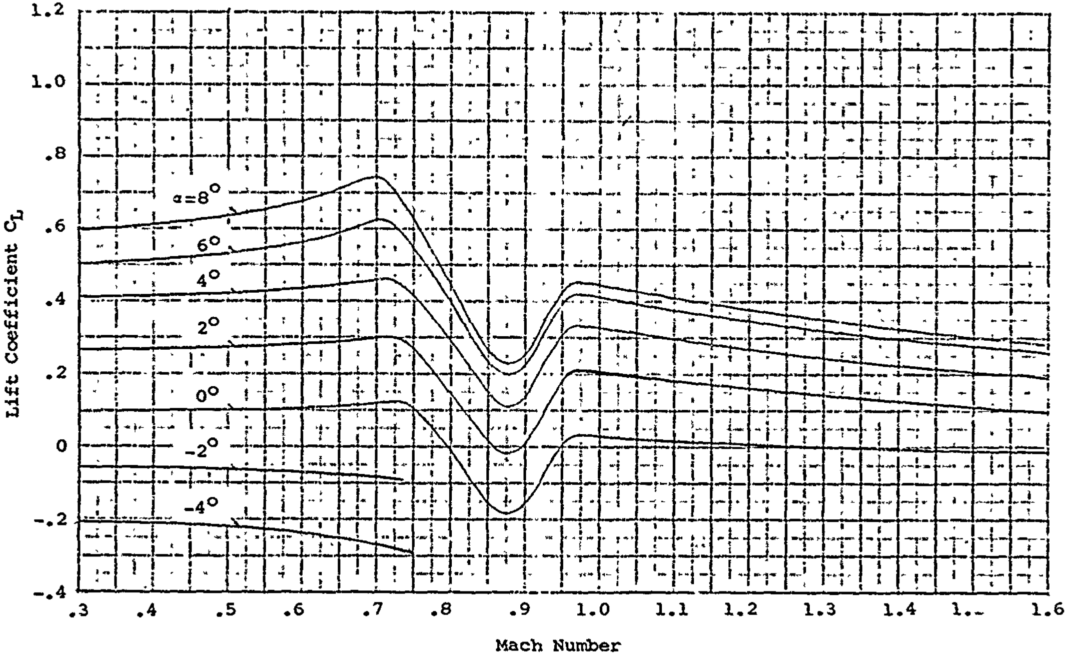

Figure 74. Two-Dimensional Lift Data, NACA 16-218 Airfoil.

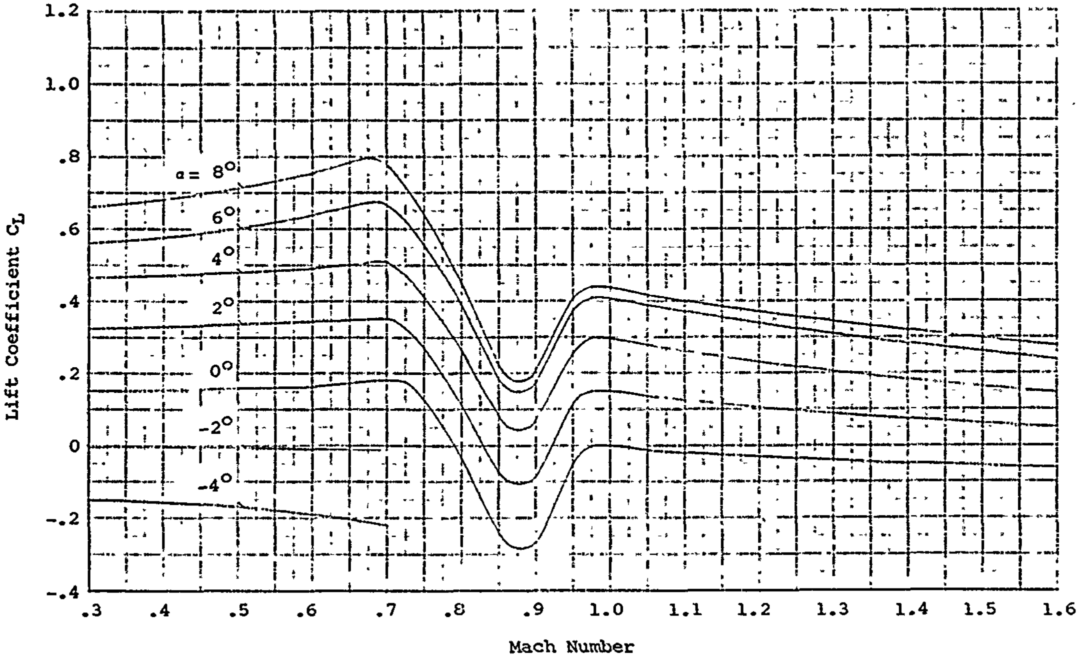

Figure 75. Two-Dimensional Lift Data, NACA 16-318 Airfoil.

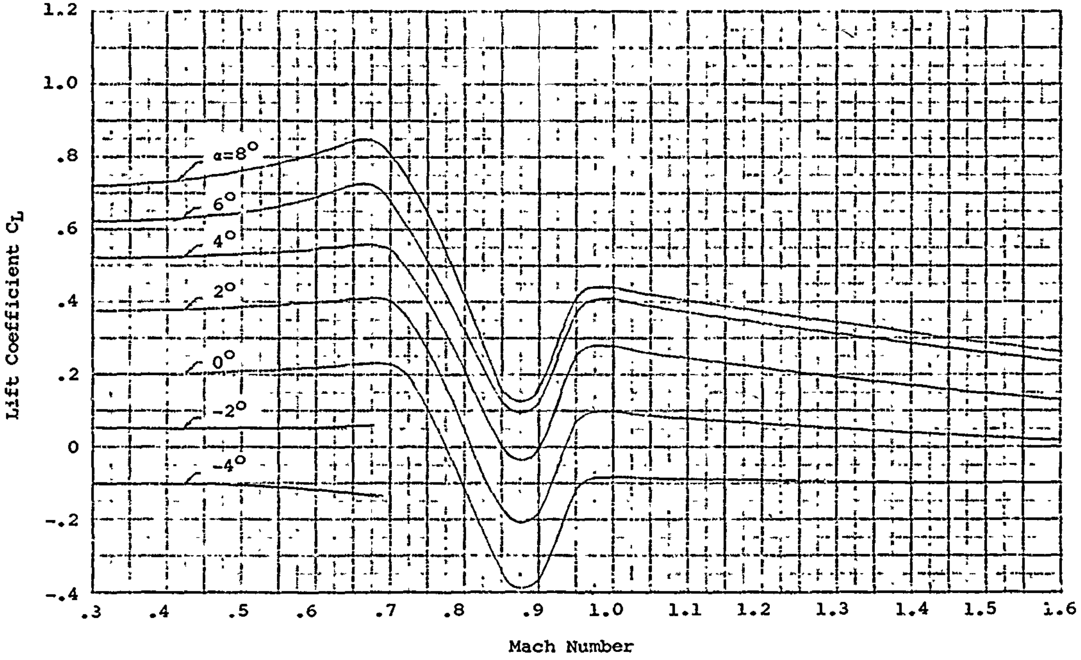

Figure 76. Two-Dimensional Lift Data, NACA 16-418 Airfoil.

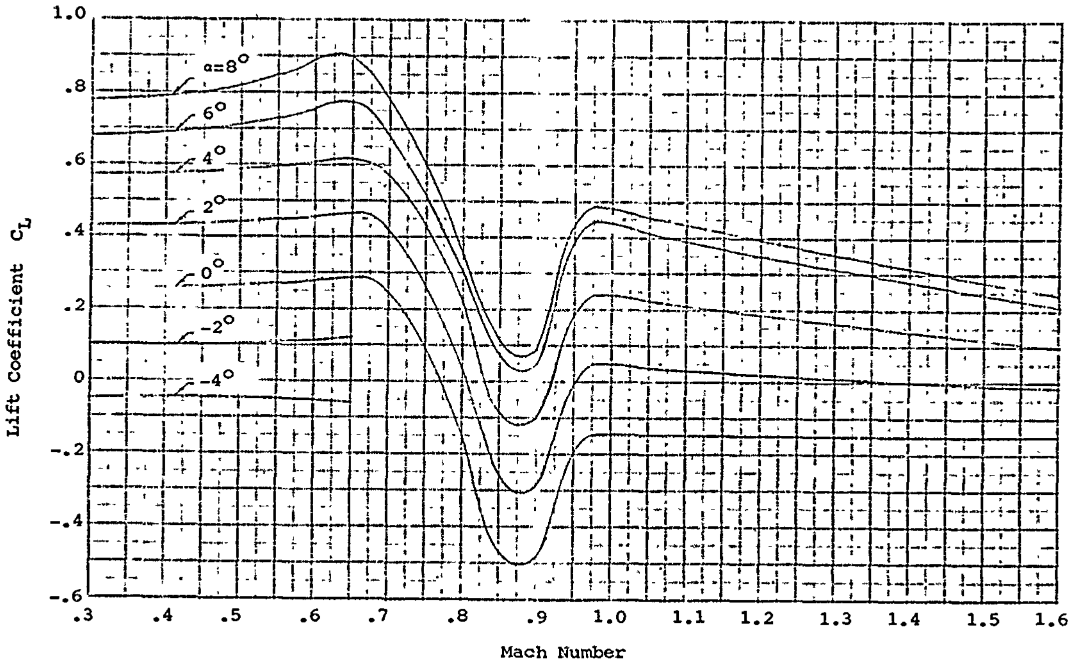

Figure 77. Two-Dimensional Lift Data, NACA 16-518 Airfoil.

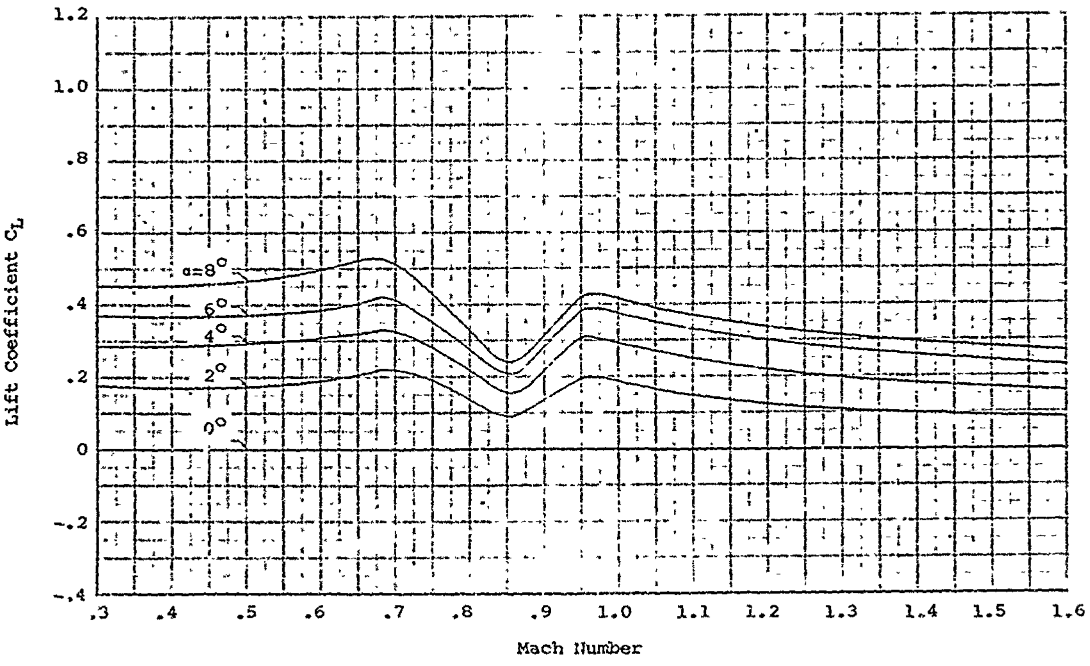

Figure 78. Two-Dimensional Lift Data,
NACA 16-021 Airfoil.

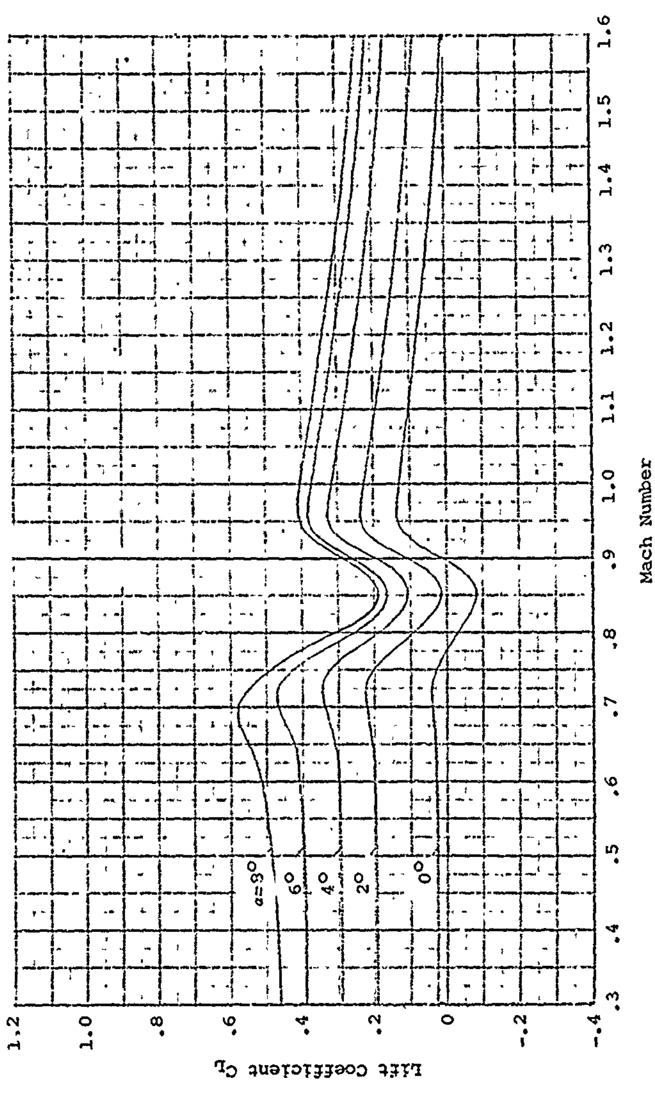

Figure 79. Two-Dimensional Lift Data, NACA 16-121 Airfoil.

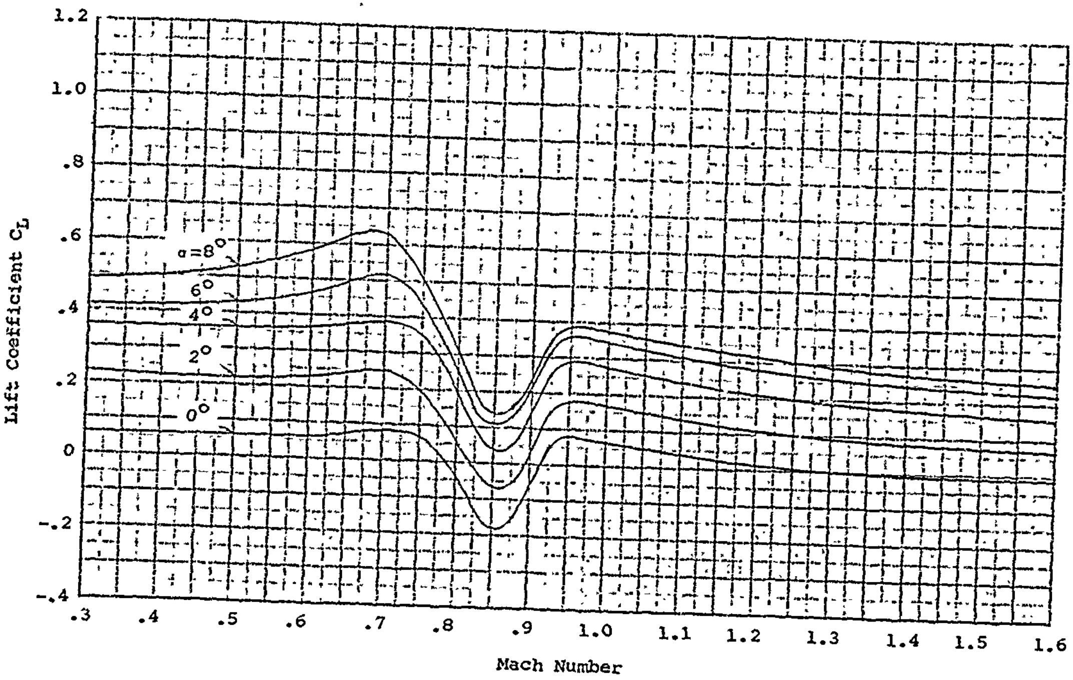

Figure 80. Two-Dimensional Lift Data, NACA 16-221 Airfoil.

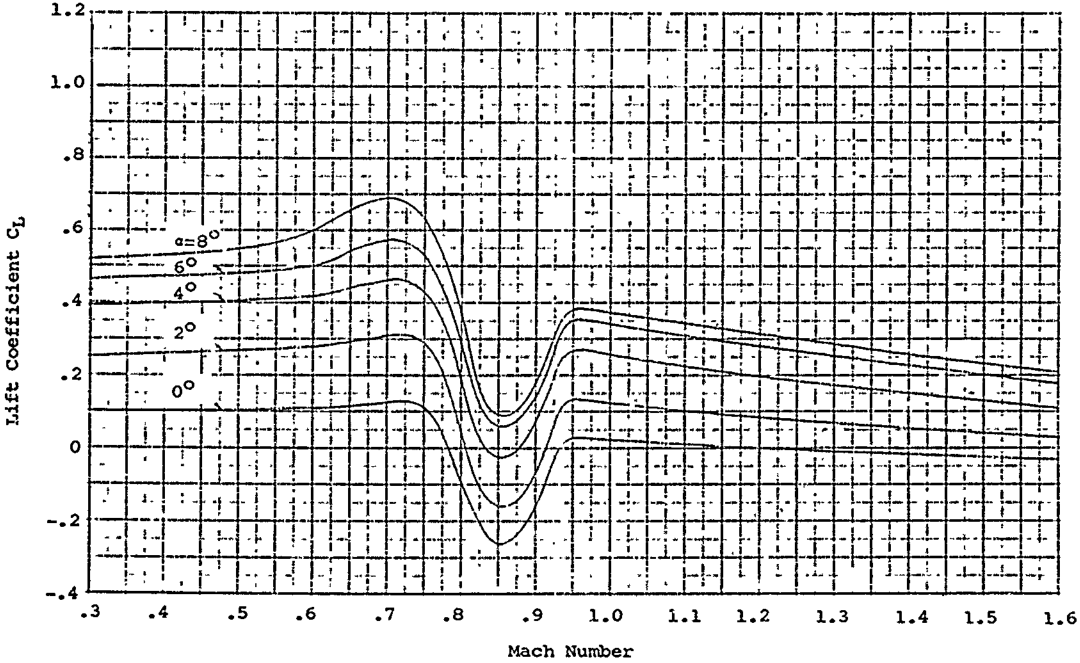

Figure 81. Two-Dimensional Lift Data, NACA 16-321 Airfoil.

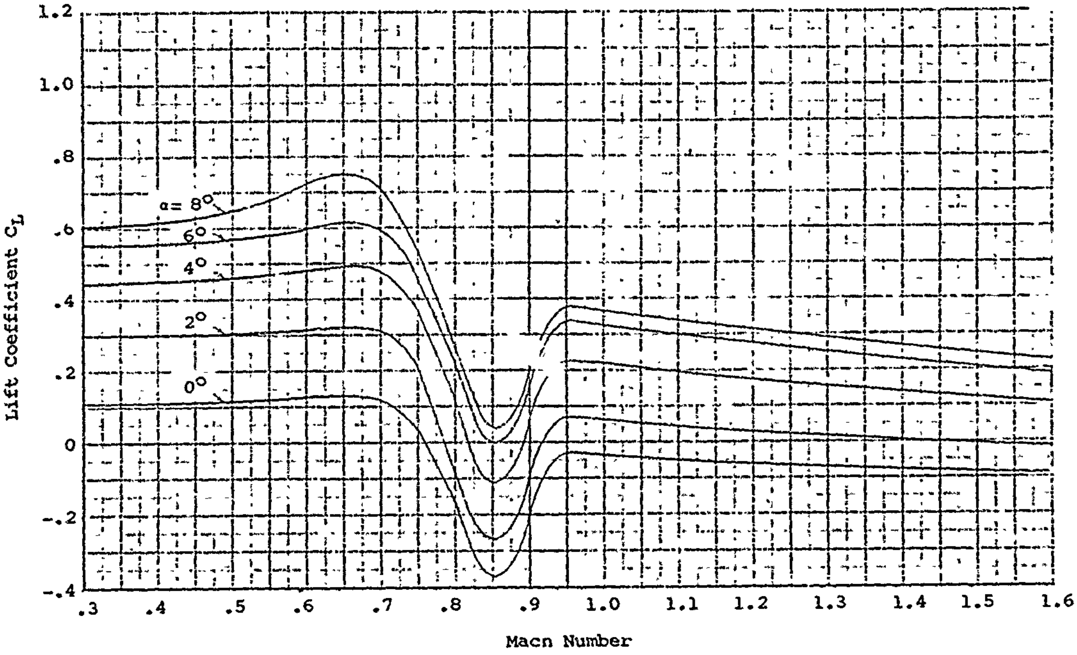

Figure 82. Two-Dimensional Lift Data, NACA 16-421 Airfoil.

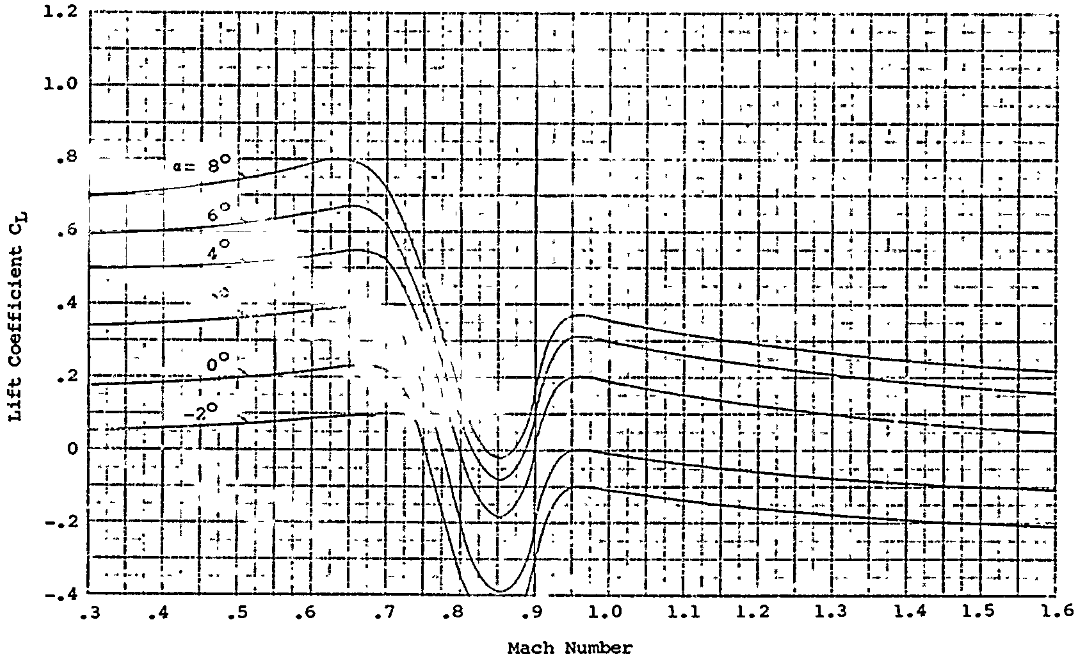

Figure 83. Two-Dimensional Lift Data, NACA 16-521 Airfoil.

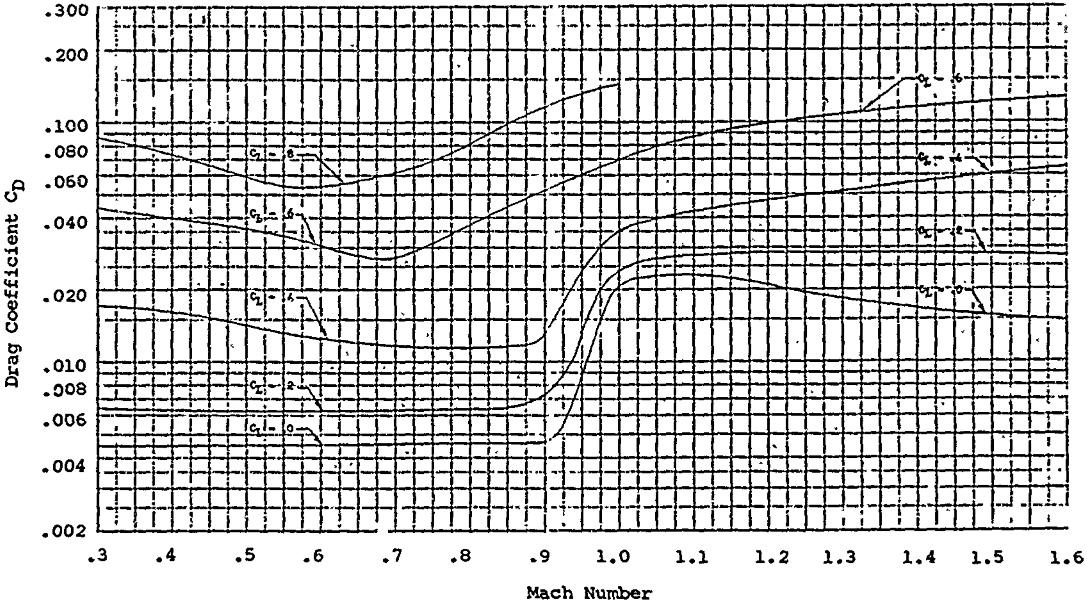

Figure 84. Two-Dimensional Drag Data, NACA 16-004 Airfoil.

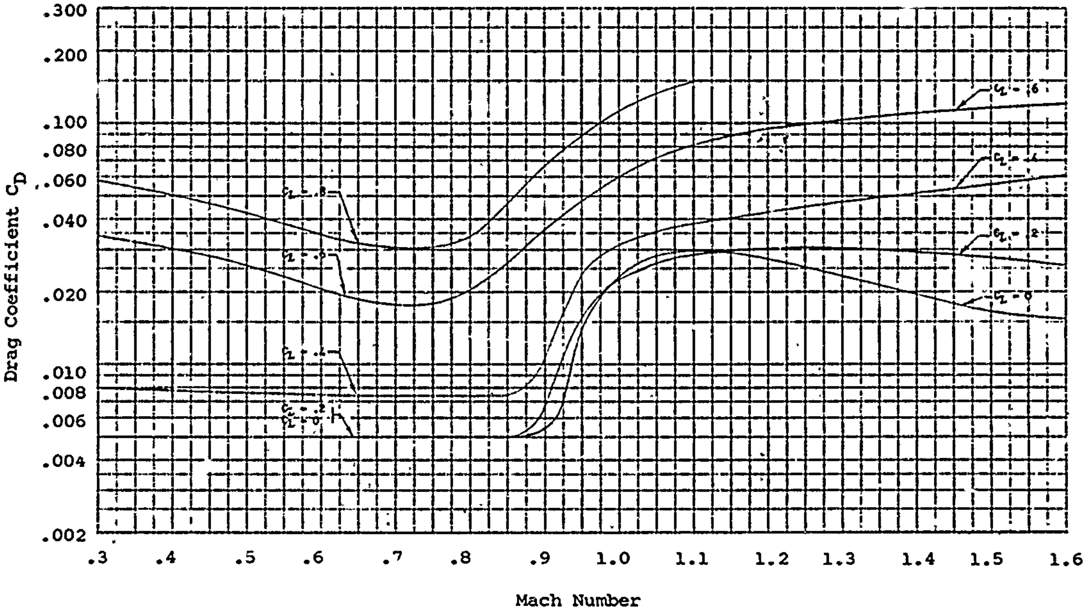

Figure 85. Two-Dimensional Drag Data, NACA 16-104 Airfoil.

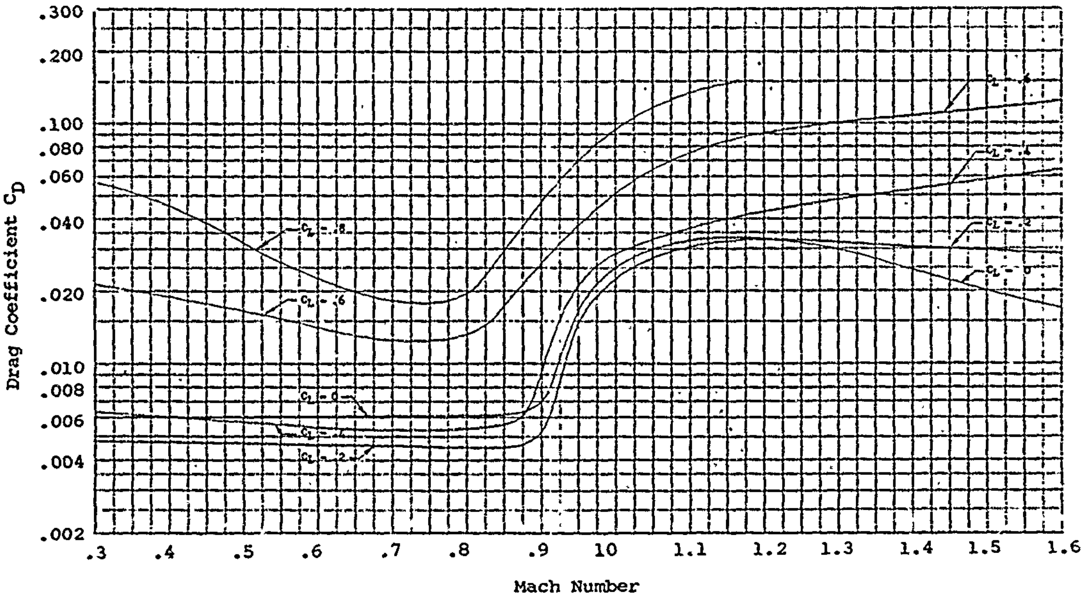

Figure 86. Two-Dimensional Drag Data, NACA 16-204 Airfoil.

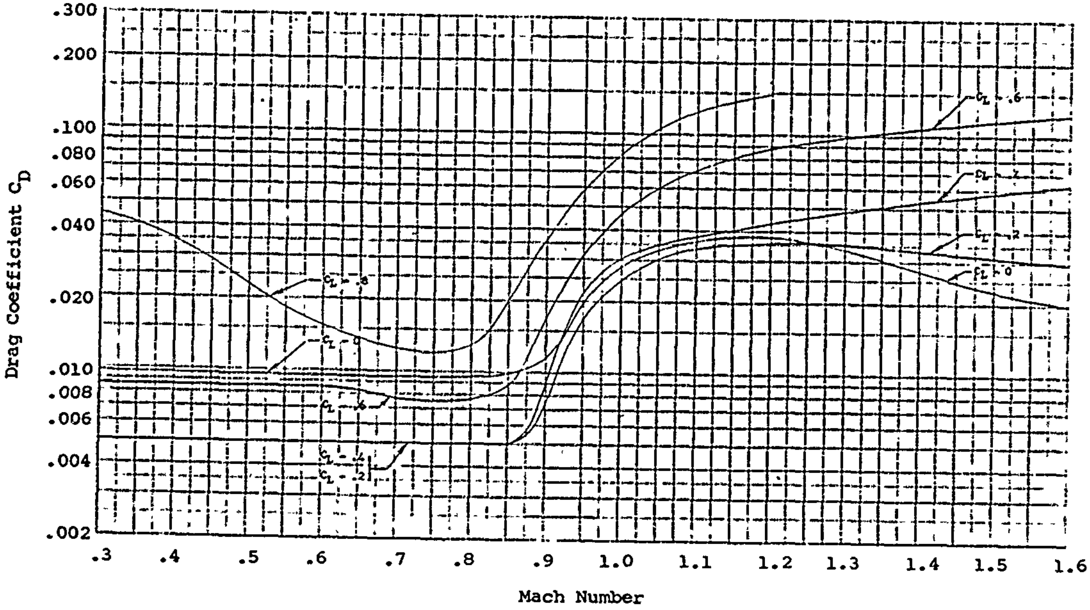

Figure 87. Two-Dimensional Drag Data, NACA 16-304 Airfoil.

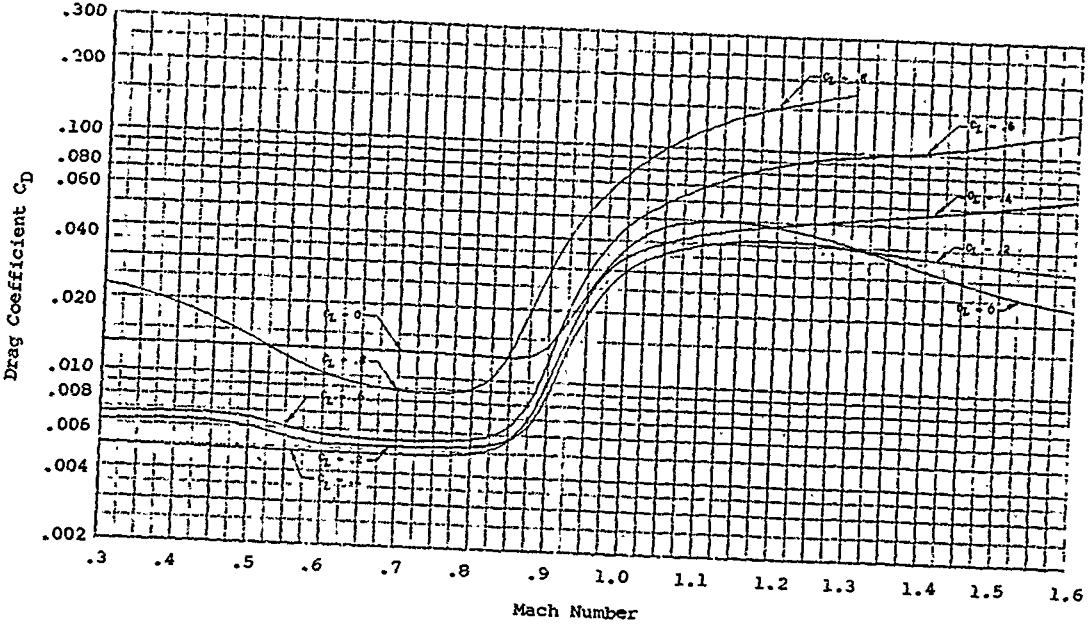

Figure 88. Two-Dimensional Drag Data, NACA 16-404 Airfoil.

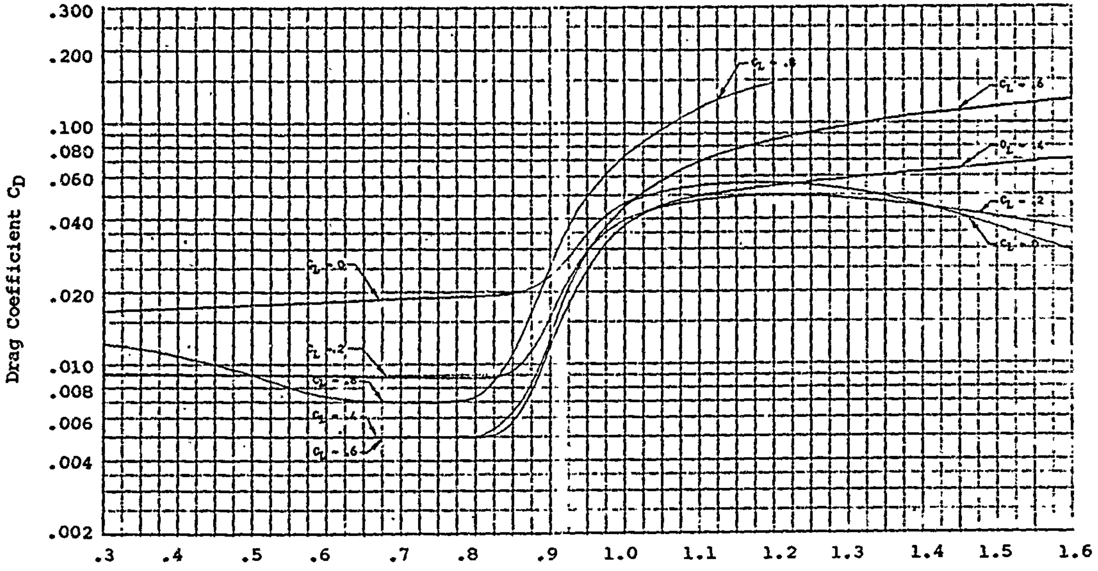

Figure 89. Two-Dimensional Drag Data, NACA 16-504 Airfoil.

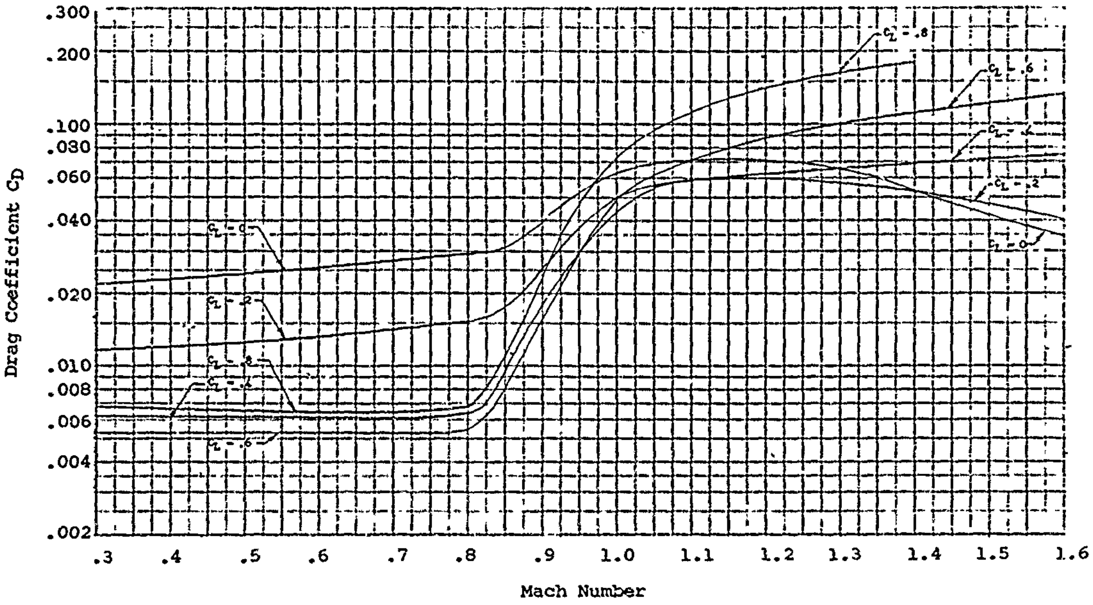

Figure 90. Two-Dimensional Drag Data, NACA 16-604 Airfoil.

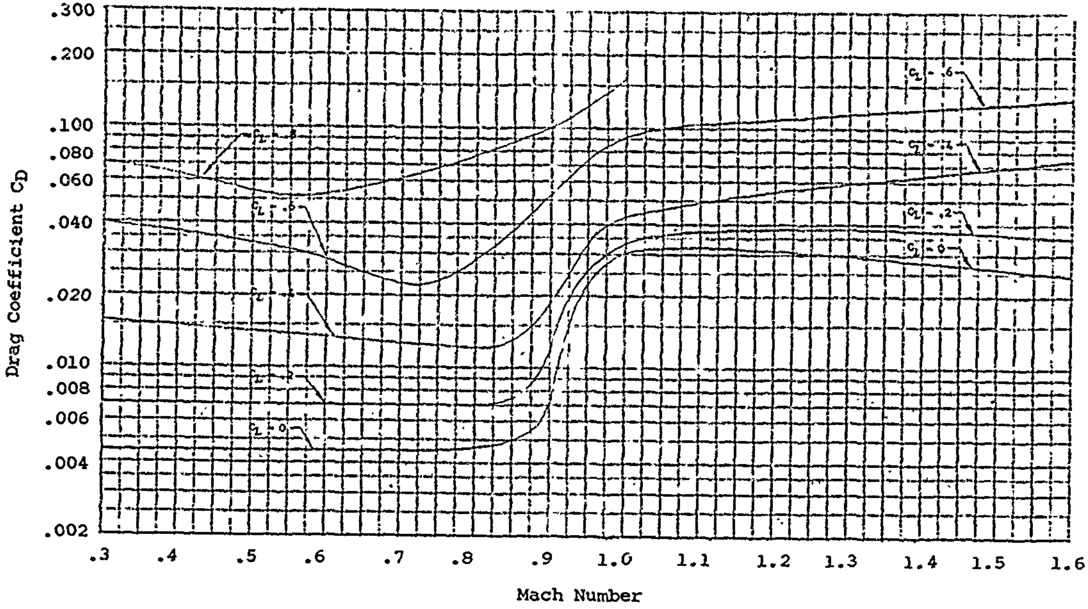

Figure 91. Two-Dimensional Drag Data, NACA 16-006 Airfoil.

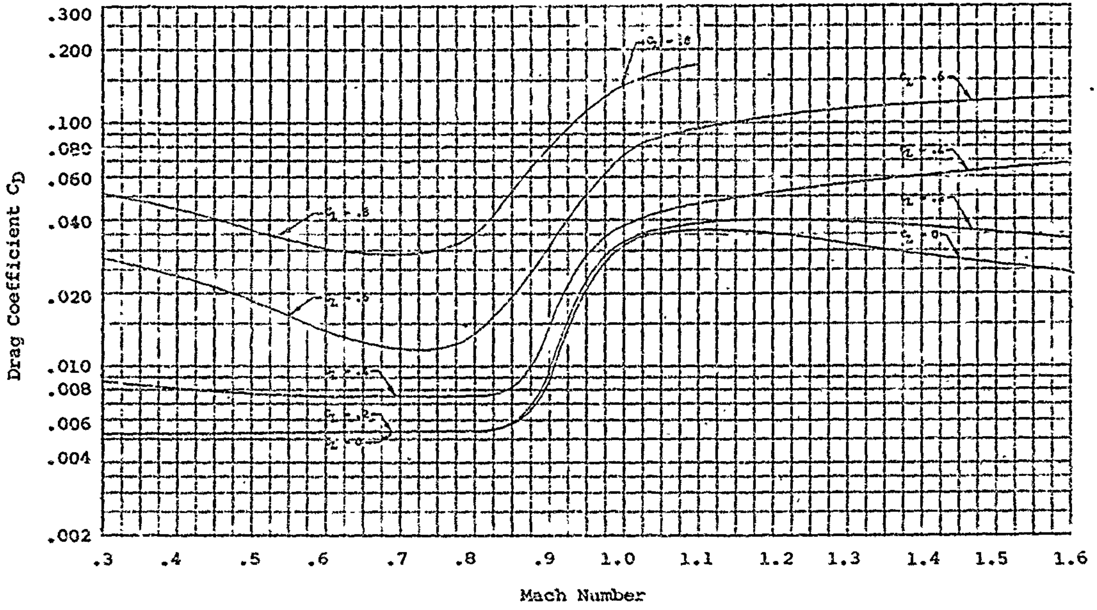

Figure 92. Two-Dimensional Drag Data, NACA 16-106 Airfoil.

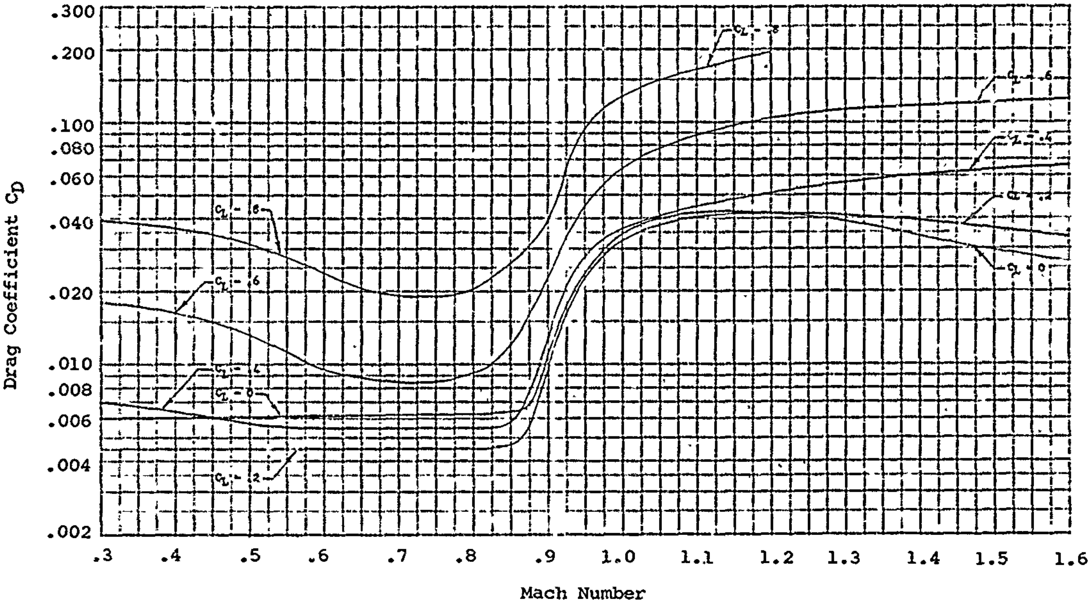

Figure 93. Two-Dimensional Drag Data, NACA 16-206 Airfoil.

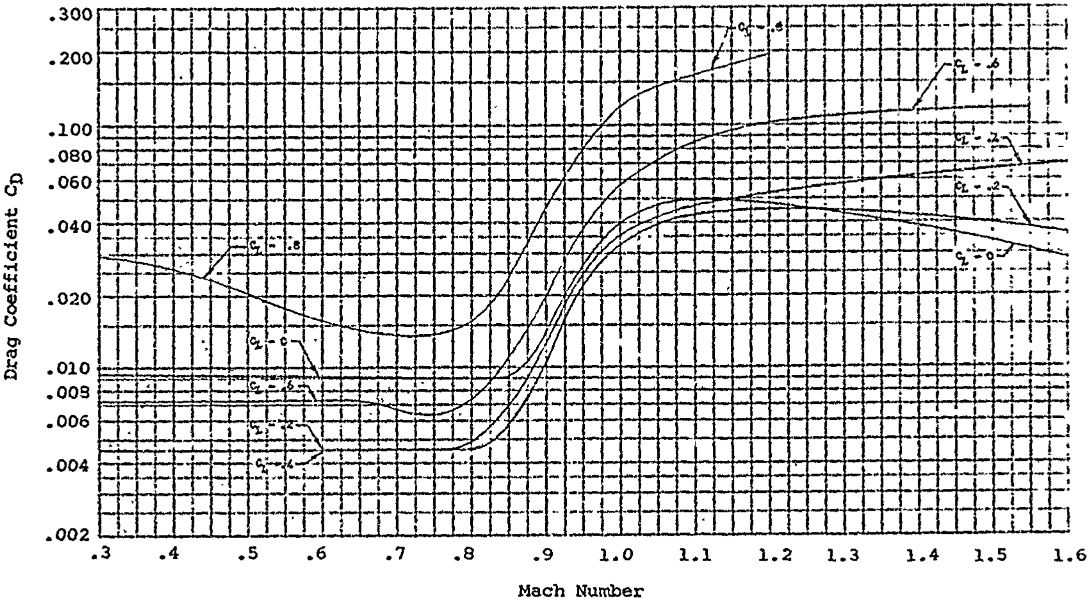

Figure 94. Two-Dimensional Drag Data, NACA 16-306 Airfoil.

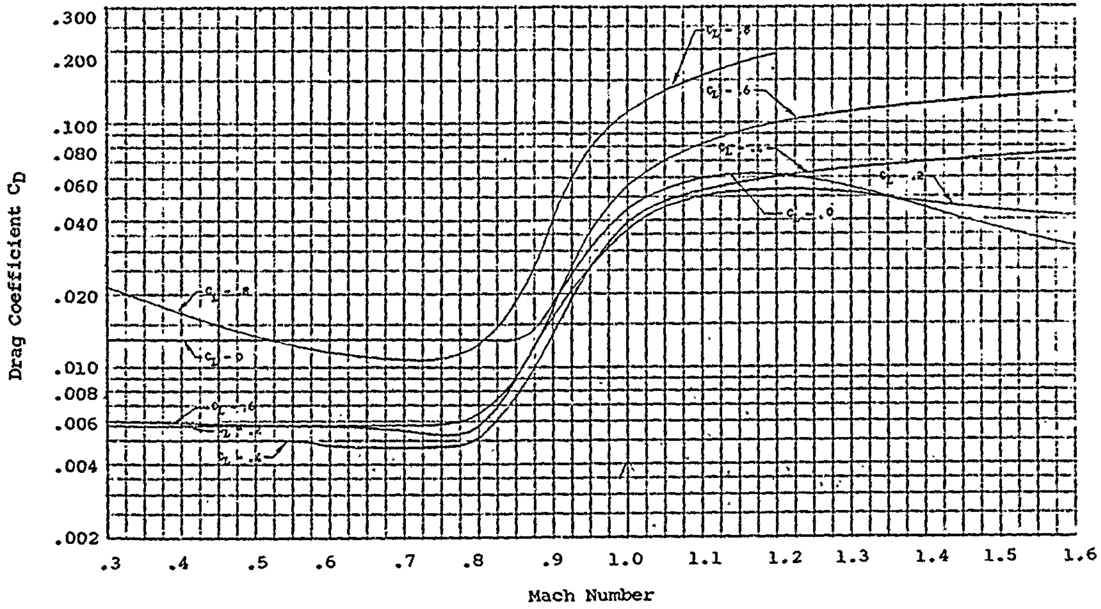

Figure 95. Two-Dimensional Drag Data, NACA 16-406 Airfoil.

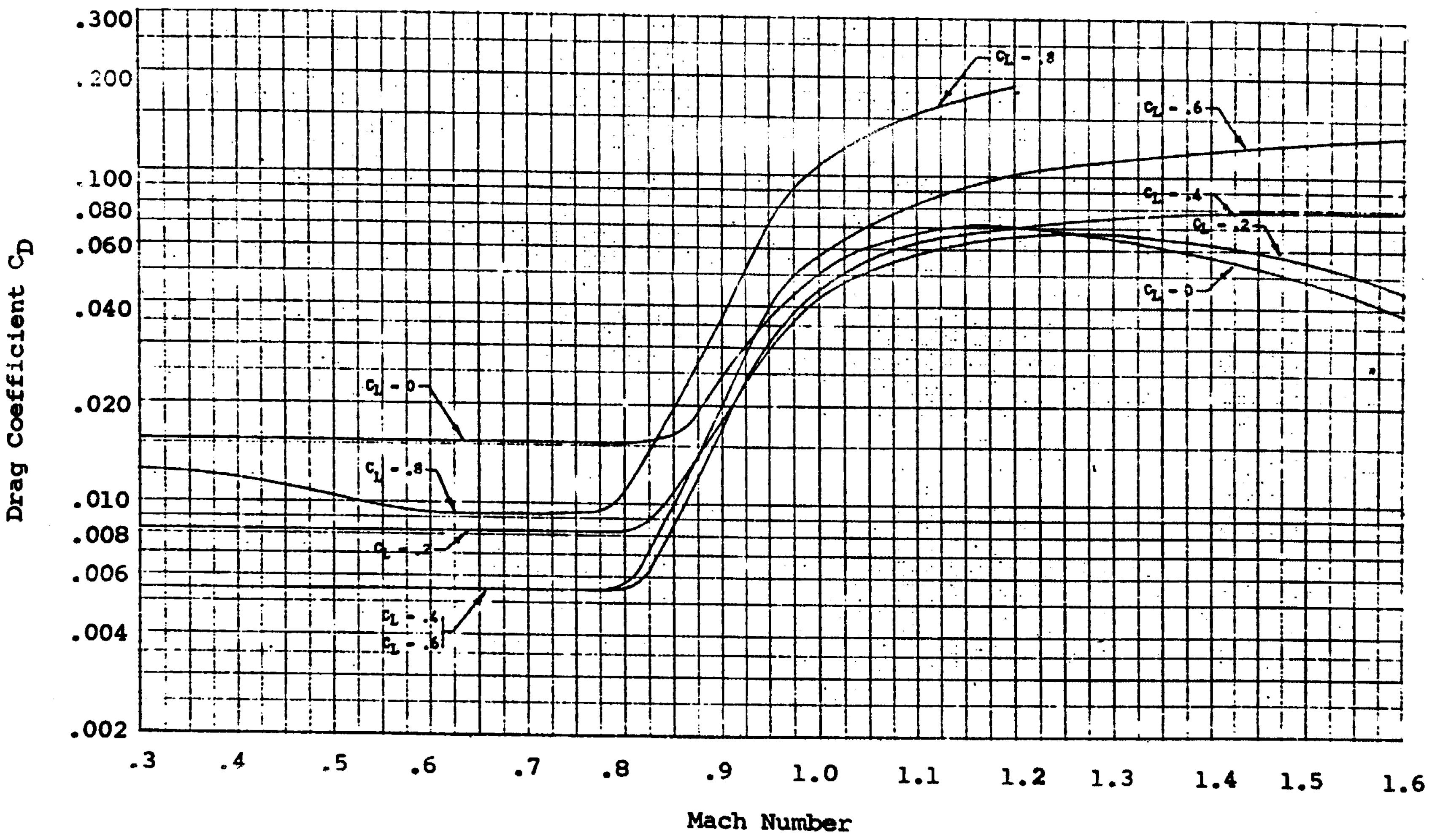

Figure 96. Two-Dimensional Drag Data, NACA 16-506 Airfoil.

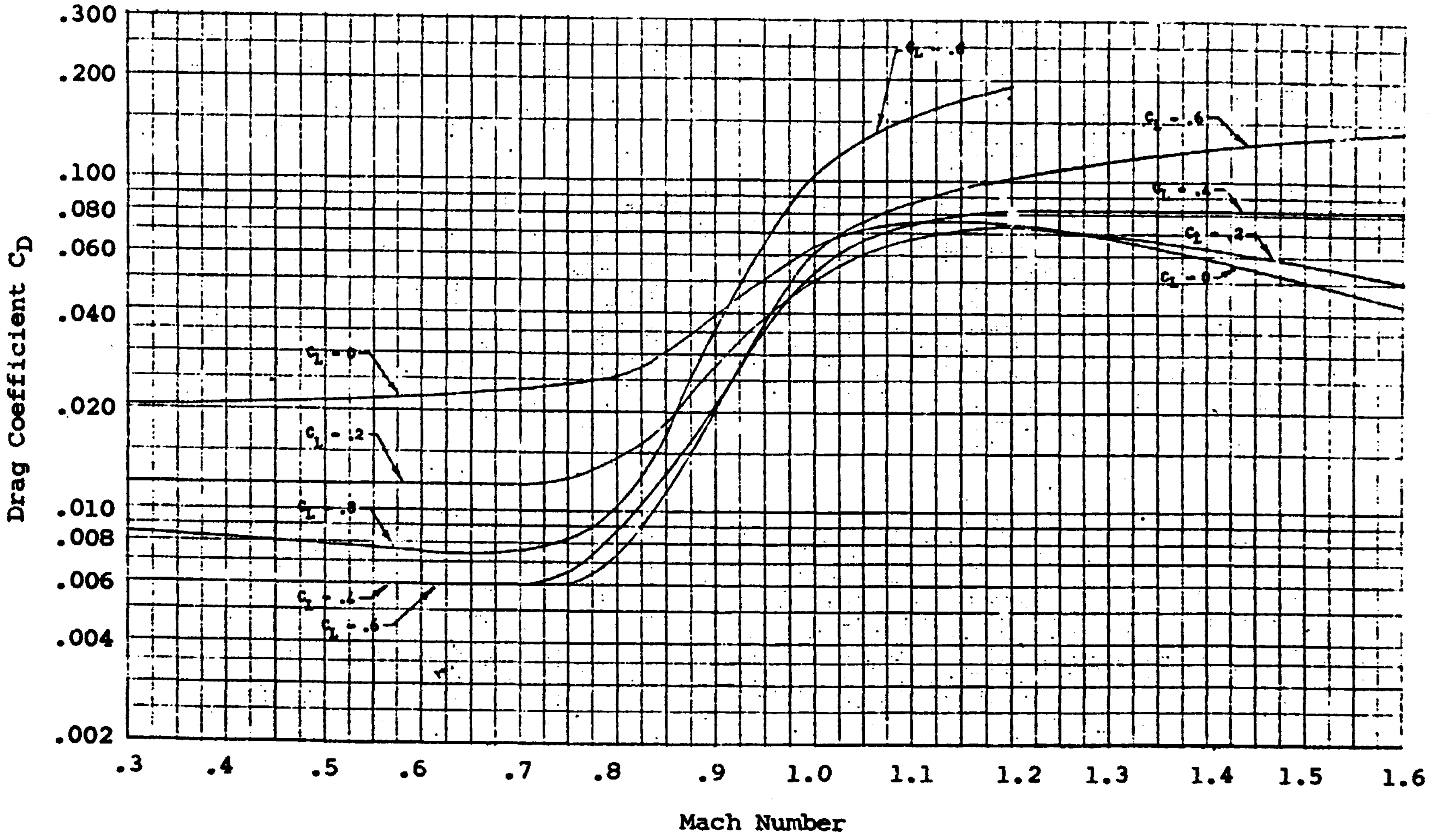

Figure 97. Two-Dimensional Drag Data, NACA 16-606 Airfoil.

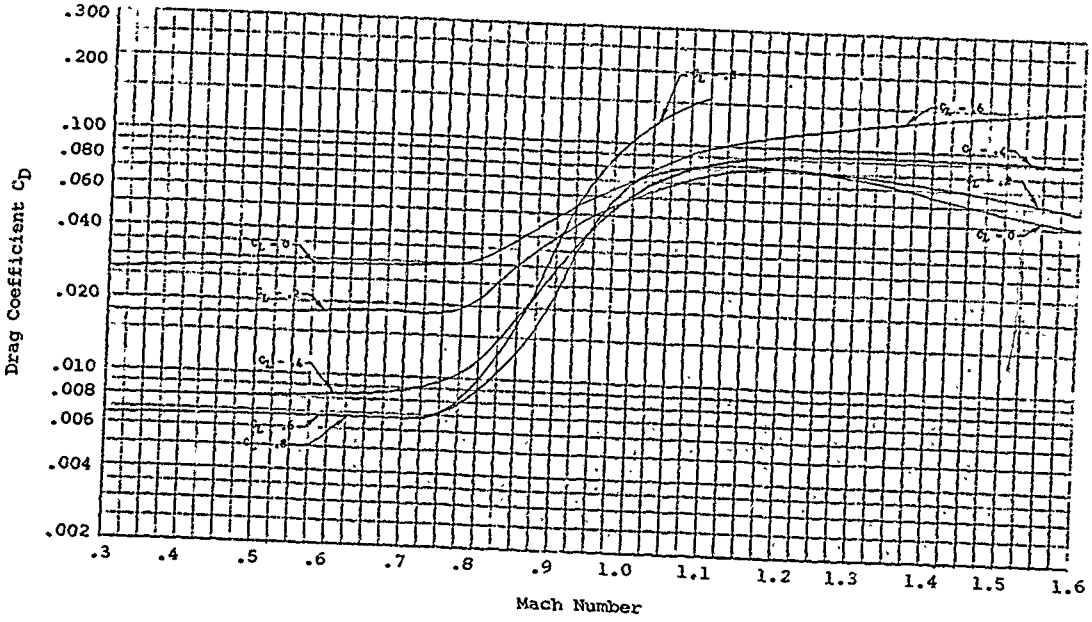

Figure 98. Two-Dimensional Drag Data, NACA 16-706 Airfoil.

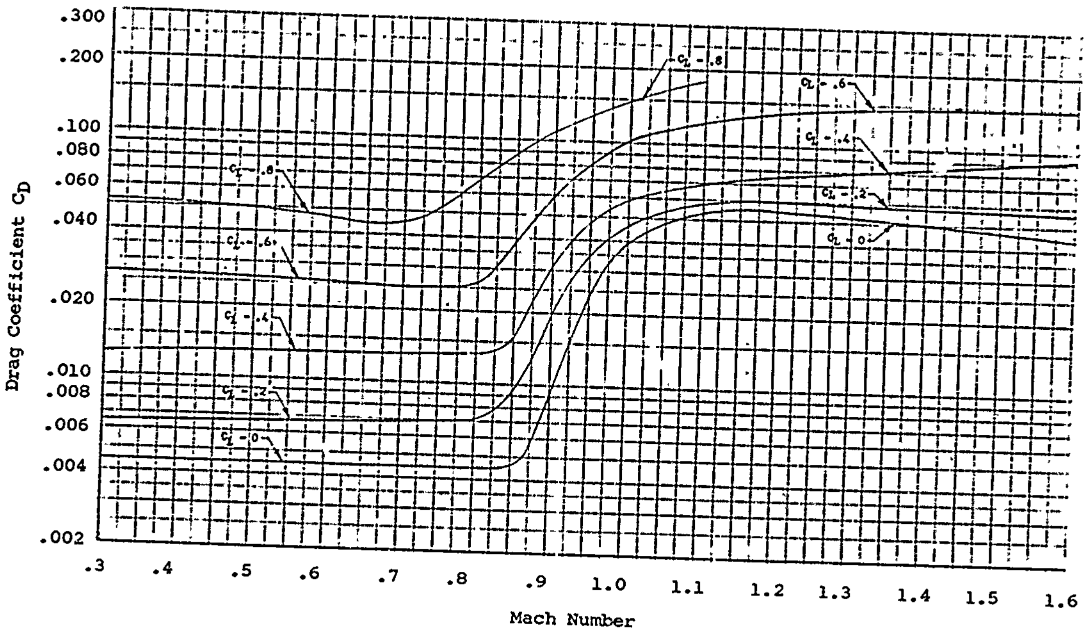

Figure 99. Two-Dimensional Drag Data, NACA 16-009 Airfoil.

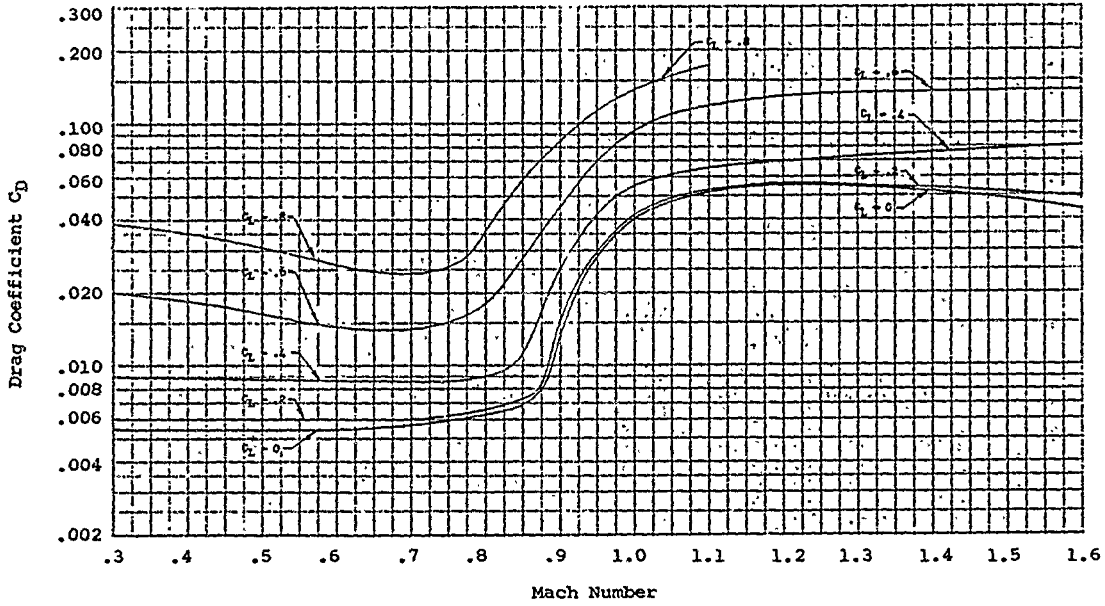

Figure 100. Two-Dimensional Drag Data, NACA 16-109 Airfoil.

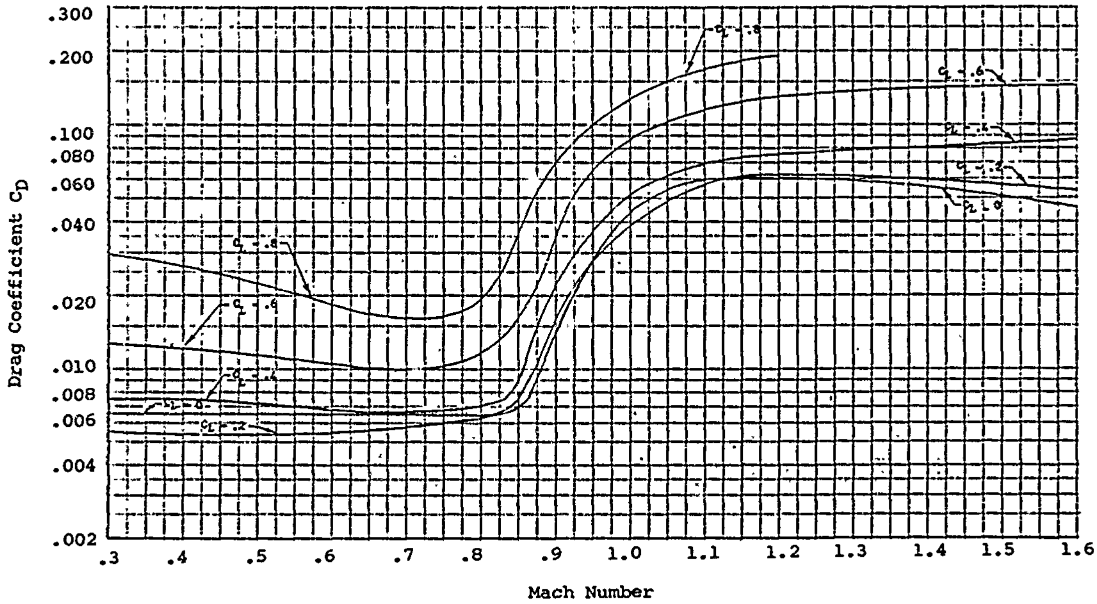

Figure 101. Two-Dimensional Drag Data,
NACA 16-209 Airfoil.

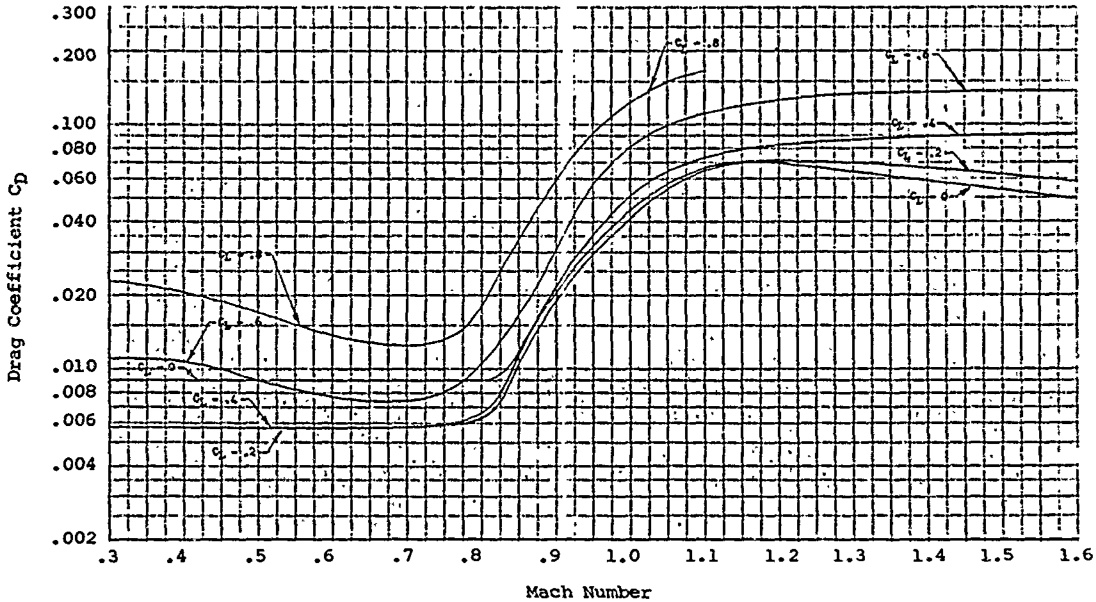

Figure 102. Two-Dimensional Drag Data, NACA 16-309 Airfoil.

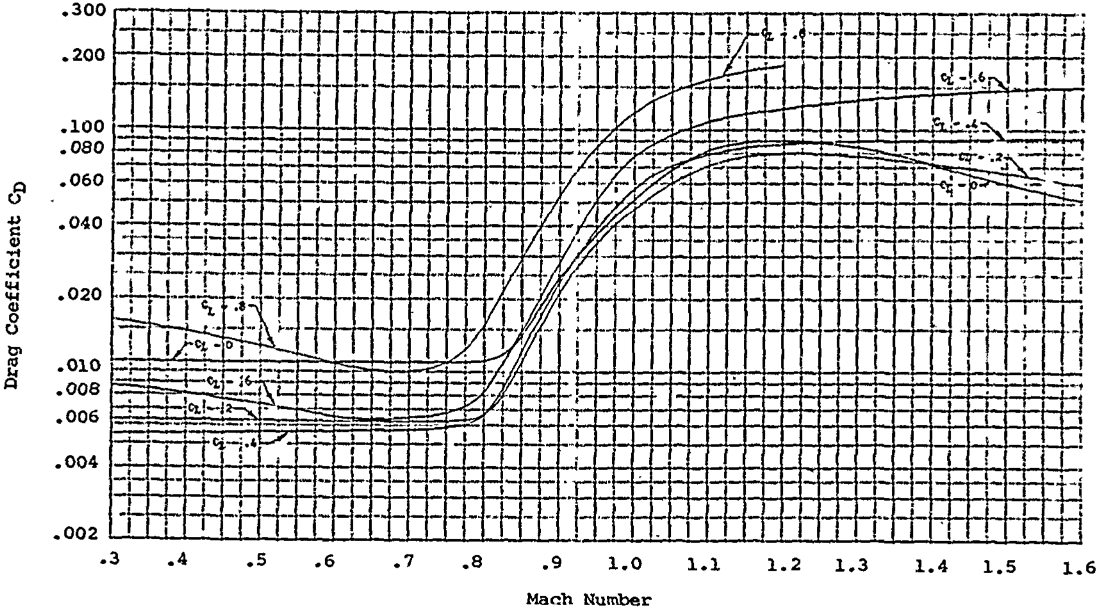

Figure 103. Two-Dimensional Drag Data, NACA 16-409 Airfoil.

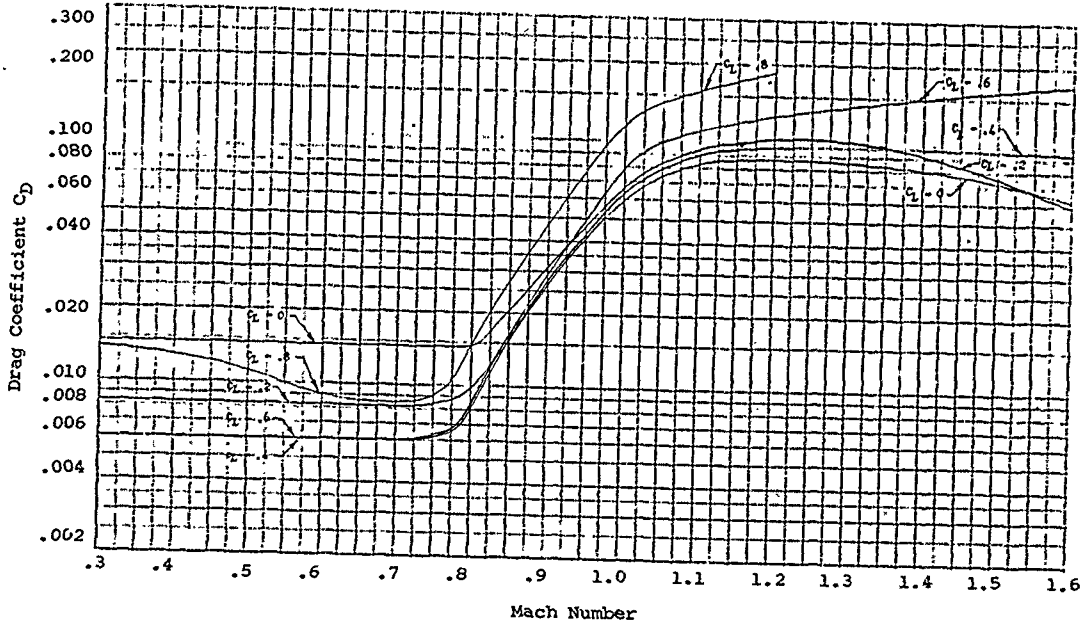

Figure 104. Two-Dimensional Drag Data, NACA 16-509 Airfoil.

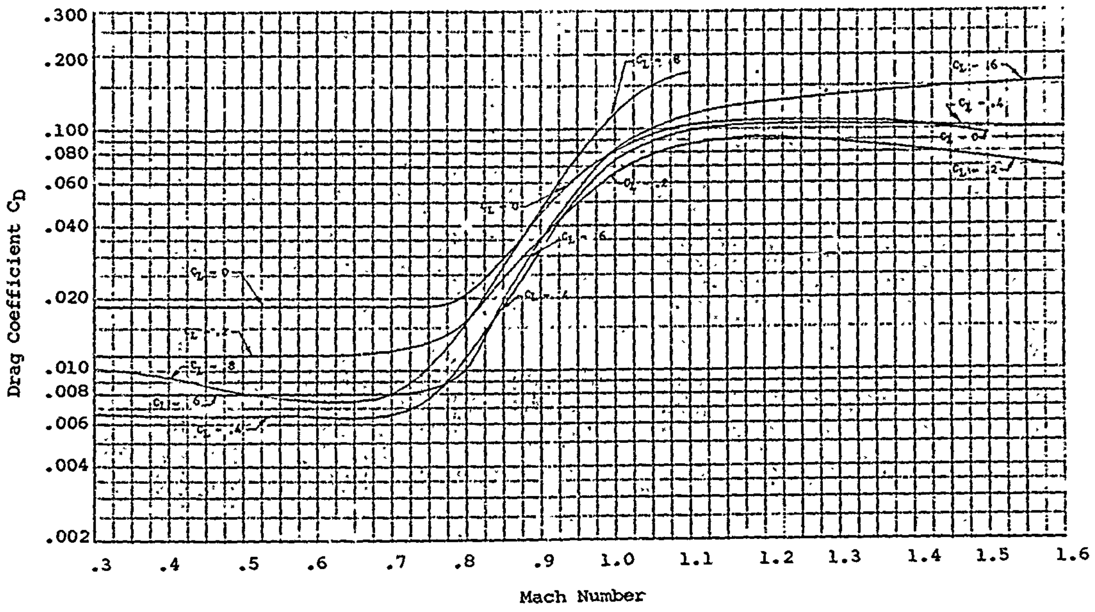

Figure 105. Two-Dimensional Drag Data, NACA 16-609 Airfoil.

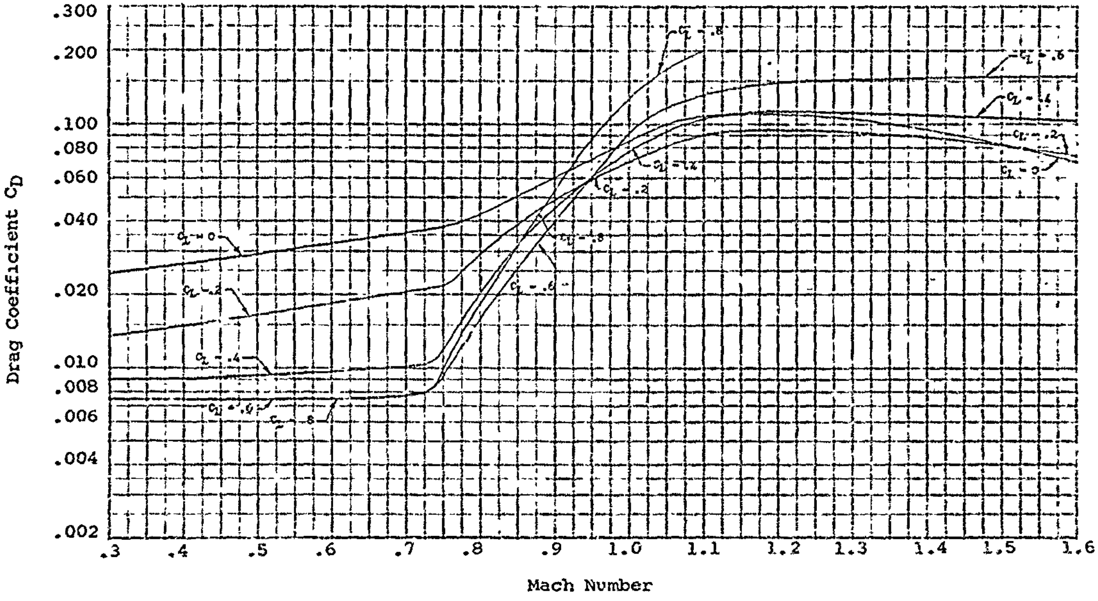

Figure 106. Two-Dimensional Drag Data,
NACA 16-709 Airfoil.

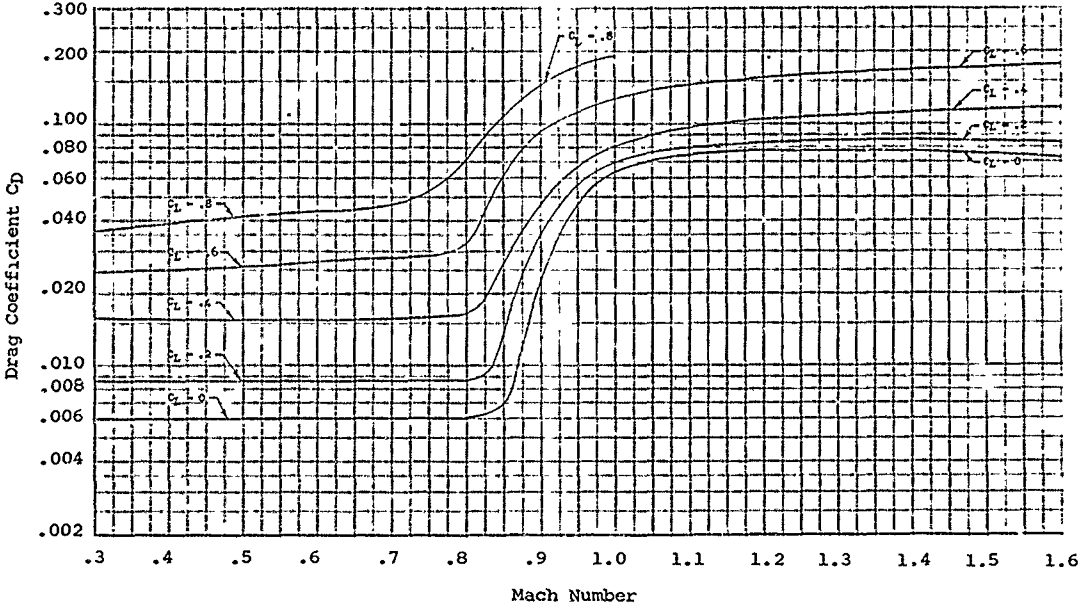

Figure 107. Two-Dimensional Drag Data, NACA 16-012 Airfoil.

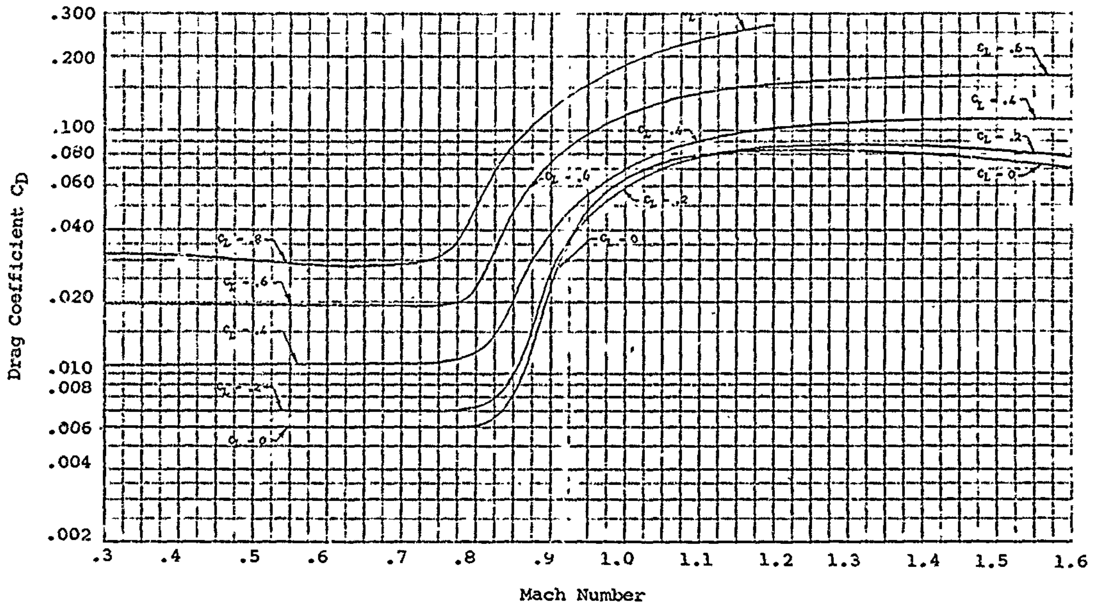

Figure 108. Two-Dimensional Drag Data, NACA 16-112 Airfoil.

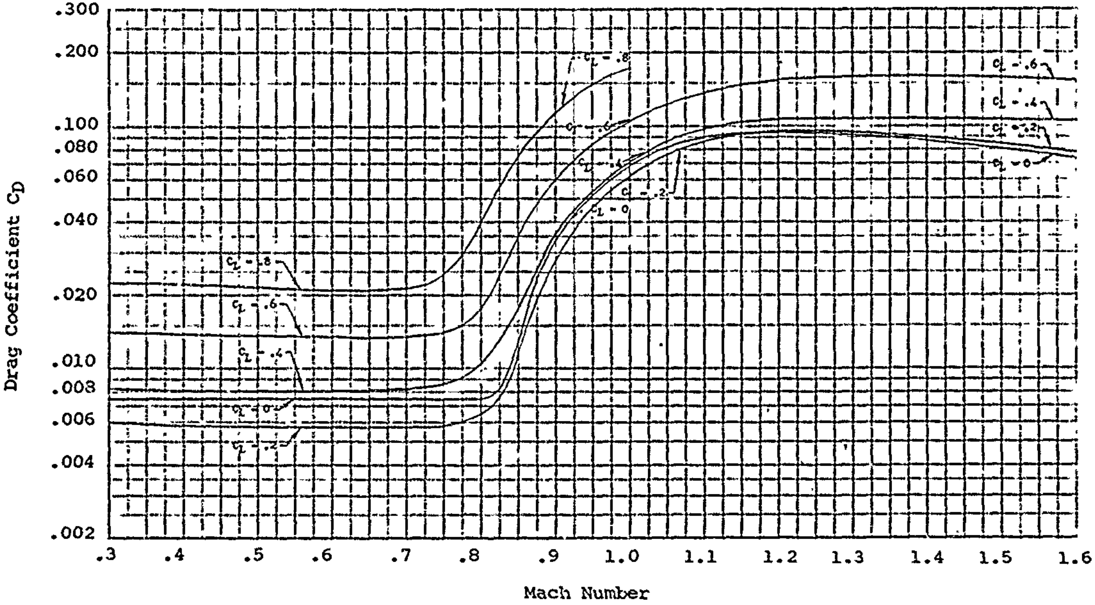

Figure 109. Two-Dimensional Drag Data, NACA 16-212 Airfoil.

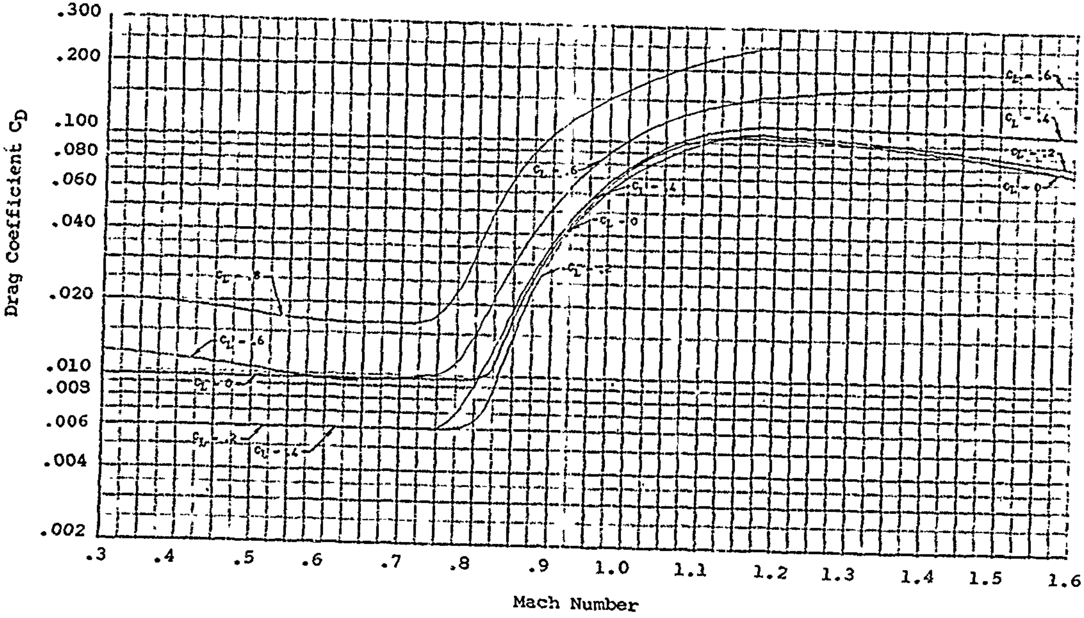

Figure 110. Two-Dimensional Drag Data, NACA 16-312 Airfoil.

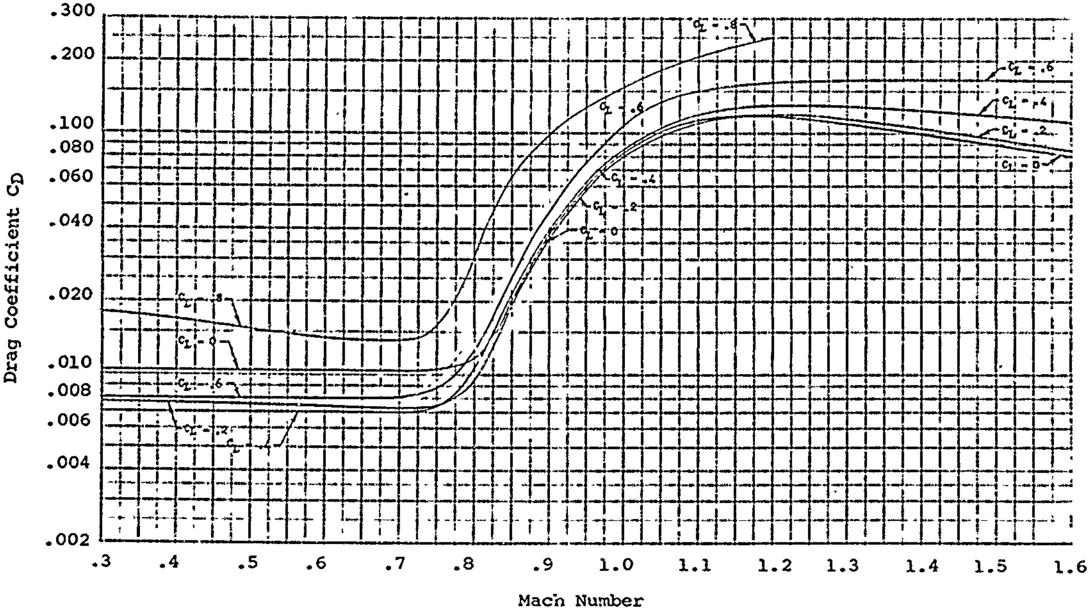

Figure 111. Two-Dimensional Drag Data,
NACA 16-412 Airfoil.

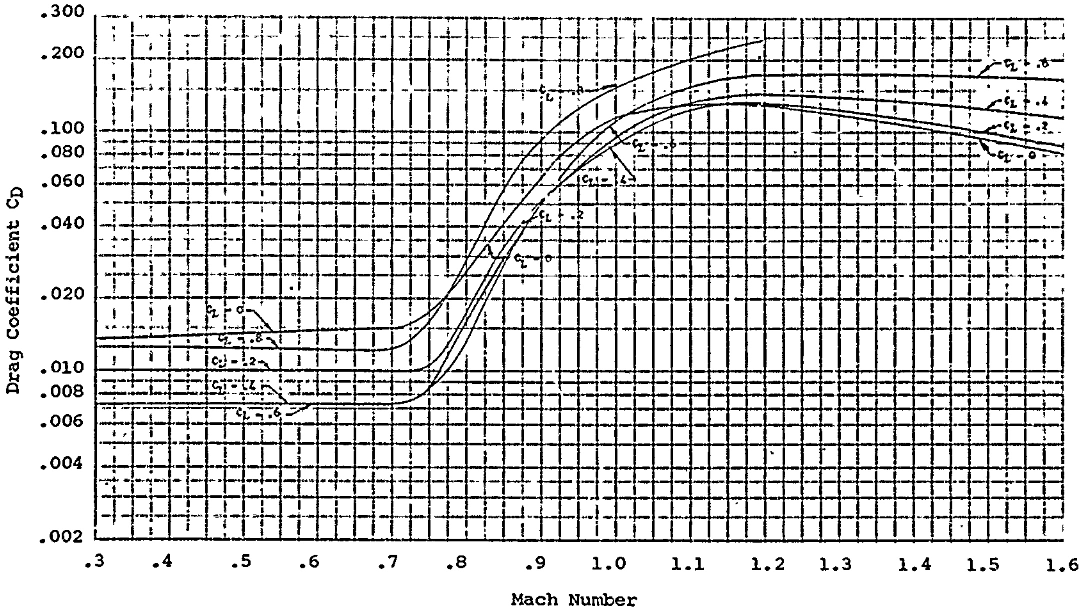

Figure 112. Two-Dimensional Drag Data, NACA 16-512 Airfoil.

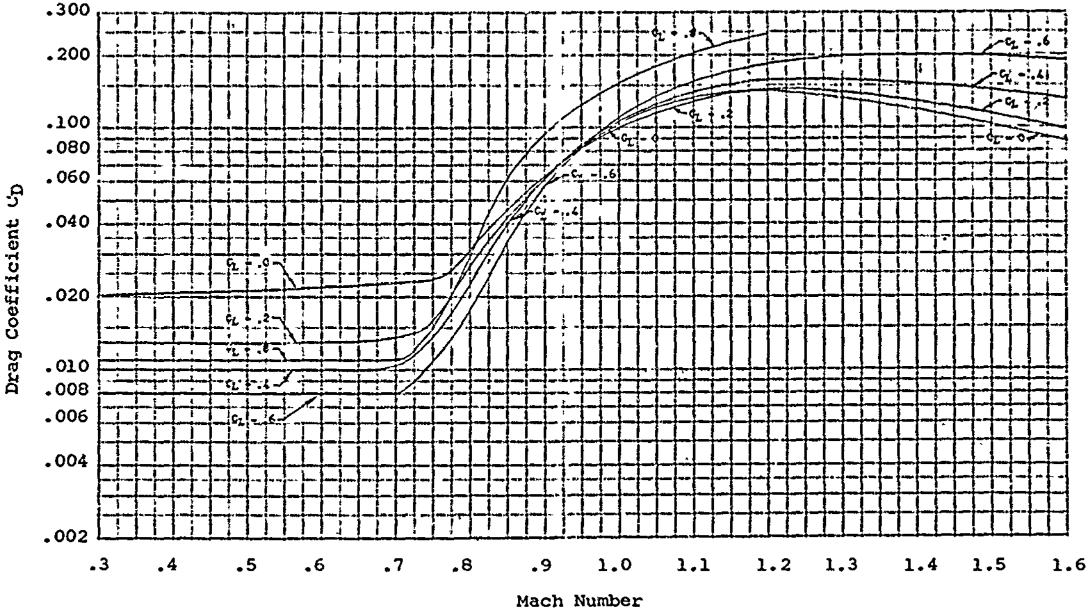

Figure 113. Two-Dimensional Drag Data, NACA 16-612 Airfoil.

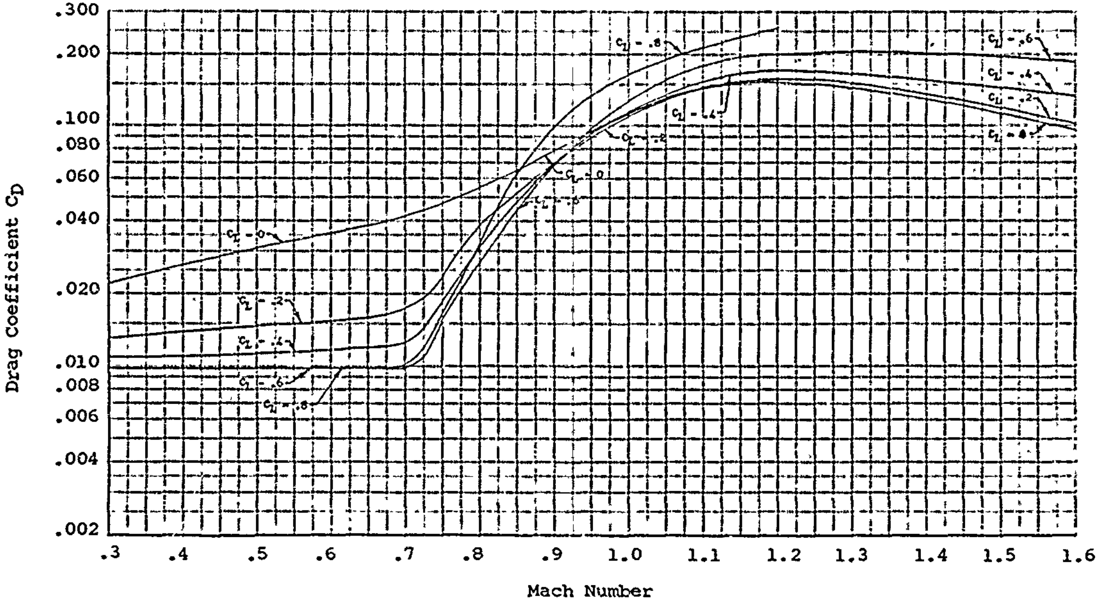

Figure 114. Two-Dimensional Drag Data,
NACA 16-712 Airfoil.

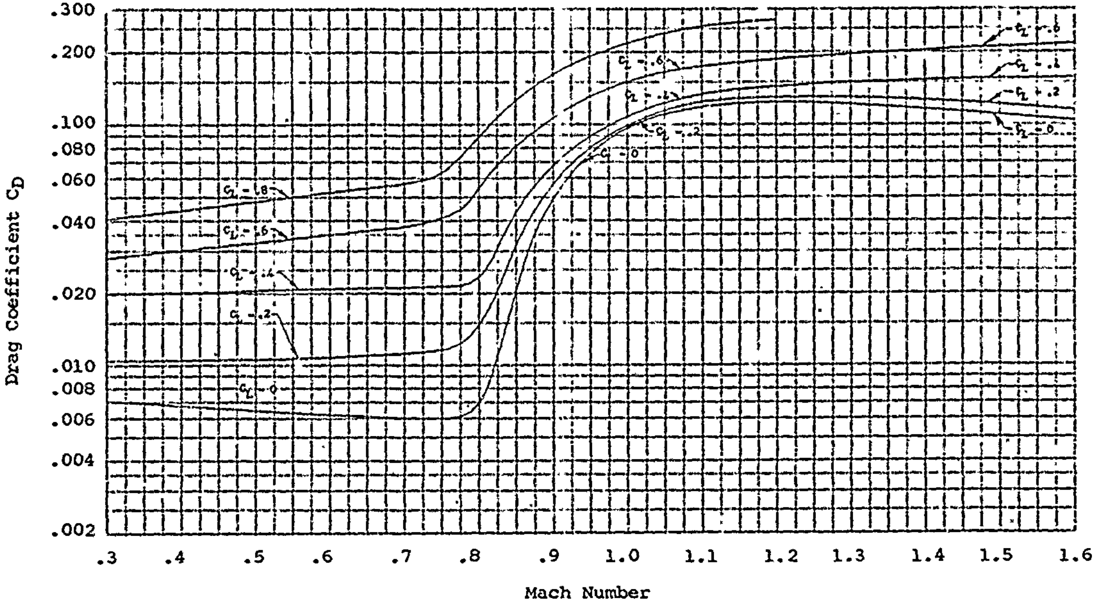

Figure 115. Two-Dimensional Drag Data,
NACA 16-015 Airfoil.

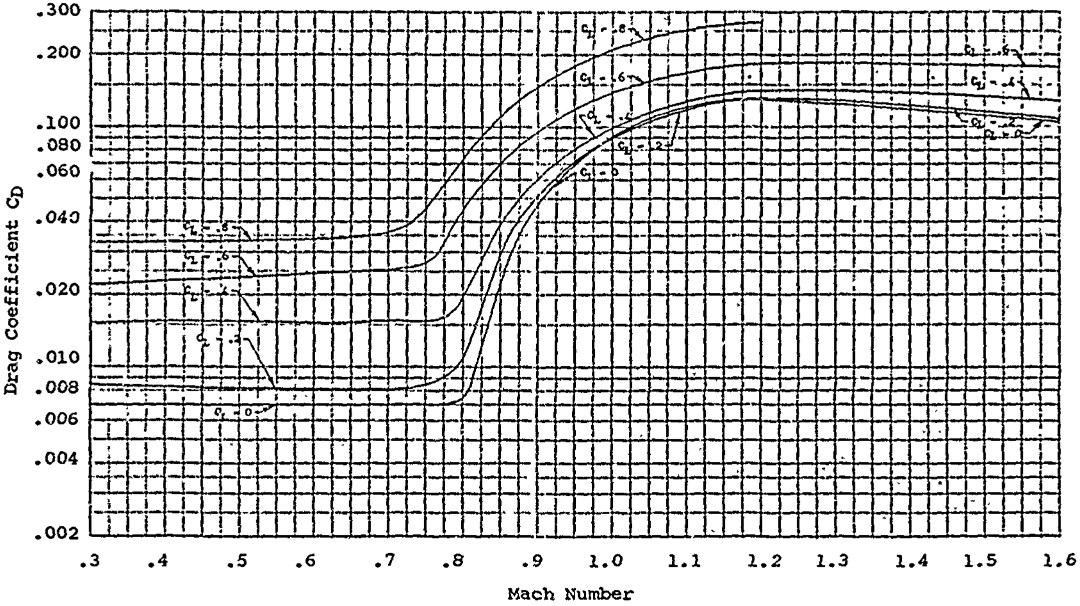

Figure 116. Two-Dimensional Drag Data, NACA 16-115 Airfoil.

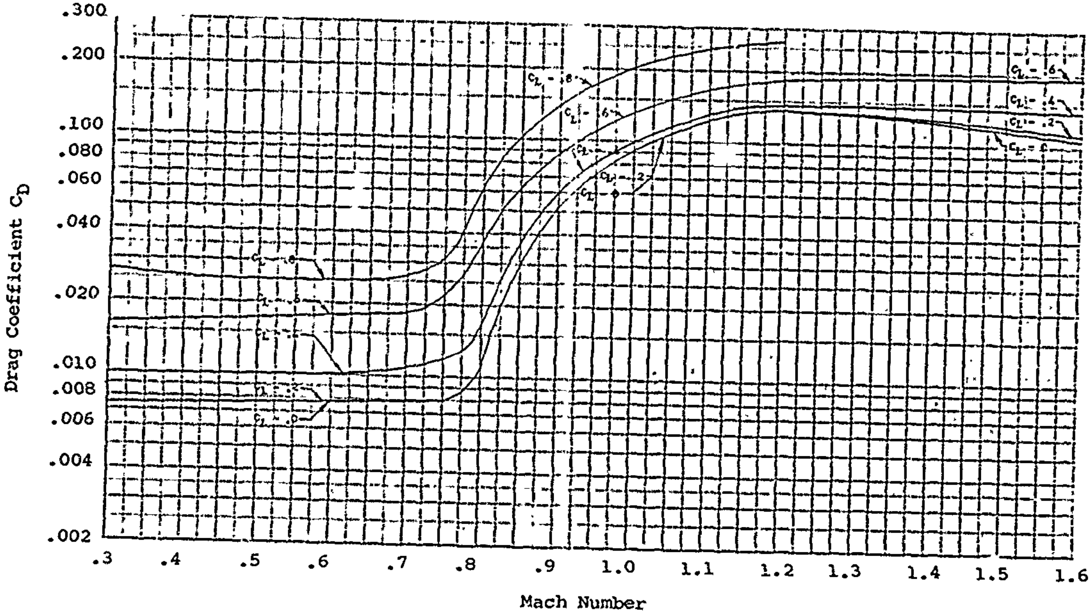

Figure 117. Two-Dimensional Drag Data, NACA 16-215 Airfoil.

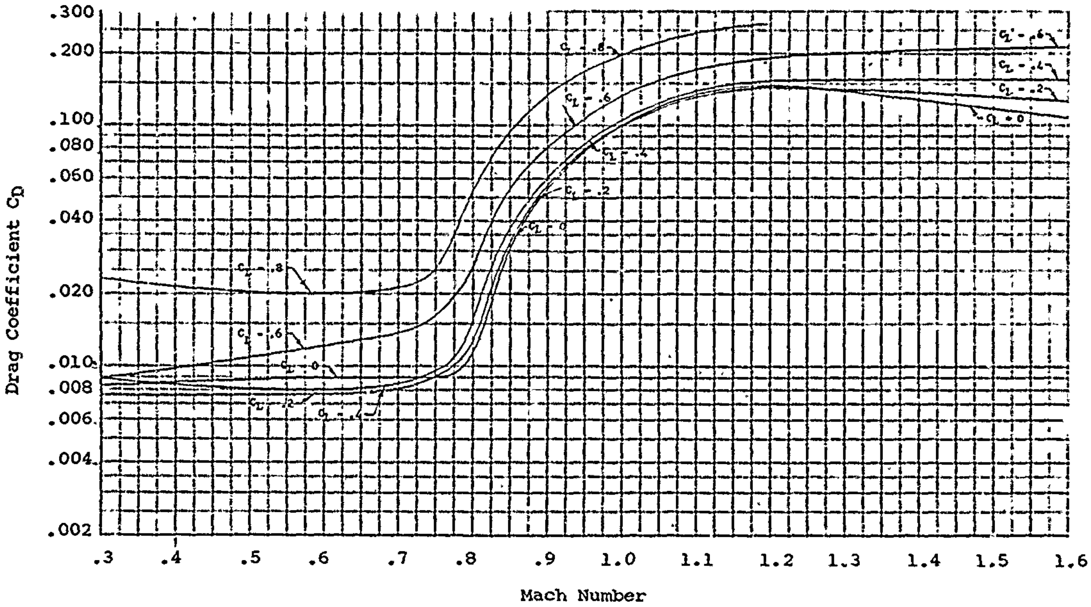

Figure 118. Two-Dimensional Drag Data, NACA 16-315 Airfoil.

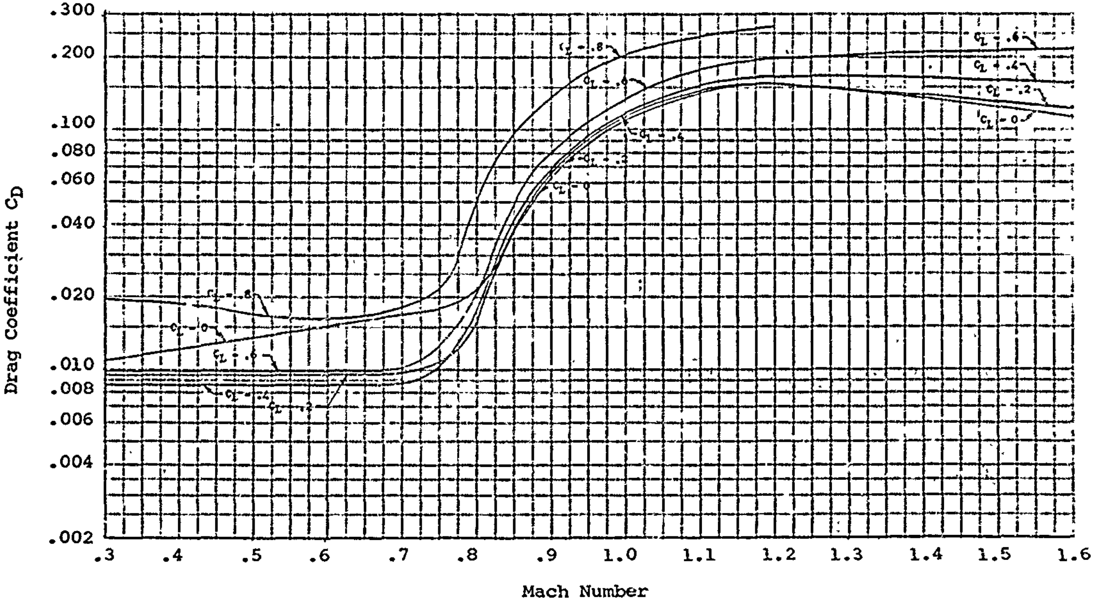

Figure 119. Two-Dimensional Drag Data, NACA 16-415 Airfoil.

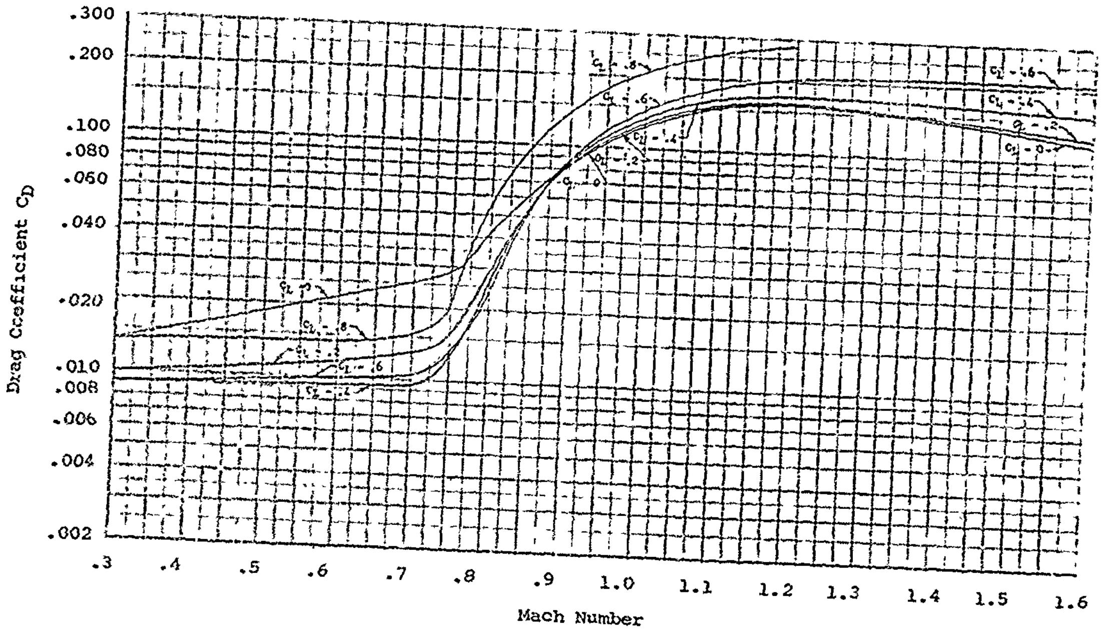

Figure 120. Two-Dimensional Drag Data, NACA 16-515 Airfoil.

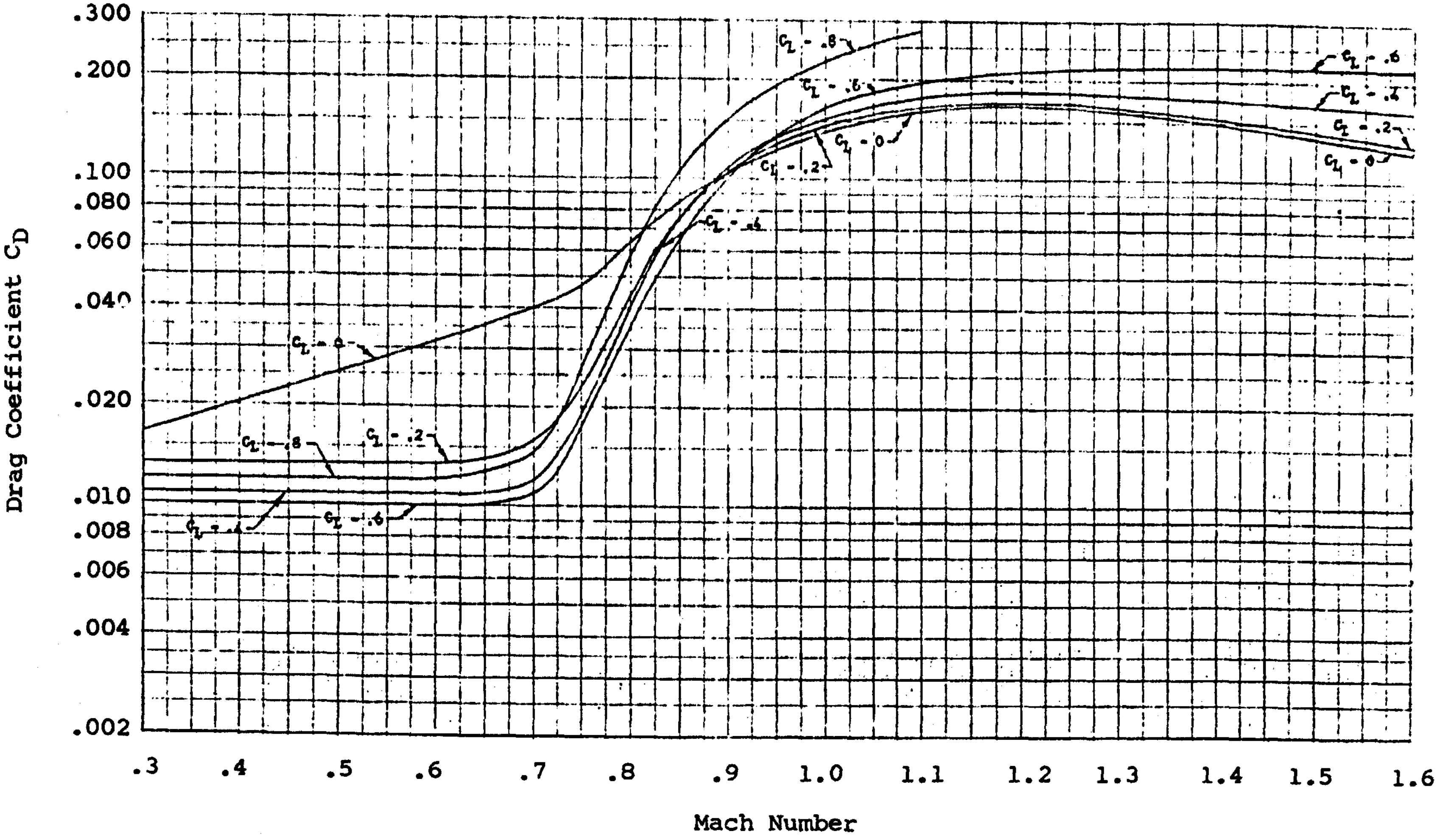

Figure 121. Two-Dimensional Drag Data, NACA 16-615 Airfoil.

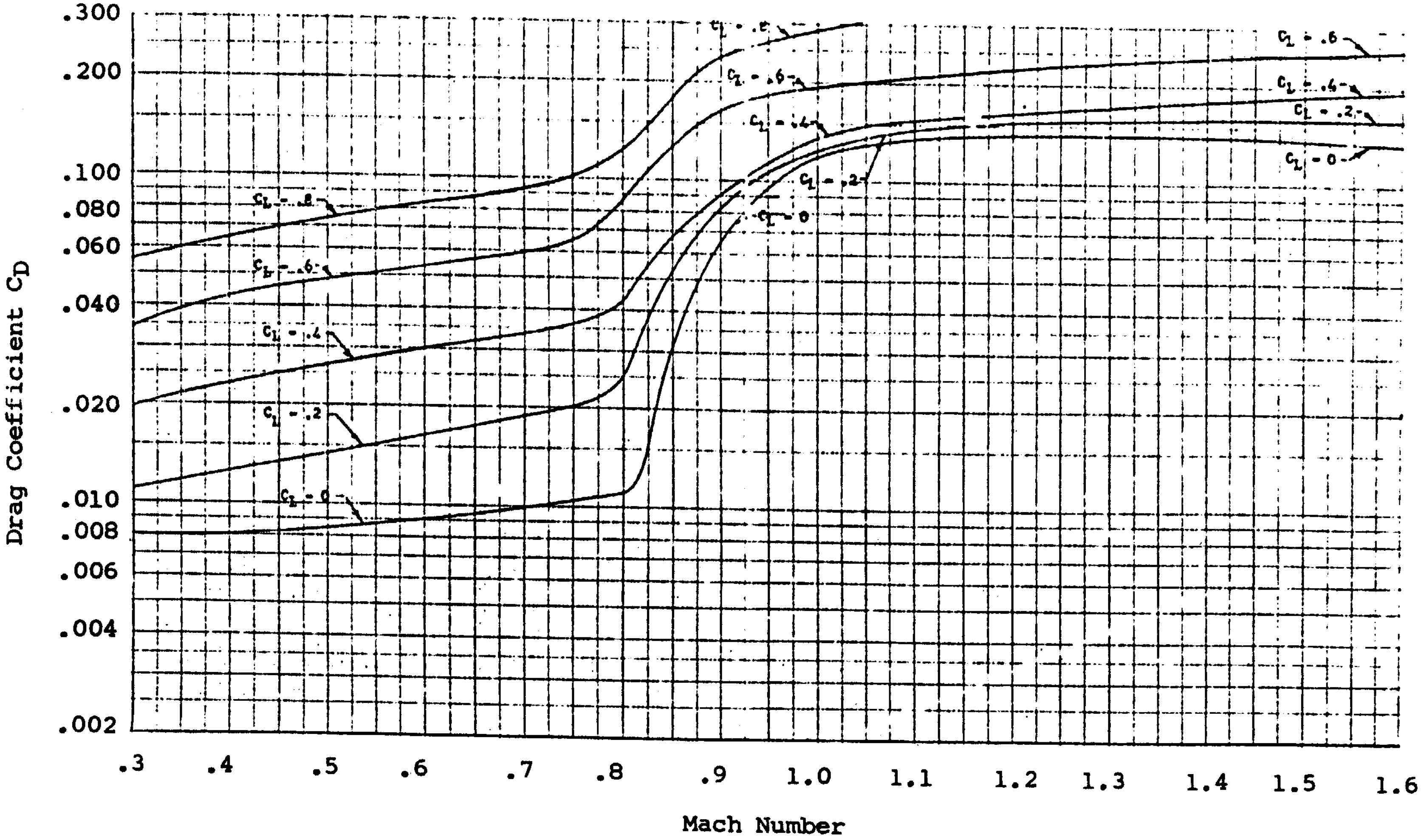

Figure 122. Two-Dimensional Drag Data, NACA 16-018 Airfoil.

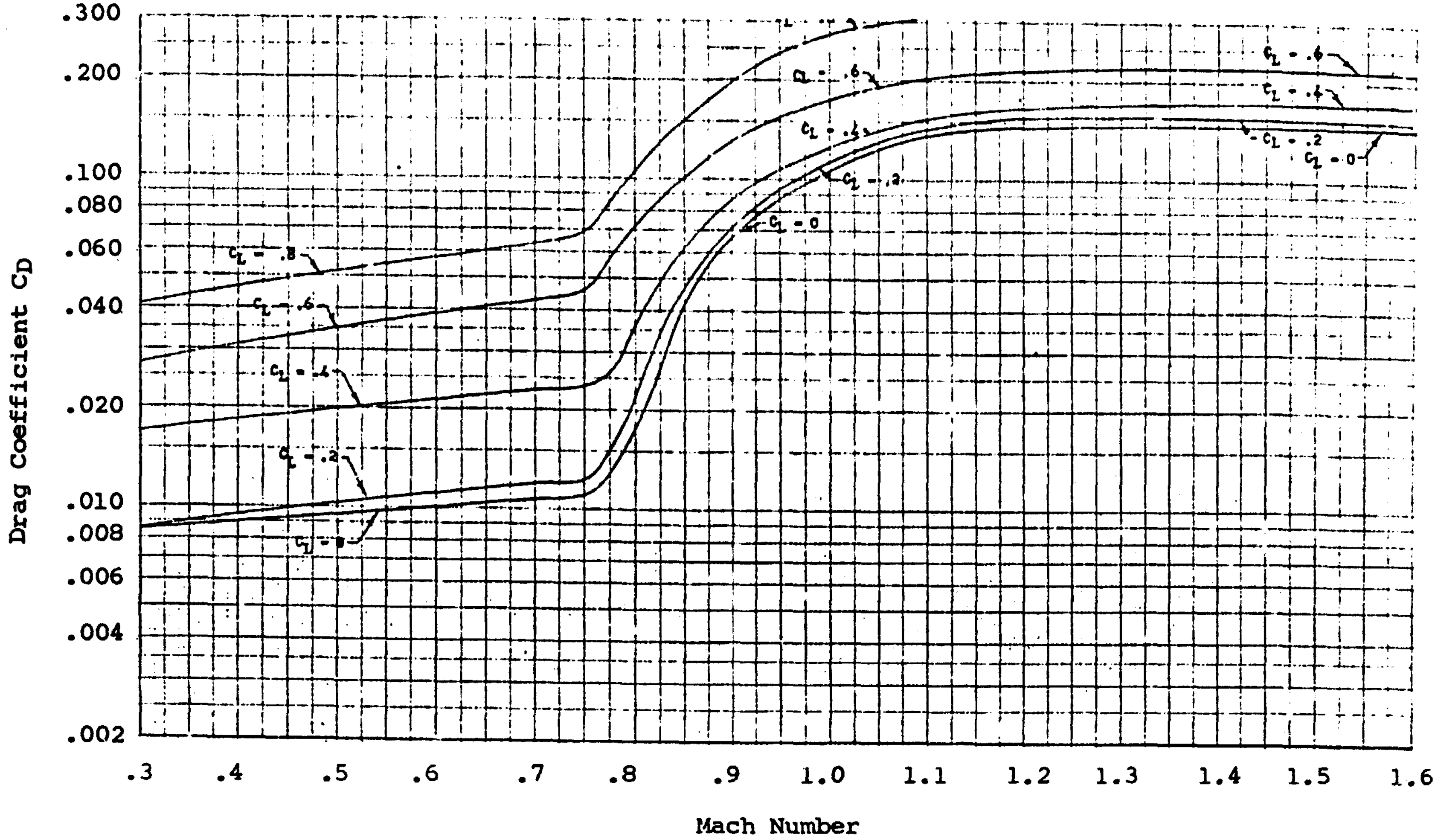

Figure 123. Two-Dimensional Drag Data, NACA 16-118 Airfoil.

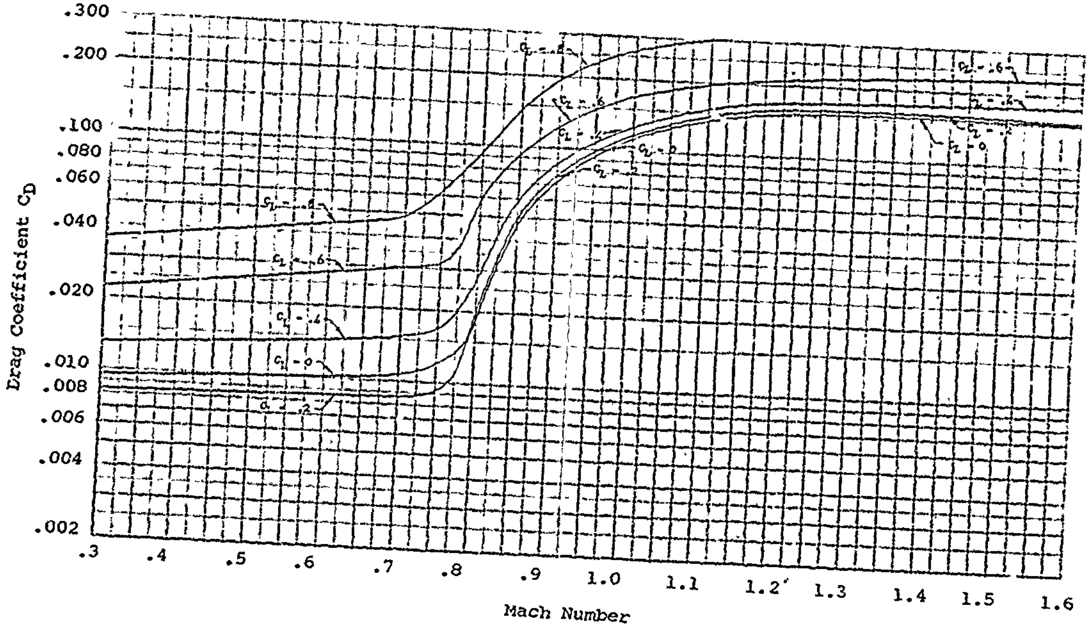

Figure 124. Two-Dimensional Drag Data,
NACA 16-218 Airfoil.

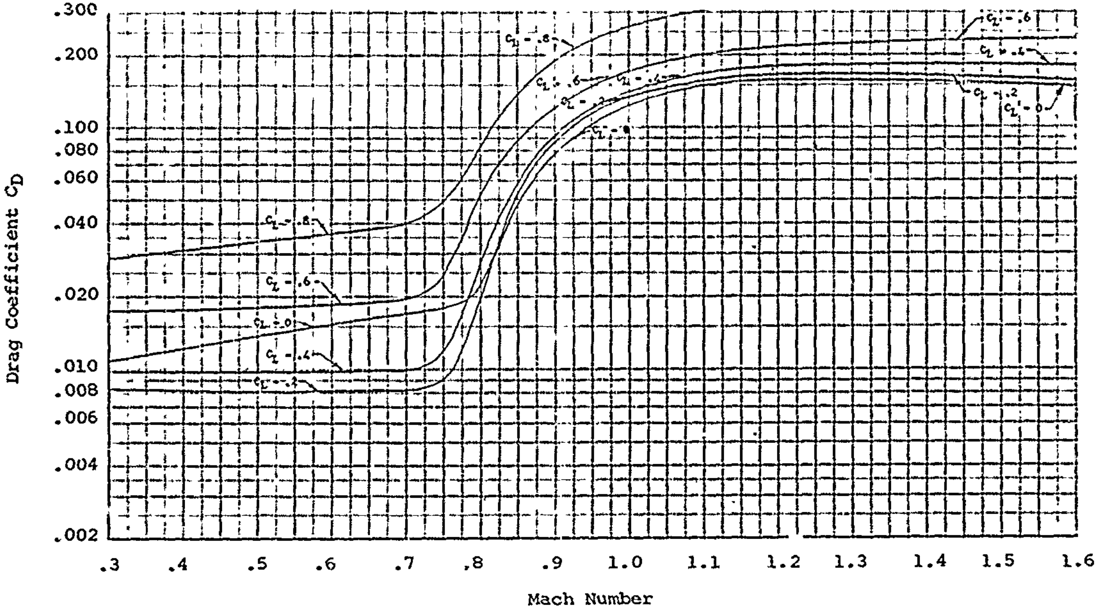

Figure 125. Two-Dimensional Drag Data, NACA 16-318 Airfoil.

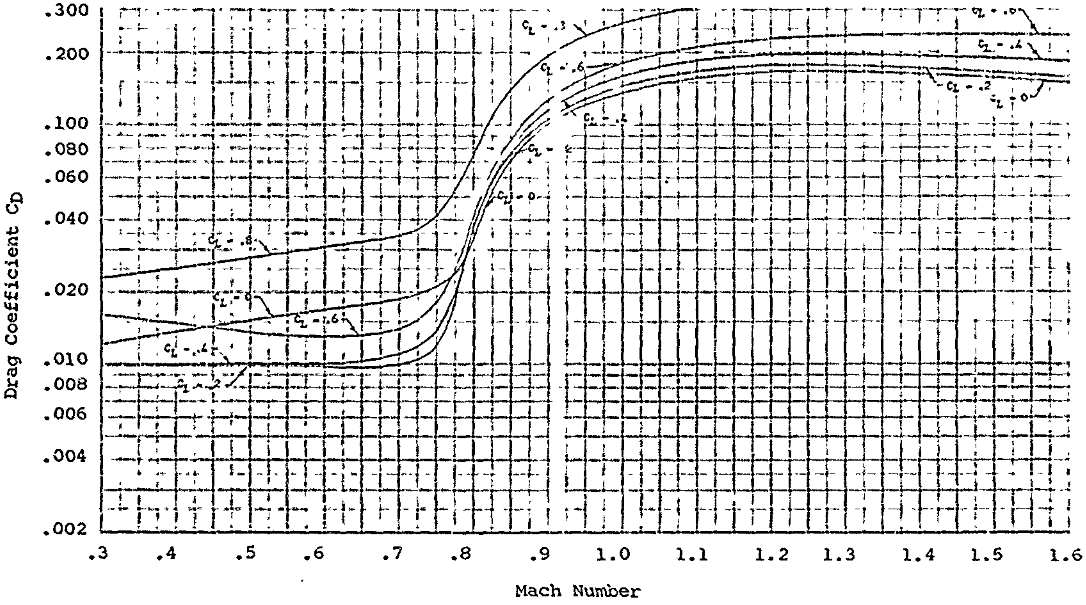

Figure 126. Two-Dimensional Drag Data, NACA 16-418 Airfoil.

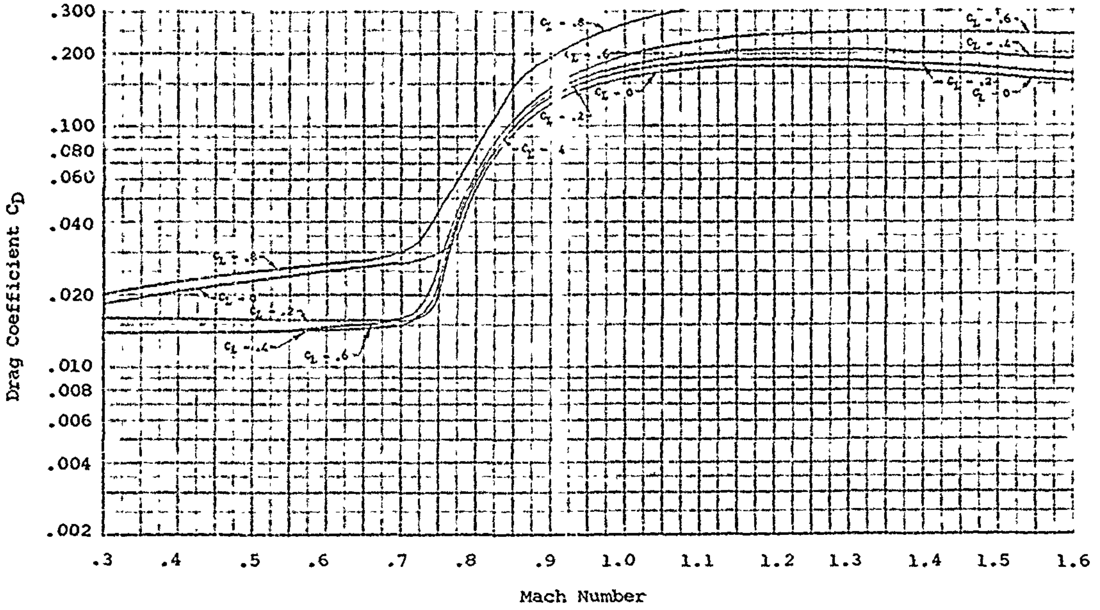

Figure 127. Two-Dimensional Drag Data, NACA 16-518 Airfoil.

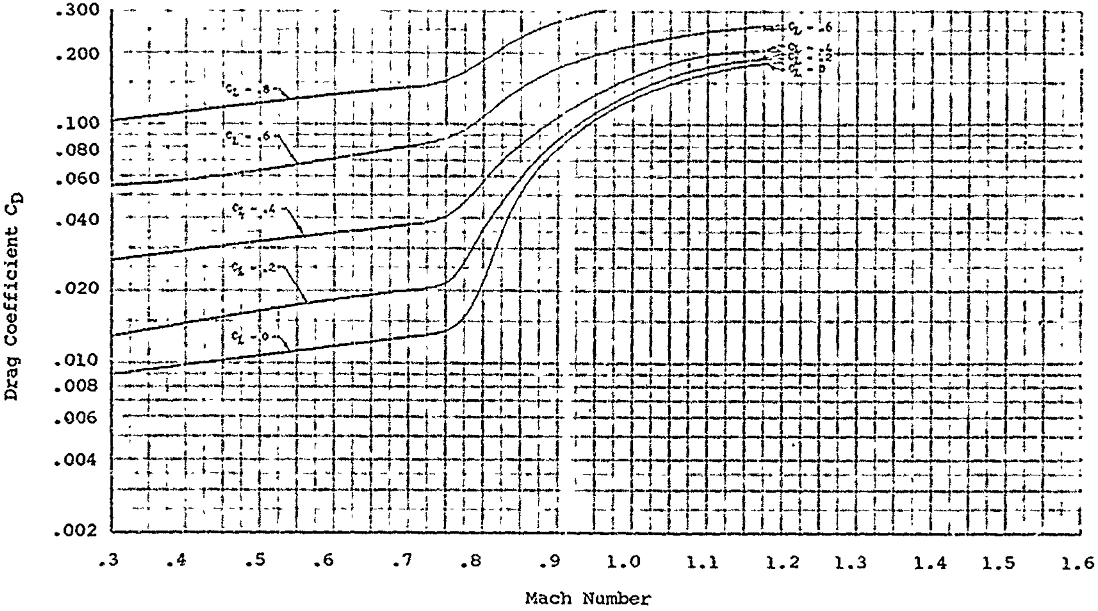

Figure 128. Two-Dimensional Drag Data, NACA 16-021 Airfoil.

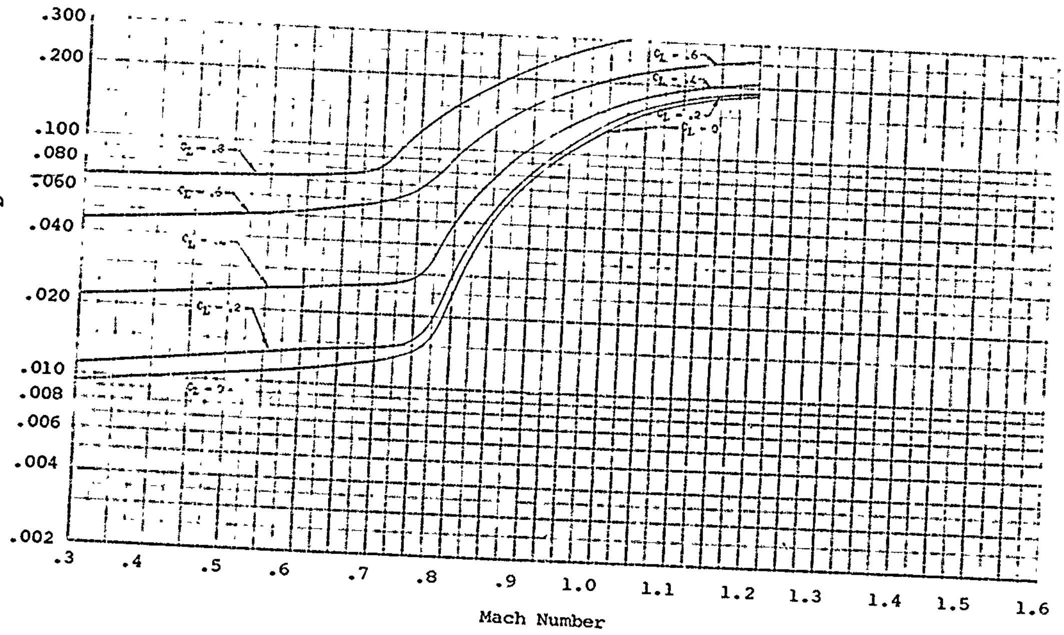

Figure 129. Two-Dimensional Drag Data, NACA 16-121 Airfoil.

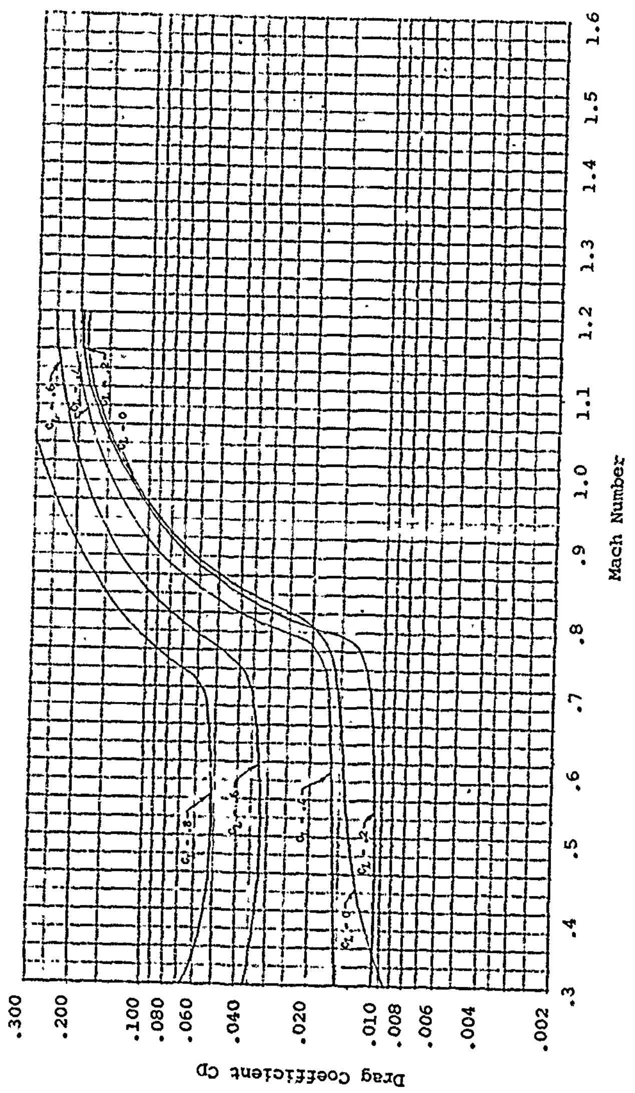

Figure 130. Two-Dimensional Drag Data, NACA 16-221 Airfoil.

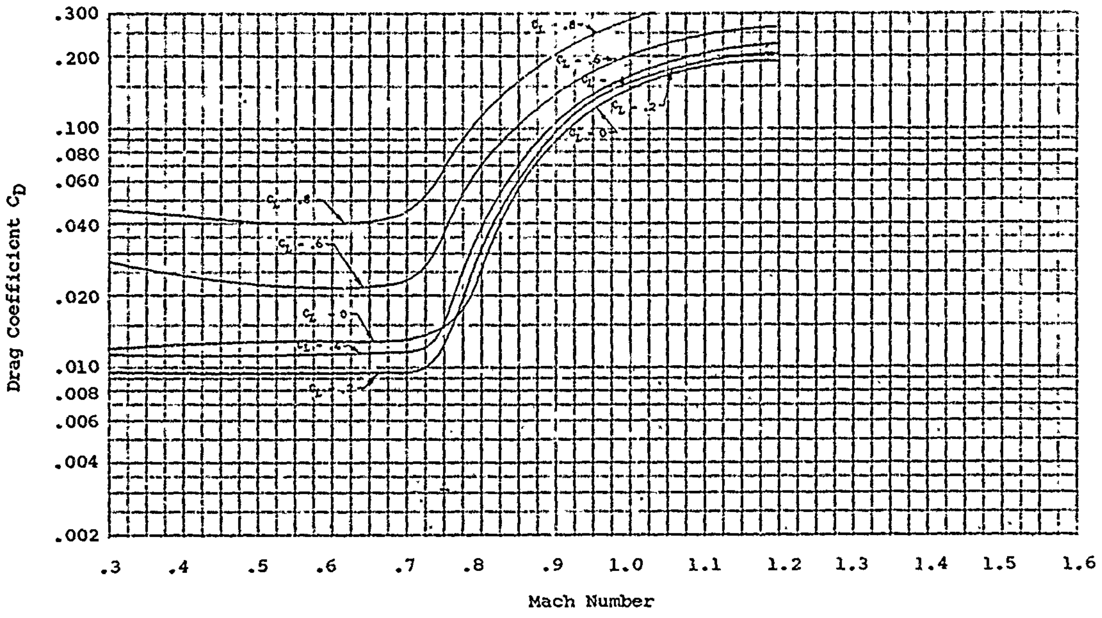

Figure 131. Two-Dimensional Drag Data, NACA 16-321 Airfoil.

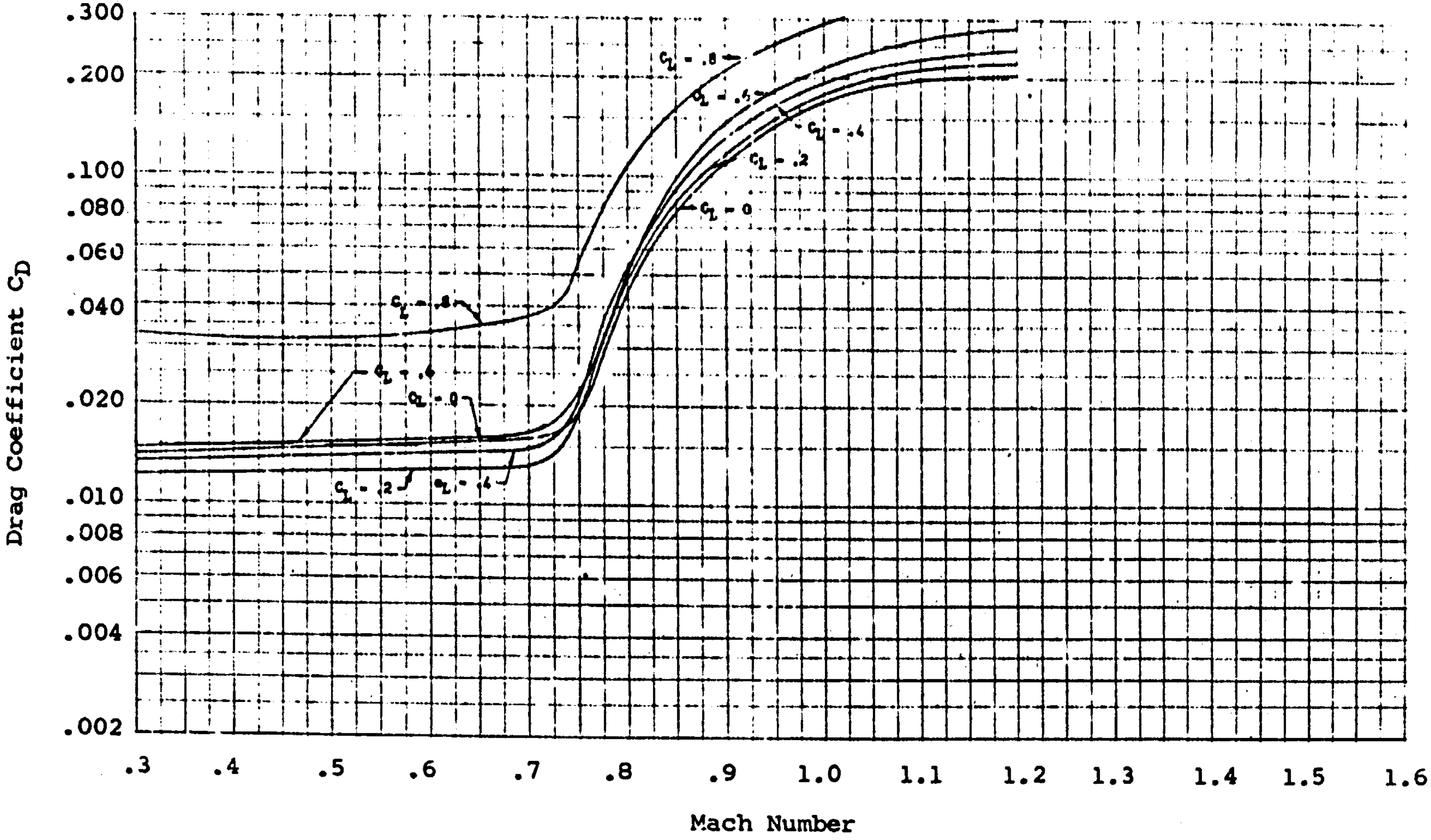

Figure 132. Two-Dimensional Drag Data, NACA 16-421 Airfoil.

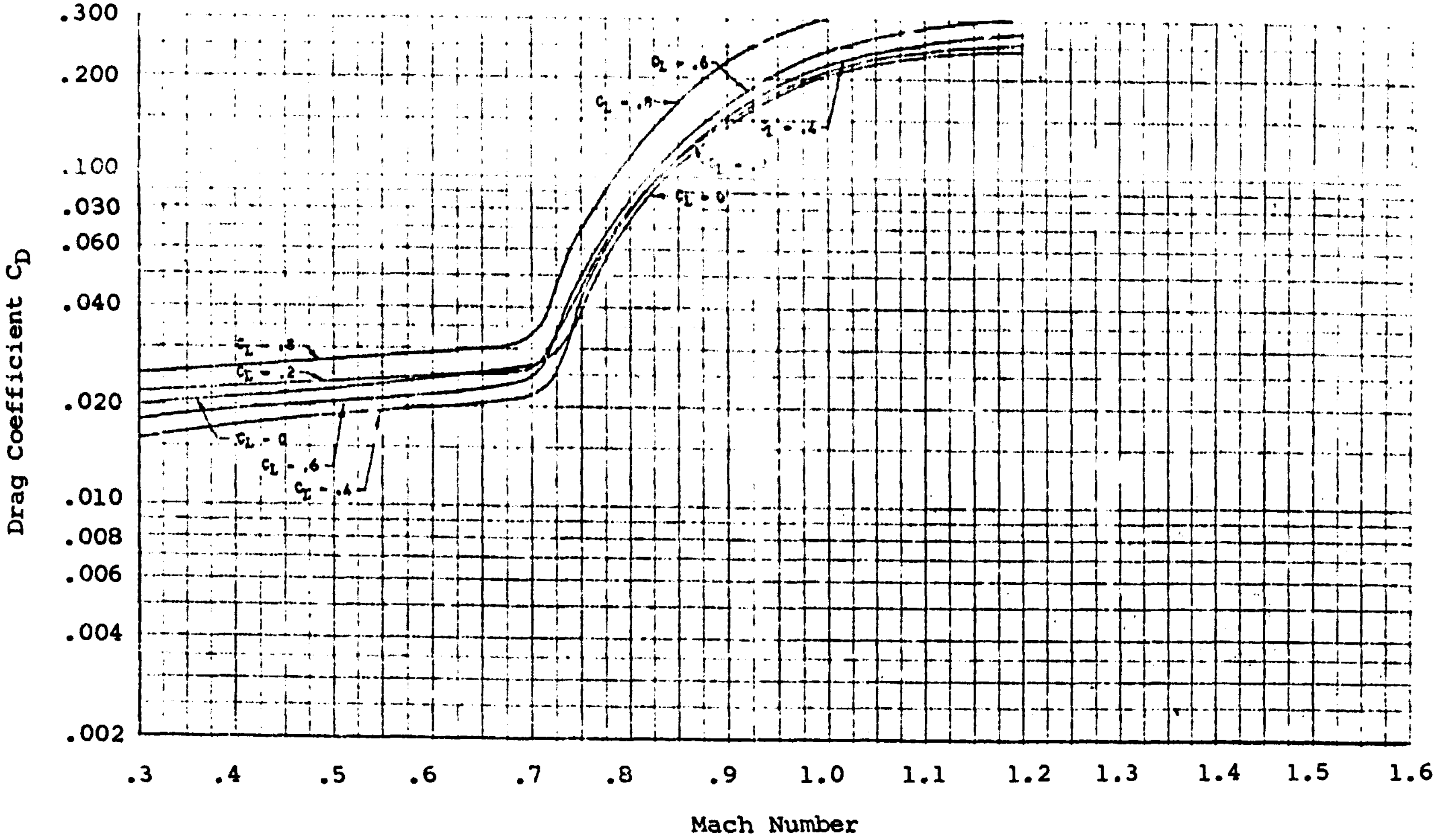

Figure 133. Two-Dimensional Drag Data, NACA 16-521 Airfoil.

TABLE II. CALCULATION PROCEDURE FOR OPERATING LIFT COEFFICIENT THICK AIRFOILS - 25% TO 100%

	AIRFOIL SECTION TYPE		
	Symmetrical	Elliptic	Cambered
Angle of attack = α	Given	Given	Given
Thickness ratio h/b	Given	Given	Given
Reynolds number = RN	Given	Given	Given
Mach number = M_o	Given	Given	Given
Basic low speed $C_L = C_{LB}$	Fig. 134 @ α & h/b	Fig. 134 @ α & h/b	Fig. 134 @ α & h/b
Shape correction	None	C_{Le}/C_{LB} Fig. 135	C_L^C Fig. 136 & f_c Fig. 137
Low speed $C_L = C_{LL}$	$C_{LB} \times 1.0$	$C_{Le}/C_{LB}(C_{LB})$	$C_{LB} + (C_L^C)(f_c)$
Critical Mach No. = M_{CR} =	Figure 138	Figure 138	Figure 138
M_{CR} correction for C_L	ΔM_{CRL} @ Fig. 139	ΔM_{CRL} @ Fig. 139	ΔM_{CRL} @ Fig. 139
Critical Mach No. = M_{CR}	$M_{CR} + \Delta M_{CR}$	$M_{CR} + \Delta M_{CRL}$	$M_{CR}^S + \Delta M_{CRL}$
Mach number increment (positive values only)	$M_o - M_{CR} = \Delta M$	$M_o - M_{CR} = \Delta M$	$M_o - M_{CR} = \Delta M$
ΔC_L due to Mach No. = ΔC_{LM} =	Fig. 140 @ ΔM	Fig. 140 @ ΔM	Fig. 140 @ ΔM
Operating C_L	$C_{LL} + \Delta C_{LM}$	$C_{LL} + \Delta C$	$C_{LL} + \Delta C$

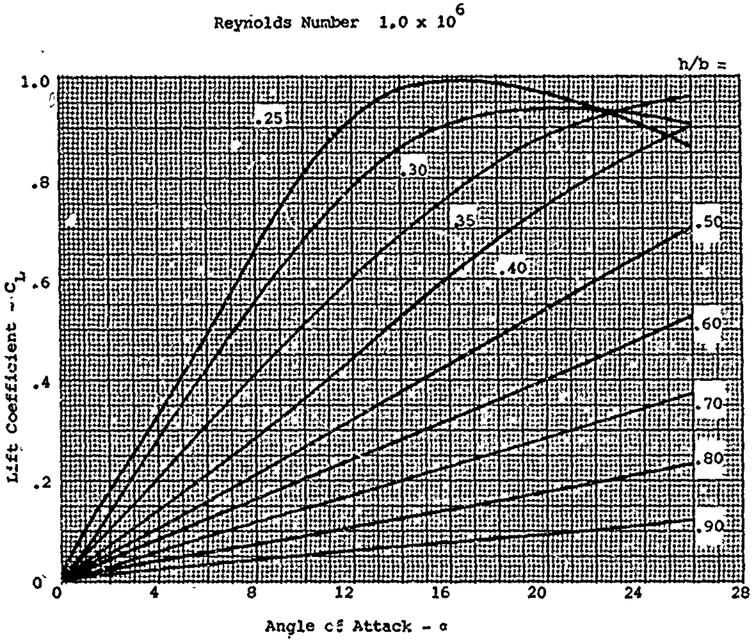

Figure 134. Basic Low-Speed Lift Coefficient - C_{LB} Symmetrical Sections - 25% to 90%.

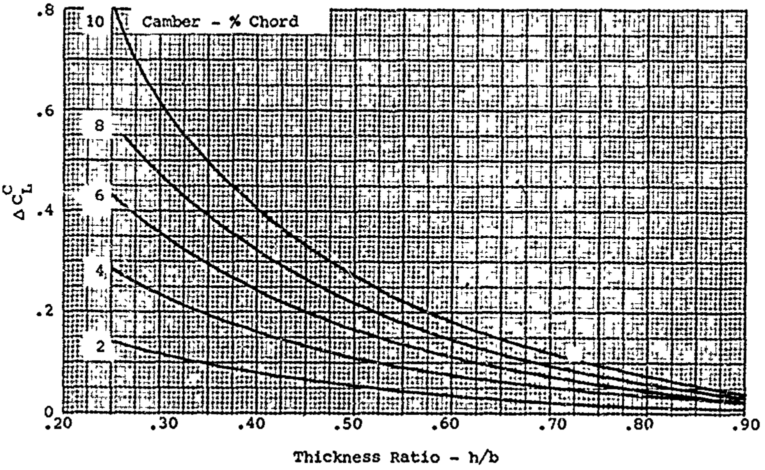

Figure 135. Correction to Basic Lift Coefficient for Camber C_L^C.

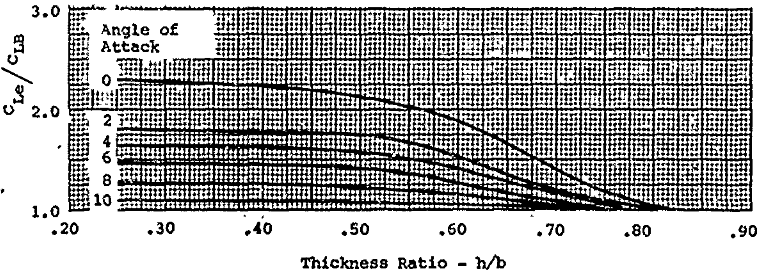

Figure 136. Shape Correction to Basic Lift Coefficient C_{LC}/C_{LP}.

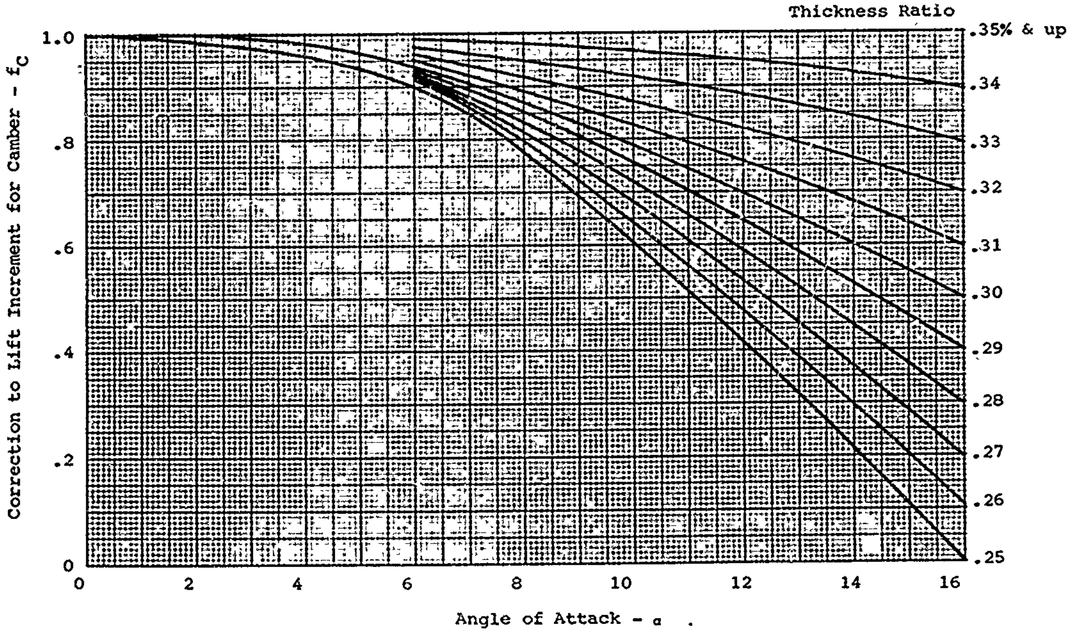

Figure 137. Correction to Lift Increment for Camber - fc.

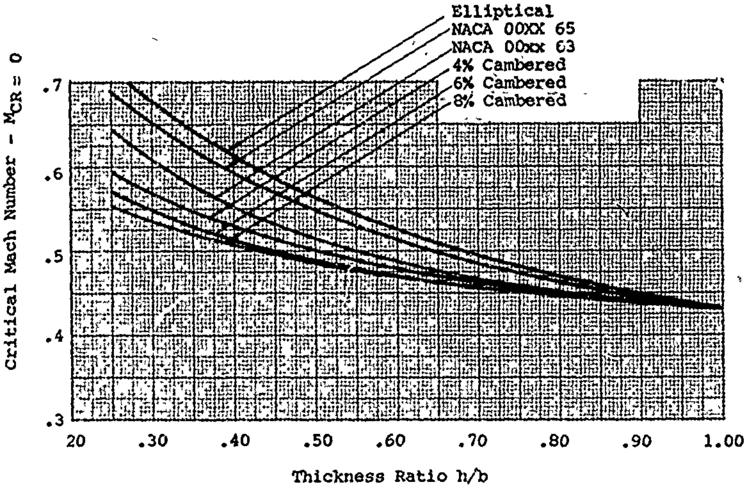

Figure 138. Critical Mach Number, Thick Airfoils, $C_L = 0$.

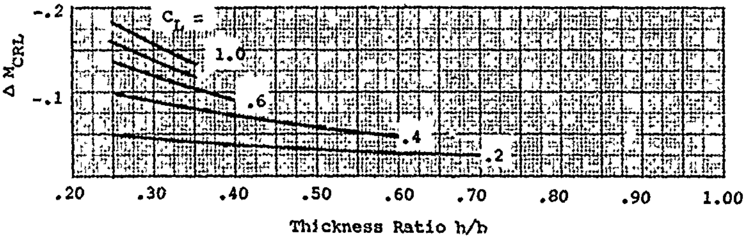

Figure 139. Critical Mach Number Correction for Lift - ΔM_{CRL}.

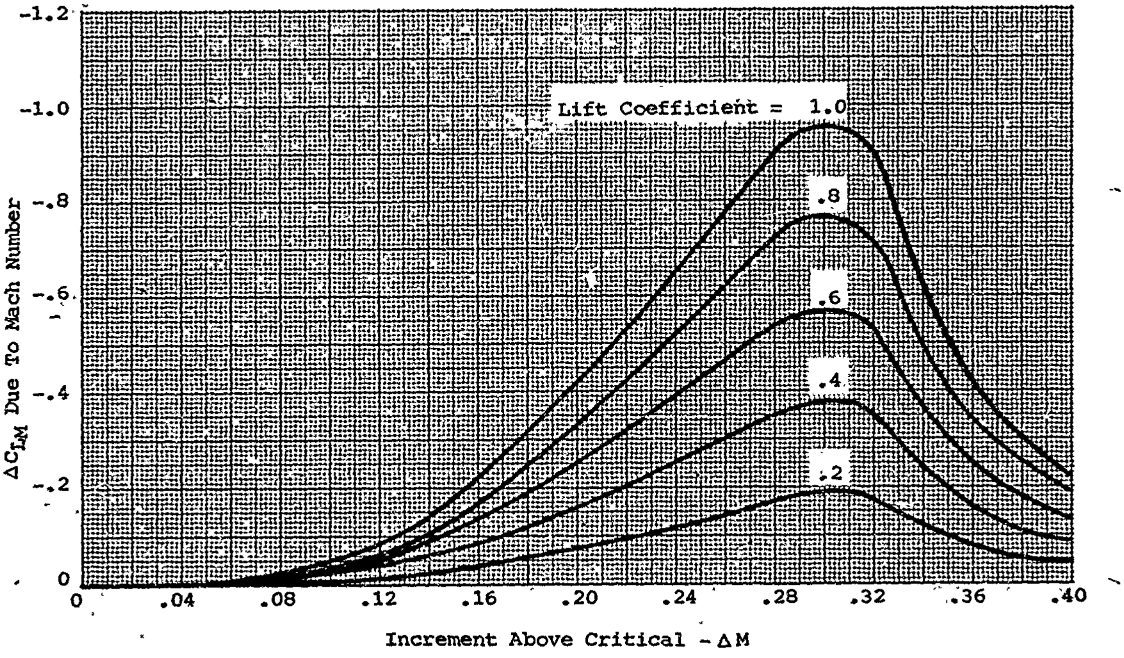

Figure 140. Lift Coefficient Increment at Mach Numbers Above the Critical.

TABLE III. CALCULATING PROCEDURE FOR OPERATING DRAG COEFFICIENT OF THICK AIRFOILS - 25% TO 100%

	AIRFOIL SECTION TYPE		
	Symmetrical	Elliptic	Cambered
Angle of attack = α	Given	Given	Given
Thickness ratio = h/b	Given	Given	Given
Reynolds Number = RN	Given	Given	Given
Mach Number = M_O	Given	Given	Given
Drag Coeff. $\alpha = 0 = C_{DOM}$	Figure 174	Figure 174	Figure 174
$\Delta C_{DO\alpha}$ for α	Figure 175	Figure 175	Figure 175
Drag Shape Correction	None	C_{DOe}/C_{DO} (Fig.176)	C_{DO}^{c} (Fig. 177)
C_{DO} low speed =	$C_{DOM} + \Delta C_{DO\alpha}$	$(C_{DOM} + \Delta C_{DO\alpha})\frac{C_{DOe}}{C_{DOS}}$	$C_{DOM} + C_{D\delta} + \Delta C_{DO\alpha}$
Mach Number increment, (positive values only)	Table II	Table II	Table II
Drag coeff. increment due to Mach No. = ΔC_{DOM}	Figure 178	Figure 178	Figure 178
Drag C_D	$C_{DO} + C_{DOM}$	$C_{DO} + C_{DOM}$	C_{DOM}

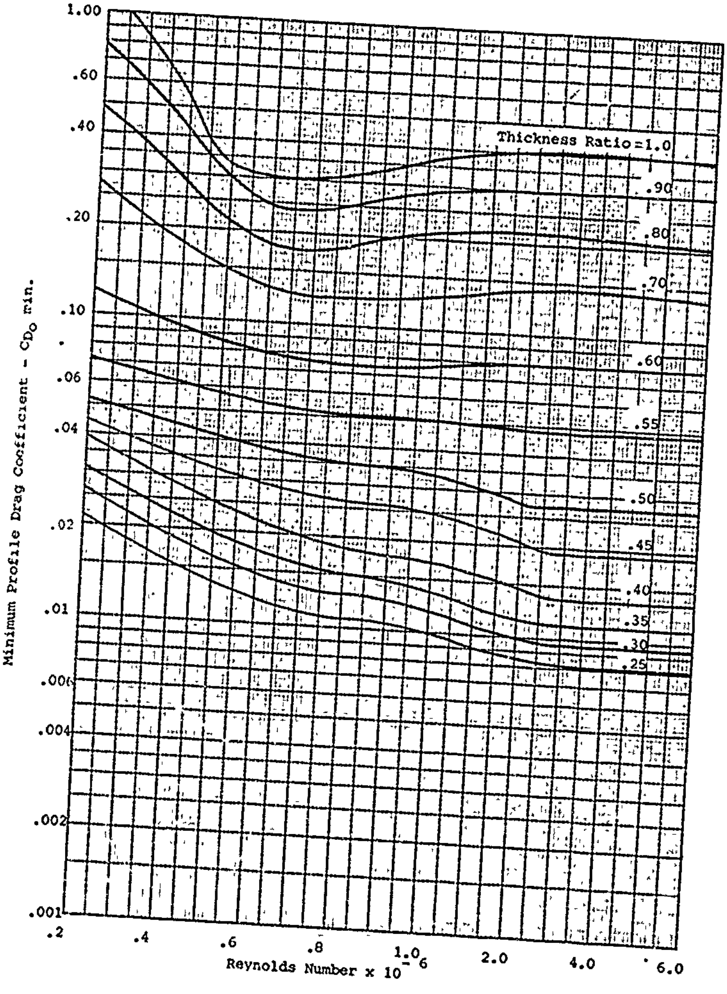

Figure 141. Minimum Profile Drag for Thick Airfoil Sections.

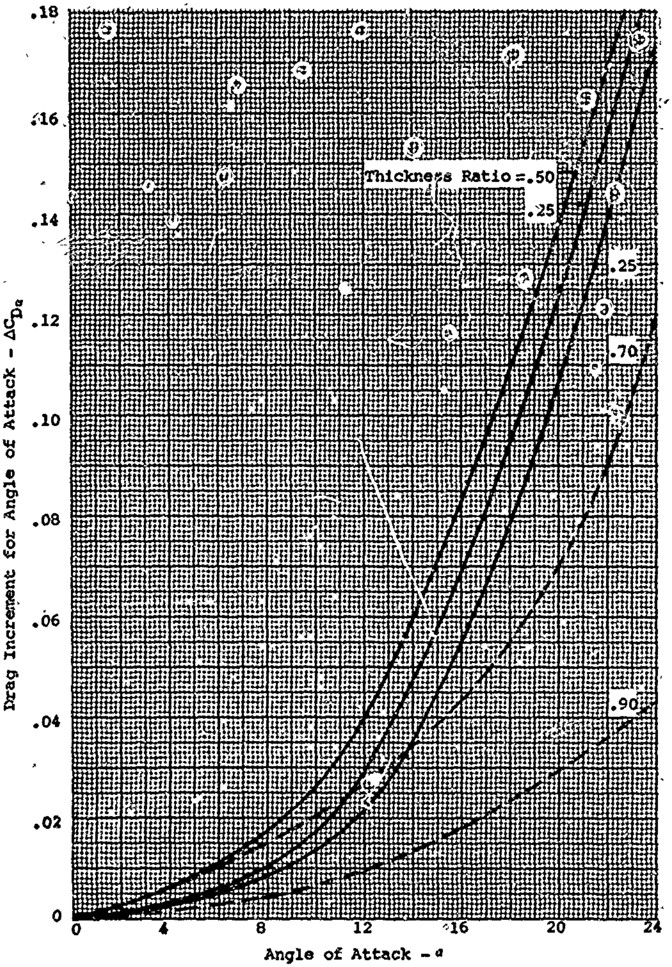

Figure 142. Drag Coefficient Increment for Angle of Attack - $\Delta C_{D\alpha}$.

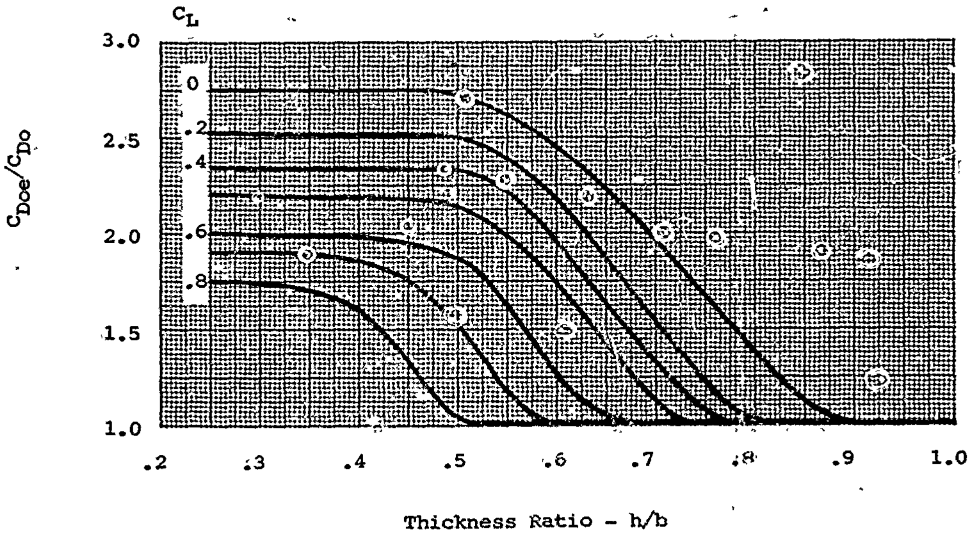

Figure 143. Drag Correction for Elliptic Airfoil Sections.

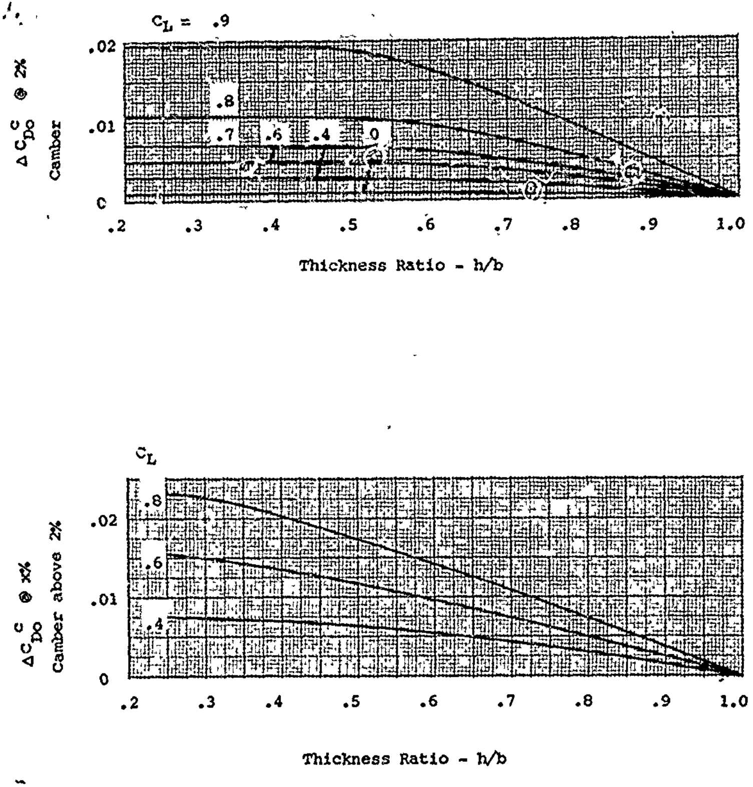

Figure 144. Drag Correction for Camber Sections.

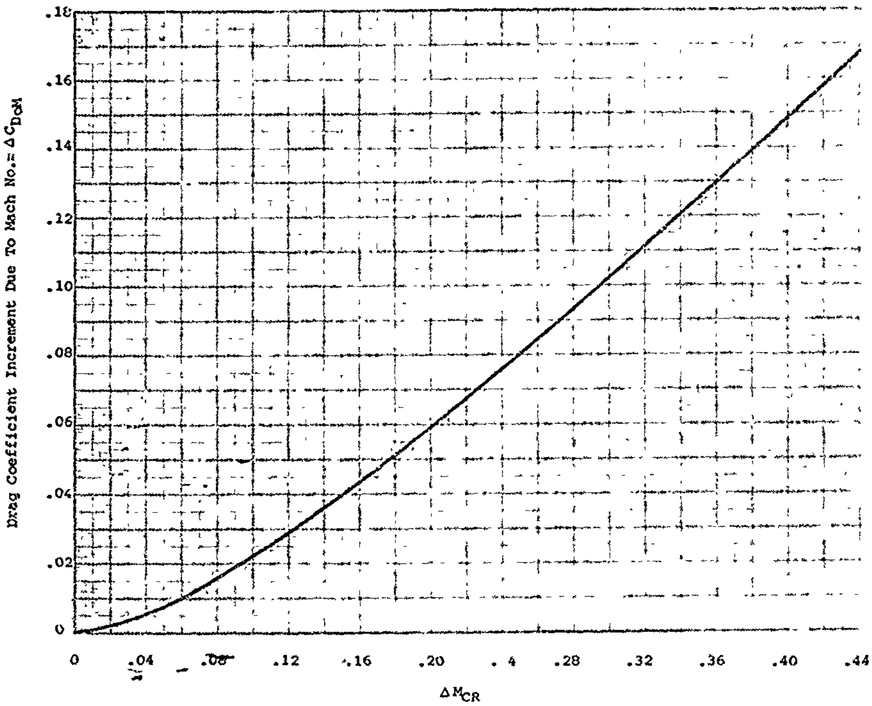

Figure 145. Drag Coefficient Increment at Mach Numbers Above the Critical.

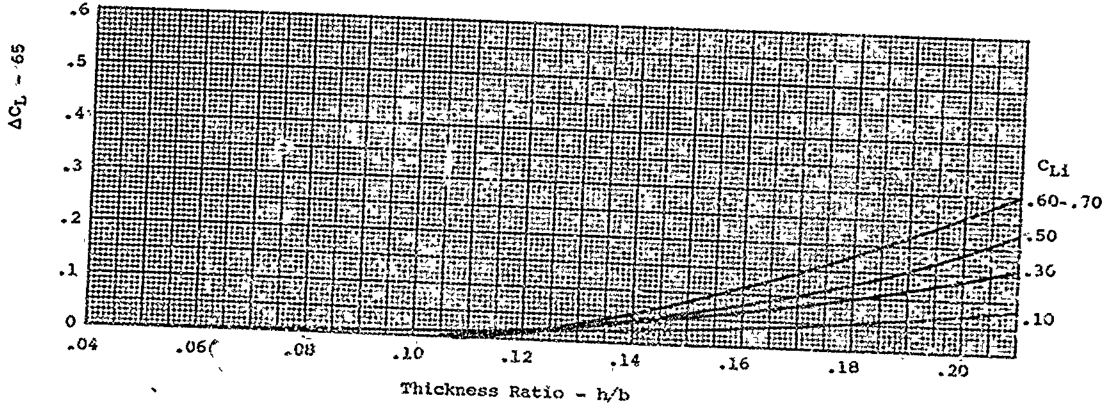

Figure 146. Incremental Lift Coefficient for 65 Airfoil Sections.

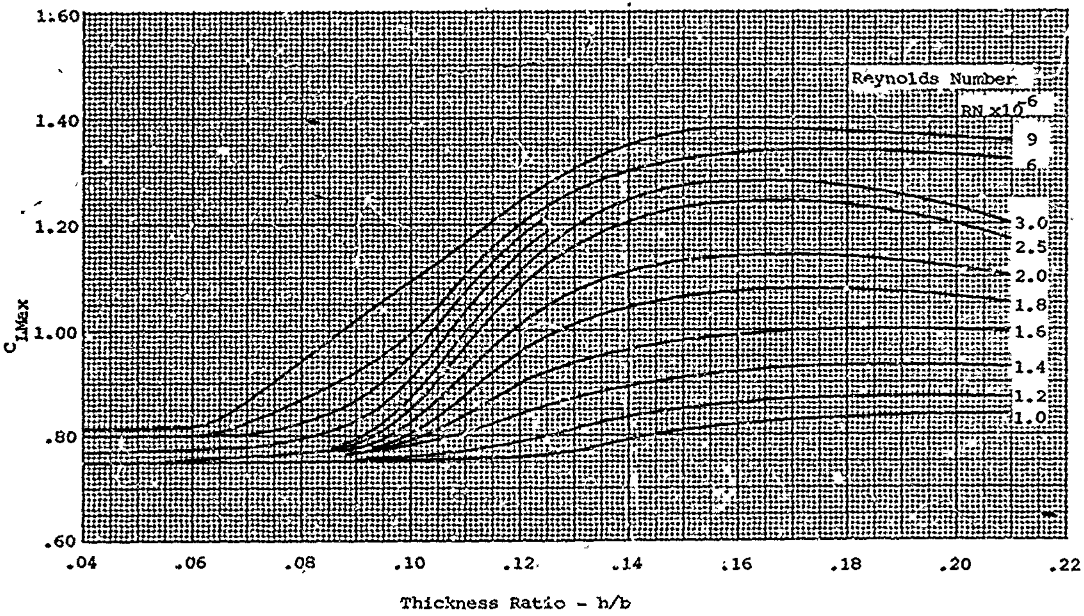

Figure 147. Lift Increment Correction to NACA-16 Sections.

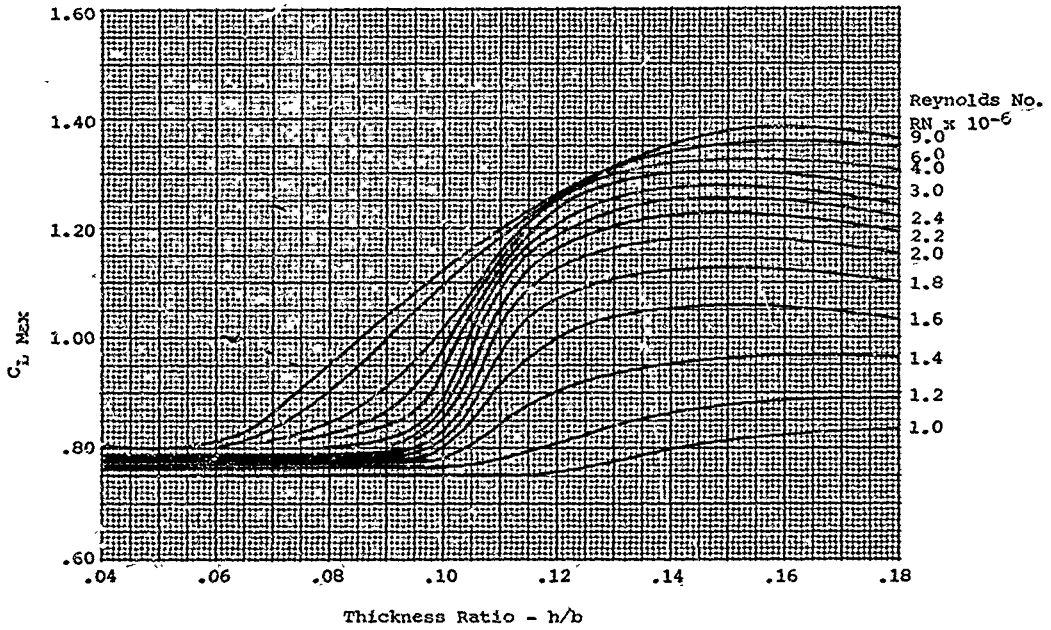

Figure 148. Maximum Lift Coefficient NACA-66 Sections.

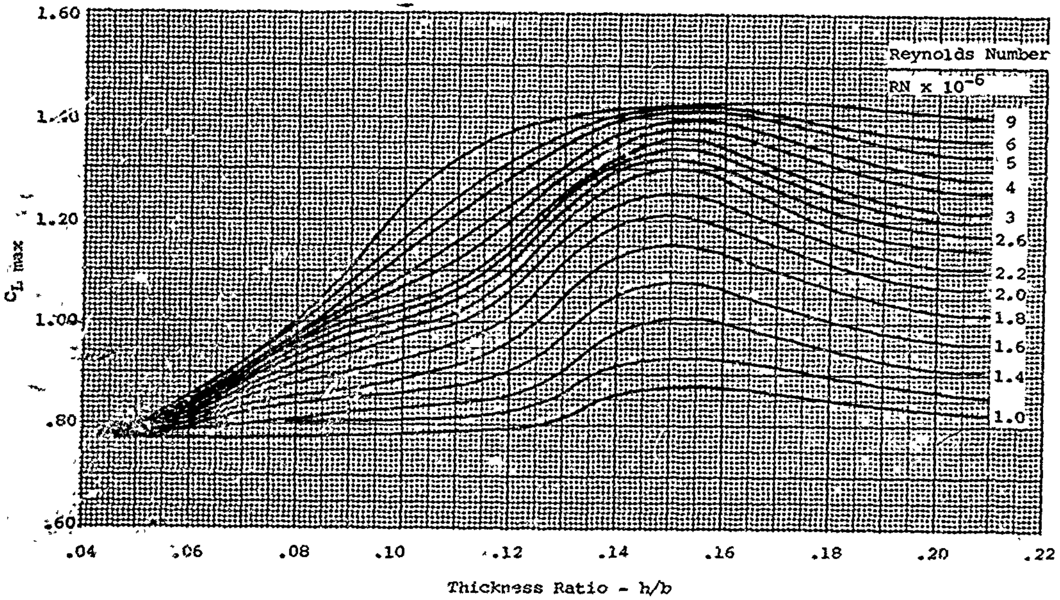

Figure 149. Maximum Lift Coefficient NACA-65 Sections.

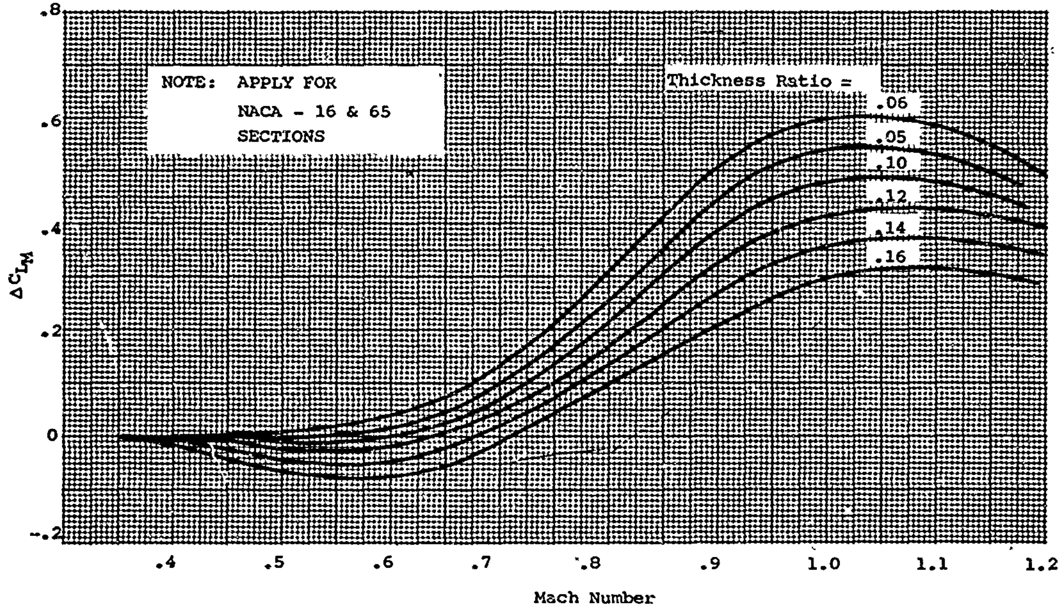

Figure 150. Change in Maximum Lift Coefficient Due to Mach Number.

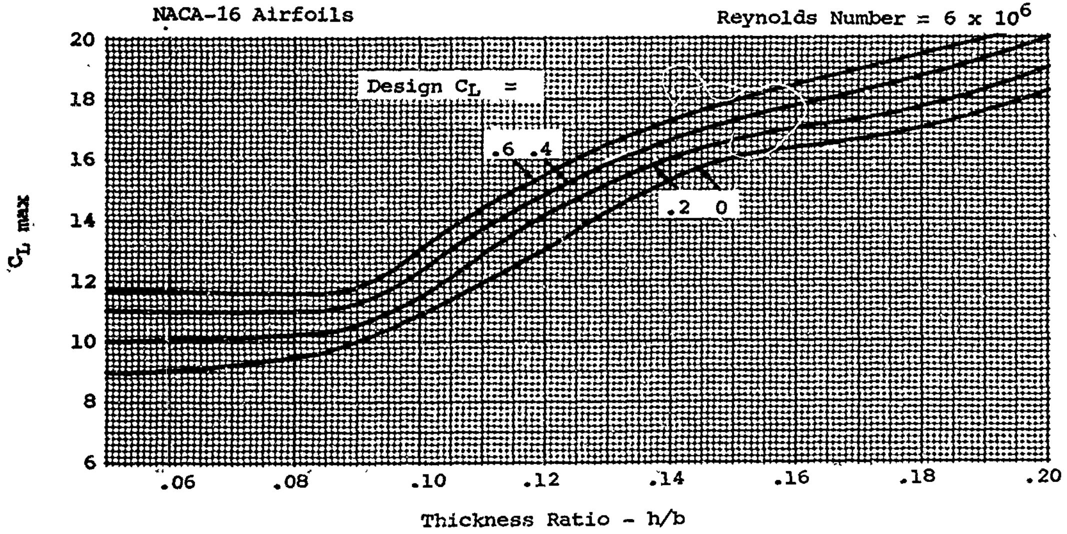

Figure 151. Angle of Attack at Stall.

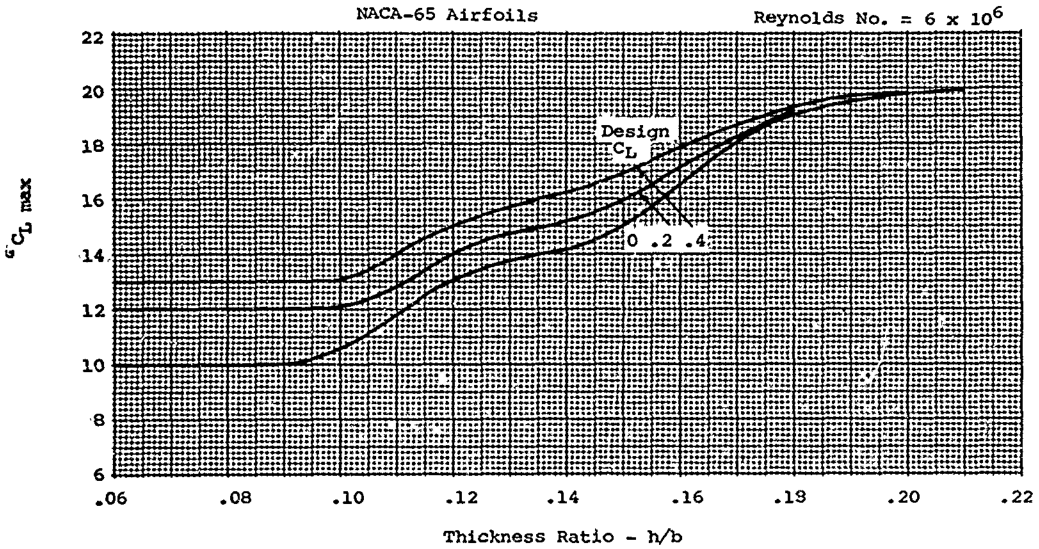

Figure 152. Angle of Attack at Stall.

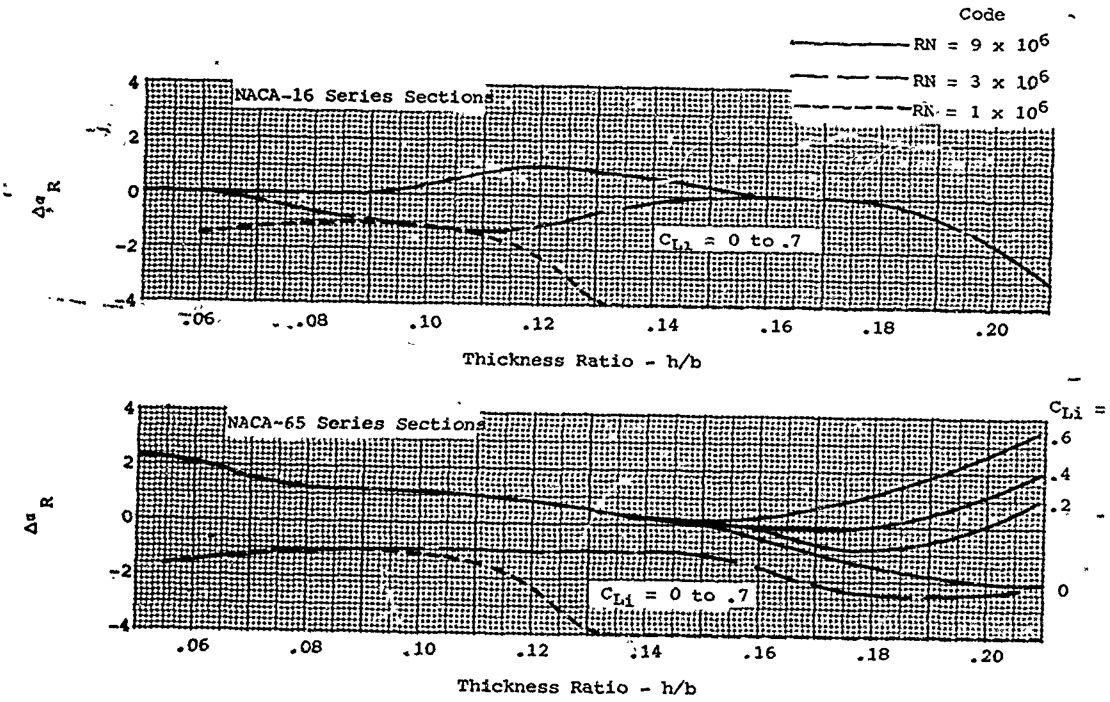

Figure 153. Stall Angle Increment Due to Reynolds Number NACA-16 and NACA-65 Sections.

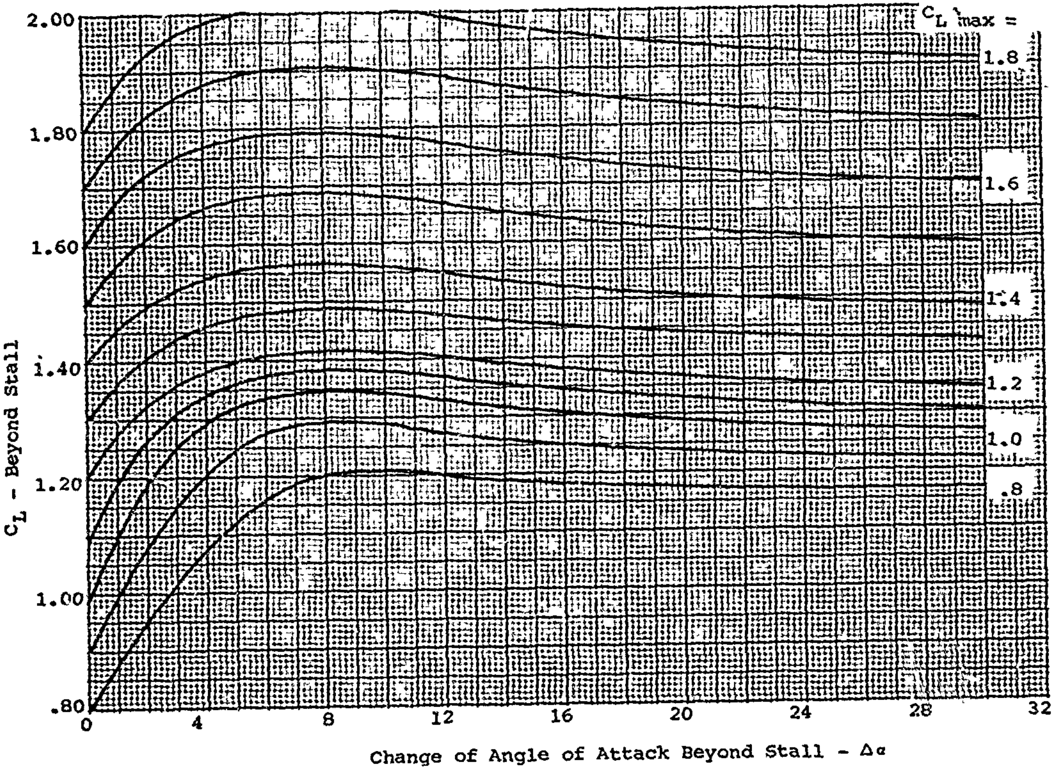

Figure 154. Variation of Lift Beyond the Stall.

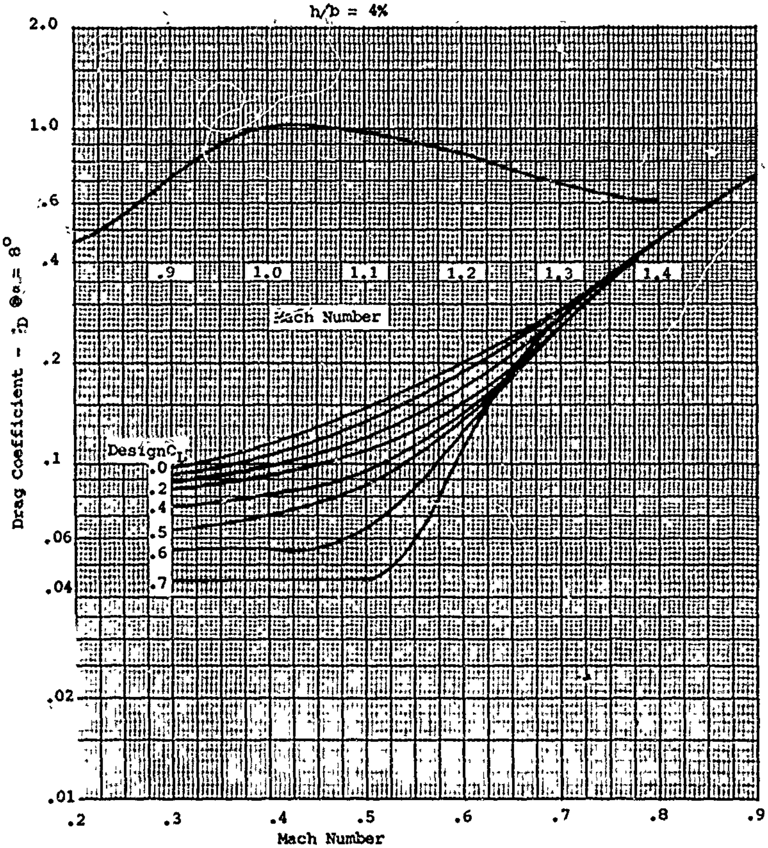

Figure 155. Drag Coefficient at 8° Angle of Attack
Thickness Ratio = 4%.

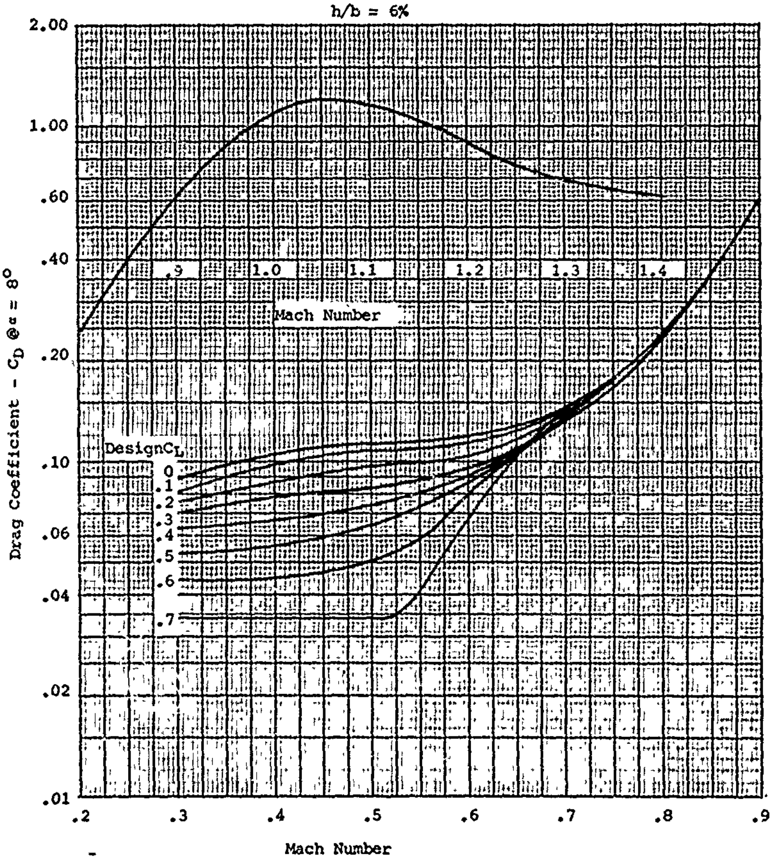

Figure 156. Drag Coefficient at 8° Angle of Attack Thickness Ratio = 6%.

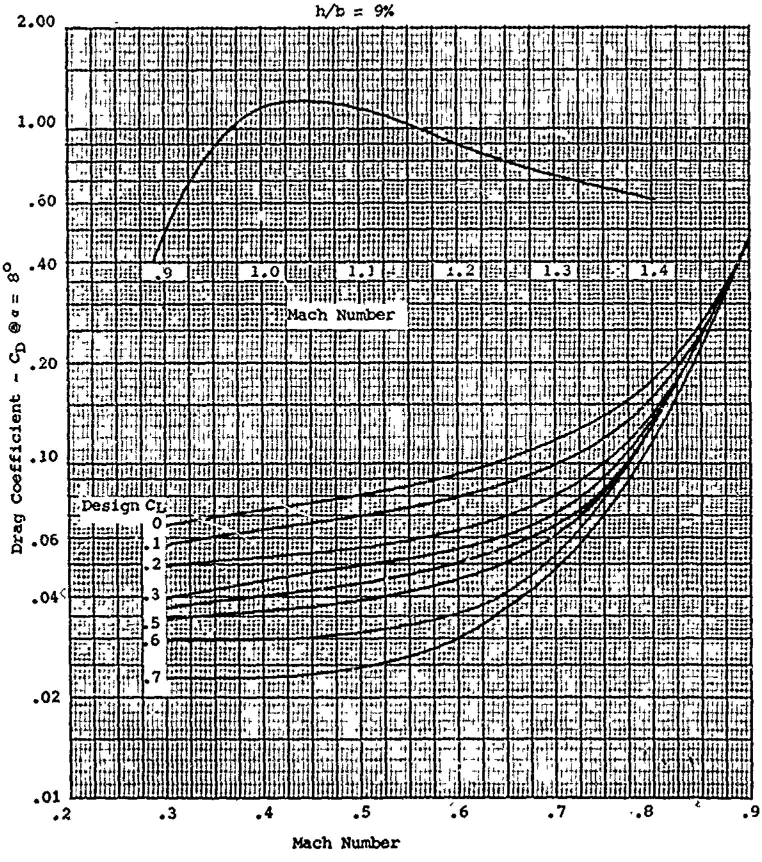

Figure 157. Drag Coefficient at 8° Angle of Attack Thickness Ratio = 9%.

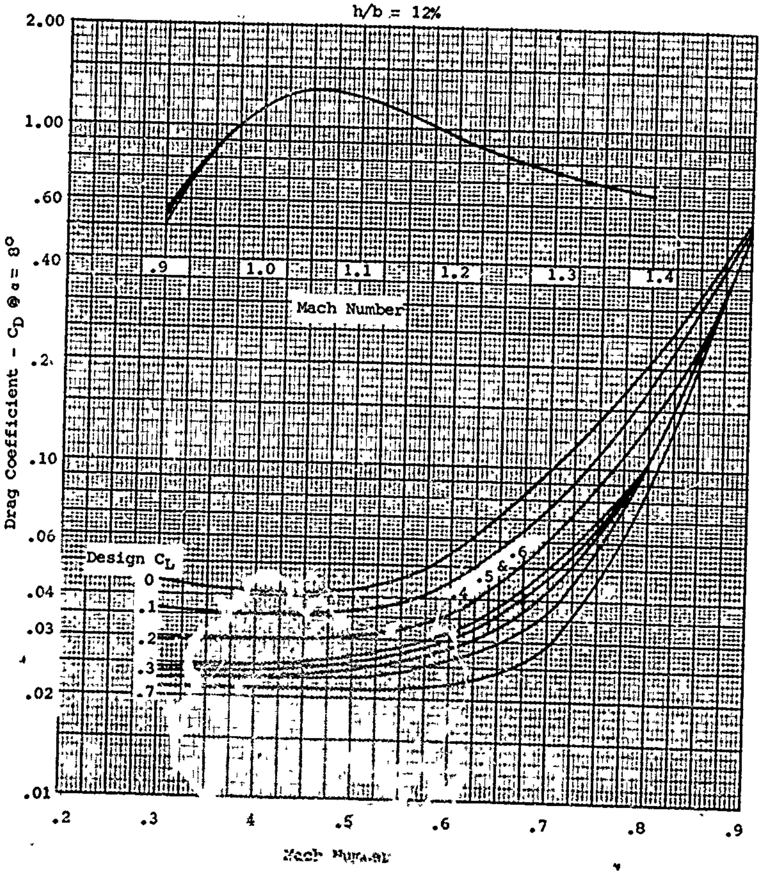

Figure 158. Drag Coefficient at 8° Angle of Attack Thickness Ratio = 12%.

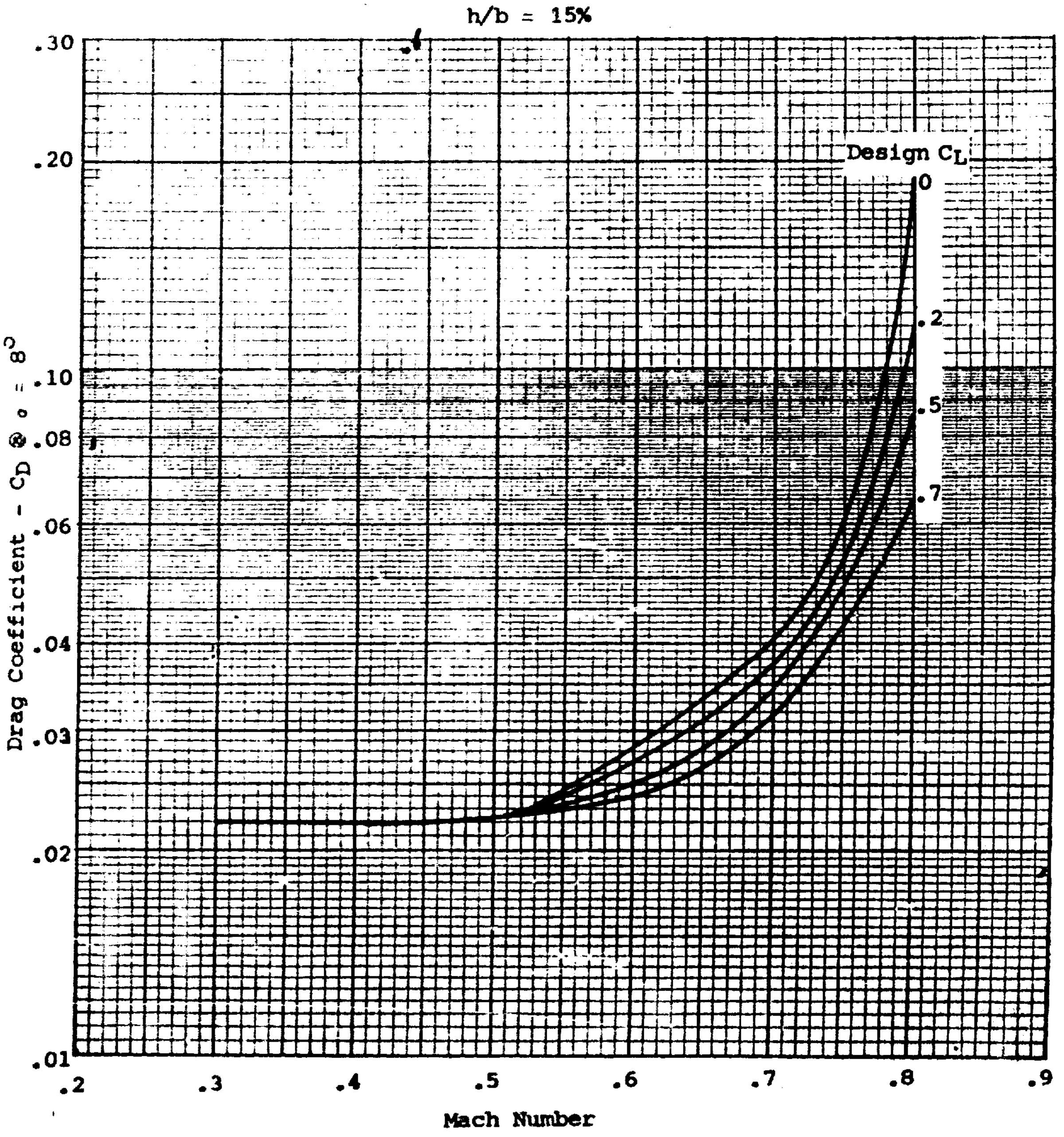

Figure 159. Drag Coefficient at 8° Angle of Attack Thickness Ratio = 15%.

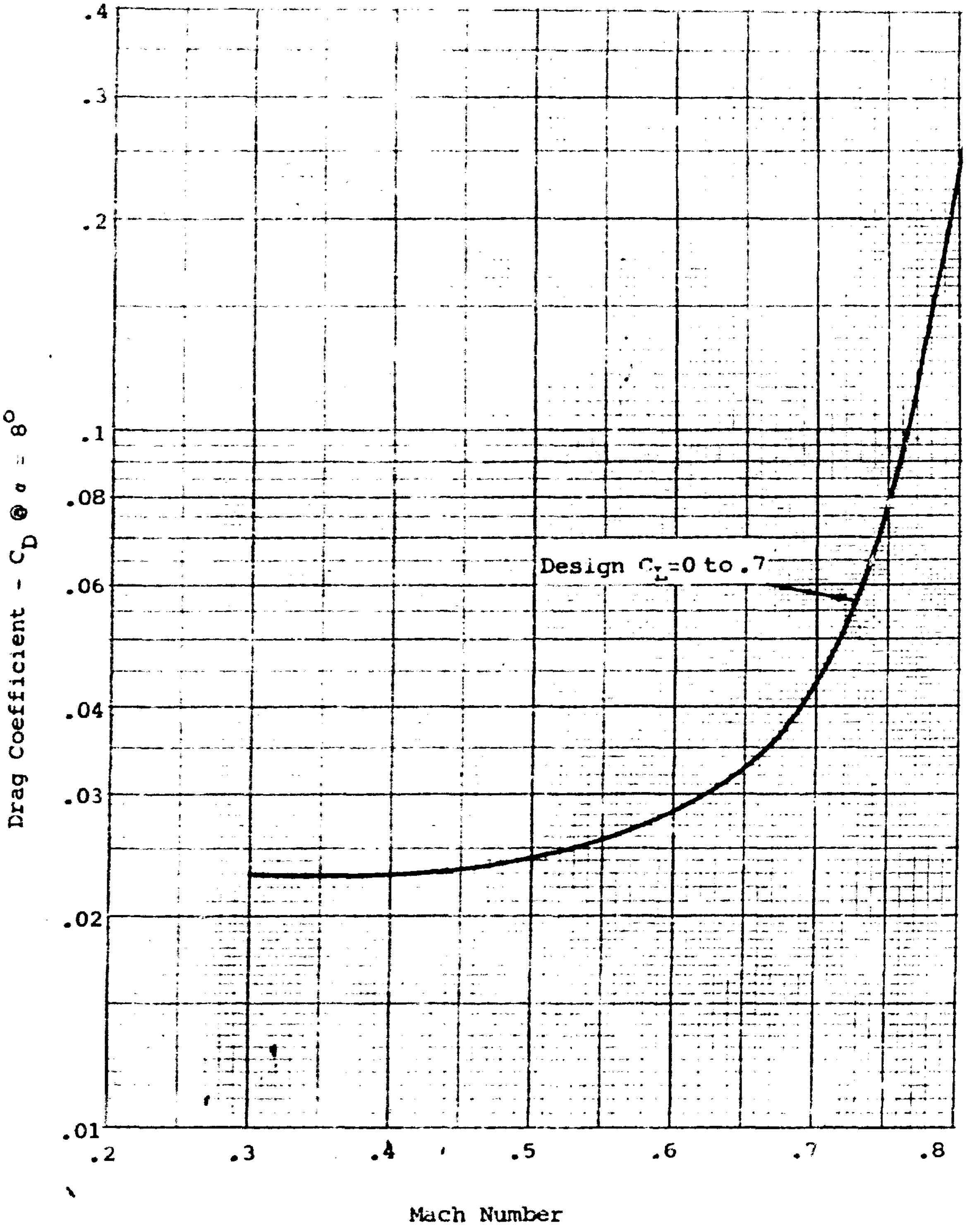

Figure 160. Drag Coefficient at 8° Angle of Attack Thickness Ratio = 18%.

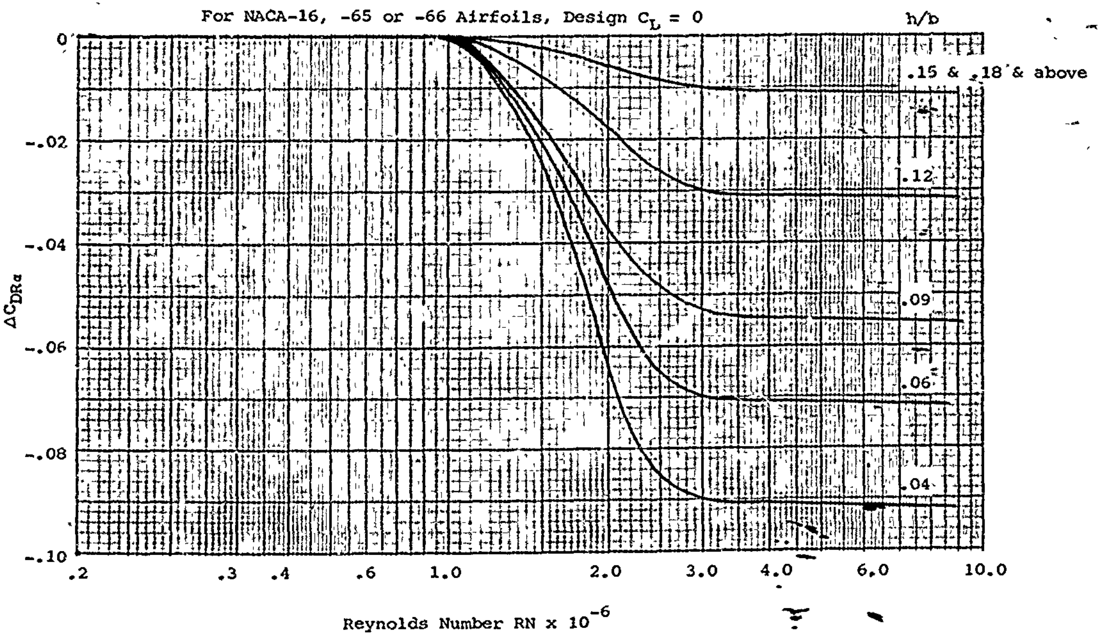

Figure 161. Change in Drag Coefficient at $\alpha = 8^{\circ}$ With Reynolds Number.

NOTE: Apply at all values of
M, RN for NACA-16, -65 Sections

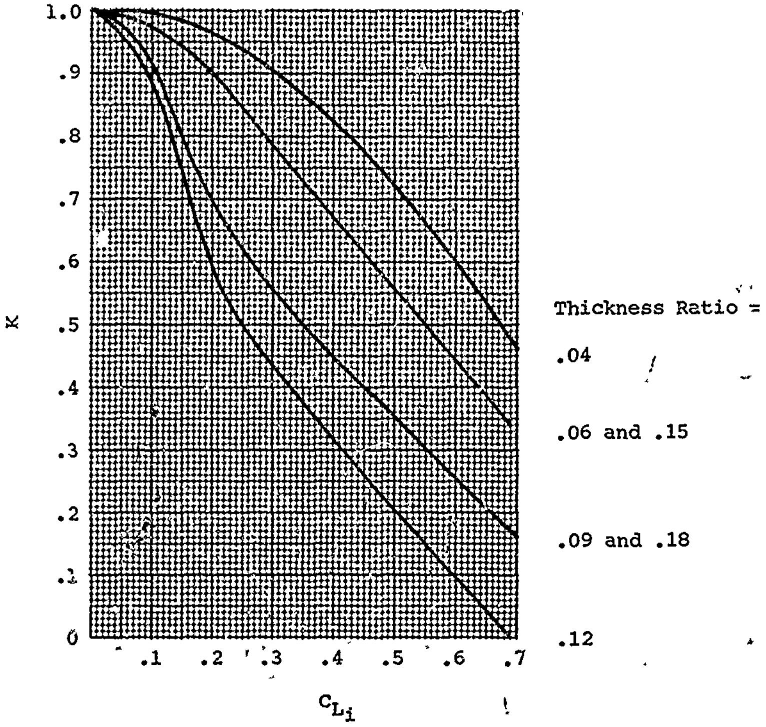

Figure 162. Design C_L Drag Factor.

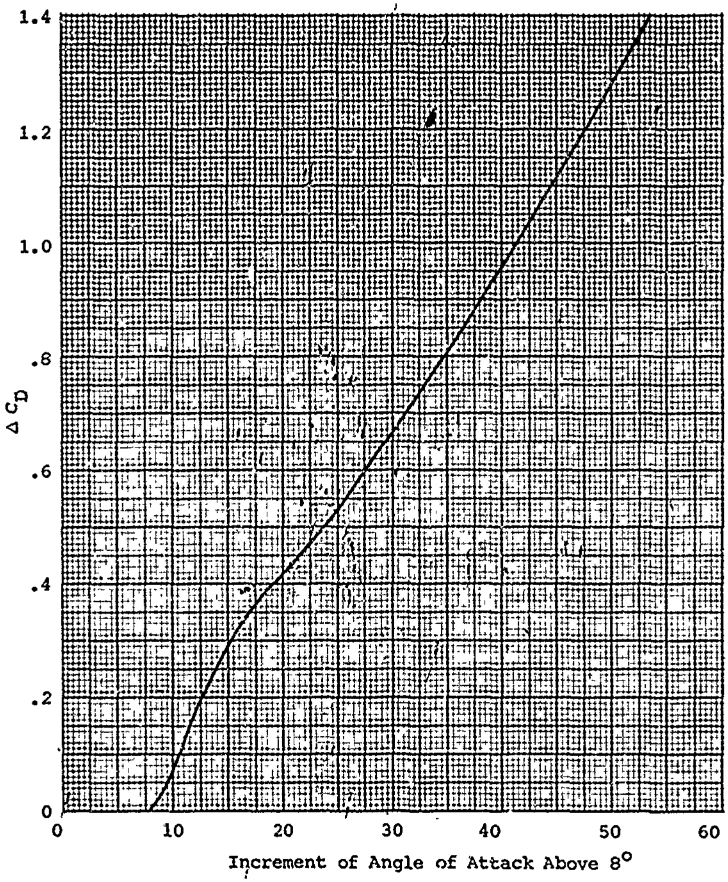

Figure 163. Increment in Drag Coefficient Beyond $\alpha = 8°$.

APPENDIX III
COMPUTER PROGRAM PROCEDURE FOR PROPELLER FORWARD FLIGHT STRIP ANALYSIS

The following generalized procedure has been developed for calculating the performance of single-rotation propellers operating at the forward flight condition. This procedure has been developed for programming on high-speed computers.

The input to the program must be available and filled in on Tables I-1 to I-10. A detailed description of the input is given as follows: .

INPUT

Location	Description
0001	No. of flight conditions from this input
0002	No. of blades
0003	Propeller diameter (FT)
0004	Altitude (FT)
0005	Temperature °F (if zero assumes standard atmos)
0006	Radial station input option 1. standard 2. input
0007	Blade cut out (for option 1)
0008	No. of radial stations (for option 2)
0009	Velocity distribution input option 1. Constant with M. 2. Variable with M
0010	Input option for flight conditions 1. Dimensional. 2. Nondimensional

Input Option 1

0013	Engine rpm
0014	Gear ratio
0015	Flight velocity KTS
0016	Horsepower
0017	Delta flight velocity for succeeding cases
0018	Total No. of flight velocities
0019	Delta h.p.
0020	Total No. of h.ps.'s

Input Option 2

0024	Flight Mach No.
0025	Advance ratio J
0026	Cp
0027	Delta J
0028	Total No. of J's
0029	Δ Cp
0030	Total No. of Cp's

COMPUTER INPUT FOR PROPELLER PERFORMANCE

Date ______ Engineer ______________ Dept. _____ Est. Time ________

Title

0001		No. of cases from this input
0002		No. of blades
0003		Diameter (ft)
0004		Altitude (ft)
0005		Temperature (°F)-if zero, assumes standard day

0006		Radial station input option, 1.-Std. 2.-Input
0007		Blade cut out (for option 1)
0008		No. of radial stations (for option 2)
0009		Velocity distribution input option -
		1. constant w/Mach No. 2. variable w/Mach No.
0010		Input option below 1. or 2.

Fill in Option 1 or 2, but not both

0011		Option 1
0012		
0013		Engine rpm
0014		Gear ratio
0015		Flight velocity (knots)
0016		Horsepower
0017		Delta flight velocity for succeeding cases
0018		Total No. of flight velocities
0019		Delta horsepower
0020		Total No. of pitch angles
0021		Option 2
0022		
0023		
0024		Flight Mach No.
0025		Advance ratio J
0026		Cp
0027		Delta J
0028		Total No. of J's
0029		Delta
0030		Total No. of Cp's

PROPELLER PARAMETERS

	Must be filled in if input No. 6 = 2	
	Table No. I-1	
Radial Station	Radial Stations (r/r_o)	
1	0031	
2	0032	
3	0033	
4	0034	
5	0035	
6	0036	
7	0037	
8	0038	
9	0039	
10	0040	
11	0041	
12	0042	

Table No. I-3		Table No. I-4	
Blade Chord Inches or (x/D) B/D		C_{Li}	
0071		0091	
0072		0092	
0073		0093	
0074		0094	
0075		0095	
0076		0096	
0077		0097	
0078		0098	
0079		0099	
0080		0100	
0081		0101	
0082		0102	

							Fill in only when input No. 9 = 1	
	Table No.I-5		Table No.I-6		Table No.I-7		Table No.I-8	
Radial Station	h/b		Twist		Airfoil Type (16 or 65)		Constant Velocity Distribution Coefficient	
1	0111		0131		0151		0171	
2	0112		0132		0152		0172	
3	0113		0133		0153		0173	
4	0114		0134		0154		0174	
5	0115		0135		0155		0175	
6	0116		0136		0156		0176	
7	0117		0137		0157		0177	
8	0118		0138		0158		0178	
9	0119		0139		0159		0179	
10	0120		0140		0160		0180	
11	0121		0141		0161		0181	
12	0122		0142		0162		0182	

WHEN INPUT NO. 9 = 2 FILL IN TABLES 9 & 10

Table No. I-9	
Mach No.	
0191	
0192	
0193	
0194	
0195	

Table No. I-10

VELOCITY DISTRIBUTION COEFFICIENT

	Mach No. =		Mach No. =		Mach No. =		Mach No. =		Mach No. =	
1	0196		0216		0236		0256		0276	
2										
3										
4										
5										
6	0201		0221		0241		0261		0281	
7										
8										
9										
10										
11	0206		0226		0246		0266		0286	
12										

Table No. I-1	Locations 0031 through 0042 to be filled in if loc (6) = 2	radial stations blank if loc (6) = 1
Table No. I-3	Locations 0071 through 0082	blade chord inches or b/D
Table No. I-4	Locations 0091 through 0102	C_{Li}
Table No. I-5	Locations 0111 through 0122	thickness distribution h/b
Table No. I-6	Locations 0131 through 0142	twist distribution $\beta (x)$
Table No. I-7	Locations 0151 through 0162	airfoil type 16 or 65 series
Table No. I-8	Locations 0171 through 0182 only when input 9 = 1 velocity distribution coeff.	to be filled in VDx
Table No. I-9	To be filled in only if location 9 = 2. Locations 0191 through 0195 Mach No.'s at which VDx values are defined.	
Table No. I-10	To be filled in only if location 9 = 2. Locations 0196 through 0287. Velocity distribution coefficients.	

End of Input

The computer method to calculate the performance of propellers requires the use of two-dimensional airfoil data and the constants K(x) for finding the induced angle. This information is given in Appendix II and the body of the report, and has to be read and placed on tapes for use as described in the calculation procedure described below.

Calculation Procedure

Step 1 Convert input chords from inches to ft.

$$b_F = b_{input}/12$$

Step 2 If input chords are in form b/D compute

$$b_F = (b/D)D \qquad x = x_1 \ldots\ldots x_{12}$$

Step 3 Read and interpolate C_L and C_D data for C_{Li} and h/b combinations used on blade
$x = x_1 \ldots\ldots x_{12}$ store

Step 4 For a given blade No. B read circulation constants from tape $b_1\ b_2\ b_3 \ldots\ldots b_{11}$ for each x station. (Use interpolation to find values for intermediate x values).

Step 5 Calculate local $b/D = b_F/D$
if input vs input values

Compute Activity Factor

$$AF = \frac{100,000}{16} \int_{x_1}^{x_n} (b/D)_x\, x^3 dx$$

Compute integrated design lift coeff.

$$C_{L_I} = 4 \int_{x_1}^{x_n} (C_{Li})_x\, x^3 dx$$

C_{Li} = input Table 4

Step 6 If input Option 1 compute M_{flight}
C_P ΔC_P ΔM_{flight} J ΔJ

If input Option 2 compute dimensional values for output later

Step 7 Compute Prop rpm = engine rpm x gear ratio
or from M_F J

Step 8 Compute atmospheric conditions

Test is altitude ≥/36,089 ft

If yes
$a = 968.465$ ft/sec
$\mu = .29603 \times 10^{-6}$ lb-sec/ft^2
$\rho = \rho^* \times 10^{-B(H-H^*)}$
$H^* = 36,089$ ft
$B = .2087367 \times 10^{-4}$
$\rho^* \doteq .00070612$ slugs/ft^3
H = operating altitude

If no Use equations

$$a = \sqrt{1116.89 \quad 1 - a^1 H/T_O}$$

$$\rho = .00237 \ (1 - a^1 H/T_O)^{4.2501}$$

$$\mu = .37472 \times 10^{-6} (1 - a^1/T_O)^{1.5} \ \cdot \left(\frac{734.658}{T_O(1 - a^1/T_O) + 215.97} \right)$$

$a^1 =$

NOTE: * Refers to Tropopause

Subscript zero refers to sea level

Step 9 Calculate local Mach No.

$$M(x) = \frac{1}{a} \sqrt{2.15111 \ V_x^2 + \frac{(\pi x \ ND)^2}{3600}}$$

$V_x = V_{FWD}$ x velocity dist. coeff.

N = rpm (prop)

V_{FWD} (mph)

If J input V x computed from J

$$Re_x = \frac{\rho a}{\mu} b_f \ M(x)$$

Step 10 Read airfoil data (previously obtained from tape) and interpolate with respect to M(x) and Re(x) and store

Step 11 Compute advance ratio

$$J = \frac{101.4 \ V(KTS)}{ND}$$

unless non-dim input used

Step 12 Calculate local J_x

$$J_x = J_x \text{ vel dist coeff}$$

for all values of x

Step 13 Compute C_P

$$C_P = \frac{(.0005)HP}{\rho\,(N/1000)^3 (D/10)^5} = \frac{(\rho_o/\rho)\,SHP}{2000\,(N/1000)^3 (D/10)^5}$$

unless C_P input

Step 14 Calculate ϕ_o

$$= \phi_o = \tan^{-1} \frac{J}{\pi x} \qquad \text{for } x = .7$$

$$= \tan^{-1} \frac{J}{2.19893}$$

Step 15 Determine induced angle of attack α_i

$$\frac{C_P}{\alpha_i} = (0.01597\,J + .0261)\,J + .00531$$

$$\alpha_i = 3(C_P/B)/(C_P/\alpha_i)$$

B = blade no.

Step 16 Compute initial ϕ

$$\phi = \phi_o + \alpha_i$$

Step 17 Determine A

If $0 < \phi \leq 11$ (ϕ in degrees)

$$A = 0.000877\,\phi + 0.000276$$

If $11 < \phi \leq 80$

$$A = \frac{(\phi - 3393.388)\phi + 12847.13}{-131811.1\,\phi - 993321.1}$$

Step 18 Calculate initial C_L

$$C_L = \frac{1562.5\,\alpha\,i\,A}{AF}$$

Step 19 Determine α by looking up the airfoil data at $x = 0.7$ and using C_L from Step 18 and the M_n & R_e specified for $x = .7$

Step 20 Calculate $\beta_{r=.7R}$

$$\beta_{r=.7R} = \phi + \alpha$$

from Step 19

Step 21 Compute β correction

$$\epsilon = \beta_{.7R} - \beta^1_{.7R} \qquad \beta^1_{.7R} = 0.0 \text{ on 1st iteration}$$

Step 22 Compute values of β

$$\beta(x) = \beta(x)_{\text{Input}} - \beta_{.7\text{Input}} + \epsilon \text{ (1st iteration)}$$

$$\beta(x) = \beta(x) + \epsilon \text{ (2nd and subsequent)}$$

Step 23 Compute local solidity at each radial station

$$\sigma_x = \frac{bB}{\pi D x} \qquad b = \text{chord}(x)$$

Step 24 Assume initial value of inflow velocity

$\bar{w} = -0.3$ (1st iteration

Step 25 Compute inflow angle

$$\phi(x) = \tan^{-1}\left[\left(1 + \frac{\bar{w}}{2}\right)\frac{J(x)}{\pi x}\right]$$

$J_{(x)}$ from Step 12

Step 26 Calculate local angle of attack

$$\alpha(x) = \beta(x) - \phi(x)$$

Step 27 Calculate

$$\bar{J} = J_{(x)}(1 + \bar{w}) \qquad \text{for all } x$$

Step 28 For each x determine $K(x)$ as follows

For given x read $b_1\ b_2\ b_3 \ldots\ldots b_{11}$ from tape

If $2. \geq \bar{J}$ $\quad K(x) = \dfrac{\bar{J} + b_4}{b_5 J^{-2} + b_6 \bar{J} + b_7}$

28(a) If $2. \geq \bar{J}$ and $0.75 \leq K(x)$ as calculated above ≤ 1.0

Recalculate $K(x) = b_1 \bar{J}^2 + b_2 \bar{J} + b_3$

28(b) If $2. < \bar{J} \leq 7.$ $\quad K(x) = \dfrac{\bar{J} + b_8}{b_9 \bar{J}^2 + b_{10} \bar{J} + b_{11}}$

Step 29 Compute σC_L (local)

$$(\sigma C_L)_x = \frac{2\bar{w}\,(1 + \bar{w})K(x)(1 - \cos^2\phi)}{(1 + \frac{\bar{W}}{2})(1 + \frac{\bar{W}}{2}\cos^2\phi)\cos\phi}$$

Step 30 Compute local $C_{L(x)}$

$$C_{L(x)} = (\sigma C_L)_x / \sigma_x$$

Step 31 Determine $C_{L(x)}$ from airfoil data using $\alpha(x)$ from Step 26

Step 32

Test

If $C_{L(x)}$ (Step 31) $\geq C_{L(x)}$ (Step 30)

then $\bar{W} = \bar{W} + \Delta \bar{W}$

$\bar{W} = 0.1$

Go to Step 25 and reiterate

If $C_{L(x)}(31) < C_{L(x)}$ (30)

Proceed.

Step 33

$$\left(\frac{\sigma C_L}{\sigma x}\right)_{x_1} = m_a \; \alpha_1 + b_A$$

$$\left(\frac{\sigma C_L}{\sigma x}\right)_{x_2} = m_a \; \alpha_2 + b_a$$

Subscripts 1 & 2 refer to the penultimate and last iterations respectively

$\left(\frac{\sigma C_L}{\sigma x}\right)_x$ computed in Step 30

α_1 & α_2 from Step 26 on successive iterations

Solve for m_a & b_a

Step 34

Solve for m_B & b_B

$$C_L(x)_1 = m_B \, \alpha_1 + b_B$$

$$C_L(x)_2 = m_B \, \alpha_2 + b_B$$

$C_{L(x)}$ from Step 31

α from Step 26

1 & 2 have the same significance as for Step 33.

Step 35 Determine angle of attack & C_L

$$\alpha(x) = \frac{b_B - b_a}{m_a - m_B}$$

Step 36 $C_L(x) = m_a \alpha + b_a$ α from Step 35

Step 37 Determine $C_D(x)$ by table look-up using $\alpha(x)$ from Step 35

Step 38 Calculate $\emptyset$ sin $\emptyset$ cos $\emptyset$

$\emptyset = \beta(x) - \alpha(x)$ (x) from 35

Step 39 $\overline{w} = 2 \left(\frac{\tan \emptyset}{J / \pi x} \right) - 2$

J(x) from 12

Step 39(a) Compute Δx values

$$\Delta x(1) = \frac{x(2) - x(1)}{2}$$

$$\Delta x(n) = \frac{x(n+1) - x(n-1)}{2} \qquad 1 < n < 11$$

$$\Delta x(11) = \frac{x(12) - x(11)}{2}$$

Step 40 Calculate Z

$$Z = \frac{\pi}{2} \left[\frac{J(x) \cdot x}{2} \left(1 + \frac{\pi}{2} \cos^2 \emptyset \right) \right]^2 \frac{1}{\sin\emptyset}$$

Step 41 If $C_L = 0.0$ $C_Q = \frac{C_D \sigma Z \Delta x}{\tan\emptyset}$

If $C_L \neq 0.0$ $\tan \gamma = C_D/C_L$

$$\Delta C_Q = C_L \sigma Z \Delta x \left[1 + \frac{\tan \gamma}{\tan\emptyset} \right]$$

Step 41(a)

$$\frac{dC_Q}{dx} = \Delta C_Q / \Delta x$$

Step 42 — Test - have all radial stations been computed. If not return to 23 and do next x value.

Step 43 — Compute C_Q, C_p and CPH

$$C_Q = \Sigma \Delta C_Q$$

$$C_p = 2 \pi C_Q$$

$$CPH = CP/24.354$$

Step 44 — for each x compute ΔC_T and dC_T/dx

If $C_L = 0$ $\quad G = \frac{-2 C_D \sigma Z \Delta x}{x}$

If $C_L \neq 0$ $\quad C_T = \frac{2}{x} \sigma C_L \Delta x Z \left(\frac{1}{\tan \phi} - \tan \gamma\right)$

$$\frac{dG}{dx} = \Delta C_T / \Delta x$$

Step 45 — Test - have values of ΔC_T & dC_T/dx been computed for all x's

Step 46 — Calculate C_T, C_{TH} and Thrust

$C_T = \Sigma \Delta C_T$'s $\quad C_{TH} = C_T / 7.752$

$$\text{Thrust} = \frac{C_T \rho N D^4}{3600}$$

Step 47 — Calculate efficiency

$\eta = J C_T / C_p$

J step 11
C_T step 46
C_p step 43

Step 48 Test

$$0.97 < \frac{C_P\ (43)}{C_P(inp)} < 1.03$$

if $\frac{C_P\ (43)}{C_P(inp)} \leq 0.97$ or ≥ 1.03

$$C_L = C_L \text{ step } 18 \Big/ \left(\frac{C_P \text{ step } 43}{C_P \text{ inp}}\right)$$

go to step 19 and reiterate

OUTPUT

The first page of computer output lists the propeller physical characteristics.

If the number of cases called for in the input is less than 7 (seven), then the local blade information is printed out for each case. If ≥ 7, the program assumes that the "thumbprint" option is required and gives only the total performance values.